

University of Groningen

FOP

Drenth, Jeroen

DOI:
[10.33612/diss.571741561](https://doi.org/10.33612/diss.571741561)

IMPORTANT NOTE: You are advised to consult the publisher's version (publisher's PDF) if you wish to cite from it. Please check the document version below.

Document Version
Publisher's PDF, also known as Version of record

Publication date:
2023

[Link to publication in University of Groningen/UMCG research database](#)

Citation for published version (APA):
Drenth, J. (2023). *FOP: on the (bio)synthesis and biocatalytic applications of the artificial deazaflavin cofactor FO-5'-phosphate*. [Thesis fully internal (DIV), University of Groningen]. University of Groningen. <https://doi.org/10.33612/diss.571741561>

Copyright

Other than for strictly personal use, it is not permitted to download or to forward/distribute the text or part of it without the consent of the author(s) and/or copyright holder(s), unless the work is under an open content license (like Creative Commons).

The publication may also be distributed here under the terms of Article 25fa of the Dutch Copyright Act, indicated by the "Taverne" license. More information can be found on the University of Groningen website: <https://www.rug.nl/library/open-access/self-archiving-pure/taverne-amendment>.

Take-down policy

If you believe that this document breaches copyright please contact us providing details, and we will remove access to the work immediately and investigate your claim.

Downloaded from the University of Groningen/UMCG research database (Pure): <http://www.rug.nl/research/portal>. For technical reasons the number of authors shown on this cover page is limited to 10 maximum.

FOP

**On the (Bio)Synthesis and Biocatalytic Applications of
the Artificial Deazaflavin Cofactor FO-5'-Phosphate**

Jeroen Drenth



rijksuniversiteit
 groningen

FOP

On the (Bio)Synthesis and Biocatalytic Applications of the Artificial Deazaflavin Cofactor FO-5'-Phosphate

Proefschrift

ter verkrijging van de graad van doctor aan de
Rijksuniversiteit Groningen
op gezag van de
rector magnificus prof. dr. C. Wijmenga
en volgens besluit van het College voor Promoties.
De openbare verdediging zal plaatsvinden op
dinsdag 28 februari 2023 om 12.45 uur

door

Jeroen Drenth

geboren op 29 oktober 1991
te Winschoten

Colofon

The research described in this thesis was carried out in the Molecular Enzymology group of the Groningen Biomolecular Sciences and Biotechnology Institute (GBB) at the University of Groningen, The Netherlands, and was funded by the Dutch Research Council (NWO VICI grant)

Promotores

Prof. dr. M.W. Fraaije

Prof. dr. D.B. Janssen

Beoordelingscommissie

Prof. dr. D.J. Slotboom

Prof. dr. A.J. Minnaard

Prof. dr. W. Kroutil

Table of contents

Chapter 1 General introduction – Setting the scene	9
Chapter 2 Natural flavins: Occurrence, role and non-canonical chemistry	15
2.1 Introduction	16
2.2 Flavin biosynthesis	18
2.3 Flavin redox states	18
2.4 Reductive and oxidative halfreactions	21
2.5 Covalently bound flavin cofactors	24
2.6 Naturally occurring riboflavin analogues and modified flavins – roles and occurrence	32
2.7 N5-substrate and N5-oxygen adducts	39
2.8 F ₄₂₀ – a natural deazaflavin	43
2.9 Conclusion	46
Chapter 3 Chemoenzymatic synthesis of an unnatural deazaflavin cofactor that can fuel F420-dependent enzymes	49
3.1 Introduction	50
3.2 Materials and Methods	52
3.3 Results	56
3.4 Discussion	61
3.5 Supporting information Chapter 3	66
Chapter 4 Introducing an artificial deazaflavin cofactor in <i>Escherichia coli</i> and <i>Saccharomyces cerevisiae</i>	85
4.1 Introduction	86
4.2 Materials and methods	89
4.3 Results	95
4.4 Discussion	107
4.5 Conclusion	111
4.6 Supporting information Chapter 4	113

Chapter 5 A tailor-made deazaflavin-mediated recycling system for artificial nicotinamide cofactor biomimetics	123
5.1 Introduction	124
5.2 Materials and Methods	127
5.3 Results	130
5.4 Discussion	135
5.5 Supporting information Chapter 5	138
Chapter 6 Boosting the reductive power of OYE1 by cofactor engineering	149
6.1 Introduction	150
6.2 Materials and methods	153
6.3 Results	154
6.4 Discussion	157
Appendices Summary and Conclusions	162
References	167
Nederlandse samenvatting	191
Acknowledgements	196
Curriculum vitae	200
List of publications	201

CHAPTER 1

General introduction – Setting the scene

Jeroen Drenth & Marco W. Fraaije

*Molecular Enzymology Group, University of Groningen, Nijenborgh 4, 9747AG Groningen,
The Netherlands*

As many countries around the globe strive to become climate neutral under the Paris Agreement, there is a growing interest in green chemistry, including many biology inspired strategies. Enzyme and whole-cell mediated biocatalysis are important tools for environmentally friendly production and recycling of compounds.

There are a few reasons why enzymes and microorganisms are particularly appealing for chemical synthesis. For instance, these water soluble catalysts generally work at ambient temperature and pressure, and they show excellent chemo-, stereo- and regioselectivity, as well as stereospecificity. Therefore, they hardly produce any waste products and require low energy input. Moreover, enzymes are produced at low cost and minimum impact for the environment by microorganisms that only require a cheap carbon source and certain minerals. Just as with the biosynthesis of enzymes, microorganisms can also be exploited for the biosynthesis of compounds with the same benefits.^{1–5} Moreover, the use of microorganisms can facilitate *de novo* biosynthesis of valuable compounds, using an intracellular enzyme-cascade with appropriate cofactor recycling when necessary.

As a wealth of organisms are known with their specific metabolic properties, a plethora of enzymes with their specific characteristics are available to biocatalysis. Advances in protein structure determination, molecular systems biology, computational chemistry and DNA sequencing, manipulation and synthesis techniques allow for efficient engineering of proteins and microbial strains, enabling the design of custom-made efficient biocatalysts that further expand the biocatalytic toolbox.^{6–8}

The large array of enzyme-mediated catalytic strategies available to chemists is not only facilitated by the 20 canonical amino acids that make up the protein, but is also – to a large extent – made possible by cofactors.⁹ Redox chemistry in biological systems requires cofactors, of which heme, flavins and nicotinamides are the most used in nature and the lab. There are many examples of redox enzymes used for biocatalysis. The heme-containing cytochrome P450s are exploited for their regio- and stereospecific oxidation of non-activated hydrocarbons.^{10–12} The NAD(P)-utilizing dehydrogenases are excellent catalysts for the oxidation of alcohols and reduction of ketones, aldehydes and imines, forming enantiopure alcohols and amines.^{13–15} Among the most versatile cofactors in biocatalysis are the flavins flavin mononucleotide (FMN) and flavin dinucleotide (FAD), which are able to reduce imines, carbonyl compounds and activated olefins, oxidize alcohols, aldehydes and amines by dehydrogenation, oxygenate an array of heteroatoms and activated carbons, and can even perform (de)halogenation.^{16,17}

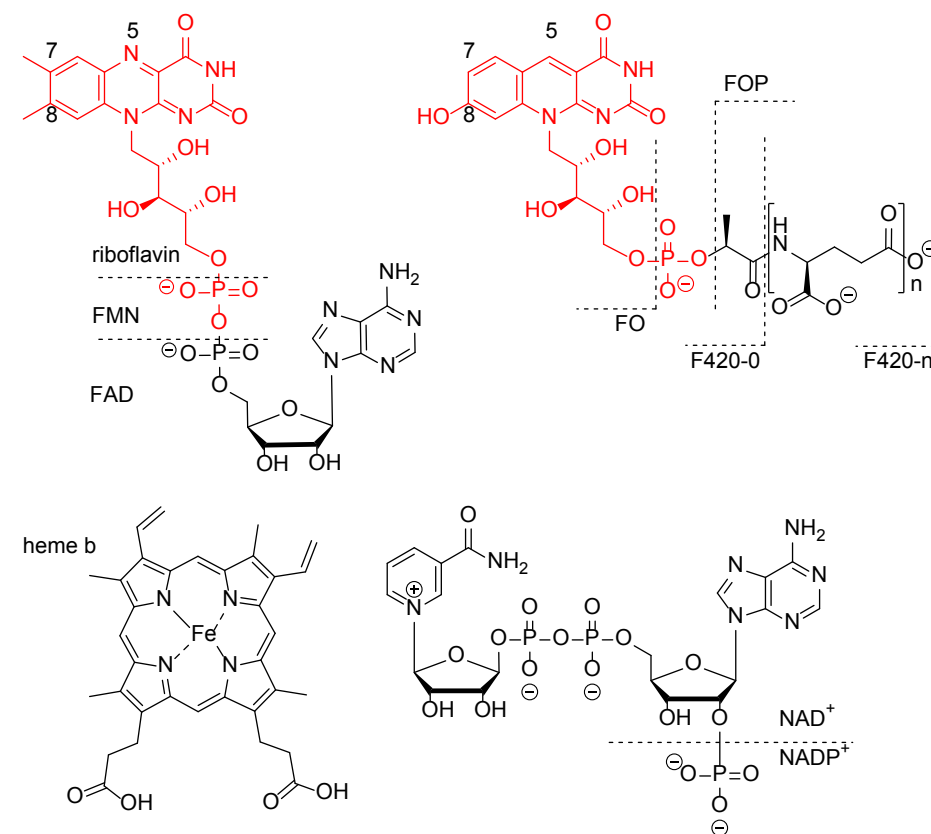


Figure 1.1: Structures of redox cofactors discussed in the text. FMN and FOP are highlighted in red.

Unlike the previously mentioned cofactors, the natural redox cofactor F_{420} , has not yet been exploited to its full potential for biocatalytic applications.^{18,19} This 5-deazaflavin structurally resembles the flavin cofactors²⁰ (see **Figure 1.1**) but its reactivity resembles more that of nicotinamides, as it only performs hydride transfer and is relatively inert to molecular oxygen.^{21,22} The very low redox potential of -340 mV up to -380 mV, however, sets it apart from the flavins and nicotinamides.^{21,23,24} Although its extraordinary attributes are vastly exploited by a broad range of organisms (e.g., as a cofactor in the C1-metabolism of methanogens and methanotrophs and in the secondary metabolism of many Actinobacteria), it has not yet been used in biocatalysis.^{25–27} Its significantly low redox potential and stability in the presence of oxygen would, however, make it an ideal candidate for the industrial reduction of low redox potential compounds, that are otherwise relatively inert to flavin and nicotinamide mediated catalytic strategies.¹⁸

A reason for its absence in biocatalysis is the low availability of the cofactor. Many of the F_{420} -producing microorganisms are hard to cultivate and have slow growth rates. Moreover, some F_{420} -producing organisms, such as *Mycobacterium tuberculosis*, are very pathogenic. As an alternative to extraction from organisms, chemical synthesis of this cofactor – with its complex structure – also results in relatively low yields.^{28,29} The synthesis of its biosynthetic precursor FO, however, is relatively straightforward, but this cofactor is unfortunately not accepted by all F_{420} -utilizing enzymes.^{30–32}

The main aim of the research presented in this thesis is to boost biocatalysis with F_{420} -dependent enzymes, by synthesizing an artificial 5-deazaflavin cofactor biomimetic that could replace the scarce F_{420} cofactor. We took inspiration from both F_{420} , as well as the structure and biosynthesis of FMN to create the artificial cofactor FOP, FO-5'-phosphate (see **Figure 1.1**). This compound is easily produced on larger scale and is accepted by an array of F_{420} -dependent enzymes with comparable activities to the native coenzyme.

Before we discuss our research on the (bio)synthesis and applications of FOP we first give an overview of naturally occurring (deaza)flavins, including F_{420} , and discuss their biosynthesis, biological roles and flavoprotein chemistry in **Chapter 2**. Flavoproteins catalyze a wealth of chemical reactions through a plethora of different ingenious mechanisms, carefully fine-tuned by the enzyme scaffold. This chapter discusses noncanonical flavin chemistry and the many modified flavins found in nature that make for surprising reactivity. It concludes with an overview of the natural deazaflavin cofactor F_{420} , discussing its biosynthesis, intriguing physicochemical properties and natural roles.

Further research on novel and known flavin-containing enzymes could reveal new activities on new substrates, with even more intriguing mechanisms and could be used for novel applications that expand the toolbox for biocatalysis. Especially F_{420} -dependent enzymes – with their extremely low redox potentials and their apparent inertness to molecular oxygen – could make for great biocatalysts.¹⁹

Chapter 3 discusses the chemoenzymatic synthesis of the artificial cofactor FOP. This cofactor has the catalytically active FO-core structure – the natural precursor of F_{420} – with a phosphoryl group at the 5'-position. It can also be regarded as a mimic of FMN. We show that an engineered riboflavin kinase can conveniently phosphorylate chemically synthesized FO *in vitro* and, therefore, produce FOP. We then show that this easily synthesized, and relatively cheap cofactor biomimetic can replace F_{420} in a range of different F_{420} -dependent oxidoreductases, with gratifyingly similar

activities. This showcases that this artificial cofactor might be a feasible replacement for F_{420} in scalable biocatalytic applications.

In **Chapter 4** we show that FOP can also be produced via *de novo* biosynthesis in *Escherichia coli* and by a hybrid synthesis method that employs *Saccharomyces cerevisiae* (baker's yeast). We demonstrate the possibility of scalable FOP biosynthesis by heterologous expression of a FO synthase and an engineered riboflavin kinase on a two-plasmid system in *E. coli*. With strain and medium engineering we can produce FOP with higher space-time yields than F_{420} production in the often used production organism *Mycobacterium smegmatis*. The possibility of using this FOP production system for whole-cell biocatalysis is showcased by the successful FOP-mediated reduction of ketoisophorone. By supplying chemically synthesized FO in the growth medium we can also produce FOP in yeast cells that express an engineered riboflavin kinase. The introduction of FOP in yeast and *E. coli* could potentially facilitate the production of novel fermentation products.

In **Chapter 5** we combine the artificial deazaflavin FOP with artificial nicotinamide biomimetics (NBCs). These are scalable, stable, easily synthesizable, and cheap replacements for the pyridine redox cofactors nicotinamide adenine dinucleotide (NAD) and nicotinamide adenine dinucleotide phosphate (NADP). The major bottleneck for their application in biocatalysis is the poor recyclability of these cofactors. We show that $F_{420}H_2$ and FOPH₂ are effective recycling agents for NBCs. By engineering a thermostable F_{420} :NADP oxidoreductase we were able to create tailor-made recycling systems for several of these NBCs for use at ambient and elevated temperatures.

In **Chapter 6** we use the reductive power of FOP to broaden the substrate scope of ene-reductases. Ene-reductases of the old yellow enzyme family (OYE) are efficient FMN-containing enzymes for the asymmetric reduction of α,β -unsaturated ketones, aldehydes and nitro groups, but are not active on lesser activated double bonds. We exploit the extremely low redox potential of FOP for the reduction of less activated olefinic bonds, by replacing FMN in the ene-reductase from brewer's bottom yeast (OYE1) with FOP. We then demonstrate that when OYE1 is reconstituted with FOP it is able to convert cinnamic acid, a compound that is normally not accepted by OYEs.

CHAPTER 2

Natural flavins: Occurrence, role and non-canonical chemistry

Jeroen Drenth & Marco W. Fraaije

This chapter is based on a published book chapter In:

Flavin-Based Catalysis: Principles and Applications Cibulka, R., Fraaije, M.W. Eds.;
Wiley-VCH: Weinheim, Germany, 2021; pp 29-65.

*Molecular Enzymology Group, University of Groningen, Nijenborgh 4, 9747AG Groningen,
The Netherlands*

Abstract

Flavoproteins are of key importance to all life on earth for both primary and secondary metabolism. Most flavin-dependent enzymes utilize flavin mononucleotide (FMN) or flavin adenine dinucleotide (FAD) as redox cofactor for single-electron and hydride transfer as well as oxidation and oxygenation chemistry at the C4a-locus. Over the last decades several naturally occurring modified flavins have been discovered, like 8-formylFAD, F_{420} , and prenylFMN, as well as covalently bound flavins, and were found to further expand the toolbox of flavin chemistry, showcasing extraordinary redox potentials and unprecedented chemistry. Recently, also several examples of ‘exotic’ flavin chemistry, such as N5-oxygenation, have been identified in enzymes that utilize the standard flavins FMN and FAD. This shows that nature has been extremely inventive in exploiting flavins and flavin derivatives as cofactors for an exceptionally wide variety of reactions. Future research will reveal whether other, so far hidden, flavoenzyme-catalyzed chemistries exist.

2.1 Introduction

Flavin-dependent enzymes are versatile biocatalysts involved in numerous cellular oxidation and reduction reactions over a wide range of substrates, many of which are of key importance to primary and secondary metabolism. Since their discovery about a century ago,³³ these flavin mononucleotide (FMN) and flavin adenine dinucleotide (FAD) utilizing oxidoreductases have been well studied, and currently much is known about flavin chemistry. Some examples of the wide range of reactions catalyzed by flavins include: reduction of activated C=C double bonds,³⁴ oxidation of alcohols,^{35,36} oxidations and reductions of aldehydes^{37,38} and lactols,^{39,40} as well as (cyclic) alkane hydroxylation,⁴¹ aromatic hydroxylation,^{42,43} Baeyer-Villiger oxidation,^{44,45} epoxidation, sulfoxidation, phosphite ester, selenide, organoboron and amine oxidations,⁴⁶ dehalogenation, halogenation,⁴⁷ decarboxylation,^{48,49} and even light production.⁵⁰ Part of the chemical versatility is derived from the ability to undergo both one and two electron reduction/oxidation reactions, to form several thermodynamically and kinetically accessible stable redox states.⁵¹ The mode of flavin reactivity and substrate specificity are dictated by the protein part of the enzyme, as it fine-tunes the flavin redox potential, directs specific substrates to the cofactor and stabilizes certain redox states and covalent adducts.^{51–53} Most enzymes do this through non-covalent interactions, but there are cases where the flavin cofactor is actually covalently bound to the protein scaffold, enabling more drastic changes in flavin reactivity and substrate acceptance. Sometimes, enzymes may even stabilize super oxidized flavin states, as in the case of the recently discovered flavin-N5-oxide ($Fl_{N5(O)}$).⁵⁴ Modified flavins can greatly enhance the ‘canonical’ activity of

flavoenzymes. Canonical flavin chemistry is hydride transfer to and from the N5 locus and molecular oxygen activation at C4a, and is responsible for almost all the reported activities. But modified flavins can also harbor new activities. A recently discovered means of steering the flavin reactivity is prenylation of the isoalloxazine catalytic core structure.⁵⁵ This highly modified cofactor is of key importance in reversible decarboxylations. In addition to the riboflavin derived cofactors also the 5-deazaflavin F_{420} exists in nature. This flavin analogue is synthesized mainly by archaea and Actinobacteria from an intermediate in riboflavin biosynthesis. This underexplored cofactor with its extraordinarily low redox potential, could be a very valuable tool in biocatalysis and medicinal chemistry.^{25,56} This chapter will deal with F_{420} and the ‘exotic’ cases of flavin chemistry found in nature, where the cofactor is covalently modified or performs noncanonical flavin chemistry, further expanding the toolbox of flavin biocatalysis.

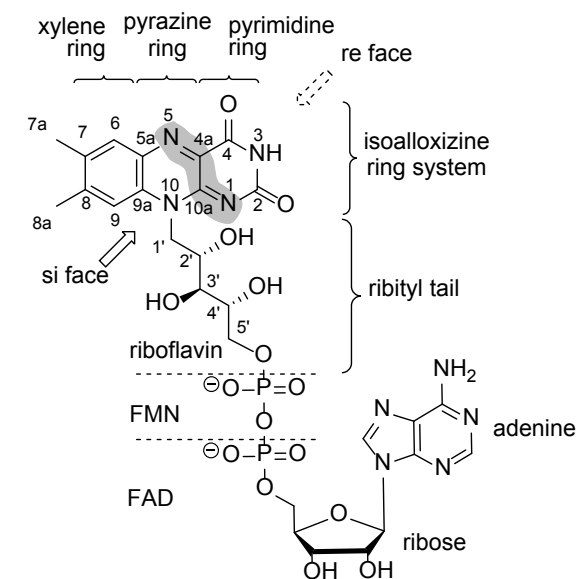


Figure 2.1: Flavin structure. The catalytic core structure of all flavins is the 7,8-dimethylisoalloxazine ring system, which is comprised of an electron rich xylene ring, an electron deficient pyrimidine ring and a bridging electrophilic pyrazine ring. The catalytically important locus N5–C4a–C10a–N1 is highlighted in grey shading. Riboflavin, FMN and FAD also have a ribityl unit fused to the 7,8-dimethylisoalloxazine moiety at N10. The ribityl tail of flavin mononucleotide (FMN) is decorated with a 5'-phosphoryl group and flavin adenine dinucleotide (FAD) is further lengthened with adenosine monophosphate.

2.2 Flavin biosynthesis

Riboflavin, the precursor of FMN and FAD, also known as vitamin B₂, is essential to all known organisms, but not all organisms –including humans– can actually synthesize this important cofactor. The structure of flavin cofactors is shown in **Figure 2.1**. Plants and many fungi and bacteria, however, can produce this cofactor from one equivalent of guanosine triphosphate (GTP) and two equivalents of ribulose-5-phosphate (R5P). Both are common metabolites in primary metabolism.^{57,58} The first steps in biosynthesis are the hydrolytic removal of C8 from the guanine ring from GTP as formate and the hydrolytic release of pyrophosphate (PP_i), both catalyzed by GTP cyclohydrolase II.⁵⁷ In bacteria, the product of these reactions, 2,5-diamino-6-(5-phospho-D-ribosylamino)pyrimidin-4(3H)-one ((2) in **Figure 2.2**) then undergoes deamination at C2 of the ring, and subsequent NAD(P)H-dependent reduction of the phosphoribosyl sidechain (reactions B and D in **Figure 2.2**, respectively) to form 5-amino-6-(1-D-ribitylamino)uracil. In bacteria both reactions are catalyzed by a bifunctional enzyme.⁵⁹ Fungi, however, first reduce the phosphoribosyl side chain of 2,5-diamino-6-(5-phospho-D-ribosylamino)pyrimidin-4(3H)-one and then deaminate the reduced product. Both reactions, depicted by arrows C and E in **Figure 2.2**, are catalyzed by separate enzymes.⁶⁰ The 5'-phosphoryl group is then removed by a phosphatase⁶¹ and the product, 5-amino-6-(1-D-ribitylamino)uracil, is then condensed with L-3,4-dihydroxybutan-2-one 4-phosphate to form 6,7-dimethyl-8-(D-ribityl)lumazine by 6,7-dimethyl-8-ribityllumazine synthase^{62–64} (arrow G in **Figure 2.2**). L-3,4-dihydroxybutan-2-one 4-phosphate is formed from R5P in a peculiar reaction, involving several tautomerizations and a sigmatropic rearrangement, catalyzed by L-3,4-dihydroxybutan-2-one 4-phosphate synthase.^{64–66} The last step in the biosynthesis pathway is catalyzed by riboflavin synthase, which catalyzes the unusual dismutation of two 6,7-dimethyl-8-(D-ribityl)lumazine equivalents to form one equivalent of riboflavin and one equivalent of its precursor, 5-amino-6-(1-D-ribitylamino)uracil.⁶⁷ In the case of FMN the 5'-carbon is decorated with a phosphoryl-group, and in the case of FAD this is further elongated by an adenosine-5'-monophosphate (AMP) moiety. Both steps are either done by bifunctional FAD-synthases in bacteria or by riboflavin kinase and FAD synthase in fungi and plants, respectively.⁶⁸

2.3 Flavin redox states

Electrons can easily be added to or removed from the isoalloxazine moiety –especially the N5–C4a–C10a–C1 locus– as the ring system stabilizes the two-electron oxidized quinone (Fl_{ox}), the two-electron reduced hydroquinone (Fl_{red}, FlH₂ or FlH⁻) and one-electron semiquinone radical states (Fl_{sq}), see **Figure 2.3**. Also stable covalent adducts with oxygen and other nucleophiles can be made at the electrophilic N5–C4a locus.^{51,69}

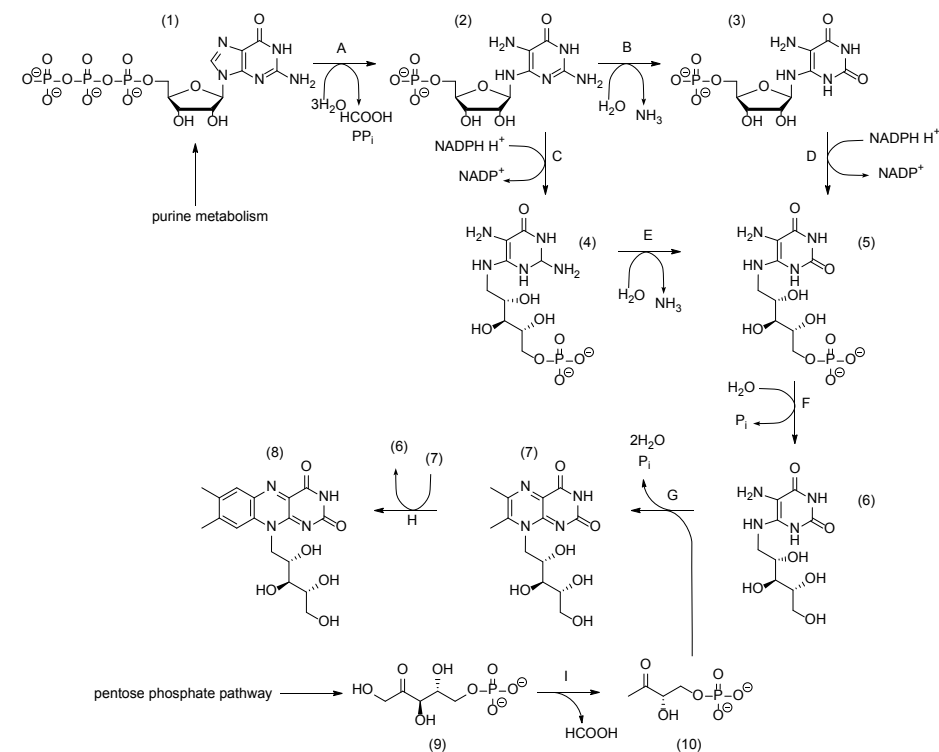


Figure 2.2: Riboflavin biosynthesis pathway. Riboflavin (**8**) is synthesized out of one equivalent of guanosine triphosphate (GTP (**1**)) and two equivalents of ribulose-5-phosphate (R5P (**9**)). **A:** The C8 and two phosphate groups of GTP are hydrolyzed by GTP cyclohydrolase II, forming pyrophosphate, formate and 2,5-diamino-6-(5-phospho-D-ribosylamino)pyrimidin-4(3H)-one (**2**). **B:** In bacteria (**2**) is deaminated at the C2 position by diaminohydroxyphosphoribosylaminopyrimidine deaminase, forming 5-Amino-6-(5'-phosphoribosylamino)uracil (**3**) and ammonia. **D:** 5-amino-6-(5-phosphoribosylamino)uracil reductase then catalyzes the NADPH-dependent reduction of the ribose moiety of (**3**), forming 5-amino-6-(5'-phospho-D-ribitylamino)uracil (**5**). **C:** In fungi (**2**) is first reduced to form 5-diamino-6-(5-phospho-D-ribitylamino)pyrimidin-4(3H)-one (**4**), which is catalyzed by 2,5-diamino-6-(ribosylamino)-4(3H)-pyrimidinone 5'-phosphate reductase. **E:** 2,5-diamino-6-(5-phospho-D-ribitylamino)-pyrimidin-4(3H)-one deaminase then catalyzes the deamination of (**4**), creating (**5**). **F:** (**5**) is dephosphorylated to form amino-6-(1-D-ribitylamino)uracil (**6**), catalyzed by 5-amino-6-(5-phospho-D-ribitylamino)uracil phosphatase. **G:** Condensation of (**6**) and L-3,4-dihydroxybutan-2-one 4-phosphate (**10**) by 6,7-dimethyl-8-ribityllumazine synthase, forms 6,7-dimethyl-8-(D-ribityl)lumazine (**7**). **H:** two equivalents of (**7**) are condensed to form one equivalent of riboflavin (**8**) and one equivalent of (**6**). **I:** 3,4-dihydroxy 2-butanone 4-phosphate synthase catalyzes the formation of (**10**) out of R5P (**9**).

The redox potential or midpoint potential (E_h) of free FAD in watery solutions at pH 7.0 is in the range of -219 mV, going from the oxidized quinone (Fl_{ox}) to the fully reduced hydroquinone state (Fl_{red}).⁷⁰ In enzymes, however, the active site environment can dramatically alter the flavin E_h by electrostatic, H-bonding and hydrophobic effects, as well as through the formation of covalent enzyme–flavin adducts. The redox potentials of enzyme-bound flavins span from $+100$ to -400 mV, an astonishing range of 500 mV.⁷¹ Enzymes can also kinetically and thermodynamically stabilize semiquinone radical states (Fl_{SQ}), thus, catalyze one electron transfers. Kinetic stabilization of semiquinone states occurs when the transition state between Fl_{ox} and Fl_{SQ} is more stabilized by the active site than the transition state between Fl_{SQ} and Fl_{red} . Thermodynamic stabilization occurs when the E_h for the formation of Fl_{SQ} out of Fl_{ox} is far more positive than that for the formation of Fl_{red} out of Fl_{SQ} . Specific wavelengths of light can also mediate the formation of semiquinone flavin states in certain aqueous solutions.⁷² Free Fl_{SQ} is thermodynamically unstable and will disproportionate very rapidly without the stabilization of the active site environment.

The different flavin redox states can be discriminated spectroscopically, as each state has a specific color.⁷³ The distinct UV/visible absorption spectra and fluorescence absorption/emission spectra of each state –with specific A_{max} values– make it possible to determine the exact redox state and the kinetics of its formation. The oxidized quinone form (Fl_{ox}) is bright yellow, with absorption maxima at around 370 and 450 nm. Whereas, the two-electron reduced hydroquinone form (Fl_{red}) has a very weak broad absorption spectrum, both in its anionic (FlH^-) and neutral (N1 -protonated; FlH_2) form, giving it a faint straw-like color. The anionic form seems to be the prevalent protonation state of Fl_{red} in enzymes.⁷⁴ One-electron reduced semiquinone radical states (Fl_{SQ}) are either blue or red, depending on the protonation state of N5. In the case of neutral, N5-protonated, Fl_{SQ} (FlH^\bullet) a characteristic strong absorbance band around 570 nm is observed, giving it a blue color. A strong absorption peak at 370 nm is observed when Fl_{SQ} is in its red anionic N5-deprotonated form ($\text{Fl}^{\bullet-}$). The semiquinone state has a pK_a of 8.3 . It seems that oxidases mainly stabilize the red, anionic semiquinone, while electron transferases mainly stabilize the blue neutral semiquinone over the whole pH range, thus drastically altering the pK_a of Fl_{SQ} .⁷⁵ In addition, some enzymes are capable of stabilizing both protonation states of the semiquinone, showing an observable pK_a value, as is the case for glucose oxidase.⁷³

The kinetically and thermodynamically favorable –and reversible– one- and two-electron transfer reactions over a broad range of redox potentials make enzyme-bound flavins powerful redox catalysts. They are capable of reducing and oxidizing

a great variety of different compounds, and can act as a bridge between obligate two-electron and obligate one-electron redox systems. Flavins are even capable of activating triplet oxygen under physiological conditions.

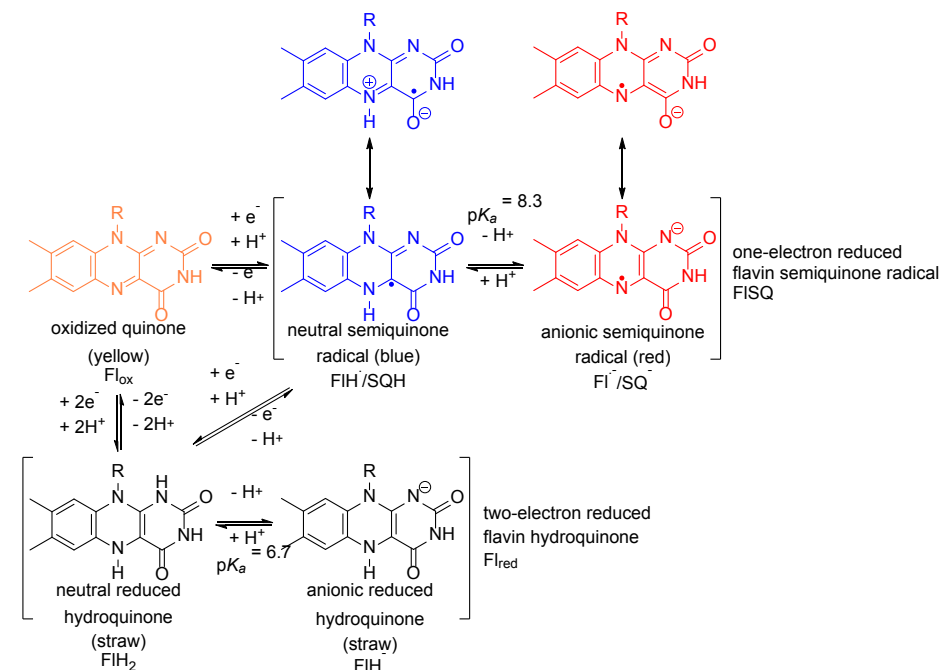


Figure 2.3: Flavin redox states. The 7,8-dimethylisalloxazine ring system can reside in a yellow oxidized quinone state, which can be either two-electron reduced (hydride transfer) or one-electron reduced. The one-electron reduced radical semiquinone states can be stabilized in the enzyme active site as a blue neutral (protonated), or anionic red species. The two-electron reduced hydroquinone state can also exist in a protonated and deprotonated form, both have a faint straw-like color.

2.4 Reductive and oxidative halfreactions

Flavins go through a catalytic cycle which can be dissected into two distinct events: the reductive and (re)oxidative half reactions. See **Figure 2.4A**. In the reductive half reaction the oxidized flavin quinone becomes two-electron reduced by the oxidation of a (co)substrate (event 1 in **Figure 2.4A**). In the (re)oxidate half reaction the two-electron reduced hydroquinone gets reoxidized to the Fl_{ox} ground state.

2.4.1 The reductive halfreaction

Many reductases –including dehydrogenases– and oxygenases use either reduced nicotinamide adenine dinucleotide or reduced nicotinamide adenine dinucleotide phosphate (NAD(P)H) as electron donating cosubstrate.^{69,76} The

electrons are transferred in the form of a direct hydride transfer from C4 of the dihydronicotinamide to the N5 of the flavin, see **Figure 2.4B**.⁷⁷ Oxidized flavins are also readily reduced by direct hydride transfer from α,β -unsaturated carbonyl compounds *in vivo*, as catalyzed by dehydrogenases like butyryl-CoA dehydrogenase and succinate dehydrogenase. Alcohols, amines, aldehydes and lactols in saccharides serve as reducing agents in, for instance, alcohol oxidase, D-aminoacid oxidase and glucose oxidase. These reductive half reactions go through direct hydride transfer or a radical mechanism.^{78–81} In some cases the mechanism of Fl_{ox} reduction involves covalent intermediates at the N5–C4a locus, due to its electrophilic nature. Sulfhydryl (thiol) groups are oxidized to their corresponding disulfides through the formation of a covalent flavin–C4a–sulfide adduct.⁸² Nitroethane, β -chlorolactate and β -chloroalanine are oxidized through a covalent adduct of a carbanion intermediate and the N5 of the isoalloxazine ring system.⁸³

Once the flavin cofactor is reduced it can give its electrons to a broad range of substrates. The most extraordinary of which is molecular oxygen. In the case of reductases an organic substrate gets two-electron reduced, whereas oxidases reduce molecular oxygen with two electrons, forming hydrogen peroxide. Monooxygenases reduce molecular oxygen and then insert an oxygen atom into an organic substrate, producing water as a byproduct. These reactions are shown in **Figure 2.4**.

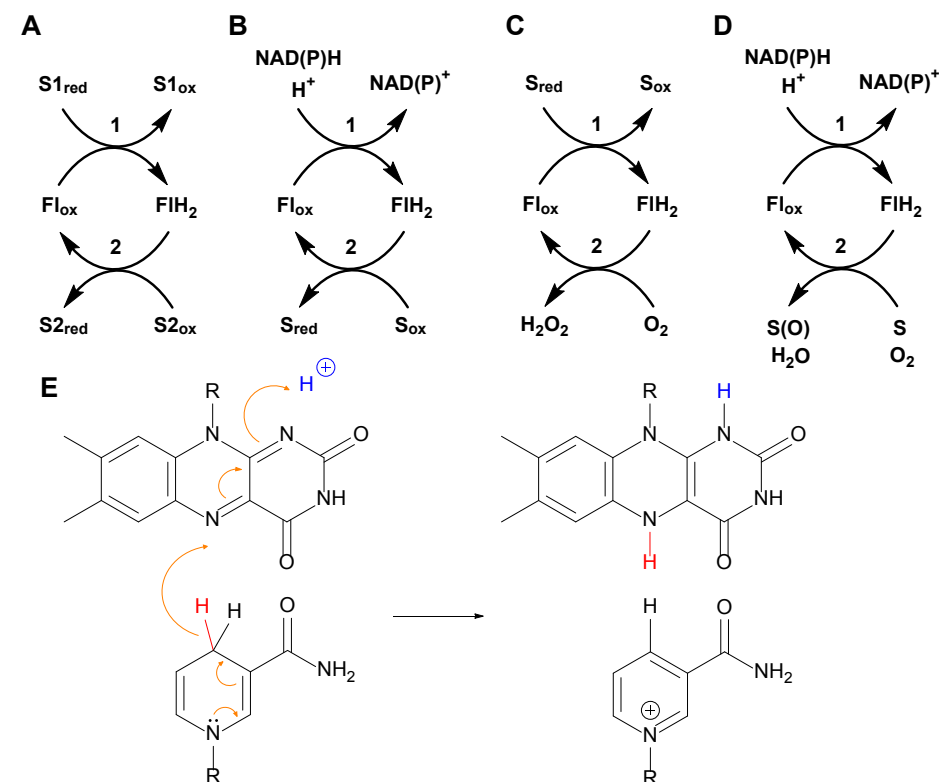


Figure 2.4: Reductive (1) and oxidative half reactions (2) for **A:** general flavoprotein **B:** reductases, **C:** oxidases and **D:** oxygenases. **E:** Reductive half reaction by direct hydride transfer between the C4 of NAD(P)H and N5 of FMN_{ox} or FAD_{ox}, forming NAD(P)^+ and FMNH_2 or FADH_2 . S = substrate.

2.4.2 Oxygen activation and oxygenation

A remarkable feature of flavins is that these organic cofactors can activate molecular oxygen in its triplet state under physiological conditions. The two-electron reduced flavin hydroquinone can react with molecular oxygen in several ways, forming H_2O_2 , $\text{O}_2^{\bullet-}$ or water and an oxygenated substrate. A direct two-electron transfer between singlet reduced flavin and triplet oxygen is spin forbidden, thus cannot happen. Therefore, first step in this reaction is the one-electron transfer from the reduced flavin to triplet molecular oxygen, forming a caged radical pair. Spin inversion (inter system crossing) of the initially formed radical pair will form an open shell singlet radical pair (arrow B in **Figure 2.5**). This radical pair can now form a C4a-peroxyflavin adduct, which can be protonated to form a C4a-hydroperoxy adduct.^{84–86} This is depicted by reaction D and compounds 3 and 4 in **Figure 2.5**, respectively. In the case of *p*-hydroxyphenylacetate 3-hydroxylase (HPAH) and pyranose 2-oxidase (P2O) the initial electron transfer between reduced flavin and oxygen is coupled with a simultaneous proton transfer to oxygen, and a second electron transfer step

forms C4a-hydroperoxy flavin directly.^{87,88} Apart from P2O, all known oxidases are believed to produce hydrogen peroxide by a second electron transfer reaction from the semiquinone radical flavin to super oxide, without forming the C4a-peroxy adduct.^{84,87} This is depicted as arrow C in **Figure 2.5**. The C4a-peroxy flavin and C4a-hydroperoxy flavin can oxygenate substrates through a nucleophilic or electrophilic mechanism, respectively, as depicted by arrows E1 and E2 in **Figure 2.5**.^{53,84} These reactions form a C4a-hydroxy flavin adduct (compound 5 in **Figure 2.5**), which then undergoes heterolytic fission, consequently forming oxidized flavin and water.

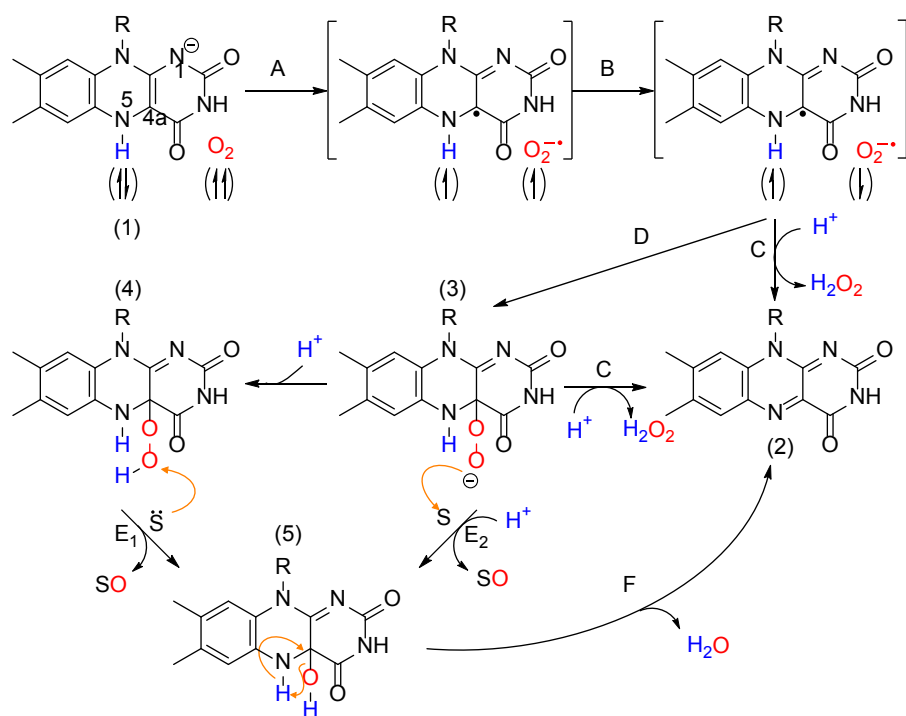


Figure 2.5: The canonical reactions of reduced flavin with molecular oxygen at the C4a locus.

2.5 Covalently bound flavin cofactors

Cofactors can be transiently or permanently bound to enzymes. Coenzymes or cosubstrates are only temporarily bound to the enzyme during a catalytic cycle, as is normally the case for coenzyme A, coenzyme Q and nicotinamides. On the other hand, prosthetic groups are tightly and permanently bound to the enzyme, and may only dissociate upon enzyme denaturation. Examples are metal ions, heme groups, iron-sulfur clusters, thiamine pyrophosphate (TPP), pyridoxal phosphate (TPP) and biotin. In some cases the nicotinamide cofactors can also serve as a prosthetic group.⁸⁹

Most of these cofactors are tightly but not covalently bound to the enzyme. Some prosthetic groups, however, are actually covalently linked to the polypeptide, as is the case for lysine bound biotin and lipoic acid, which enables these cofactors to ‘swing’ in between different active sites of an enzyme complex.⁹⁰ Other covalently bound cofactors are formed *in situ* out of amino acid side chains, like topaquinone and analogous cofactors.^{91–93} FMN and FAD are special in the sense that these cofactors can both serve as coenzyme and prosthetic group, and as a prosthetic group they can either be covalently or noncovalently attached to the enzyme. In fact, hemes and flavins are the only cofactors which can be found as both covalently and non-covalently bound prosthetic groups. It is estimated that about 10% of the flavoproteins contain a covalently bound flavin.⁹⁴

2.5.1 Types and occurrence of covalent protein–flavin bonds

The first covalent flavoprotein, succinate dehydrogenase, was identified in 1955, and later experimental work revealed that it contained 8 α -N³-histidyl-FAD.^{95,96} Thus far, seven additional covalent flavin–enzyme linkages have been identified after this discovery. Covalent bonds can be formed between histidine, cysteine, tyrosine, aspartate, and the C8a and C6 position of the isoalloxazine ring system or between the 5'-phosphoryl group of FMN and a threonine residue, and the resulting linkages found in nature are 8 α -N¹-histidyl-FAD/FMN, 8 α -N³-histidyl-FAD/FMN, 8 α -S-cysteinyl-FAD/FMN, 8 α -O-tyrosyl-FAD, 8 α -O-aspartyl-FAD, 6-S-cysteinyl-FMN and phosphoester-threonyl-FMN, respectively (see **Figure 2.6**).^{94,97,98} In some cases, FAD is linked to the protein via two covalent bonds. The bicovalent 8 α -N¹-histidyl-6-S-cysteinyl-FAD is found in several enzymes, among which are gluco-oligosaccharide oxidase (GOOX), aclacinomycin oxidoreductase, berberine bridge enzyme (BBE), cannabidiolic acid synthase, hexose oxidase, and chito-oligosaccharide oxidase (ChitO).^{99–104} The 8 α -N-histidyl-FAD linkage is the most abundant form, found in a large array of proteins. This type of linkage is especially prevalent in enzymes that belong to the vanillyl alcohol oxidase (VAO) family. In fact, studies on the VOA family in the genome database predict that one in four proteins contains a covalent FAD, due to the presence of a conserved active site histidine.^{105,106} Apart from the 8 α -N¹-histidyl-FAD and 8 α -N³-histidyl-FAD linkages, some VOA members also contain 8 α -N¹-histidyl-6-S-cysteinyl-FAD and 8 α -O-tyrosyl-FAD. Another large protein family, the glucose oxidase/methanol oxidase/cholesterol oxidase family (GMC), contains far less members with a covalently bound flavin cofactor. This suggests that the fold type of the enzyme might be important for promoting covalent flavin–protein bonds. Strikingly, the residues in the VAO family that form the covalent bond between the polypeptide and C8a of FAD are not fully conserved. The histidine residue which is responsible for 8 α -N¹-histidyl-FAD bond is found near

the N-terminus, which is part of the FAD binding domain, whereas the histidine responsible for the 8α -N³-histidyl-FAD is found in different positions on the cap domain, the same holds for the tyrosine that forms 8α -O-tyrosyl-FAD. No consensus sequence for covalent flavin incorporation has been identified. In fact, most binding motifs in covalent flavoproteins are similar to their noncovalent counterparts.^{94,97}

The 8α - and 6-S-cysteinyll bound flavins are less widespread than the 8α -N-histidyl bound flavins, moreover the 8α -O-tyrosyl-FAD, 8α -O-aspartyl-FAD and phosphoester threonyl FMN are thus far only identified in isolated cases. Histidyl-FAD/FMN and 8α -S-cysteinyll-FAD are found in all domains of life, whereas all the other bond types have only been identified in bacterial proteins. Extensively studied proteins containing 8α -S-cysteinyll-FAD are monoamine oxidase (MAO) and bacterial monomeric sarcosine oxidase (MSOX)^{107,108} and a well-studied example of an 6-S-cysteinyll-FMN containing enzyme is trimethylamine dehydrogenase (TMADH).^{109,110} 8α -O-tyrosyl-FAD, 8α -O-aspartyl-FAD and phosphoester threonyl FMN are found in *p*-cresol methyl hydroxylase (PCMH),^{111,112} chloramphenicol halogenase¹¹³ and the NprB/C subunits of a Na⁺-translocating NADH:quinone reductase,^{114,115} respectively.

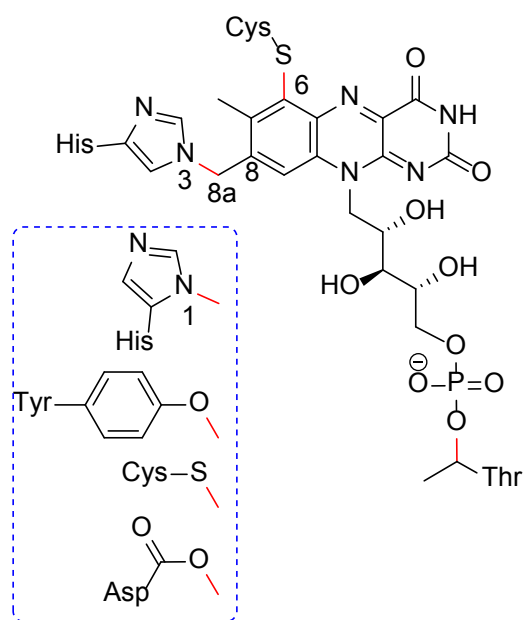


Figure 2.6: Identified covalent flavin–protein linkages. 8α -N¹-histidyl-FAD/FMN, 8α -N³-histidyl-FAD/FMN, 8α -S-cysteinyll-FAD/FMN, 8α -O-tyrosyl-FAD, 8α -O-aspartyl-FAD, 6-S-cysteinyll-FMN, 8α -N¹-histidyl-6-S-cysteinyll-FAD and phosphoester-threonyll-FMN.

2.5.2 The mechanisms of protein–flavin bond formation

A wealth of structural and biochemical data on covalently bound flavins has led to a consensus on the general mechanisms of covalent flavinylation at the isoalloxazine ring system. The formation of a covalent bond between the protein and the C8a and C6 positions was long believed to be a fully autocatalytic post-translational process, but recent studies have shown that covalent tethering at the 8-methyl group might be assisted by a small helper protein in some cases.

2.5.2.1 Formation of the protein–flavin bond at the C8a position

The proposed general mechanism for the autocatalytic formation of a covalent bond between the C8a of the isoalloxazine ring system and the nucleophilic side chain of tyrosine, cysteine, aspartate and histidine is shown in **Figure 2.7**, as was first proposed by Walsh.⁷⁶ The first step in this mechanism is the deprotonation of the 8a-methyl group by an active site base, forming an iminoquinone methide intermediate. This intermediate was first discovered by Bullock and Jardetzky in high temperature deuterium exchange NMR experiments,¹¹⁶ and was later also found in biomimetic 8a-functionalization studies of 2',3',4',5'-tetraisobutyrylriboflavin with morpholine and imidazole, using base catalysis.¹¹⁷ The nucleophilic amino acid residue then performs a nucleophilic attack on the C8a-position, accompanied by a concerted protonation of N5, creating a covalent adduct between the protein and reduced flavin hydroquinone. Oxidation of the hydroquinone results in the oxidized 8α -peptidyl–flavin resting state. The formation of the reduced flavin intermediate was observed when the apo-form of bacterial monomeric sarcosine oxidase (MSOX), expressed and purified from a riboflavin auxotrophic *Escherichia coli* strain, was reconstituted with FAD *in vitro*. This aerobic reconstitution process, forming 8α -S-cysteinyll-FAD, produced a stoichiometric amount of hydrogen peroxide with apparent second order kinetics, which suggests an autocatalytic process.¹⁰⁸ The same experiments were conducted for vanillyl alcohol oxidase, showing the same results.¹¹⁸ The formation of reduced and quinone methide intermediates, and the production of stoichiometric amounts of hydrogen peroxide *in vitro* show that this is an autocatalytic process. Autocatalytic 8-S-cysteinyll–flavin formation was also seen for the A394C mutant of putrescine oxidase from *Rhodococcus erythropolis* NCIMB 11540. This enzyme normally binds FAD noncovalently as a prosthetic group, but the introduced cysteine, that faces the C8a position of FAD, can actually form a covalent bond.¹¹⁹

Replacement of FAD by 1-deaza and 5-deaza analogues does not lead to covalent bond formation in MSOX, as well as in *p*-cresol methyl hydroxylase (PCMH) and 6-hydroxy-D-nicotine oxidase (6-HDNO),¹²⁰ as can be explained by the lower redox

potentials and lower electrophilicity, making the 8 α -protons less acidic. Some flavin analogues with redox potentials higher than 5-deaza FAD were shown to covalently bind PCMH.¹²¹

In some cases, covalent flavinylation might need some stabilizing factors, like helper proteins. PCMH is a $\alpha_2\beta_2$ tetramer, containing two flavoprotein α -subunits (PchF) and two c-type cytochrome β -subunits (PchC), and can only form a covalent 8 α -O-tyrosyl-FAD bond when the full complex is formed. Apo-PchF can be noncovalently reconstituted with FAD, but the cofactor and the enzyme are only covalently linked in the presence of PchC. Binding of PchC to holo PchF causes a conformational change that leads to the covalent bond formation. The reduced flavin that is formed in this process in turn reduces the cytochrome, which also happens in its normal catalytic scheme.^{122,123} The autocatalytic formation of the histidyl- N^1 -FAD bond in purified 6-HDNO needs the presence of additives like glycerol-3-phosphate *in vitro*.^{120,124} For PCMH one could still argue that covalent bond formation is fully autocatalytic, as the whole tetramer that is needed for the 8 α -O-tyrosyl-FAD bond formation is also necessary to form a normal catalytically active unit. And for 6-HDNO one could say the same, as these small molecules naturally occur in living cells and do not directly contribute to the catalytic process.

Studies on human succinate dehydrogenase, however, have suggested that a small ~10 kDa protein, SdhAF2, is needed as an assembly factor for the formation of the covalent flavin-protein bond.¹²⁵ This factor has homologues in all kingdoms of life, like Sdh5 in yeast and SdhE in bacteria.¹²⁶ Structural, biochemical and mutagenesis experiments on SdhE and Sdh5 have shown that this protein has a conserved motive for binding succinate dehydrogenase and quinol:fumarate reductase (RGXXE) and does not bind FAD itself.¹²⁷⁻¹²⁹ Moreover, circular dichroism studies show that these flavoproteins are already completely folded and contain FAD before treatment with SdhE. Therefore, it is believed to stabilize the protein in a locked active site conformation, promoting autocatalysis.^{130,131} The lack of SdhE homologues in some extreme thermophiles, containing succinate dehydrogenases that share high homology with their mesophilic counterparts, agrees with this hypothesis.¹³²

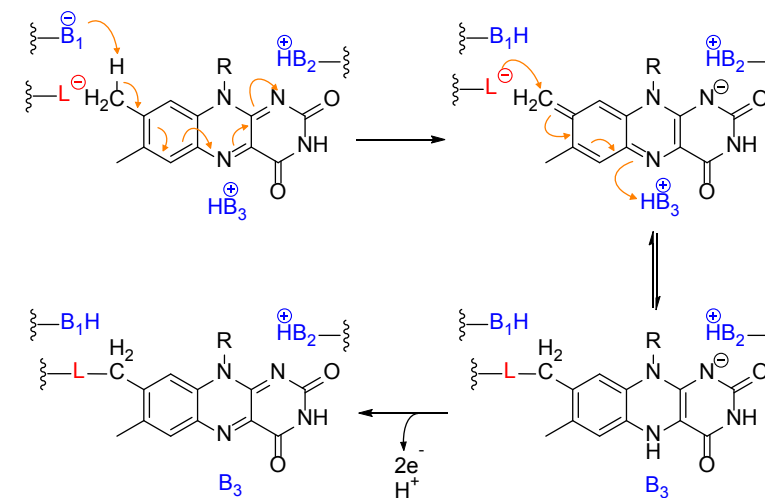


Figure 2.7: Proposed mechanism for the formation of a covalent flavin-enzyme bond at the C8a position of the isoalloxazine ring system. B1, B2 and B3 are active site bases and L- is the nucleophilic side chain of tyrosine, histidine, cysteine or aspartate. B3 might be an amino acyl side chain or an acidic water molecule. The formed product can be 8 α -N1-histidinyl-flavin, 8 α -N3-histidinyl-flavin, 8 α -S-cysteinyl-flavin, 8 α -O-tyrosyl-flavin or 8 α -O-aspartyl-flavin. Adapted from Heuts et al.⁹⁴

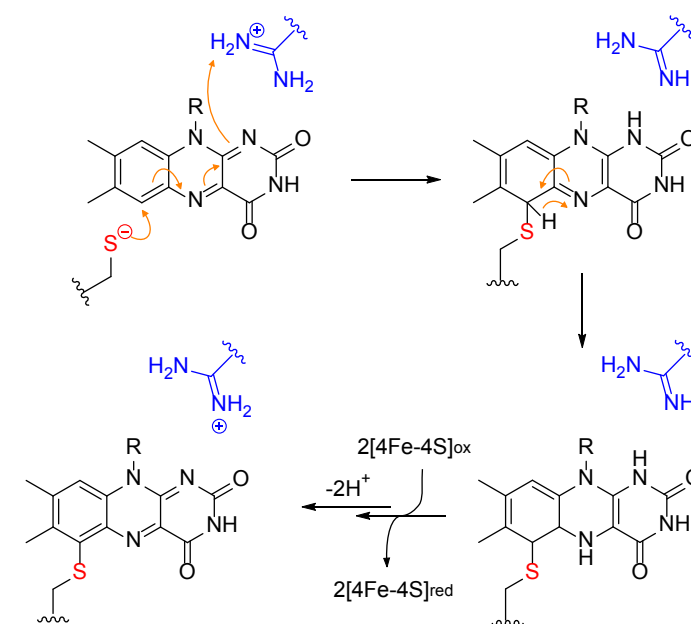


Figure 2.8: Proposed mechanism for the formation of 6-S-cysteinyl-FMN. The cysteinyl thiolate anion attacks C6 of the isoalloxazine ring system. The positively charged arginine (blue) assists by stabilizing the negative charge on N1. Picture adapted from Scrutton et al.¹⁰⁹

2.5.2.2 Formation of the 6-S-cysteinyl–flavin bond

The formation of the 6-S-cysteinyl–FMN bond in trimethyl amine dehydrogenase (TMADH) is believed to happen autocatalytically by nucleophilic attack of the Cys30-thiolate anion on the C6 position. Tautomeric re-aromatization creates a reduced 6-S-cysteinyl–FMN intermediate. This hydroquinone then donates electrons to a nearby [4Fe–4S] cluster by two consecutive 1-electron transfer reactions, forming the oxidized 6-S-cysteinyl–flavin ground state.¹⁰⁹ See **Figure 2.8**.

2.5.2.3 Formation of the phosphoester threonyl-FMN bond

Unlike covalent bond formation at the isoalloxazine ring system, phosphoester threonyl-FMN bond formation is non-autocatalytic and needs assistance from a FMN transferase that incorporates FMN into the polypeptide. When the phosphoester threonyl-FMN containing Na⁺-translocating NADH:quinone oxidoreductase (Na⁺-NQR) from *Vibrio cholera* was heterologously expressed in *E. coli*, no flavin incorporation was seen.¹³³ This led to the discovery of a ‘chaperone’ protein, ApbE, through bioinformatic analysis of the genomes of all *nqr* operon-containing bacteria. AphE was later renamed as Ftp (flavin trafficking protein). Co-expression of the *V. harveyi* NqrC (a subunit of Na⁺-NQR) and ApbE (Ftp) genes in *E. coli* resulted in the production of a covalently flavinylated NqrC, and also *in vitro* covalent flavinylation was seen when incubating FAD, ApbE and NqrC in one pot.¹³⁴ A homologue of ApbE (Ftp) from *Treponema pallidum* (Ftp_Tp) was shown to have metal-dependent FAD pyrophosphatase activity, hydrolyzing FAD into AMP and FMN, as well as flavin-transferase activity. Mutating the active site residue asparagine-55 to tyrosine changed its activity to a FAD binding protein. And mutating the metal binding aspartate-284 to an alanine abolished catalytic activity.¹³⁵ The same loss of activity was seen for ApbE when it was incubated with EDTA.¹³⁴ Crystal structures of *S. enterica* and *T. pallidum* ApbE indeed showed that these enzymes can bind FAD.^{135,136} This led to the conclusion that FtPs are not just chaperones, but are enzymes that catalyze the formation of the phosphoester threonyl-FMN bond. A consensus sequence for the covalent targeting was identified as: DgxtsAT/S, in which T/S is the residue that is covalently modified.¹³⁷ A conserved histidine, which is in close proximity to the FAD pyrophosphate in Ftp proteins, is believed to activate threonine or serine as a nucleophile for flavin transfer, or acts as a general acid to activate AMP as a leaving group. Mutagenesis studies indeed showed that this histidine is essential for catalysis.¹³⁵ Furthermore, it is also believed that a lysine (Lys-211) in Na⁺-NQR is involved in activating the threonine or serine as nucleophile by polarization. A possible mechanism is shown in **Figure 2.9**.

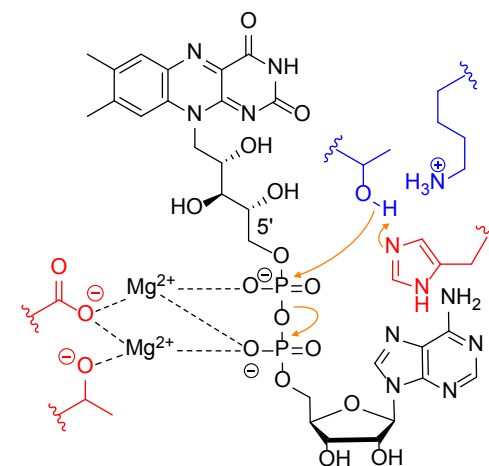


Figure 2.9: Phosphoester threonyl-FMN bond formation. Residues in red are from AphE/Ftp and residues in blue are from Na⁺-NQR. Adapted from Fang et al.¹³⁸

2.5.3 The function of covalent flavinylation

Covalent flavinylation can serve different purposes in enzymes. Studies on enzymes with covalently bound flavins suggest a number of roles, namely increasing the redox potential, structural integrity, holoenzyme lifetime, flavin and substrate orientation, and flavin reactivity.

2.5.3.1 Redox potential

The protein environment can alter the redox potential (midpoint potential, E_h or E_m) of flavins by noncovalent interactions,^{139,140} but not as drastically as compared to covalent modifications. Substitutions at position 7 and 8 of the isoalloxazine system (ortho and para to N5) with electron withdrawing and donating substituents have a dramatic effect on the redox potential, and the correlation follows a linear Hammett relationship.¹⁴¹ Mutagenesis studies on several enzymes with flavins tethered to the polypeptide chain through C8a showed that these enzymes have a higher redox potential than their noncovalent counterparts. The same is observed at the C6 position. The high redox potential of covalent flavoenzymes, which is in many cases above 0, results in a very limited array of electron acceptors. Therefore, most of these enzymes are indeed oxidases, using dioxygen as electron acceptor. A drastic drop in redox potential from +55 mV to –65 mV and an accompanying 10-fold decrease in catalytic activity was seen for vanillyl alcohol oxidase (VAO) when the His-422, responsible for the covalent FAD linkage, was replaced by an alanine. The structure and protein stability, however, seem not to be affected by this mutation, suggesting that covalent flavinylation is purely influencing the redox potential in these enzymes.^{142,143} A similar trend was seen for PCMH when the covalent anchoring point Tyr-384 was mutated

to a phenylalanine. This mutation prevented covalent binding and resulted in a drop in redox potential (from +84–93 mV to +34–48 mV) and an astonishing drop in k_{cat} (from 121 s⁻¹ to 3.8 s⁻¹), whereas the K_m remained virtually unchanged.^{121,144} The same effects were also seen in studies on cholesterol oxidase type II (CholO), where drastic drops in turnover numbers and redox potential were seen and no deviations in crystal structures.^{145,146} Changes in turnover number can be correlated to a decrease in the flavin reduction rate when the redox potential is lowered.

Bicovalent attachment at both C8a and C6 results in an even higher redox potential, as is seen in *E. coli* reticuline oxidase, GOOX and ChitO.^{147,148} Breaking either covalent attachment results in a decrease in reduction rate and decrease in redox potential. So, both covalent anchoring events contribute to the elevation in redox potential.

2.5.3.2 Structural integrity and holoenzyme lifetime

Covalent flavinylation increases the redox potential and therefore also influences the reduction rate and the electron acceptor scope, but it can also affect the stability and substrate scope in some cases. A clear effect on the substrate scope and holoenzyme lifetime is seen in enzymes with a bicovalently anchored flavin, which have a very open active site that allows the conversion of bulky substrates and polymers, without loss of the cofactor.^{101,148} Removal of the C6-cysteinyl bond in ChitO influences the redox potential, as was discussed in section 1.5.3.1, but also influences the K_m of the substrate, indicating that this bond is also important for the correct positioning of FAD in the active site for Michaelis complex formation with the substrate. A similar effect is seen for MSOX.¹⁴⁹ ChitO mutants with only one covalent attachment tend to be less stable and aggregate over time. Moreover, mutants with none of the covalent linkages hardly express at all, which shows the stabilizing effects these attachments have on the protein.¹⁴⁸ Lower stability is also seen for CholO and 6-HDNO.^{120,150}

2.6 Naturally occurring riboflavin analogues and modified flavins – roles and occurrence

Several flavin analogues have been identified over the last couple of decades. These analogues are made by variations in biosynthesis or by enzyme-mediated modifications of FMN or FAD. Some are modified in such a way that they are better catalysts for the job than the standard riboflavin derivatives FMN and FAD (see **Figure 2.1**), but others are believed to be artifacts of faulty catalysis.

2.6.1 6-Hydroxy and 7-methyl-8-hydroxyflavins

6-Hydroxyflavin mononucleotide (6-hydroxyFMN; **Figure 2.10A**) is one of these cases where a flaw in the catalytic mechanism results in an inactive flavin derivative. It

was discovered in two mutants of trimethylamine dehydrogenase from *Methylophilus methylotrophus* (sp. W₃A₁). Active site mutants W355L and C30A – which is normally responsible for a C6-cysteinyl flavin–protein bond – showed substrate induced and substrate independent formation of this compound, respectively, which severely reduced the oxidative demethylation activity.⁹⁷ Wild type enzyme seemed to also produce 6-hydroxyFMN, but in much lower quantities. This is yet another advantage of covalent flavinylation: controlling the reactivity of the bound flavin.

At first it was thought to be conceived by hydration of the electrophilic iminoquinone methide, which is the intermediate responsible for C8a and C6 covalent flavin–protein bonds, but a later isotope labeling study found that the 6-hydroxyl group was derived from molecular oxygen.¹⁵¹

Also 6-hydroxy modified FAD and FMN analogues were detected in an electron-transferring flavoprotein (ETF) from *Peptostreptococcus elsdenii* and glycolate oxidase from pig liver, respectively. These were serendipitous discoveries, due to the peculiar green color of these compounds at pH 9.¹⁵² The reason for the existence of these compounds and a possible function in these enzyme systems was never found.

Not long after the discovery of 6-hydroxyFAD in *P. elsdenii* FTR, the orange 7-methyl-8-hydroxyFAD was isolated from the same organisms as a prosthetic group of a NADH dehydrogenase.¹⁵³ The enzymes with this cofactor were actually not active, and therefore it was thought that both newly identified cofactors in *P. elsdenii* were artifacts that were somehow created in the purification process.

2.6.2 6-(3'-(R)-Myristyl)flavin mononucleotide

6-(3'-(R)-myristyl)flavin mononucleotide (MyrFMN or Myristylated FMN; **Figure 2.10B**) is another covalently modified FMN, which is also believed to be an artifact of a faulty enzyme-mediated chemical reaction. It was found in bioluminescent bacteria in several genera, like *Photobacteria*, *Aliivibrio* and *Vibrio* that use the FMN-dependent bacterial luciferase,^{154,155} and a direct correlation between light production and MyrFMN production was seen. Bacterial luciferase catalyzes the oxidation of long chain aldehydes to long chain fatty acids, like myristic acid (tetradecanoic acid), through a chemically-induced electron exchange luminescence (CIEEL) mechanism, which produces a short-lived excited state of FMN.¹⁵⁶ It is thought that rearrangement of the alkoxy radical to a carbon radical results in the covalent attachment of myristic acid to FMN.¹⁵⁵ Luciferase is strongly inhibited by MyrFMN,^{157,158} and a gene product from *LuxF*, a homologue to the β -subunit of luciferase, is believed to be a scavenger for MyrFMN,¹⁵⁵ and co-expression greatly enhances light production.

2.6.3 Chizoflavins

Two riboflavin derivatives, coined chizoflavins, were isolated in the culture broth of *Schizophyllum commune*, which had the 5'-hydroxyl group oxidized to an aldehyde or carboxylic acid functionality, yielding 7,8-dimethyl-10-(2,3,4-trihydroxy-4-formylbutyl)isoalloxazine and 7,8-dimethyl-10-(2,3,4-trihydroxy-4-carboxybutyl)isoalloxazine, respectively,^{159,160} see **Figure 2.10C** and **D**. An NADPH-dependent enzyme was later identified as the 5'-aldehyde forming enzyme.¹⁶¹ Thus far, no physiological role has been assigned to these chizoflavins.

2.6.4 7-Hydroxymethyl and 8-hydroxymethyl riboflavin

Nekoflavin (**Figure 2.10E**) was discovered in cat choroids as a pigment molecule.¹⁶² This compound was later identified as 7 α -hydroxymethyl riboflavin.¹⁶² Both nekoflavin and 8 α -hydroxymethyl riboflavin are found in human and rat urine, and may be pigments necessary for vision. 7-Carboxy and 8-carboxy lumichrome, also both found in milk, are probably degradation products of these compounds (**Figure 2.10H**). Hydroxymethyl flavin, shown in **Figure 2.10G**, is also found in urine as a degradation product of riboflavin, which is probably produced by symbiotic bacteria in the urinal tract.¹⁶³

2.6.5 Plant root iron uptake cofactors

Some plants excrete reduced riboflavin and riboflavin analogues that contain either a 3' or 5'-sulfate group from their roots upon iron starvation, as was seen for sugar beet.¹⁶⁴ It is hypothesized that reduced flavin is used to reduce iron(III) to iron(II) and the riboflavin sulfates are then used for iron uptake. See **Figure 2.10F**.

2.6.6 Roseoflavin –an antimicrobial flavin analogue

Roseoflavin, 8-dimethylamino-8-demethyl-D-riboflavin (RoF), see **Figure 2.10J**, was originally isolated from *Streptomyces davawensis* in 1974 and was found to have antimicrobial properties.¹⁶⁵ RoF is especially active against Gram-positive bacteria, and has a minimal inhibitory concentration (MIC) of 1.56 $\mu\text{g}/\text{mL}$ for *Bacillus subtilis* and 0.25–6.25 $\mu\text{g}/\text{mL}$ for *Staphylococcus aureus*.^{165,166}

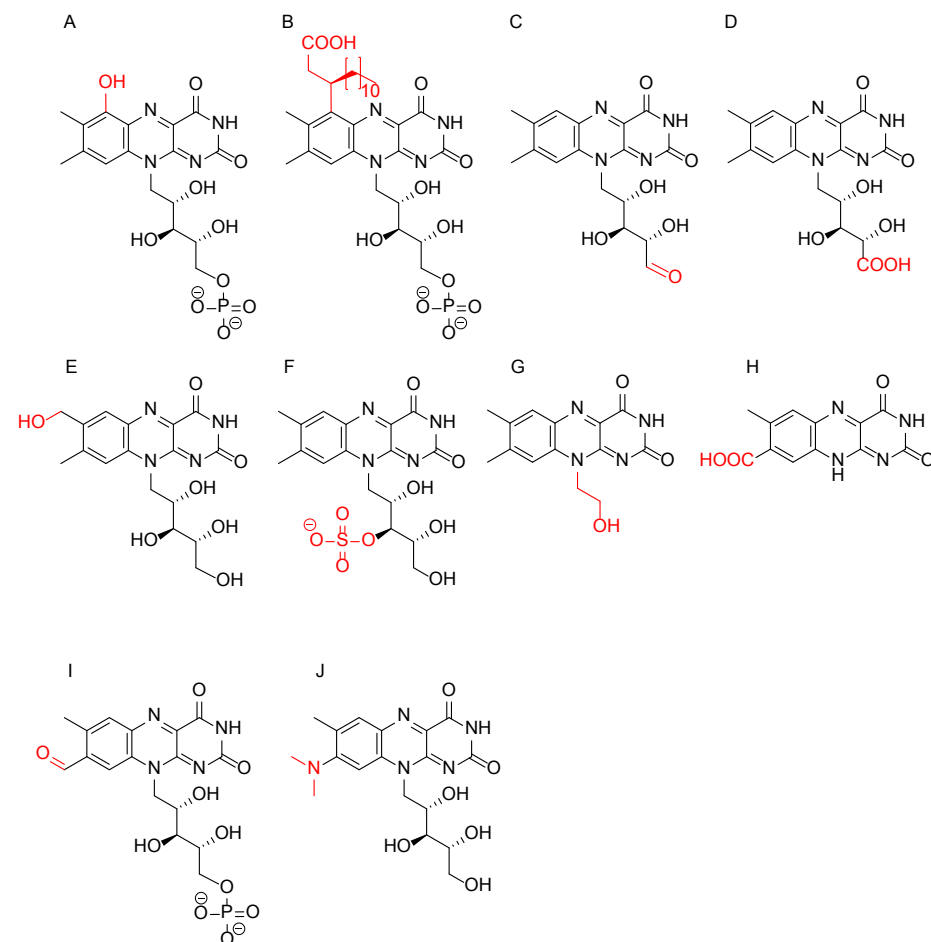


Figure 2.10: Structures of natural modified flavins. **A:** 6-hydroxyFMN, **B:** 6-(3'-(R)-myristyl)FMN, **C:** 7,8-dimethyl-10-(2,3,4-trihydroxy-4-formylbutyl)isoalloxazine (a chizoflavin), **D:** 7,8-dimethyl-10-(2,3,4-trihydroxy-4-carboxybutyl)isoalloxazine (a chizoflavin), **E:** Nekoflavin; 7 α -hydroxymethyl riboflavin, **F:** riboflavin-3'-sulfate, **G:** 10-hydroxymethyl-7,8-dimethylisoalloxazine (hydroxymethyl flavin), **H:** 8-carboxy lumichrome, **I:** 8-formylFMN, **J:** roseoflavin.

Although the exact nature of the antimicrobial effect is not well understood, it is postulated that roseoflavin inhibits FMN- and FAD-dependent enzymes as a competitive inhibitor, after being converted to roseoflavin-5'-phosphate and roseoflavin adenine dinucleotide.^{167–170} Another possible mode of action is the binding of roseoflavin in FMN-dependent riboswitches that control the expression of the riboflavin biosynthesis machinery.¹⁷¹

RoF is synthesized from FMN in several steps by 3 enzymes. The first enzyme, RosB, oxygenates FMN on the 8a-position to form 8-formyl-FMN, which is then further oxidized to 8-demethyl-8-carboxylFMN and then a thiamine-dependent decarboxylation/glutamate-dependent amination results in 8-demethyl-8-aminoriboflavin-5'-phosphate (AFP). RosB is a flavodoxin-like enzyme, composed of four subunits, which has evolved from an electron- or hydride-transferring flavoprotein to a 'FMN 8-aminase'.^{172,173} AFP is subsequently dephosphorylated to form 8-amino-8-demethyl-D-riboflavin (AF).¹⁷⁴ And AF is then subjected to two S-adenosyl methionine-dependent N-methylations, catalyzed by 8-Amino-8-demethyl-D-riboflavin dimethyltransferase (RosA), to form roseoflavin.¹⁷⁵

2.6.7 8-Formyl flavins

Formyl flavin analogues were reported three times in the last twenty years. A mutagenesis study on two strictly conserved active site arginines in a FMN-dependent lactate oxidase from *Aerococcus viridans* showed the slow formation of so-called 8-formylFMN (8-demethyl-8-formylFMN).¹⁷⁶ Its structure is shown in **Figure 2.10I**. In another study, 8-formylFAD (8-fFAD) was found in wild type formate oxidase from *Aspergillus oryzae*. This enzyme seems to slowly and autocatalytically produce 8-fFAD after reconstitution of the apoenzyme with FAD, which makes the enzyme 10-fold more active.¹⁷⁷ An rationale for the increasing activity would be the increase in redox potential due to the electron-withdrawing group on the 8-position, as is also the case for flavins covalently attached to the polypeptide. It is actually thought that the 8-formyl group is formed through the same mechanism as covalent protein-flavin formation, involving the quinone-methide tautomer, which is hydrated to form the 8-fFAD product. Substitution of lysine-87, which is believed to act as a base in this mechanism, with an alanine prohibited the formation of 8-fFAD, thus strengthens this suggested mechanism.¹⁷⁷

8-fFAD was also discovered in the heterodimeric human electron transferring flavoprotein (hETF).¹⁷⁸ This enzyme is responsible for the transfer of electrons from at least thirteen different flavin-dependent dehydrogenases to the mitochondrial respiratory chain through a non-covalently bound FAD cofactor. This non-covalently bound FAD cofactor undergoes the same time-dependent 8-formyl formation in the active site as was shown for formate oxidase, and seems to be pH dependent. Higher pH values promote 8-fFAD formation. The 8-fFAD cofactor in hETF seemed to reside in the semiquinonic state for longer period than is seen for FAD, which slightly lowered the observed rates. But, surprisingly, the 8-fFAD containing hETF had a 5-fold enhanced affinity to human dimethylglycine dehydrogenase, which shows that 8-fFAD must modulate the binding affinity somehow. Furthermore, it

was shown that two mutations that prohibit the formation of 8-fFAD are a cause of glutaric aciduria type II, a rare genetic metabolic disease.¹⁷⁸ Thus, formation of this 8-formylFAD compound results in better enzyme activities and the absence of it can even result in a life-threatening chronic disease.

2.6.8 Prenyl-FMN

Another recent discovery of a highly modified flavin was done while investigating a decarboxylase in the ubiquinone biosynthesis pathway of fungi and bacteria. Biochemical and crystallographic studies on *Aspergillus niger* FdcI and the *E. coli* homologue UbiD have detected a prenylated FMN in their active sites.^{179,180} The prenylated FMN, prenyl-FMN (prFMN), is provided by a FMN-prenyl transferase, which is UbiX in *E. coli* and Pad1 in *A. niger*. The substrate for the transferase is dimethylallyl-monophosphate and is initially linked to N5 by nucleophilic attack of the nitrogen atom on C1', releasing phosphate through nucleophile displacement. The active site then assists in a conformational change of the olefin adduct through the formation of carbocation species, which then promotes the formation of the C6-C3' dimethylallyl bond,¹⁸¹ see **Figure 2.11A**. After the formation of holo-UbiD/FdcI the reduced prenyl-FMN undergoes oxidative maturation, most probably through proton-coupled electron transfer.¹⁷⁹ Oxidized prenyl-FMN has an azomethine ylide character, and two isomeric forms – a secondary N5-ketamine and a N5-iminium adduct – have been observed in the crystal structure of FdcI, with very different ring structures. The hexameric holoenzyme catalyzes the reversible decarboxylation of cinnamic acid *in vitro*, which is placed directly on top of the azomethine ylide. The substrate and cofactor undergo a 1,3-dipolar cycloaddition – the first to be described in nature – and the formed substrate-prFMN^{iminium} pyrrolidine adduct is then decarboxylated through a Grob-type fragmentation reaction. A second prFMN^{iminium} pyrrolidine adduct is then formed, upon protonation of C2', which results in product (styrene) release through a *retro*1,3-cycloaddition,¹⁸⁰ see **Figure 2.11B**. The stabilized iminium adduct of prFMN is the first discovered modification that facilitates noncanonical flavin chemistry, as it enables covalent 1,3-cycloaddition catalysis – something not seen before in nature.

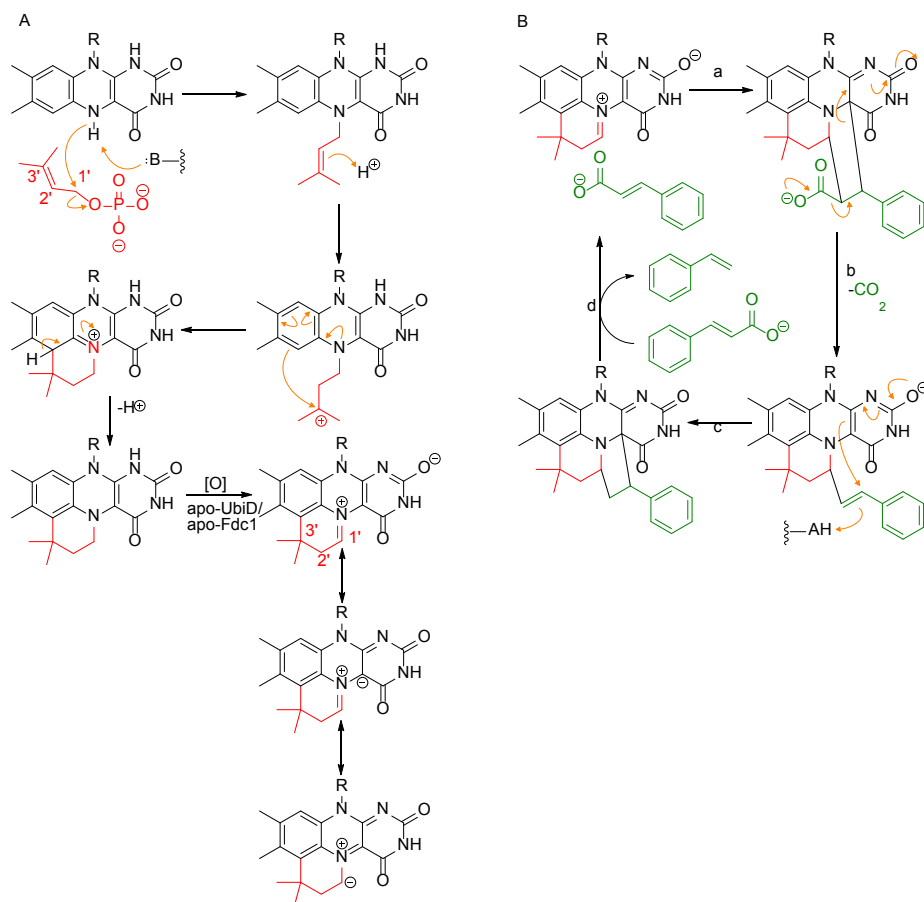


Figure 2.11: Prenyl-FMN formation and UbiD/Fdc1 decarboxylase activity. **A:** the UbiX/Pad1 catalyzed formation of prenyl-FMN and oxidative maturation in UbiD/Fdc1. **B:** Catalytic cycle of UbiD/Fdc1 with cinnamic acid. a.) formation of substrate-prFMNiminium pyrrolidine adduct through a 1,3-dipolar cycloaddition, b.) Grob-type fragmentative decarboxylation, c.) intermediate-prFMNiminium pyrrolidine adduct formation and protonation, d.) product release by retro1,3-dipolar cycloaddition. Adapted from Marshal et al.¹⁸² and Payne et al.¹⁸⁰

2.6.9 Artificial cofactors and novel catalytic activity

Artificial flavin analogues have been used extensively as active site probes for the elucidation of flavoenzyme mechanisms and flavin chemistry.^{75,141,183–185} Artificial flavins have also been successfully introduced as a means to create or change enzyme activity. The dehalogenase activity of iodotyrosine deiodinase could be changed to nitroreductase activity by exchanging FMN with 5-deazaFMN, using NaBH_4 as the reductant.¹⁸⁶ Unlike most native nitroreductases, which convert the substrate only to the hydroxylamine, this artificial enzyme could fully reduce its substrate to the amine product.

Similarly, monooxygenase activity could be introduced to a riboflavin binding protein by exchanging riboflavin with several *N*-alkylated flavins. These artificial flavoenzymes could perform H_2O_2 -driven sulfoxidations, for which the enantioselectivity could be switched by using different *N*-alkylated flavin analogues.¹⁸⁷

Three F_{420} -dependent reductases, MSMEG_2027, MSMEG_6848 and MSMEG_3356, are capable of using both F_{420} and FMN as a cofactor to either reduce or oxidize the aflatoxins AFG1 and AFG2.¹⁸⁸ So, also natural systems can adopt different activities by switching naturally occurring cofactors. Cofactor exchange may continue to be an interesting method of creating novel activities in existing flavoproteins.

2.7 N5-substrate and N5-oxygen adducts

The canonical reactivity of flavin cofactors is redox chemistry through N5-hydride transfer or oxygen activation at C4a, as discussed above in section 1.4. Most dehydrogenases, oxidases and monooxygenases utilize these catalytic strategies. Section 1.6.8. discussed prenyl-FMN and its ability to do 1,3-dipolar cycloadditions. The stabilized N5-iminium ion in the cyclic azomethine ylide functionality of this highly modified flavin is the cause of this novel reactivity. Although the majority of enzymes containing unmodified FMN or FAD cofactors perform the standard 'canonical' redox chemistry, a few flavoenzymes have recently been shown to catalyze redox neutral processes with covalent flavin-N5-substrate intermediates. The best studied enzyme in flavin-dependent covalent catalysis is UDP-galactopyranose mutase (UGM), which catalyzes the isomerization to UDP-galactopyranose to UDP-galactofuranose.

2.7.1 Redox neutral covalent catalysis

A wealth of studies have resulted in the elucidation of the mechanism of UGM. Crystal structures indicate that the substrate, UDP-galactopyranose, binds close to reduced FAD, and that the O4 of FAD hydrogen bonds with the sugar moiety.¹⁸⁹ Positional isotope exchange then showed that the O-glycosidic bond is cleaved before isomerization, which implies that a highly electrophilic oxocarbenium cation is formed.¹⁹⁰ This can then react with the nucleophilic N5-position of the isoalloxazine ring, creating a covalent intermediate between N5 and the anomeric carbon. A covalent FAD-galactose intermediate was indeed seen in a crystal structure.¹⁹¹ The N5-anomeric carbon bond promotes sugar ring opening by iminium ion formation, which later acts as an electron sink for ring closure. Nucleophilic attack by a phosphate oxygen of UDP, forms UDP-galactofuranose and the reduced flavin ground state, ending the catalytic cycle. See **Figure 2.12**.

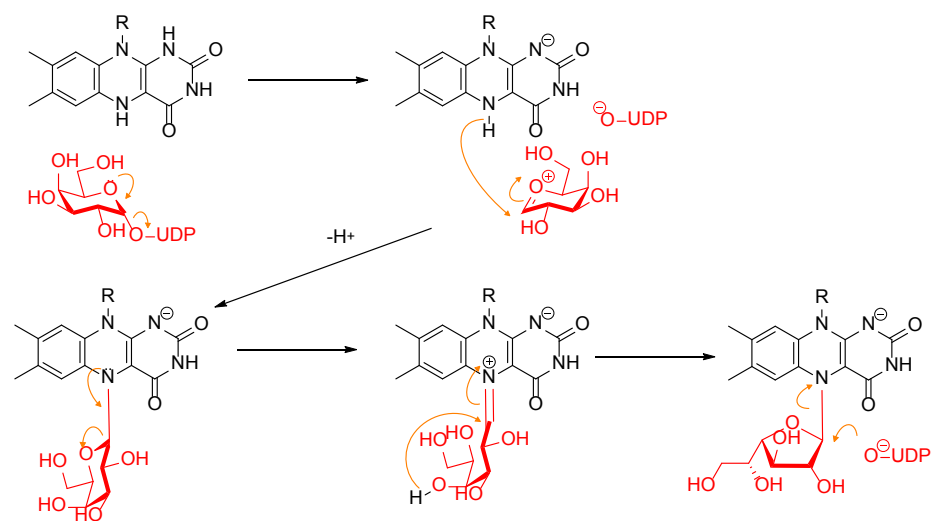


Figure 2.12: Proposed UGM mechanism. Adapted from Tanner et al.¹⁹²

A similar iminium-adduct intermediate is seen in alkyl-dihydroxyacetone phosphate synthase, which is involved in the biosynthesis of important ether lipids. In this enzyme the covalent N5-substrate adduct is formed by a nucleophilic attack from C1 of the enolate form of the substrate, acyldihydroxyacetone phosphate, which is stabilized by active site histidine residues. Strikingly, the flavin needs to be in the oxidized state for catalysis, contrary to UGM. The iminium adduct acts as an electron sink for further catalysis and promotes ether formation with fatty alcohols.¹⁹³ See **Figure 2.13**. Another fascinating observation is that the active site architecture and the whole protein structure are very similar to that of VAO enzymes. This shows that minor evolutionary changes can greatly alter protein function.

Two other bacterial enzymes, namely tRNA methyl-transferase (TrmFO)¹⁹⁴ and flavin-dependent thymidylate synthase (FDTS),¹⁹⁵ catalyze the methylenetetrahydrofolate-dependent methylation of uracil in tRNA or dUMP, respectively. Both enzymes utilize the flavin cofactor as a covalent methyl-transfer catalyst, again exploiting the flavin N5-iminium intermediate, but the two structurally unrelated enzymes catalyze the reaction differently.^{196–198} This shows that covalent catalysis might be more abundant in nature and that very unrelated enzymes can exploit the same N5 iminium-adduct in different ways.

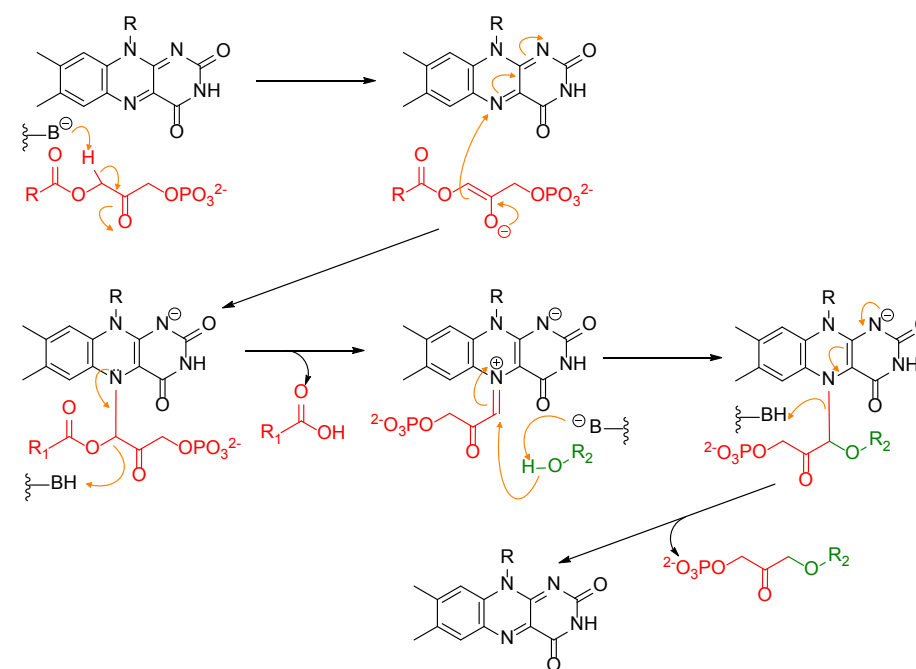


Figure 2.13: Proposed ADPS mechanism. Adapted from Sobrado.¹⁹⁹

2.7.2 N5-oxygen adducts

The majority of flavin-dependent monooxygenases utilizes the C4a-(hydro) peroxyflavin intermediate as a form of activated oxygen.⁵² A few flavoenzymes, however, were found to utilize a N5-peroxy flavin intermediate. The first discovered enzyme that was shown to harbor an N5-oxide ($\text{Fl}_{\text{N5(O)}}$) is EncM from *Streptomyces maritimus*, which is involved in the enterocin biosynthesis pathway.²⁰⁰ UV/VIS spectroscopic and mass spectrum analysis showed that the covalently bound FAD prosthetic group was present as an N5-oxide adduct.^{54,201} This $\text{FAD}_{\text{N5(O)}}$ forms a covalent adduct with an enolic carbon of the substrate, which then results in the oxygenated substrate and oxidized FAD. The formed alcohol then reduces FAD and forms a ketone product, which subsequently undergoes a Favorskii-type rearrangement, inside the enzyme. The reduced flavin can then again form the N5-oxide by reaction with molecular oxygen. See **Figure 2.14**.

The C4a-peroxyflavin is thought to be formed by a single electron transfer between the C4a carbon and molecular oxygen upon ‘face-on’ approach. Apolar or amphipathic oxygen binding pockets around this flavin locus facilitate this reaction. O_2 -pressurized X-ray crystallography showed that EncM has such a binding pocket on the *re*-face of FAD, facing the N5 in a reactive position.²⁰³ The same was seen for

the crystal structure of another N5-oxide containing protein, RutA, where O₂ has a distance of 2.1 Å from N5 and a dihedral angle of 99° with respect to the FMN plane, ideal for covalent bond formation.²⁰⁴ The current opinion is that N5 reacts with oxygen in a similar fashion as C4a (see section 1.4.), in which the reduced hydroquinone form and oxygen have a single electron transfer, resulting in a negatively charged semiquinone radical, in which the radical resides on the N5. Radical pairing yields flavin N5-hydroperoxide, which can form N5-oxide by elimination of water.^{54,204} See **Figure 2.15**.

E. coli RutA is a group C monooxygenase which catalyzes the first step in the Rut pathway, which is the conversion of uracil to 3-ureindoacrylic acid.^{205,206} Reactions with isotopically labelled oxygen, oxygen pressurized crystallography and quantum mechanical modelling suggest that the N5-peroxyflavin is responsible for substrate oxygenation through a peroxyacid intermediate, forming the product and flavin N5-oxide, as is shown in **Figure 2.16**.^{204,206} It was shown that two other members from the same group C monooxygenase also exploit the N5-peroxide/N5-oxide for catalysis. These enzymes are DszA from *Rhodococcus erythropolis*²⁰⁷ and HcbA1 from *Nocardioides* sp. (Strain PD653).²⁰⁸ Both enzymes use the N5-peroxyflavin as a weak nucleophile, oxygenating dibenzothiophene sulfone and hexachlorobenzene through nucleophilic aromatic substitutions.

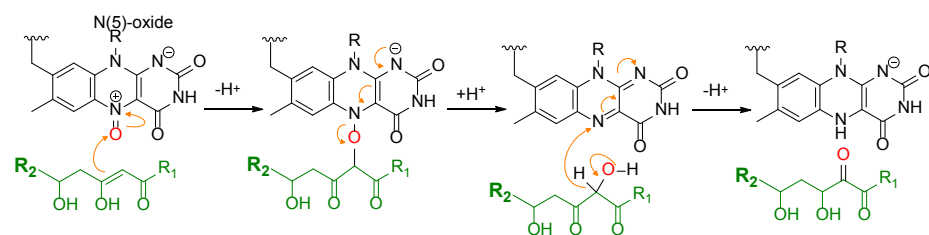


Figure 2.14: EncM mechanism involving a crucial FADN5[O]. Adapted from Teufel et al.²⁰²

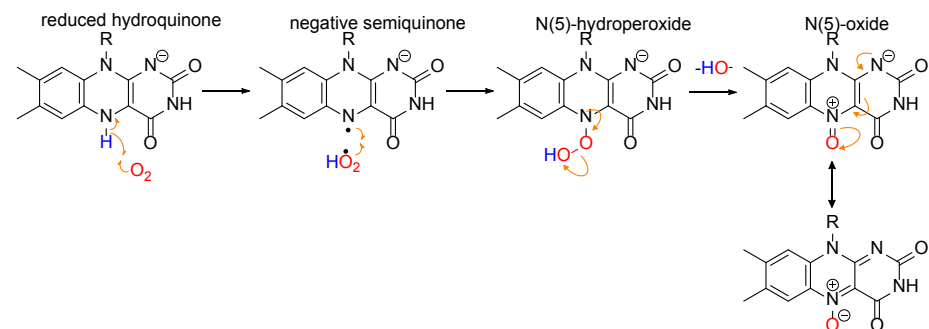


Figure 2.15: Proposed mechanism for the formation of flavin N5-oxide. Adapted from Matthews.²⁰⁴

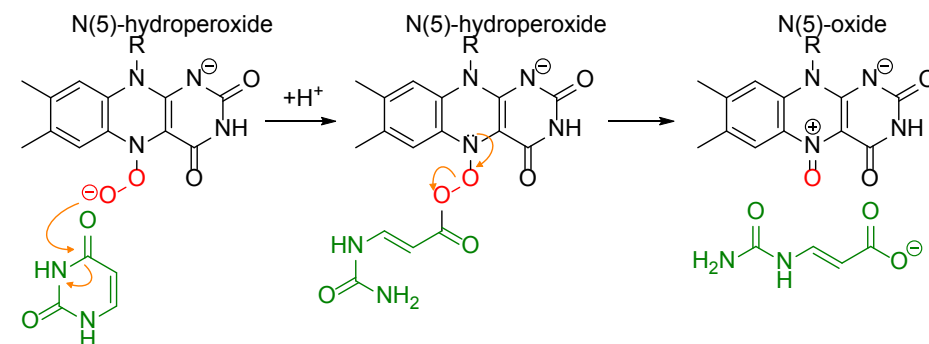


Figure 2.16: Proposed mechanism for RutA. Adapted from Adak And Begley.²⁰⁶

The identification of three monooxygenases from the same group as N5-peroxyflavin utilizing enzymes in different bacterial species suggests that more enzymes in this superfamily might exploit this type of catalysis. It could be that the N5-oxide intermediate was overlooked in previously characterized monooxygenases from this and other superfamilies. The UV/VIS-spectrum of the N5-oxide intermediate is in fact very similar to that of oxidized flavin. EncM is structurally not related to the group C monooxygenases, but has a mechanism that also proceeds through the N5-oxide intermediate. This indicates that this type of flavin chemistry is not restricted to a specific class of flavoproteins.

2.8 F₄₂₀ – a natural deazaflavin

F₄₂₀ is sometimes seen as a rare cofactor, but this naturally occurring deazaflavin is actually wide spread in nature, as it is found in methanogenic, halophilic and sulphate reducing archaea as well as many Actinobacteria.^{26,209,210} It was first discovered in lysates of *Methanobacterium bryantii* in which it is responsible for the characteristic blue-green fluorescence at 420 nm, hence the name.²¹¹ The extremely low redox potential and electrochemical and photochemical properties make F₄₂₀ an attractive cofactor for various other purposes.²¹²

2.8.1 Structure and properties of F₄₂₀

The structure of F₄₂₀ was solved in the same decade as its discovery.²⁰ It has a tricyclic 8-hydroxy-5-deazaalloxazine catalytic core structure, which is attached to a ribityl moiety at N10. This 8-hydroxy-5-deazariboflavin compound, called FO (or Fo), is further decorated with a polar 5'-phospho-L-lactyl-γ-L-glutamyl tail, see **Figure 2.17**. The number of glutamyl residues varies depending on the organism and ranges from 2 in methanogens to sometimes 9 in *Mycobacteria*.²¹³ The 5-deaza and 8-hydroxy modifications have a large effect on the chemical properties of this flavin analogue,

as compared to FMN and FAD. The redox potential of free F_{420} , being -340 mV, is dramatically lower than that of FMN, FAD and NAD(P)H, and can be even -385 mV under some physiological conditions.^{22,23} Furthermore, F_{420} is an obligate hydride transfer agent, as semiquinone radical states cannot be stabilized in the absence of N5.²¹ This makes reduced F_{420} ($F_{420}H_2$) a relatively stable compound under aerobic conditions. This deazaflavin cofactor has a distinctive absorbance maximum at 420 nm, which shifts to lower wavelengths at lower pH values, with an isobestic point at 400 nm ($\epsilon_{400\text{ nm}} = 25.7 \text{ mM}^{-1} \text{ cm}^{-1}$). It has a fluorescence emission maximum at 470 nm.²⁰

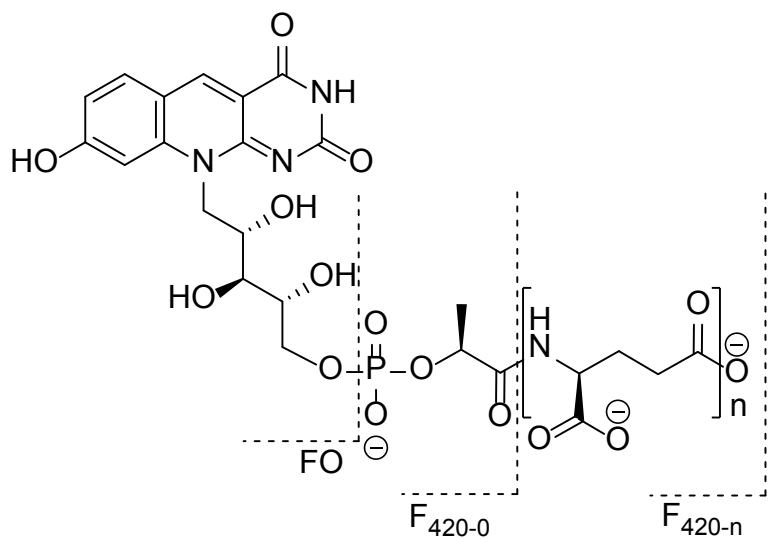


Figure 2.17: Structure of F_{420} .

2.8.2 Physiological functions of F_{420}

F_{420} has several important roles in methanogens. Reduced F_{420} is of key importance in the CO_2 -reducing pathway, and therefore these organisms exploit several means of reducing F_{420} , like molecular hydrogen, formate and secondary alcohols, catalyzed by Frh, Ftd and Adf, respectively.^{214–218} $F_{420}H_2$ is then used as a cofactor for Mer and Mtd that reduce methenyl-tetrahydromethanopterin.^{219,220} It can also be used in the methanogenic electron transport chain, oxygen detoxification, sulfur mobilization and NADP^+ -reduction for biosynthesis.^{221–225} Although not much is known about most of these organisms it is believed that F_{420} also performs a crucial role in the central metabolism of sulfate-reducing archaea and halobacteria.²²⁶

F_{420} is also present in various Actinobacteria, in which it does not seem to have a role in central metabolism. Knock-outs in the F_{420} -biosynthesis machinery did not affect *Mycobacteria* under optimal growth conditions, but prohibited survival under oxidative and nitrosative stress.^{227,228} Therefore, it is believed that this cofactor plays an important role in stress relieve. A F_{420} -dependent glucose-6-phosphate dehydrogenase seems to be the source of reduced cofactor for the protection against stress.^{228–230} Some enzymes in a subgroup of the flavin/deazaflavin oxidoreductases (with a β -roll topology), the FDOR-As, can reduce menaquinone with reduced F_{420} , assuring that the respiratory chain stays in a reduced state.²²⁷ A set of prodrugs were found to be activated by these F_{420} -dependent reductases, releasing toxic nitrogenoxides into the cytosol.²³¹ Another *Mycobacterial* F_{420} -dependent enzyme, hydroxymycolic acid dehydrogenase, is directly involved in the biosynthesis of virulence factors that make these cells less susceptible to antibiotics.²³² Several F_{420} -dependent reductases from the flavin/deazaflavin oxidoreductase (FDOR) superfamily are involved in secondary metabolism of *Mycobacteria*, which perform fatty acid modifications and reduce degradation products of heme, some of which may form potent antioxidants.²³³ Members of the same superfamily are involved in the biosynthesis of tetracycline and its homologues, as well as lincosamide and pyrrolbenzodiazapine antibiotics in *Streptomyces* species.^{234–236}

2.8.3 F_{420} biosynthesis

F_{420} -synthesis utilizes 5-amino-6-ribitylamino-2,4[1H,3H]-pyrimidinedione from the riboflavin biosynthesis pathway. But this compound is instead condensed with tyrosine to form the 7,8-didemethyl-8-hydroxyriboflavin compound FO. FO synthesis is catalyzed by either two separate enzymes in archaea, CofG and CofH, or by the bifunctional FbiC in Actinobacteria, which proceeds through a radical mechanism that involves *S*-adenosyl methionine.^{237,238} FO is decorated with a 5'-phosphoryl-L-lactyl tail or phosphoryl-enolpyruvyl tail from enolpyruvyl-diphospho-5'-guanosine (EPPG) or L-lactyl-2-diphospho-5'-guanosine (LPPG) by the action of CofD in archaea or FbiA in Actinobacteria. LPPG and EPPG can be synthesized from phosphoenol pyruvate or lactate and GTP by CofC or FbiD. Dehydro- F_{420-0} , the product of FbiA, is reduced by the FMN-dependent bifunctional enzyme FbiB to form F_{420-0} . The same enzyme then finalizes the synthesis by attaching several (2 to 9) glutamyl residues to F_{420} , forming F_{420-n} .²³⁹ See Figure 2.18 for an overview of the biosynthetic pathway. A peculiar F_{420} variant was found in the Gram-negative, endofungal bacterium *Paraburkholderia rhizoxinica*. This bacterium produces 3PG- F_{420} , which has a phosphoglycerol tail, instead of a phospholactyl tail.²⁴⁰

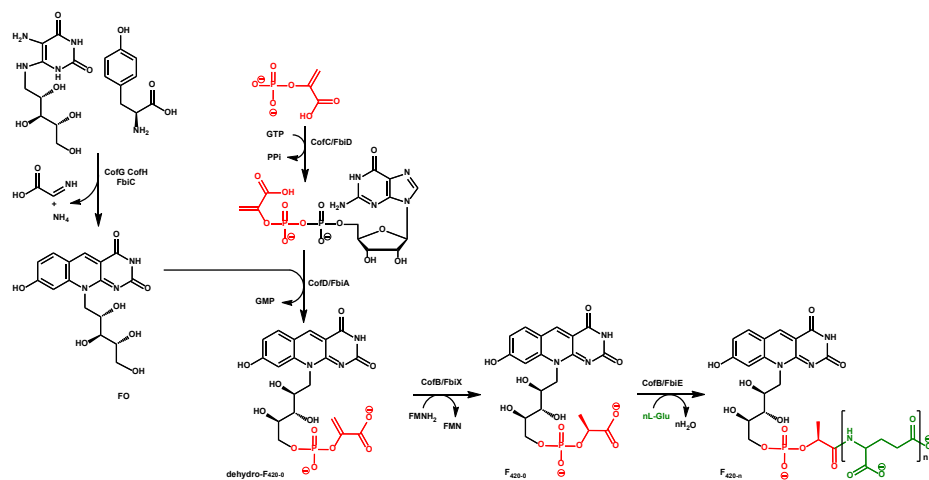


Figure 2.18: F420-biosynthesis pathway in Actinobacteria. Fbi enzymes are found in Actinobacteria and the corresponding Cof enzymes are found in archaea.

2.8.4 F_{420} -dependent enzymes in biocatalysis

The very low redox potential and its stability under aerobic conditions make F_{420} a very attractive cofactor for biocatalytic purposes. The members of the FDOR and luciferase-like hydride transferases superfamily (LLHT; having TIM barrel topology) show a diverse range of substrates, some of which are recalcitrant to other enzymatic systems. F_{420} -dependent ene reductases, imine reductases and secondary alcohol dehydrogenases in these superfamilies could be valuable redox catalysts in the future, as well as many more enzymes that have yet to be discovered. Glucose-6-phosphate dehydrogenases and F_{420} -NADPH oxidoreductases, as well as other well-characterized enzymes, could be used as cofactor recycling systems.¹⁹ The special photochemical properties of deazaflavins could also be exploited for light-driven reactions, omitting the necessity for cofactor recycling systems or yielding completely new catalytic mechanisms.

2.9 Conclusion

The flavin cofactors FMN and FAD can convert a wealth of compounds through their canonical N5-hydride transfer and C4a-(hydro)peroxide exploiting catalytic strategies. Oxidases, monooxygenases and reductases that exploit this chemistry are capable of aromatic, aliphatic and heteroatom oxygenations and oxidations, dehalogenation, halogenation and even light production. Covalent flavin-protein adducts and other modified flavins, like 8-formyl and prenylated flavins, can greatly enhance the catalytic properties of FMN and FAD. The modifications that nature made to flavins can serve as inspiration for man-made artificial cofactor systems that can boost the field of

biocatalysis. Cofactor replacement studies with artificial cofactors have already shown novel activities in existing enzymes.

Noncanonical flavin chemistry exploits the catalytic power of the N5 locus on the isoalloxazine ring, and expands the known flavin chemistry even further. Redox neutral covalent catalysis, through N5-imminium intermediates opens up a whole new field of flavin chemistry. Which is even more expanded by covalent modifications, like the highly modified prenyl-FMN cofactor, making it possible to do reversible decarboxylations of aromatic compounds. N5-peroxy and N5-oxide catalysis also shows that flavins utilize several pathways for oxygenation. The notion that different types of flavin chemistry can exist in one family of enzymes, shows that flavins are far more versatile and – maybe – less predictable than we thought. This makes one wonder what is still to be discovered in the field of flavin catalysis.

CHAPTER 3

Chemoenzymatic synthesis of an unnatural deazaflavin cofactor that can fuel F420- dependent enzymes

Jeroen Drenth, Milos Trajkovic, Marco W. Fraaije

This chapter is based on a published article: ACS Catal. 2019, 9, 7, 6435–6443

*Molecular Enzymology Group, University of Groningen, Nijenborgh 4, 9747AG Groningen,
The Netherlands*

Abstract

F_{420} -dependent enzymes are found in many microorganisms and can catalyze a wide range of redox reactions, including those with some substrates that are otherwise recalcitrant to enzyme-mediated reductions. Unfortunately, the scarceness of the cofactor prevents application of these enzymes in biocatalysis. The best F_{420} producing organism, *Mycobacterium smegmatis*, only produces 1,4 μmol per liter of culture. Therefore, we synthesized the unnatural cofactor FO-5'-phosphate, coined FOP. The FO core-structure was chemically synthesized, and an engineered riboflavin kinase from *Corynebacterium ammoniagenes* (CaRFK) was then used to phosphorylate the 5'-hydroxyl group. The triple F21H/F85H/A66I CaRFK mutant reached 80% of FO conversion in 12 h. The same enzyme could produce 1 mg (2.5 μmol) FOP in 50 mL of reaction volume, which translates to a production of 50 $\mu\text{mol/L}$. The activity toward FOP was tested for an enzyme of each of the three main structural classes of F_{420} -dependent oxidoreductases. The sugar-6-phosphate dehydrogenase from *Cryptosporangium arvum* (FSD-Cryar), the F_{420} :NADPH oxidoreductase from *Thermobifida fusca* (TfuFNO), and the F_{420} -dependent reductases from *Mycobacterium hassiacum* (FDR-Mha) all showed activity for FOP. Although the activity for FOP was lower than that for F_{420} , with slightly lower k_{cat} and higher K_m values, the catalytic efficiencies were only 2.0, 12.6, and 22.4 times lower for TfuFNO, FSD-Cryar, and FDR-Mha, respectively. Thus, FOP could be a serious alternative for replacing F_{420} and might boost the application of F_{420} -dependent enzymes in biocatalysis.

3.1 Introduction

The naturally occurring cofactor F_{420} was discovered in 1972 in methanogenic archaea where it plays a crucial role in one-carbon catabolism.²¹¹ Nowadays, F_{420} is known to be present in a wide range of archaea and bacteria in which it plays an important role in many processes as a redox cofactor.^{26,210,241,242} In several Actinobacteria, for instance, it plays a crucial role in antibiotic synthesis,^{235,236,243} as well as aflatoxin degradation,^{188,233,242} and degradation of other aromatic compounds.^{244–246} Also the notorious pathogen *Mycobacterium tuberculosis* has a high abundance of F_{420} -dependent proteins.²¹⁰ In this organism F_{420} is crucial in the regulation of oxidative and nitrosative stress.^{227,228,247} Ironically, a series of antitubercular nitroimidazole prodrugs, like pretomanid (PA-824) and delamanid (OPC-67683), are specifically activated by a F_{420} -dependent reductase *in vivo*, releasing toxic NO.^{248–250}

Structurally, the 7,8-didemethyl-8-hydroxy-5-deazariboflavin catalytic core of F_{420} , called FO, is analogous to that of riboflavin²⁰ (see **Figure 3.1**). Its chemistry, however, resembles more that of nicotinamide dinucleotide (NAD(P)⁺), as F_{420} can

only perform two-electron hydride transfers and is hardly reactive toward molecular oxygen. Its reduction potential of -360 mV is lower than that of NAD(P)⁺ and the riboflavin derived cofactors flavin mononucleotide (FMN) and flavin adenine dinucleotide (FAD), which are -320 mV and -220 mV, respectively.²¹ Apart from the FO core, the rest of the structure is very different than that of the nicotinamide and flavin cofactors. The ribityl tail of FO is extended with a 5'-phospho-L-lactyl moiety, forming F_{420} -O, and this is in turn elongated by a poly- γ -glutamyl tail.²⁰ The length of the poly- γ -glutamyl tail depends on the organism and varies from 2 to 9 monomers.^{26,251} Interestingly, the larger part of the poly- γ -glutamyl tail is not bound to the enzyme, as was seen in several crystal structures and modeled protein structures.^{229,233,252–256} Ney et al.,²⁶ however, showed that electrostatic interactions of the poly- γ -glutamyl tail with enzymes of the split β -barrel like fold flavin/deazaflavin oxidoreductase (FDOR) and TIM barrel fold luciferase-like hydride transferase (LLHT) families influences the binding affinity. It seems that a longer polyglutamyl tail results in a higher binding affinity (lower K_d and K_m), which lowers the catalytic turnover (k_{cat}), probably because of slower cofactor exchange rates.

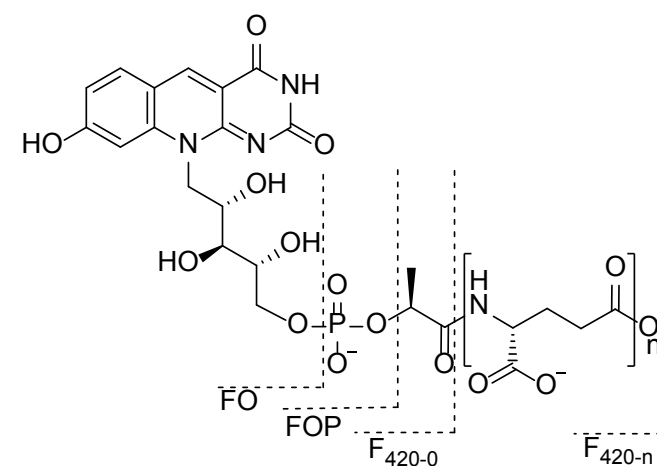


Figure 3.1: Structure of F_{420} and related compounds.

The uniquely low redox potential of the cofactor makes it an interesting candidate for the use in biocatalysis.^{19,25} F_{420} -dependent enzymes can reduce various physiologically important heterocyclic enones, unsaturated esters and imines which are inert to other enzymes.^{188,242,257,258} Recently, it was shown that F_{420} -dependent reductases (FDR), part of the split β -barrel fold FDORs, can reduce α,β -unsaturated ketones and aldehydes in an enantio- and regioselective fashion and, interestingly, yielding the opposite enantiomer as would be formed by the well-studied FMN-dependent old yellow enzyme-type reductases.²⁵⁹ Also F_{420} -dependent enantioselective

secondary alcohol dehydrogenases were characterized.^{217,252} These enzymes could also be used as cofactor recycling systems to supply reductases with reduced F_{420} . The well-studied F_{420} :NADPH oxidoreductases^{224,253,260–263} and sugar-6-phosphate dehydrogenases^{254,264–268} could also be used as recycling systems. These enzymes form a biocatalytic toolbox which is anticipated to expand, as many genomes are predicted to accommodate genes for F_{420} -dependent enzymes that have yet to be characterized.^{25,210}

The main bottleneck in the application of F_{420} -dependent enzymes thus far is the limited availability of the cofactor. Many of the organisms that produce F_{420} are hard to culture or grow relatively slowly. The best production organism, *Mycobacterium smegmatis*, still only produces 1.4 $\mu\text{mol/L}$ of culture.^{269,270} Straightforward organic synthesis cannot be used as an alternative option, because of the complicated, heterogeneous molecular structure of the cofactor. Especially the regioselectivity is very challenging as many groups in, for instance, the ribityl moiety and the poly- γ -glutamyl tail have similar reactivity. Heterologous biosynthesis in faster growing hosts was, until recently, impossible because of some missing links in the F_{420} -biosynthesis pathway. The recent elucidation of the complete biosynthesis pathway made heterologous production of the cofactor in *Escherichia coli* actually possible, but – thus far – has the same low yields as with *M. smegmatis*.²³⁹

Herein we describe the chemoenzymatic production of the unnatural F_{420} analogue FO-5'-phosphate, which we coined FOP. The structure of FOP is analogous to FMN, the cofactor that is used in enzymes that share homology with the TIM barrel fold and split β -barrel like fold F_{420} -dependent oxidoreductases, and that may be the ancestors of F_{420} -dependent oxidoreductases.^{233,252,255,265} To generate this functional alternative for F_{420} , the FO core was synthesized, as described by Hossain et al.³¹ with small modifications. FO was 5'-phosphorylated with an engineered variant of the riboflavin kinase from *C. ammoniagenes*. Site-directed mutagenesis was applied to the enzyme in order for it to accommodate FO. The enzyme activity with FOP as a coenzyme was tested for a representative member of each structural class of F_{420} -dependent oxidoreductases.^{25,265}

3.2 Materials and Methods

Reagents and chemicals were purchased from Sigma-Aldrich (St. Louis, MO, U.S.A.) unless indicated otherwise. Mutagenic primers were also ordered at Sigma-Aldrich. Ligase and restriction endonucleases were obtained from New England Biolabs (NEB, Ipswich, MA, U.S.A.). PfuUltra Hotstart PCR Mastermix (Agilent Technologies) was used for mutagenic PCR (QuikChange). Plasmid DNA was isolated using the QIAprep

Miniprep Kit and PCR products were purified with the QIAquick PCR Purification Kit (Qiagen, Valencia, CA, U.S.A.).

3.2.1 F_{420} Production

F_{420} was isolated from *Mycobacterium smegmatis* as described by Bashiri et al. and Isabelle et al.^{269,270} The production strain *M. smegmatis* mc² 4517 was a kind gift from Dr. G. Bashiri from the University of Auckland, New Zealand.

3.2.2 FO and FO-7-Methyl Synthesis

FO was synthesized using the approach described by Hossain et al.³¹ with a modification for the reductive amination procedure. These two steps are done in one step via reductive amination with sodium cyanoborohydride, instead of synthesis of the mixture of anomers and then reduction of them. FO-7-Me was synthesized using the same modified procedure as for synthesis of FO. Detailed procedures and physical data can be found in the Supporting Information.

3.2.3 Gene Cloning and Mutagenesis of *C. ammoniagenes* Riboflavin Kinase

The *C. ammoniagenes* riboflavin kinase gene (*CaRFK*) was ordered at GenScript (Piscataway, NJ, U.S.A.), codon optimized for *E. coli*. It was composed of the C-terminal kinase domain of the FAD synthetase gene, *ribF* (NCBI#: D37967.1), previously described by Iamurri et al.²⁷¹ The nucleotide sequence and protein sequence are shown in **Figures S1** and **S2** of the online supplementary information to the publication, respectively. The gene was cloned into a pBAD/*Myc*-His vector (Invitrogen, Thermo-Fisher) using restriction sites *NdeI* and *HindIII*, following standard cloning procedures.²⁷² Site-directed mutagenesis was performed on the riboflavin kinase gene with the use of mutagenic primers, degenerate at a chosen codon, using the QuikChange mutagenesis kit (Stratagene), following the procedure of the manufacturer. Primers were designed with the Agilent QuikChange primer design tool (<http://www.genomics.agilent.com/primerDesignProgram.jsp>). The used primers are listed in Table S1 of the online supplementary information to the article. Sequencing was performed at GATC (Constance, Germany). The plasmids were transformed into calcium chloride chemically competent *E. coli* NEB 10-beta (New England Biolabs Ipswich, MA, U.S.A.) for amplification and protein expression, using standard protocols.²⁷²

3.2.4 Expression and Purification of *C. ammoniagenes* Riboflavin Kinase

An *E. coli* NEB 10-beta overnight culture in Terrific broth (TB), supplemented with 50 $\mu\text{g mL}^{-1}$ ampicillin, was grown at 37 °C, 135 rpm. The overnight culture was diluted a hundred times in 200 mL of fresh TB with 50 $\mu\text{g mL}^{-1}$ ampicillin in a 500 mL

Erlenmeyer flask. This was grown at 37 °C, 135 rpm until the OD_{600} reached ~ 0.5 , at which the culture was induced with 0.2% L-arabinose and further grown at 17 °C for 36 h. Cells were harvested by centrifugation at 4000g for 20 min at 4 °C. The cell pellets were stored at -20 °C until purification. Cell pellets were resuspended in about 10 mL of 50 mM Tris/HCl pH 8.0, 200 mM NaCl, 10 mM imidazole, 1 mM β -mercaptoethanol, and cOmplete mini EDTA-free Protease Inhibitor Cocktail. The cells were lysed by sonication, using a Sonics Vibra-Cell VCX 130 sonicator with a 3 mm stepped microtip (5s on, 10s off, 70 % amplitude, 7.5 min). Cell debris were pelleted by centrifugation at 8000g for 40 min at 4 °C. The clear supernatant was incubated on 2 mL Ni-Sepharose High Performance (GE Healthcare, Eindhoven, The Netherlands) for 12 h at 4 °C, with gentle shaking. The column was washed extensively with 3 column volumes of 50 mM Tris/HCl pH 8.0, 200 mM NaCl, 20 mM imidazole, and the protein was eluted with 50 mM Tris/HCl pH 8.0, 200 mM NaCl, 300 mM imidazole. The eluted protein was then desalted and concentrated using Amicon Ultra centrifugal filter units with a 3 kDa molecular weight cutoff, exchanging the buffer with 50 mM Tris/HCl pH 8.0, 200 mM NaCl. The protein was flash-frozen in liquid nitrogen and stored at -80 °C until further use. Purity was checked with SDS-PAGE analysis and protein concentrations were measured by Bradford analysis, using the standard protocols.

3.2.5 Expression and Purification of F_{420} -Dependent Enzymes

Genes, plasmids, and host strains were already in the collection of this lab from earlier studies. *T. fusca* F_{420} :NADPH oxidoreductase (TfuFNO) was expressed and purified as described by Kumar and Nguyen et al.²⁵³ *R. jostii* RHA1 F_{420} -dependent glucose-6-phosphate dehydrogenase (RHA1-FGD) was expressed and purified as described by Nguyen et al.²⁵⁴ The sugar-6-phosphate dehydrogenase from *C. arzum* (FSD-Cryar) was expressed and purified as described by Mascotti and Kumar et al.²⁶⁵ The F_{420} -dependent reductases from *M. hassiacum* (FDR-Mha) and *R. jostii* RHA1 (FDR-RHA1) were expressed and purified as described by Mathew and Trajkovic et al.²⁵⁹

3.2.6 Riboflavin Kinase Activity Assay and HPLC analysis

The activity of wild-type CaRFK and mutant enzymes toward riboflavin and FO was measured in conversion experiments. Conversion mixtures contained 1 μ M enzyme and 50 μ M riboflavin, FO-7-methyl (FO-7-Me) or FO in 50 mM Tris/HCl pH 8, 100 mM $MgCl_2$, 10 mM ATP. The reaction mixtures with a total volume of 0.5 mL were incubated at room temperature or 37 °C for 12 h. Samples were taken either at certain intervals (0, 5, 10, 15, 30 min) or after 12 h. Conversions were measured by either high performance liquid chromatography (HPLC) or thin layer chromatography (TLC). The TLC method was previously described by Iamurri et al.²⁷¹ The HPLC method was a modified version of that of Iamurri et al. The reactions were quenched with 100%

formic acid (FA), 1:5 FA:sample, incubating on ice for 5 min. Then, the samples were spun down at 8000g in a table top centrifuge at 4 °C and neutralized with 1.6 mM NaOH, 1:9 NaOH:sample. Supernatant (100 μ L) was used for HPLC analysis. Samples were separated on an Alltech Alltime HP C18 5 μ , 250 mm column by applying a linear gradient of 50 mM ammonium acetate pH 6.0 with 5% acetonitrile (buffer A) and 100% acetonitrile (buffer B): t = 0 min / 100:0 (A:B), t = 20 min / 75:30 (A:B), t = 30 min / 5:95 (A:B), t = 35 min / 5:95 (A:B), t = 40 min / 75:30 (A:B), t = 45 min / 100:0 (A:B). The separation was monitored in time at 262 nm. The retention times for FO, FOP, FO-7-Me and FO-7-Me-P are 17, 15, 21, and 19 min, respectively.

3.2.7 Chemoenzymatic Synthesis of FOP

CaRFK F21H F85H A66I (10 μ M) was added to 50 μ M FO in 50 mL of 50 mM Tris/HCl pH 8, 100 mM $MgCl_2$, 10 mM ATP and was incubated at room temperature for 24 h. The reaction mixture was spun down at 8000g in a table top centrifuge and applied to a Reveleris C18-WP Flash cartridge column. FOP was eluted with deionized water, and purity was verified by HPLC, as described above. The product was concentrated by water evaporation under reduced pressure with a rotary evaporator. FOP was either kept at -20 °C for long-term storage or at 4 °C for short-term storage. Obtained FOP was confirmed by HRMS (result is shown in Supporting Information).

3.2.8 Steady-State Activity Assays for Selected F_{420} -Dependent Enzymes with FO, FOP, and F_{420}

The Michaelis–Menten kinetic parameters for TfuFNO with FO and FOP were obtained by the spectrophotometric assay as described by Kumar and Nguyen et al.²⁵³ In short, the measurements were performed at 25 °C by adding 25 – 50 μ M enzyme to 50 mM KPi, pH 6.0, with a constant NADPH concentration of 250 μ M and varying concentrations of FO and FOP between 0.625 and 50 μ M. The activity of RHA1-FGD and FSD-Cryar with FO, F_{420} and FOP was obtained by the spectrophotometric assay as described by Nguyen et al.²⁵⁴ and Mascotti and Kumar et al.,²⁶⁵ respectively. Glucose-6-phosphate was used as substrate at a constant concentration of 20 mM. The concentration of FO, FOP and F_{420} was varied between 1.25 and 50 μ M in the appropriate Tris/HCl-based buffers for each enzyme at 25 °C.^{254,265}

The absorbance at 400 nm was followed in time for all the experiments and observed slopes (k_{obs}) were calculated with $\epsilon_{400}(F_{420}) = 25.7 \text{ mM}^{-1} \text{ cm}^{-1}$. All experiments were performed in triplicates. The k_{obs} values were plotted against de FO/FOP/ F_{420} concentration and the data was fitted to the Michaelis–Menten (eq 1) or Hill equation (eq 2) by nonlinear regression, using GraphPad Prism v. 6.0 (GraphPad Software Inc., La Jolla, CA, U.S.A.).

$$k_{obs} = \frac{k_{cat} \cdot [S]}{K_m + [S]} \quad (1)$$

$$k_{obs} = \frac{k_{cat} \cdot [S]^h}{K_{half}^h + [S]^h} \quad (2)$$

The kinetic parameters for the F_{420} -dependent reductase FDR-Mha were obtained as follows: FOPH₂ and F_{420} H₂ were prepared by incubating 500 μ M FOP or F_{420} with 10 μ M FSD-Cryar and 20 mM glucose-6-phosphate in 50 mM Tris/HCl, pH 8.0, until the yellow color disappeared. Then, the mixture was passed through an Amicon Ultra 0.5 mL centrifugal filter, 10 kDa molecular weight cutoff. The filtrate, containing 500 μ M FOPH₂ or F_{420} H₂, was then immediately used for a spectrophotometric assay. The assay mixture contained 0.1 – 1 μ M FDR-Mha, 1.0 mM 2,6,6-trimethyl-2-cyclohexene-1,4-dione, and various concentrations of FOPH₂ and F_{420} H₂ between 1.25 and 50 μ M in 50 mM Tris/HCl, pH 8.0. The increase in absorbance at 400 nm was measured in time over several minutes. The k_{obs} values were calculated using $\epsilon_{400}(F_{420}) = 25.7 \text{ mM}^{-1} \text{ cm}^{-1}$. All experiments were performed in triplicates at 25 °C. Kinetic data was analyzed by nonlinear regression and fitted to the Hill equation for cooperative binding (eq 2), using GraphPad Prism v. 6.0 (GraphPad Software Inc., La Jolla, CA, U.S.A.).

3.2.9 Conversion Experiments with F_{420} -Dependent Reductases from *M. hassiacum* and *R. jostii* RHA1 with FO, FOP, and F_{420}

The reaction mixture contained 400 μ L of 50 mM Tris/HCl pH 8.0 supplemented with 1.0 mM cinnamaldehyde, 20 μ M FO/FOP/ F_{420} , 1.0 μ M TfuFNO, 10 mM NADPH, 25 μ M FDR-RHA1/FDR-Mha and DMSO (3% v/v). The reaction was performed in a closed 1 mL glass vial in the dark at 25 °C and 135 rpm for 3 h. The reaction was quenched by adding the mixture to an equal amount of acetonitrile and was then incubated on ice for 5 min. This mixture was spun down at 8000g in a table top centrifuge at 4 °C, and 100 μ L supernatant was used for analysis on HPLC. The depletion of substrate and formation of product were analyzed at 240 nm, using an isocratic mobile phase of 60:40 water:acetonitrile on an Alltech Alltime HP C18 5 μ , 250 mm column.

3.3 Results

3.3.1 Engineering of *C. ammoniagenes* Riboflavin Kinase Towards Activity on FO

The C-terminal riboflavin kinase domain (CaRFK) of the FAD synthetase (RibF) from *C. ammoniagenes*, previously described by Iamurri et al.²⁷¹ and Herguedas et al.,²⁷³ was chosen for the biocatalytic 5'-phosphorylation of FO. The truncated *ribF* gene (NCBI#: D37967.1), *CaRFK*, was ordered, codon optimized for *E. coli*, and was transformed into *E. coli* NEB 10-beta as a pBAD-*CaRFK* construct, equipped with a C-terminal 6 ×

histidine tag. Purification of the respective protein, CaRFK, was achieved by table-top nickel affinity chromatography, yielding about 20 mg L⁻¹ pure CaRFK.

Conversion experiments with 50 μ L FO and 1 – 50 μ M of CaRFK, analyzed by reverse-phase HPLC after 12 and 48 h at 20 or 37 °C, showed that the wild-type enzyme had no detectable activity toward FO. Therefore, structure-guided site-directed mutagenesis was performed. The crystal structure of the C-terminal riboflavin kinase domain of RibF, PDB ID 5A89,²⁷³ was used to identify suitable sites for mutagenesis. See **Figure S 3.9** for the architecture of the riboflavin binding site in CaRFK. Polar amino acids were introduced at positions 21, 85, and 122 with QuikChange-PCR to accommodate the 8-hydroxyl group of FO (numbering according to the protein sequence given in **Figure S2** of the online supplementary information). Single point mutations, as well as double mutations, however, did not result in any activity toward FO. Yet, interestingly, the apparent activity toward another deazaflavin, FO-7-methyl (8-demethyl-8-hydroxy-5-deazariboflavin, a molecule that is structurally halfway riboflavin and FO), was increased by these mutations, while the activity toward RF was significantly diminished (see **Figure 3.2**). Gratifyingly, introduction of three mutations resulted in activity on FO: mutations A66V/A66I, together with F21H/Y and F85H/Y yielded FO conversions of 61 to 81 % in 12 h (see **Figure 3.3**). Replacing alanine at position 66 by a valine or isoleucine might fill up the void that was left vacant by the missing 7-methyl group in FO, making it impossible for water to reside there. Introduction of additional polar residues at position 122 and the mutation T23S, both in the same binding pocket facing the 8-hydroxyl group of FO, did not increase the activity any further.

3.3.2 Chemoenzymatic Synthesis of FO-7-Me-P and FOP

Incubating 50 μ M FO-7-Me with 10 μ M F21Y/F85H CaRFK mutant or FO with 10 μ M F21H/F85H/A66I CaRFK mutant in a volume of 50 mL resulted in full conversion of FO-7-Me to FO-7-Me-P and FO to FOP within 24 h at 37 °C. The product could be purified from the other reaction components with the aid of a preparative reverse-phase liquid chromatography and was concentrated by rotary evaporation under reduced pressure. The yield of 50 mL of reaction volume was about 1 mg (2.5 μ mol) of FOP and FO-7-Me-P, in a final concentration of about 400 μ M (measured by absorbance at 400 nm, $\epsilon_{400} = 25.7 \text{ mM}^{-1} \text{ cm}^{-1}$). Obtained FO-7-Me-P and FOP were confirmed by HRMS (see Supporting Information).

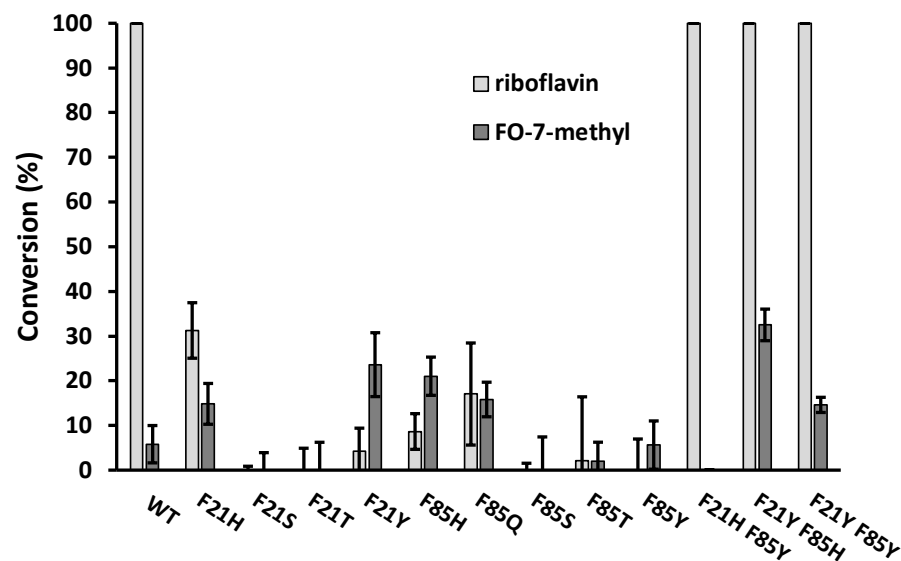


Figure 3.2: Conversion of riboflavin and FO-7-methyl by single and double CaRFK mutants within 12 h of incubation at 37 °C. Enzyme concentrations are 17 μ M for single mutants and 1 μ M for double mutants. Experiments were performed in duplicates. Error bars represent standard deviations.

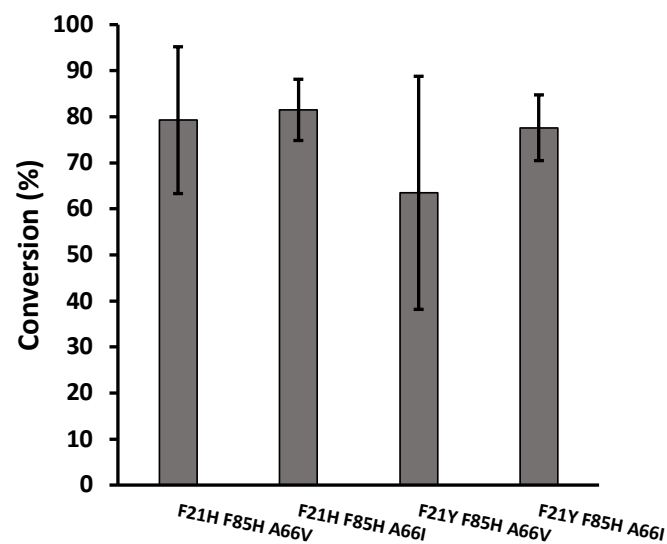


Figure 3.3: Conversion of FO to FOP within 12 h of incubation at 37 °C with several CaRFK mutants. Experiments were performed in duplicates. Error bars represent standard deviations.

3.3.3 Purification of F_{420} -Dependent Oxidoreductases

The F_{420} :NADPH oxidoreductase from *T. fusca* (TfuFNO) was expressed and purified as described by Kumar and Nguyen et al.²⁵³ with a yield of approximately 140 mg L⁻¹ pure protein. The glucose-6-phosphate dehydrogenase from *R. jostii* RHA1 (RHA1-FGD) and the sugar-6-phosphate dehydrogenase from *C. arzum* (FSD-Cryar) were expressed and purified as described by Nguyen et al.²⁵⁴ and Mascotti and Kumar et al.,²⁶⁵ respectively. Yields of purified enzyme were similar as described by the papers mentioned above. Similar results were also obtained for the expression and purification of the F_{420} -dependent reductases from *M. hassiacum* (FDR-Mha) and *R. jostii* RHA1 (FDR-RHA1), as described by Mathew and Trajkovic et al.²⁵⁹

3.3.4 Steady-State Kinetics Using FOP as Alternative Cofactor

The activity of the F_{420} -dependent enzymes TfuFNO, RHA1-FGD, FSD-Cryar, and FDR-Mha toward FO, FOP and F_{420} was measured spectrophotometrically. Steady-state kinetic parameters were measured by varying the concentration of the coenzymes FO, FOP and F_{420} , while keeping the other substrates at constant, saturating concentrations. The slopes of absorbance decrease – or increase in the case of FDR-Mha – at 400 nm were measured, and the observed rates (k_{obs}) were calculated using $\epsilon_{400} = 25.7 \text{ mM}^{-1} \text{ cm}^{-1}$. The observed rates were plotted against the cofactor concentration and fitted to the Michaelis–Menten or the Hill model for positive cooperativity (eqs 1 and 2, respectively).

Tfu-FNO showed activity with all three tested deazaflavins (FO, FOP and F_{420}). The kinetic data with FO and FOP did not fit well to the Michaelis–Menten kinetic model but could be fitted to a Hill plot for cooperative substrate binding kinetics (**Figure S 3.2** and **Figure S 3.3**). This positive cooperativity can be explained by the dimeric structure of the enzyme. Cooperativity was also observed for the FNO from *Archaeoglobus fulgidus*, using NADPH and FO, as reported by Le et al.²⁷⁴ Strangely, positive cooperativity was not seen with F_{420} as a coenzyme, as discussed by Kumar and Nguyen et al.²⁵³ The kinetic parameters for FO and FOP, however, are similar to that of F_{420} (**Figure 3.1**). Thus, FO, FOP and F_{420} are all equally well used as coenzymes in NADPH oxidation by TfuFNO. The crystal structure of TfuFNO (PDB ID 5N2I),²⁵³ superimposed with the crystal structure of the F_{420} -bound FNO homologue from *A. fulgidus* (1JAY),^{256,263} shows that only the FO part of F_{420} is bound and that the rest of the molecule is actually located outside of the enzyme. Therefore, the phosphate of FOP or phospho-L-lactyl and poly- γ -glutamyl tail of F_{420} have only minor contributions to the binding affinity.

It was found that RHA1-FGD shows no activity with FO or FOP, while it has a k_{cat} of 17 s⁻¹ and K_m of 3.8 μM for F₄₂₀.²⁵⁴ The crystal structure of RHA1-FGD (PDB ID 5LXE),²⁵⁴ superimposed with the F₄₂₀-bound crystal structure of the *M. tuberculosis* homologue (PDB ID 3Y4B),²²⁹ shows that the first glutamate moiety of the F₄₂₀ poly-γ-glutamyl tail forms hydrogen bonds with the protein backbone. This could be the reason for being unable to use FO or FOP as coenzyme, which are lacking the glutamyl tail. FSD-Cryar, however, with 57% sequence identity to RHA1-FGD, did show detectable activity toward FOP. The k_{obs} data fitted well to a Michaelis–Menten curve and gave a k_{cat} of 1.3 s⁻¹ and K_m of 7.0 μM for FOP (**Figure S 3.4** and **Figure S 3.5**, **Table 3.1**). Both values are lower than the kinetic parameters measured for the native cofactor F₄₂₀, being 33 s⁻¹ and 13.9 μM for the k_{cat} and the K_m , respectively (**Table 3.1**). Although the K_m values are in the same range ($K_{m,FOP}$ is ~ 2 times lower than $K_{m,F420}$), the k_{cat} value for F₄₂₀ is 25 times higher than that for FOP. The catalytic efficiency for FOP, however, is only 1 order of magnitude lower than that when using F₄₂₀. The measured k_{obs} values for different concentrations of FO could not be fitted with the formula for the Michaelis–Menten model. A good fit could be obtained with a sigmoidal function, but the plateau was never reached with FO concentrations up to 80 μM. Higher concentrations could not be tested because of the solubility of FO in buffer. Although the data could not be used to calculate the kinetic parameters of FSD-Cryar with FO, it is safe to say that the K_m must be significantly higher than that of FOP and F₄₂₀. The k_{obs} at a concentration of 80 μM FO, the highest concentration tested, is about 20% of the k_{cat} with FOP (see **Figure S 3.6**).

The kinetic parameters could also be established for FDR-Mha with both FOP and F₄₂₀ as coenzymes. But the kinetic parameters for FO, however, could not be measured. The reduced form of this deazaflavin could not be obtained as it could not be reduced by FSD-Cryar or RHA1-FGD. TfuFNO, which can reduce FO, could not be used as the necessary excess of NADPH would interfere with the FO absorbance at 400 nm. The k_{obs} data for both F₄₂₀ and FOP fitted well to a sigmoidal Hill-curve (eq 2; **Figure S 3.7** and **Figure S 3.8**). This could mean positive cooperativity or the fact that the lower concentrations of the coenzymes were in the same range as the enzyme concentration, so not being present in saturating conditions and, thus, not fitting to the Michaelis–Menten model. The same sigmoidal behavior was also seen for the activity of enzymes of the same structural fold class in *M. smegmatis*, denoted MSMEG_3356 and MSMEG_3380, with various concentrations of F₄₂₀.²⁴² The asymptotes to the plateau values of the curves still give a good description of the k_{cat} , and the K_{half} still gives an accurate estimation for coenzyme specificity. From **Table 3.1** it can be seen that FOP has somewhat lower k_{cat} and K_m values than F₄₂₀, but they are still in the same range.

Table 3.1: Steady-State Kinetic Parameters with Three Different Deazaflavin Cofactors.

Enzyme	Cofactor	k_{cat} (s ⁻¹)	K_m or K_{half} (h) (μM)	k_{cat}/K_m (M ⁻¹ s ⁻¹)	$\frac{k_{cat}, F_{420}}{K_m} / \frac{k_{cat}, FOP}{K_m}$
TfuFNO	F ₄₂₀	3.3 ^a	2.0 ^a	1.7·10 ⁶	2.0
	FOP	3.3	4.0 ^b (1.8)	8.3·10 ⁵	
	FO	2.2	4.8 ^b (2.9)	4.6·10 ⁵	
FSD-Cryar	F ₄₂₀	33.0	13.6	2.4·10 ⁶	12.6
	FOP	1.3	7.0	1.9·10 ⁵	
	FO	-	-	-	
FDR-Mha	F ₄₂₀	1.8·10 ⁻²	12.1 ^b (4.4)	1.5·10 ⁴	22.4
	FOP	1.3·10 ⁻²	19.3 ^b (2.9)	6.7·10 ²	
	FO	-	-	-	

^a: Values described by Kumar et al.²⁵³

^b: K_{half} values, according to eq 2, Hill coefficients (*h*) are given in between brackets. Errors are within a 10% range.

3.3.5 Conversion Experiments with FDR-Mha and FDR-RHA1

Since the catalytic parameters could not be determined spectrophotometrically for FDR-Mha and FO, conversion experiments were used to compare the activity of FDR-Mha and FDR-RHA1 with FO, FOP and F₄₂₀. The conversion of cinnamaldehyde was measured by reverse-phase HPLC after 3 h of incubation for all three coenzymes at concentration of 20 μM. The results show that the conversion of cinnamaldehyde is around 70% when using F₄₂₀ for both FDR-Mha and FDR-RHA1. The conversion when using FOP is close to 40%, which is in line with the spectrophotometric experiments. The conversion of cinnamaldehyde with FO as a coenzyme is lower than that of FOP by about 10 to 18 percentage points. These results show that the apparent activity follows the trend F₄₂₀>FOP>FO (see **Figure 3.4**).

3.4 Discussion

Enzymes that utilize F₄₂₀ could become a biotechnological tool of importance in the near future. The very low redox potential of the cofactor can be utilized for the bioconversion of compounds that would otherwise be recalcitrant to enzymes.^{21,188,242,258} The now known F₄₂₀-dependent reductases and cofactor recycling systems harbor interesting activities for biocatalysis.^{19,25} Genome studies revealed that many bacteria and archaea contain putative F₄₂₀-dependent enzymes that yet have to be characterized^{26,210,242} and could potentially yield new biocatalysts with novel interesting properties.

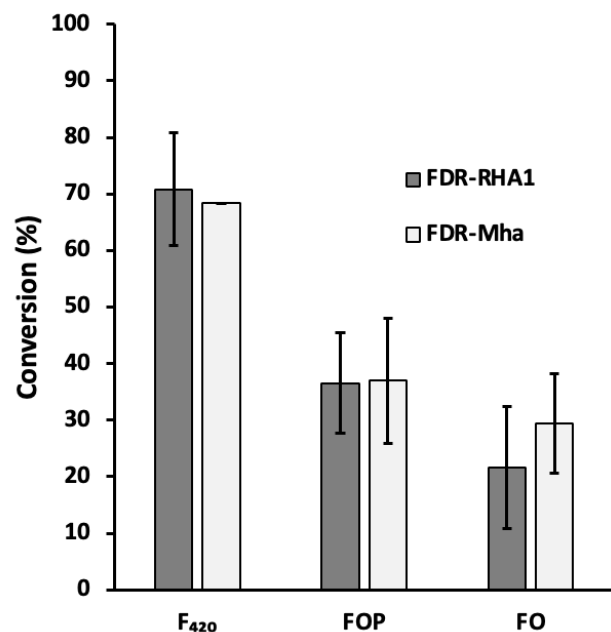


Figure 3.4: Conversion of cinnamaldehyde within 3 h of incubation at 25 °C by FDR-Mha and FDR-RHA1, using FO, FOP and F₄₂₀ as coenzymes. Experiments were performed in duplicates. Error bars represent standard deviations.

A bottleneck for application of F₄₂₀-dependent enzymes is the low availability of the cofactor, as many F₄₂₀-producing organisms are slow-growing and hard to culture, resulting in low yields.^{269,270} Furthermore, the complex structure of the cofactor prevents straightforward chemical synthesis methods. The recent and remarkable efforts by Bashiri et al.²³⁹ to heterologously produce F₄₂₀ in *E. coli* unfortunately still resulted in similar low yields as with *M. smegmatis*. This inspired us to synthesize a F₄₂₀ analogue that could replace F₄₂₀.

The crystal structures of F₄₂₀-dependent oxidoreductases show that these enzymes can mainly be divided into three distinct structural classes, namely the Rossmann fold, TIM barrel fold, and the split β -barrel like fold class.^{25,254,265} The same crystal structures also show that the major part of the poly- γ -glutamyl tail of the cofactor is not bound by the enzyme.^{229,233,252–256} The main interactions between F₄₂₀ and the enzyme are formed by the FO core structure and the phosphate group, whereas the lactyl group and poly- γ -glutamyl tail form less interactions. The TIM barrel fold and the split β -barrel like fold classes share structural homology with FMN-dependent oxidoreductases, which can explain this observed cofactor-enzyme binding pattern. Furthermore, it was recently shown by Mascotti and Kumar et al.²⁶⁵ that the TIM barrel fold clade probably has evolved from a FMN-dependent enzyme. Therefore,

we proposed FOP, 7,8-didemethyl-8-hydroxy-5-deazariboflavin-5'-phosphate, as an alternative for F₄₂₀. It is worth noting that FOP is not a naturally occurring cofactor and is also not an intermediate in the biosynthesis of F₄₂₀. Chemical hydrolysis of F₄₂₀,²⁰ in order to elucidate the structure of this cofactor by Eirich et al., however, produced FOP.²⁰ The authors then coined the term F+ for this deazaflavin compound.

The FO core structure was synthesized by a straightforward organic synthesis procedure. Similar to the biosynthesis of FMN from riboflavin, the phosphate group was then attached enzymatically at the 5'-position with the aid of an tailor-made kinase. A riboflavin kinase (RFK) was used as starting point to engineer a FO kinase since the catalytic core structure, FO, is structurally very similar to that of riboflavin. The RFK from *C. ammoniagenes*, obtained by truncation of the bifunctional FAD synthetase, RibF, was chosen as it was already well studied by Iamurri et al.²⁷¹ Previous research on the enzyme showed its ease of expression and purification and the remarkable range of riboflavin analogues that could be converted, including 5-deazariboflavin. Unfortunately, we discovered that RFK does not accept FO as substrate. Therefore, structure-inspired site-directed mutagenesis was employed to accommodate the more hydrophilic FO in the active site. Introduction of polar residues at position 21 and 85 could facilitate the hydroxyl-group of FO in an otherwise hydrophobic binding pocket. Substitutions of the phenylalanines at these positions by tyrosine and histidine yielded the most active biocatalysts. Substitution of alanine by valine or isoleucine at position 66 was crucial for introducing activity toward FO, probably to fill the space left vacant by the 7'-methyl group that is absent in FO. With these triple mutants conversion of FO into FOP could be achieved. Structure-based site-directed mutagenesis on *C. ammoniagenes* RFK can thus expand the already large substrate acceptance of riboflavin analogues even more, making it a useful tool for the synthesis of unnatural (deaza)flavin cofactors.

The drawback of riboflavin kinase is its low stability,²⁷¹ which prevents the use of cosolvents. Since the solubility of FO and other riboflavin analogues in water is quite low, relatively large reaction volumes have to be used for the production of large amounts of phosphorylated compounds. A more stable RFK could be a solution to this problem, if one would like to produce FOP or other cofactors on plant scale. Still, a 50 mL reaction resulted in the production of about 1 mg (2.5 μ mol) FOP within 24 h, which translates to a production of 50 μ mol/L. Thus, far more than the F₄₂₀ yield from *M. smegmatis*, being 1.4 μ mol/L of culture, grown over several days.

The activity of an F₄₂₀-dependent oxidoreductase from each structural class with FO, FOP, and F₄₂₀ was measured. Steady-state parameters could be determined with FOP

and F_{420} for a member of each class, spectrophotometrically. Experiments with the F_{420} -NADPH oxidoreductase from *T. fusca*, TfuFNO, a member of the Rossmann fold structural class, showed that the kinetic parameters for FO, FOP, and F_{420} are in the same range. The K_m values of FO and FOP are slightly higher, resulting in a slightly lower catalytic efficiency that is 3.7 (FO) or 2 (FOP) times lower than that for F_{420} . The similarity in kinetic parameters can be explained by the fact that only the FO core is bound to the enzyme, as can be seen in crystal structures.^{253,256}

Members from the TIM barrel fold class showed a significant decrease in activity when FO and FOP were used as coenzymes. The F_{420} -dependent glucose-6-phosphate dehydrogenase from *R. jostii* RHA1 shows no detectable activity at all for the alternative deazaflavin cofactors. The sugar-6-phosphate dehydrogenase from *C. arvum* has activity toward FOP. Although the K_m values for both FOP and F_{420} are similar, the k_{cat} for F_{420} is significantly higher than that of FOP. Still, the catalytic efficiency with FOP is only 1 order of magnitude lower, meaning that the activity with FOP is significant and that FOP could be used as an alternative non-natural cofactor for this enzyme. An ever lower activity was found for FO, indicating that the phosphate moiety of the F_{420} cofactor is important for recognition and/or productive coenzyme binding.

The kinetic parameters for both FDR-MHA1 and FDR-Mha, both members of the split β -barrel fold class for F_{420} and FOP revealed that the K_m and k_{cat} values are in the same order of magnitude, although the catalytic efficiency is 22 times higher for F_{420} than for FOP. It shows that members of this group of F_{420} -dependent enzymes, dedicated to perform reductions, also can utilize the non-natural deazaflavin cofactor that lacks the lactyl-poly glutamyl moiety. No steady-state kinetic parameters could be obtained with the reduced form of FO, because the sugar-6-phosphate dehydrogenases could not be used to prepare reduced FO. We decided to perform comparative conversion experiments with cinnamaldehyde as substrate to probe the efficiency of all three deazaflavin cofactors. Here we could see that cinnamaldehyde conversion with FOP is somewhat less effective than with F_{420} , which is in line with the results from the spectrophotometric assay. The conversions with FO are again lower than that with FOP but in the same range. It shows that all three deazaflavins are accepted by the tested reductases, suggesting that for catalysis only the FO part of the F_{420} cofactor is essential.

The experiments have shown that F_{420} -dependent enzymes of all tested structural classes are active on the non-natural, synthetic deazaflavin cofactor FOP and that the activity is typically higher when compared with its precursor, FO. It seems that

in all cases the phosphate group is important for a higher binding affinity, as seen by a lower K_m , and for a higher catalytic turnover, as seen by a higher k_{cat} . When comparing F_{420} and FOP activities the presence of a poly- γ -glutamyl tail seems to be important for higher binding affinities and higher catalytic activity. Interestingly, Ney et al. discovered that the presence of a long poly- γ -glutamyl tail of 5 to 8 glutamate residues indeed lowered the K_m , as compared with a shorter tail of two residues, because of favorable electrostatic interactions between tail and enzyme, but also lowered the k_{cat} and vice versa. The effect of higher k_{cat} with lower cofactor-affinity can be explained by higher cofactor exchange rates of enzymes at saturating conditions.²⁶ Surprisingly, the same effect on k_{cat} and K_m is not seen when the poly- γ -glutamyl tail is completely missing. It could be that the interactions between the poly- γ -glutamyl tail – however short – and the enzyme are significantly important or that the properties of the more substituted phosphate diester in F_{420} are more favorable for enzyme binding than that of the phosphate monoester in FOP.

The findings of this research show that FOP could also be used as an alternative deazaflavin cofactor *in vivo*. With having an engineered FO kinase, the introduction of a biosynthetic route toward FOP is feasible. A great advantage of FOP over FO is that it retains inside a cell, because of the charged phosphate group, similar to the conversion of riboflavin into FMN. Also, the solubility is enhanced by the addition of a phosphate group. Although the activity for FOP is lower than that for F_{420} , it is still sufficient enough for the use as a cofactor in biocatalysis, as can be seen by the relatively small differences in catalytic efficiency. The ease of production and higher product yields of the cofactor could make up for the decrease in activity when used as coenzyme in F_{420} -dependent enzyme reactions. Therefore, FOP could be the key to successful implementation of F_{420} -dependent enzymes as biocatalytic tools in industry.

Author Contributions

M.W.F., J.D. designed the project. M.T. synthesized FO and analyzed the products and intermediates of FO and FOP synthesis. J.D. Performed the mutagenesis of CaRFK, the chemoenzymatic synthesis of FOP and steady-state kinetics experiments. J.D. and M.W.F. wrote the manuscript.

Funding Sources

Funding came from the Dutch research council; NWO (VICI grant).

Notes

The authors declare no competing financial interest.

3.5 Supporting information Chapter 3

Sequences of CaRFK and the mutagenic primers can be found online, in the supporting information to the published article.

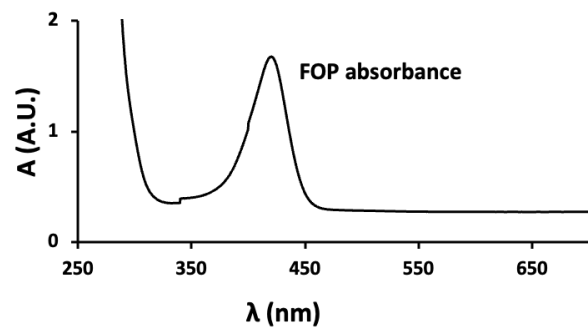


Figure S 3.1: Absorbance spectrum of FOP after purification by preparative reverse-phase liquid chromatography.

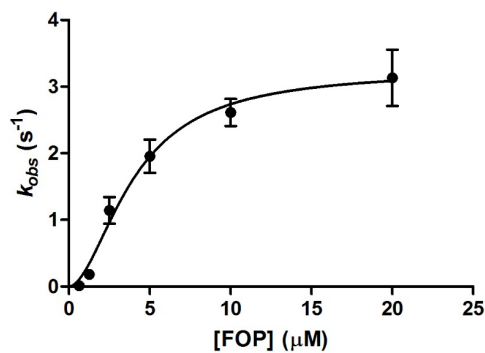


Figure S 3.2: TfuFNO activity with varying concentrations of FOP and 250 μM NADPH at 25 °C. Experiments were performed in triplicates. Data was fitted to equation 2.

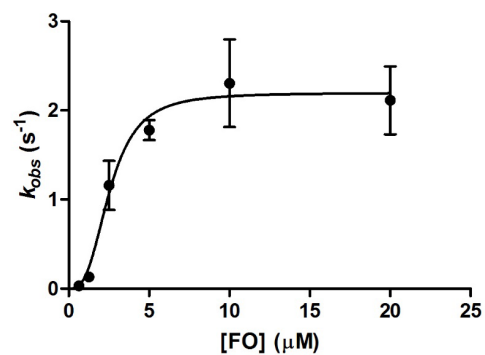


Figure S 3.3: TfuFNO activity with varying concentrations of FO and 250 μM NADPH at 25 °C. Experiments were performed in triplicates. Data was fitted to equation 2.

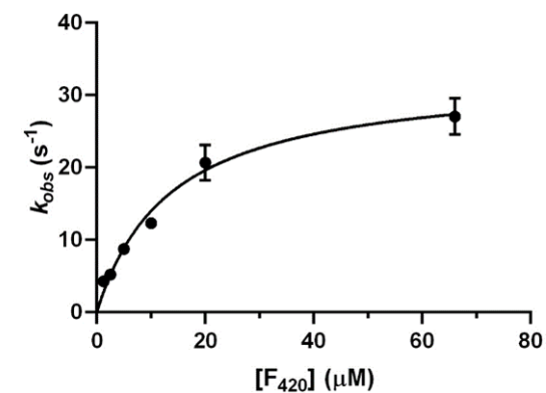


Figure S 3.4: FSD-Cryar activity with varying concentrations of F₄₂₀ and 20 mM glucose-6-phosphate at 25 °C. Experiments were performed in triplicates. Data was fitted to equation 1.

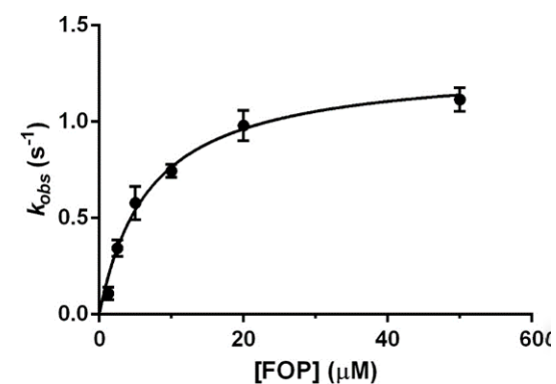


Figure S 3.5: FSD-Cryar activity with varying concentrations of FOP and 20 mM glucose-6-phosphate at 25 °C. Experiments were performed in triplicates. Data was fitted to equation 1.

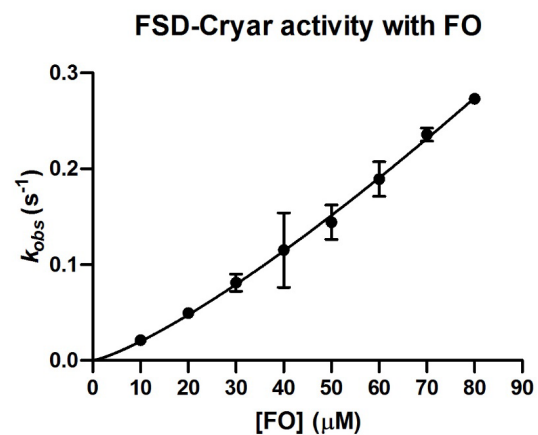


Figure S 3.6: FSD-Cryar activity with varying concentrations of FO and 20 mM glucose-6-phosphate at 25 °C. Experiments were performed in triplicates. Data was fitted to equation 1.

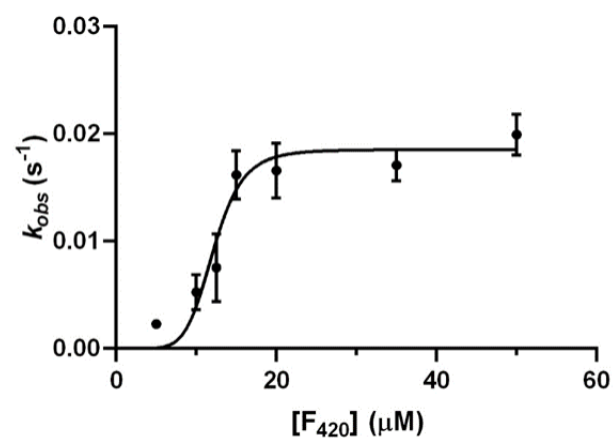


Figure S 3.7: FDR-Mha activity with varying concentrations of F420 and 1 mM 2,6,6-trimethyl-2-cyclohexene-1,4-dione at 25 °C. Experiments were performed in triplicates. Data was fitted to equation 2.

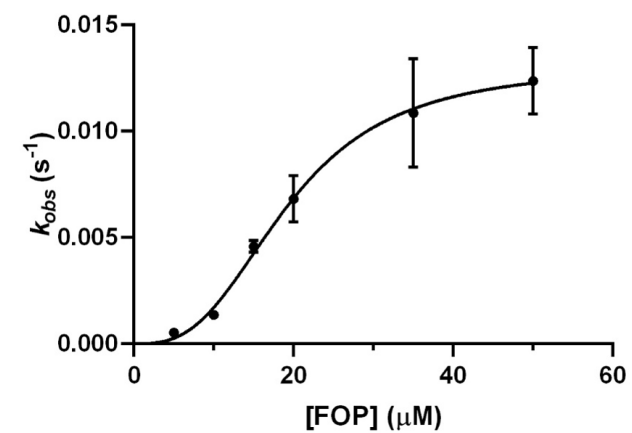


Figure S 3.8: FDR-Mha activity with varying concentrations of FOP and 1 mM 2,6,6-trimethyl-2-cyclohexene-1,4-dione at 25 °C. Experiments were performed in triplicates. Data was fitted to equation 2.

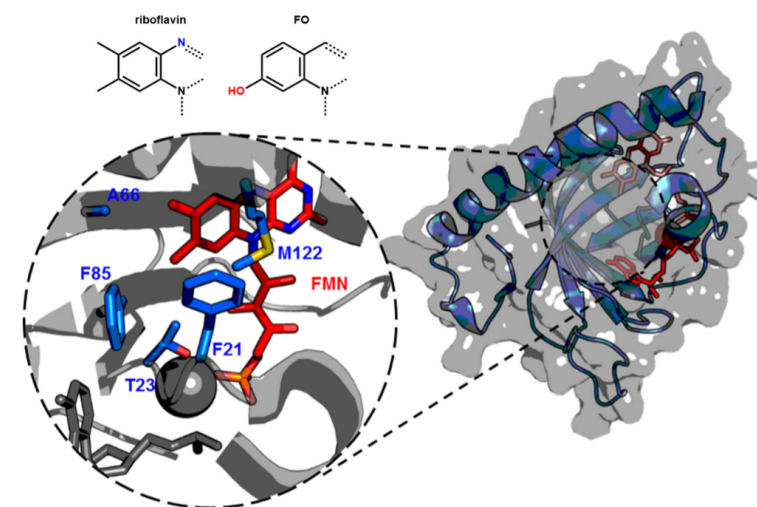


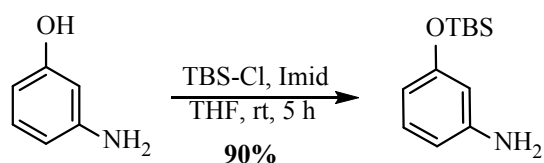
Figure S 3.9: The active site of CaRFK with residues that were selected for mutagenesis shown as blue sticks. The substrate FMN is shown in red and ATP and the magnesium ion-cofactor are shown as grey sticks and a grey sphere, respectively. PDB ID: 5A89.

Synthesis of FO and FO-7-Me

Commercially available compounds were purchased from Sigma–Aldrich, Acros Organics and Fluorochem, and used without further purification. All other solvents were obtained as analytical grade and used without further purification. Flash chromatography was performed with Silicycle silica gel SiliaFlash P60. NMR spectra were recorded on an Agilent 400-MR spectrometer (1H and 13C resonances at 400 MHz and 100 MHz, respectively). Chemical shifts are reported in parts per million (ppm) and coupling constants (J) are reported in hertz (Hz). The residual 1H signals from solvent were used as references. HRMS was measured by a Thermo scientific LTQ Orbitrap XL. The ionization mode was ESI negative and the eluent was methanol with 0.1% ammonia.

Synthesis of FO

Synthesis of 3-((tert-butyl dimethylsilyl)oxy)aniline

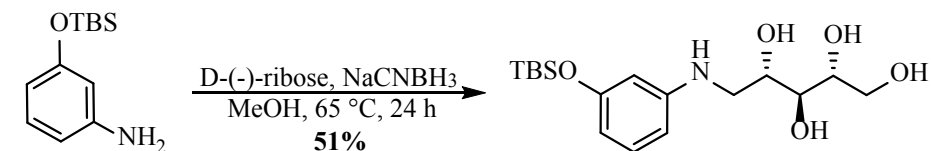


To cold solution (0 °C) of 3-aminophenol (2.00 g, 18.3 mmol) and imidazole (2.50 g, 36.7 mmol) in dry THF (100 mL) was added dropwise a solution (50% wt) of *tert*-butylchlorodimethylsilane in toluene (6.5 mL, 18.8 mmol) under N₂ during 10 minutes. A white solid formed immediately and the mixture was stirred for five additional hours at room temperature. After that, the reaction was quenched with 100 mL of water. The organic layer was separated and the water layer was extracted with diethyl ether (4 x 50 mL). Combined organic extracts were dried over anhydrous MgSO₄, filtered and concentrated by rotovap. The residue was purified by flash chromatography (SiO₂, pentane/ethyl acetate = 9/1) to yield protected aniline (3.69 g, 90%) as a colorless oil.

¹H NMR (400 MHz, DMSO-*d*₆) δ 6.84 (t, *J* = 8.0 Hz, 1H), 6.15 (ddd, *J* = 8.0, 2.1, 0.9 Hz, 1H), 6.09 (t, *J* = 2.2 Hz, 1H), 5.97 (ddd, *J* = 8.0, 2.3, 0.9 Hz, 1H), 4.99 (s, 1H), 0.93 (s, 9H), 0.15 (s, 6H).

¹³C NMR (101 MHz, DMSO-*d*₆) δ 155.8, 150.0, 129.4, 107.6, 107.2, 105.4, 25.6, 17.9, -4.4.

(2R,3S,4S)-5-((3-((tert-butyl dimethylsilyl)oxy)phenyl)amino)pentane-1,2,3,4-tetraol

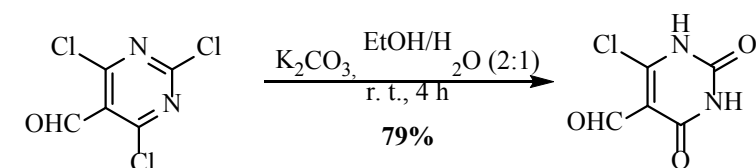


To a solution of aniline (1.46 g, 6.5 mmol) and D-ribose (2.95 g, 19.6 mmol) in dry methanol (33 mL) sodium cyanoborohydride (0.83 g, 13.2 mmol) was added under N₂ at room temperature. Then the reaction mixture was stirred and heated at 65 °C overnight. After that, the solvent was removed by rotovap and the residue was purified by flash chromatography (SiO₂, dichloromethane/methanol = 9/1) to yield product (1.18 g, 51%) as colorless solid.

¹H NMR (400 MHz, Methanol-*d*₄) δ 6.95 (t, *J* = 8.0 Hz, 1H), 6.32 (ddd, *J* = 8.2, 2.3, 0.9 Hz, 1H), 6.20 (t, *J* = 2.2 Hz, 1H), 6.13 (ddd, *J* = 8.0, 2.3, 0.9 Hz, 1H), 3.91 (ddd, *J* = 7.9, 6.3, 3.4 Hz, 1H), 3.82 – 3.72 (m, 2H), 3.69 – 3.59 (m, 2H), 3.42 (dd, *J* = 12.9, 3.4 Hz, 1H), 3.10 (dd, *J* = 12.9, 7.9 Hz, 1H), 0.97 (s, 9H), 0.17 (s, 6H).

¹³C NMR (101 MHz, Methanol-*d*₄) δ 157.9, 151.7, 130.6, 110.1, 108.1, 106.2, 74.7, 74.3, 72.2, 64.6, 47.6, 26.2, 19.0, -4.3, -4.2.

6-chloro-2,4-dioxo-1,2,3,4-tetrahydropyrimidine-5-carbaldehyde

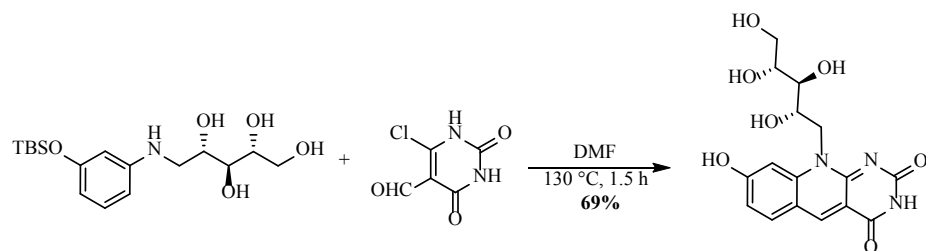


To suspension of aldehyde (1.02 g, 4.8 mmol) in mixture of ethanol/water (40 mL, v/v = 2/1) was added potassium carbonate (0.70 g, 5.1 mmol) and the resulting mixture was stirred for 4 hours at room temperature. After that the reaction was neutralized by glacial acetic acid (4-5 drops) and concentrated to 10 mL. The resulting solution was kept at 4 °C for 24 hours. The product was isolated by filtration and dried in vacuum to yield product (669 mg, 79%) as colorless solid.

¹H NMR (400 MHz, DMSO-*d*₆) δ 10.03 (s, 1H).

¹³C NMR (101 MHz, DMSO-*d*₆) δ 189.0, 171.5, 160.7, 158.8, 111.9.

Synthesis of FO



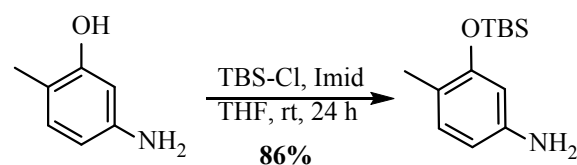
Solution of compound aminoalcohol (550.0 mg, 1.54 mmol) and aldehyde (200 mg, 1.15 mmol) in DMF (5 mL) was stirred and heated for 1.5 hours at 135 °C. After that the reaction was cooled down to room temperature and diethyl ether (10 mL) was added dropwise. The resulting mixture was kept at 4 °C for 24 hours. The product was isolated by filtration, was a small volume of cold mixture (acetonitrile/water = 1/1) and dried in vacuum to yield FO (285.5 mg, 69%) as dark red powder.

$^1\text{H NMR}$ (400 MHz, DMSO- d_6) δ 11.22 (s, 1H), 10.96 (s, 1H), 8.87 (s, 1H), 8.02 (d, $J = 8.7$ Hz, 1H), 7.39 (s, 1H), 7.03 (d, $J = 8.8$ Hz, 1H), 5.10 (d, $J = 5.4$ Hz, 1H), 4.93 (d, $J = 5.4$ Hz, 1H), 4.83 – 4.72 (m, 2H), 4.66 (d, $J = 14.6$ Hz, 1H), 4.50 – 4.43 (m, 1H), 4.23 (s, 1H), 3.69 – 3.58 (m, 3H), 3.49 – 3.44 (m, 1H).

$^{13}\text{C NMR}$ (101 MHz, DMSO- d_6) δ 164.2, 162.4, 158.1, 156.5, 144.1, 141.4, 133.7, 115.3, 115.3, 110.7, 102.2, 73.9, 72.8, 69.6, 63.4, 47.9.

Synthesis of FO-7-Me

Synthesis of 3-((tert-butyltrimethylsilyloxy)-4-methylaniline



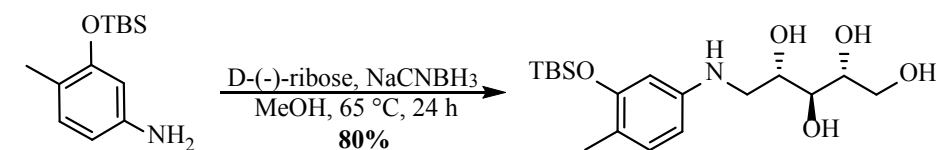
To cold solution (0 °C) of 5-amino-2-methylphenol (1.13 g, 9.2 mmol) and imidazole (1.25 g, 18.4 mmol) in dry THF (50 mL) was added dropwise a solution (50% wt) of *tert*-butylchlorodimethylsilane in toluene (4.8 mL, 13.8 mmol) under N_2 during 10 minutes. A white solid formed immediately and the mixture was stirred overnight at room temperature. After that, the reaction was quenched with 60 mL of water. Organic layer was separated and the water layer was extracted with diethyl ether (4

x 50 mL). Combined organic extracts were dried over anhydrous MgSO_4 , filtered and concentrated by rotovap. The residue was purified by flash chromatography (SiO_2 , pentane/ethyl acetate = 95/5) to afford protected aniline (1.88 g, 86%) as an orange oil.

$^1\text{H NMR}$ (400 MHz, DMSO- d_6) δ 1H NMR 6.73 (d, $J = 7.9$ Hz, 1H), 6.11 (s, 1H), 6.09 (d, $J = 7.9$ Hz, 1H), 4.77 (s, 2H), 1.97 (s, 3H), 0.97 (s, 9H), 0.17 (s, 6H).

$^{13}\text{C NMR}$ (101 MHz, DMSO- d_6) δ 153.6, 147.7, 130.7, 114.6, 107.4, 104.9, 25.7, 17.9, 15.6, -4.3.

(2R,3S,4S)-5-((3-((tert-butyltrimethylsilyloxy)-4-methylphenyl)amino)pentane-1,2,3,4-tetraol

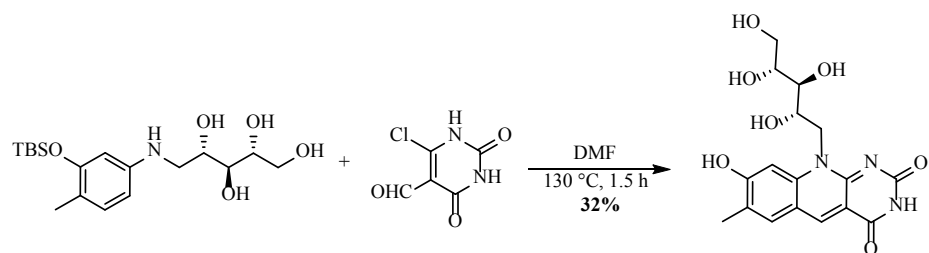


To solution of aniline (1.63 g, 6.9 mmol) and D-ribose (3.13 g, 20.8 mmol) in dry methanol (35 mL) was sodium cyanoborohydride (0.90 g, 14.3 mmol) under N_2 at room temperature. Then the reaction mixture was stirred and heated at 65 °C overnight. After that, the solvent was removed by rotovap and the residue was purified by flash chromatography (SiO_2 , dichloromethane/methanol = 9/1) to afford product (2.03 g, 80%) as colorless sticky oil.

$^1\text{H NMR}$ (400 MHz, Methanol- d_4) δ 6.86 (d, $J = 8.1$ Hz, 1H), 6.27 (dd, $J = 8.1, 2.3$ Hz, 1H), 6.23 (d, $J = 2.3$ Hz, 1H), 3.91 (ddd, $J = 7.6, 6.4, 3.4$ Hz, 1H), 3.82 – 3.73 (m, 2H), 3.69 – 3.60 (m, 2H), 3.41 (dd, $J = 12.8, 3.4$ Hz, 1H), 3.08 (dd, $J = 12.8, 7.8$ Hz, 1H), 2.06 (s, 3H), 1.02 (s, 9H), 0.21 (s, 6H).

$^{13}\text{C NMR}$ (101 MHz, Methanol- d_4) δ 155.6, 149.3, 132.1, 118.5, 108.1, 106.0, 74.8, 74.3, 72.2, 64.6, 48.1, 26.3, 19.1, 16.3, -3.9, -4.0.

Synthesis of FO-7-Me



Solution of compound aminoalcohol (433.0 mg, 1.16 mmol) and aldehyde (127 mg, 0.73 mmol) in DMF (4 mL) was stirred and heated for 1.5 hours at 135 °C. After that the reaction was cooled down to room temperature and diethyl ether (10 mL) was added dropwise. The resulting mixture was kept at 4 °C for 24 hours. The product was isolated by filtration, was a small volume of cold mixture (acetonitrile/water = 1/1) and dried in vacuum to afford FO-7-Me (87.6 mg, 32%) as yellow powder.

¹H NMR (400 MHz, DMSO-*d*₆) δ 11.34 (s, 1H), 10.92 (s, 1H), 8.79 (s, 1H), 7.87 (s, 1H), 7.42 (s, 1H), 5.08 (d, *J* = 5.6 Hz, 1H), 4.95 (d, *J* = 5.2 Hz, 1H), 4.85 – 4.75 (m, 1H), 4.69 (d, *J* = 5.2 Hz, 2H), 4.49 (s, 1H), 4.30 – 4.18 (m, 1H), 3.75 – 3.62 (m, 2H), 3.62 – 3.54 (m, 1H), 3.52 – 3.41 (m, 1H), 2.23 (s, 3H).

¹³C NMR (101 MHz, DMSO-*d*₆) δ 164.2, 162.6, 157.6, 156.5, 142.8, 140.4, 132.4, 125.1, 115.1, 109.8, 101.3, 74.0, 72.7, 69.7, 63.4, 48.0, 15.6.

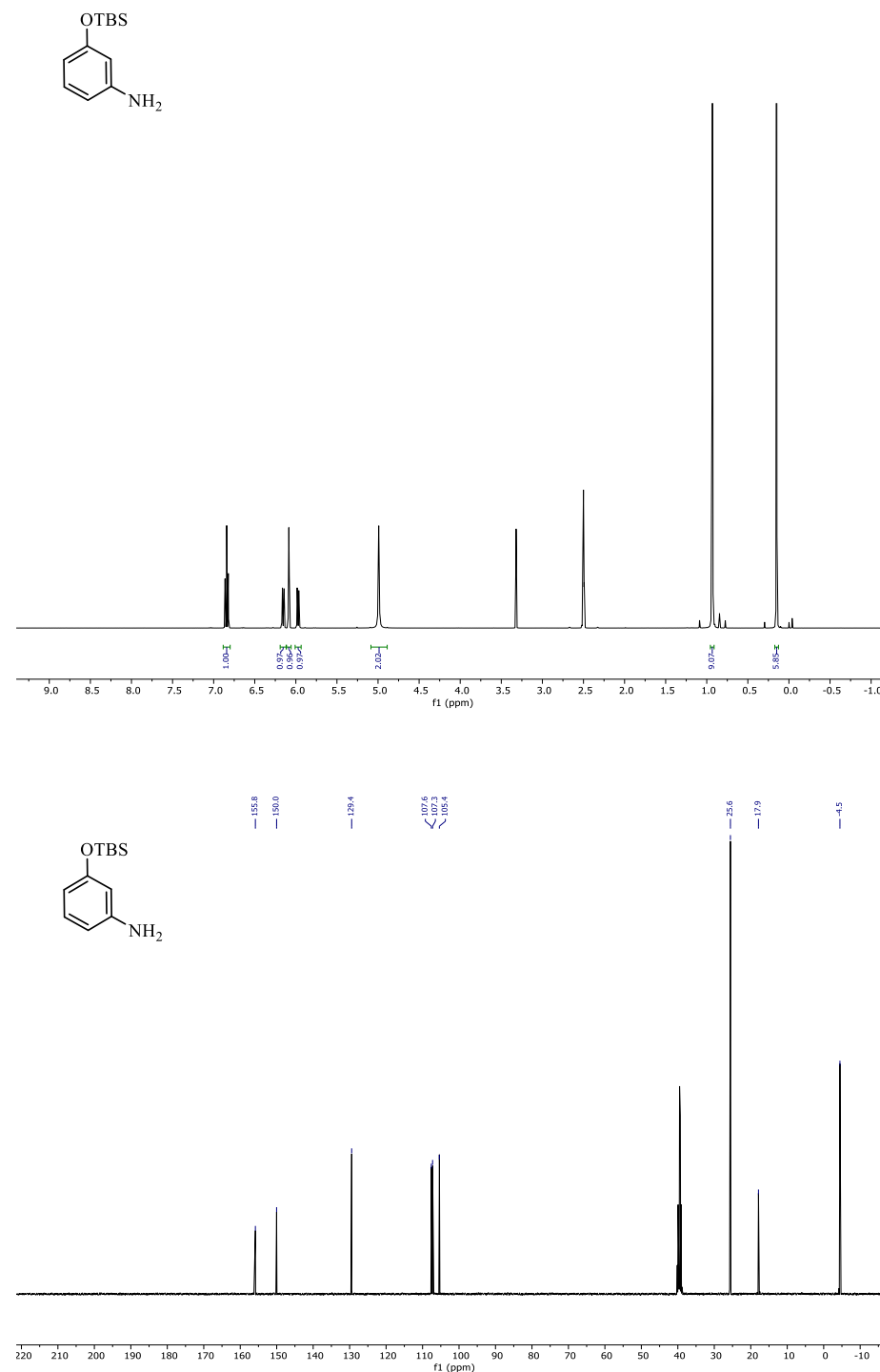
HRMS of FOP (see below)

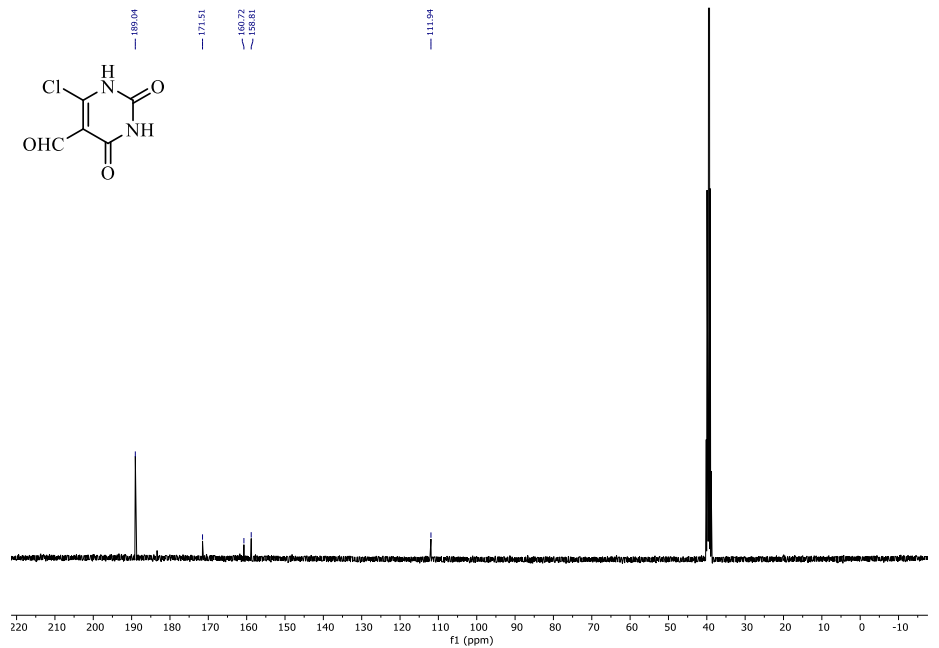
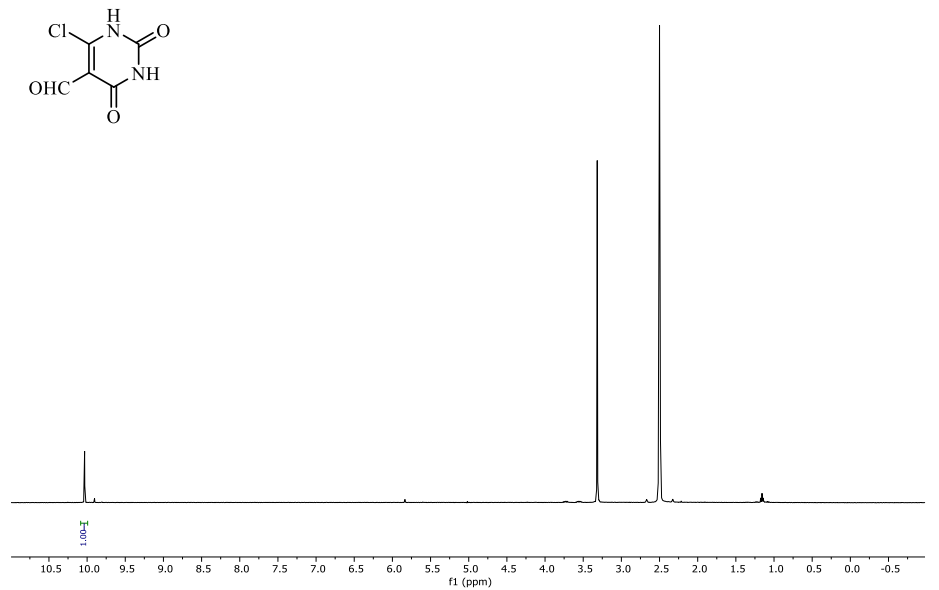
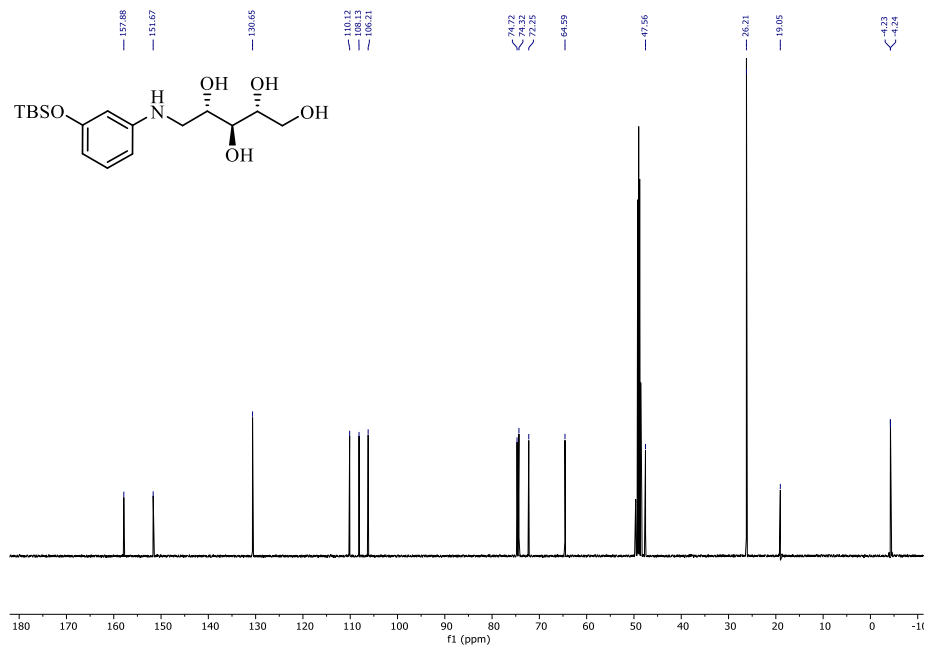
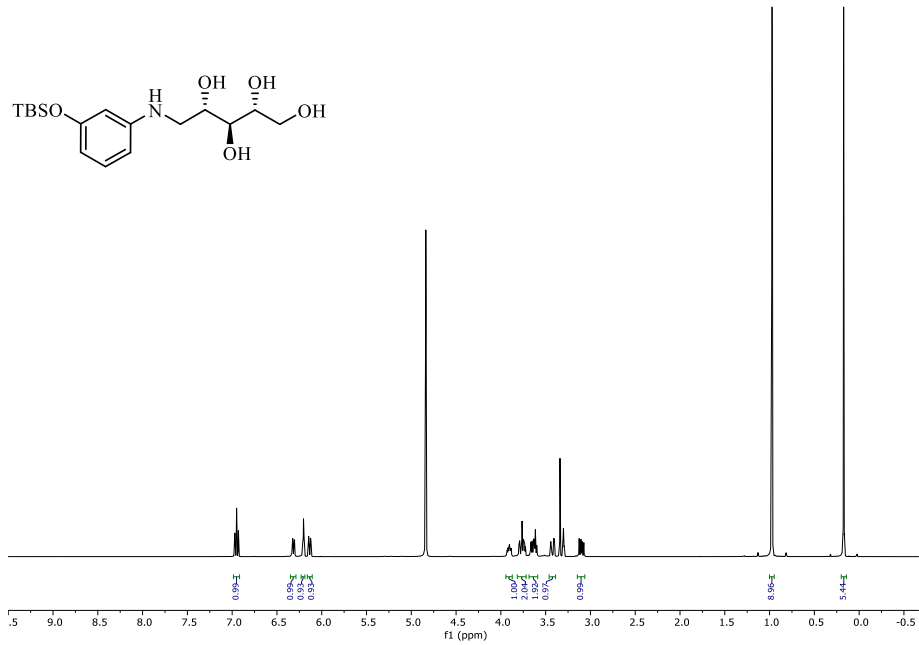
HRMS (ESI) calculated for C₁₆H₁₇N₃O₁₀P⁻ [M-H]⁻: 442.0646, found: 442.0644.

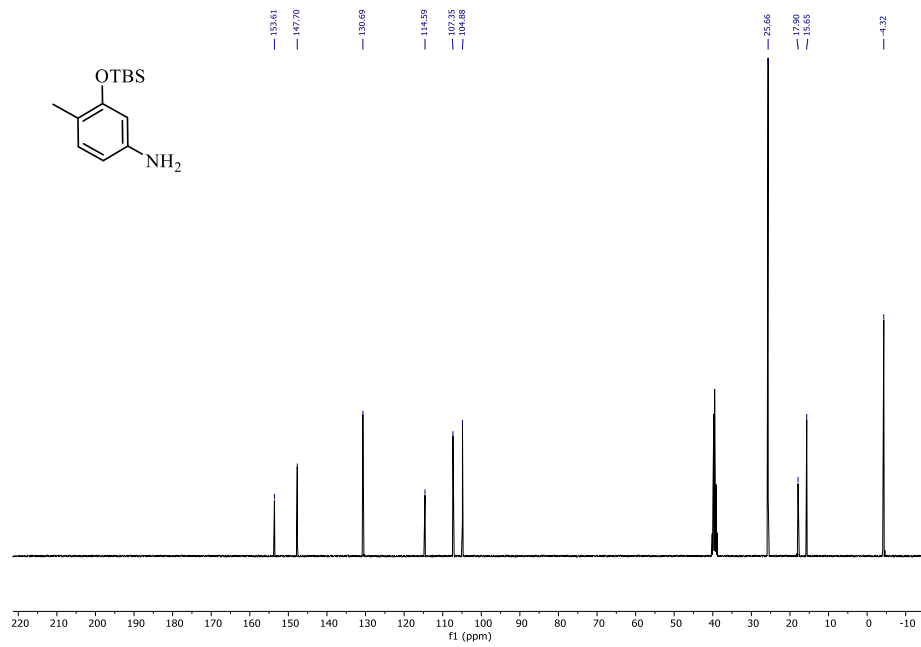
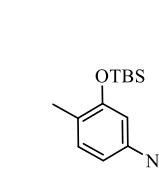
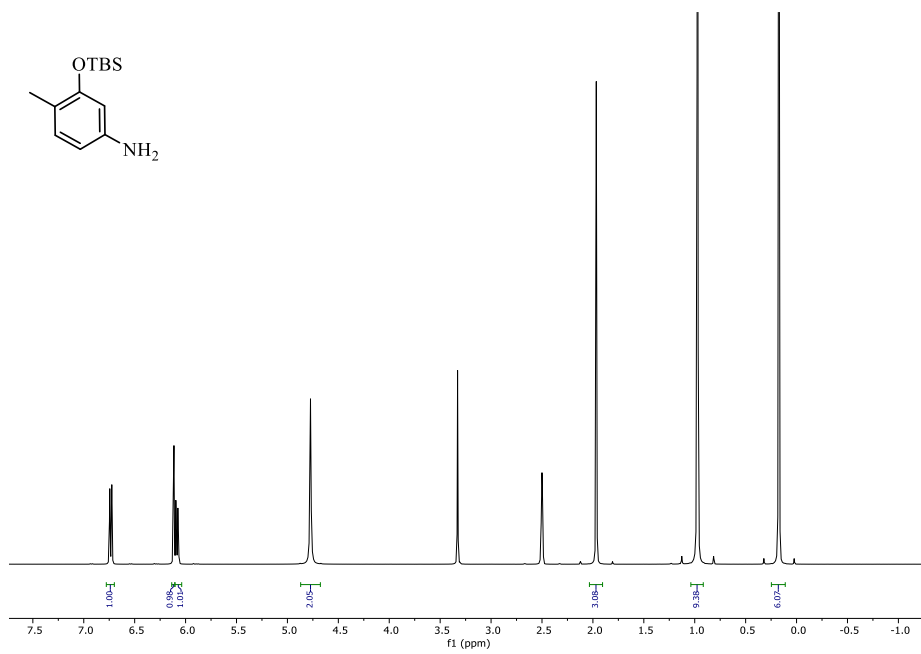
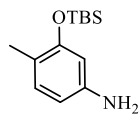
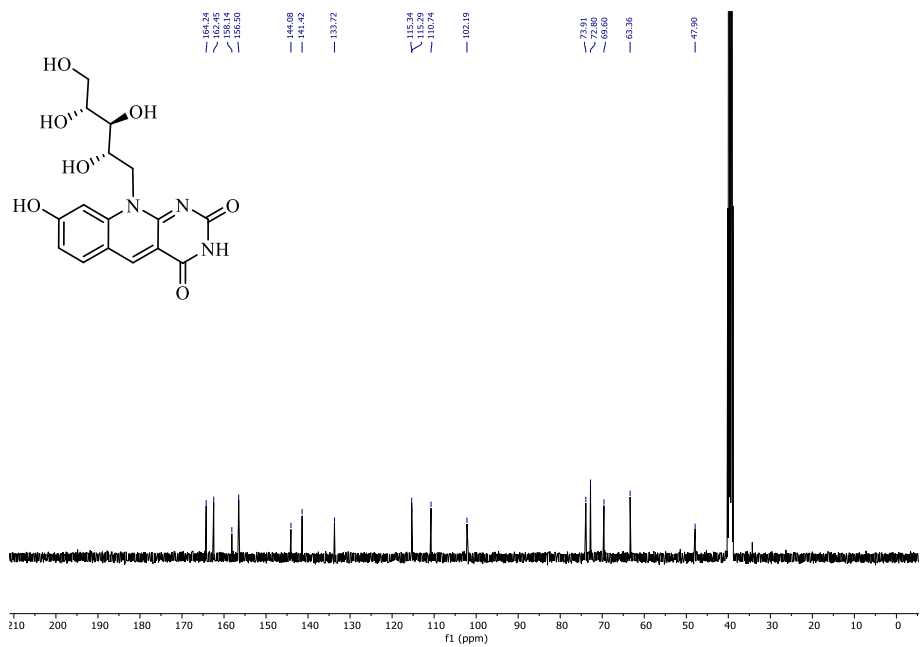
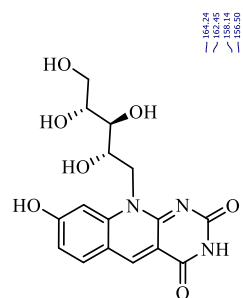
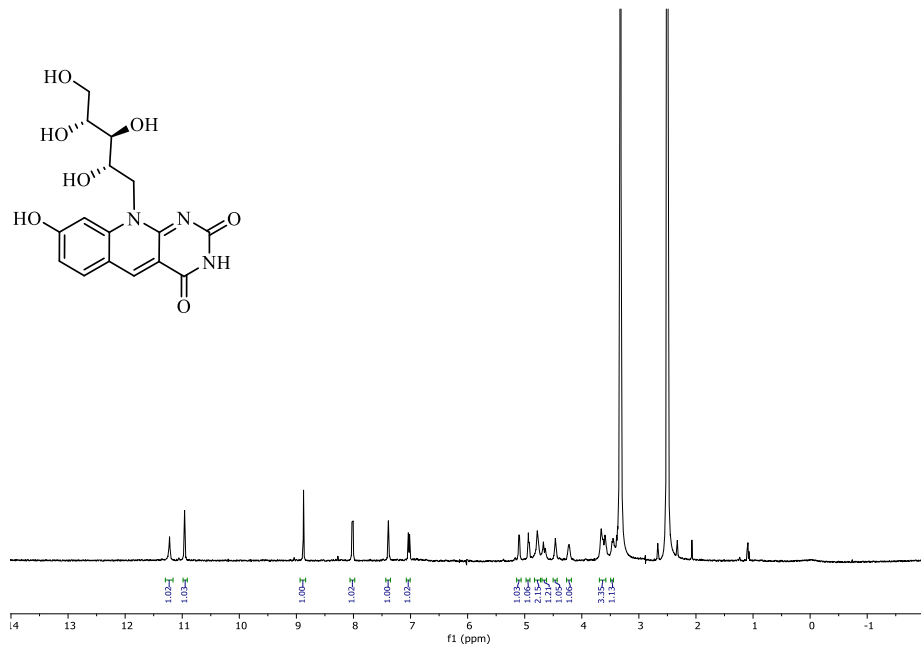
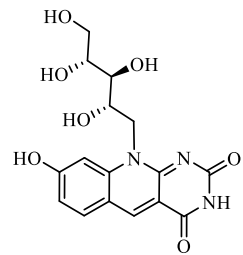
HRMS of FO-7-Me-P (see below)

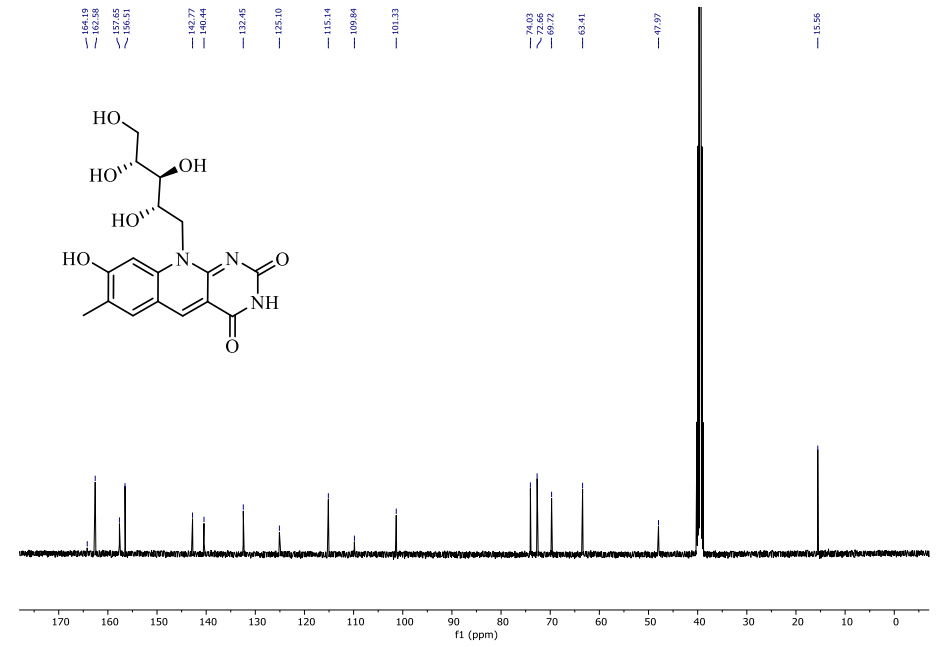
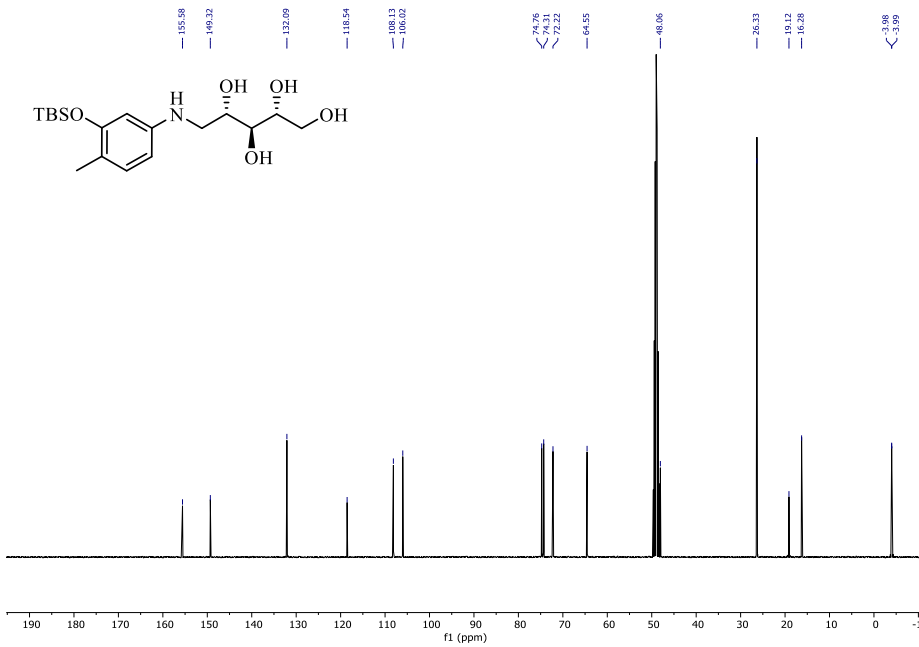
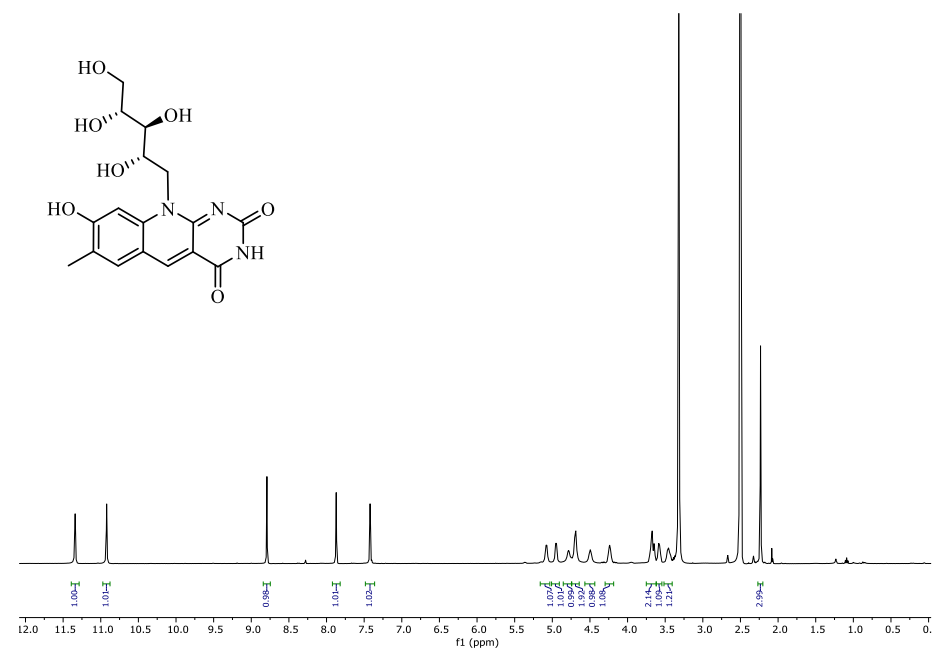
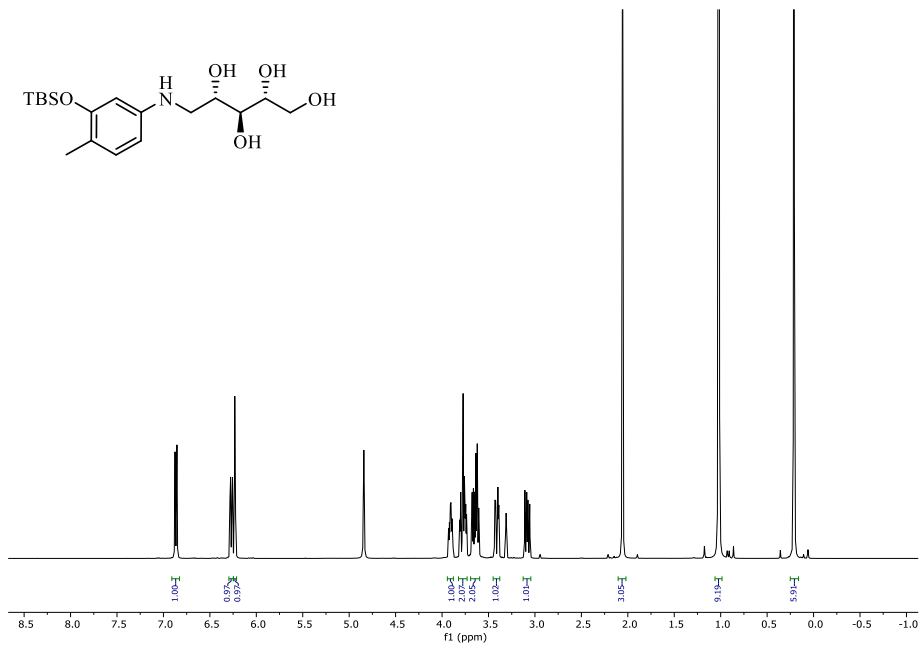
HRMS (ESI) calculated for C₁₇H₁₉N₃O₁₀P⁻ [M-H]⁻: 456.0803, found: 456.0790.

NMR spectra

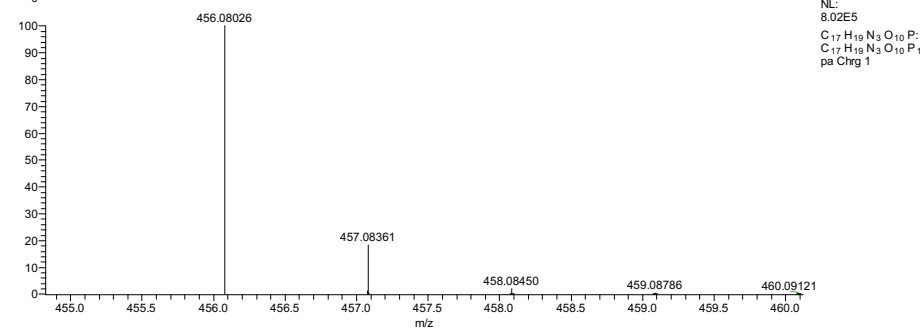
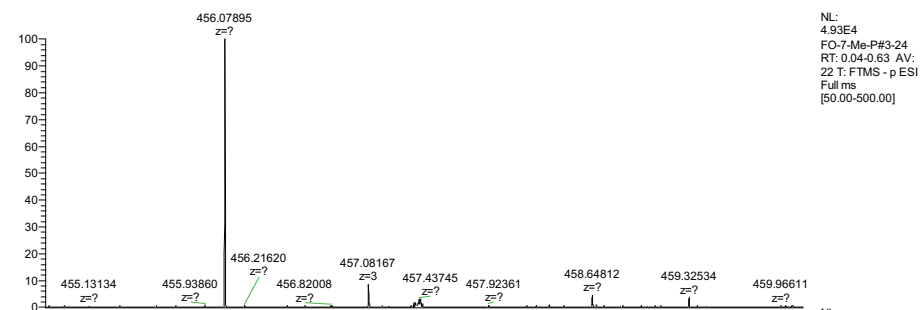
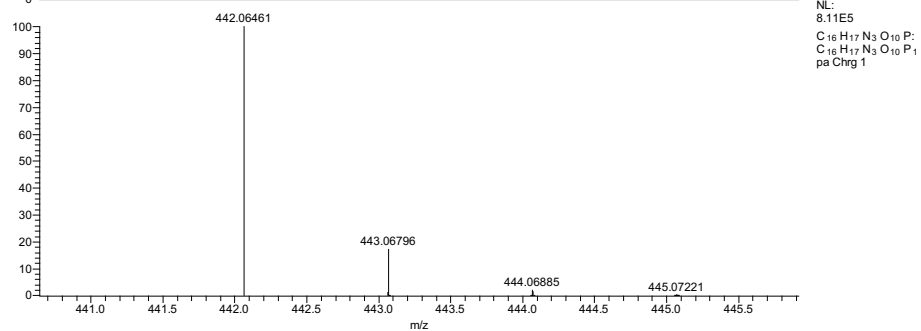
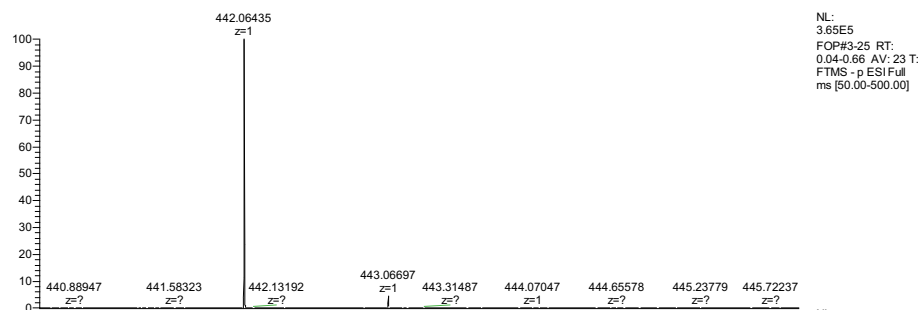








HRMS of FO-P (top) and FO-7-Me-P (bottom)



CHAPTER 4

Introducing an artificial deazaflavin cofactor in *Escherichia coli* and *Saccharomyces cerevisiae*

Jeroen Drenth^{1‡}, Misun Lee^{1‡}, Milos Trajkovic¹, René M. de Jong² and
Marco W. Fraaije^{1*}

¹Molecular Enzymology Group, University of Groningen, Nijenborgh 4, 9747AG Groningen,
The Netherlands

²DSM Biotechnology Center, Alexander Fleminglaan 1, 2613 AX Delft, The Netherlands

*These authors contributed equally

This chapter is based on a published article: ACS Synth. Biol. 2022, 11, 2, 938–952.

Abstract

Deazaflavin-dependent whole-cell conversions in well-studied and industrially relevant microorganisms such as *Escherichia coli* and *Saccharomyces cerevisiae* have high potential for the biocatalytic production of valuable compounds. The artificial deazaflavin FOP (FO-5'-phosphate) can functionally substitute the natural deazaflavin F_{420} and can be synthesized in fewer steps, offering a solution to the limited availability of the latter due to its complex (bio)synthesis. Herein we set out to produce FOP *in vivo* as a scalable FOP production method and as a means for FOP-mediated whole-cell conversions. Heterologous expression of the riboflavin kinase from *Schizosaccharomyces pombe* enabled *in vivo* phosphorylation of FO, which was supplied by either organic synthesis *ex vivo*, or by a co-expressed FO synthase *in vivo*, producing FOP in *E. coli* as well as in *S. cerevisiae*. Through combined approaches of enzyme engineering as well as optimization of expression systems and growth media, we further improved the *in vivo* FOP production in both organisms. The improved FOP production yield in *E. coli* is comparable to the F_{420} yield of native F_{420} -producing organisms such as *Mycobacterium smegmatis*, but the former can be achieved in a significantly shorter time frame. Our *E. coli* expression system has an estimated production rate of $0.078 \mu\text{mol L}^{-1} \text{h}^{-1}$ and results in an intracellular FOP concentration of about $40 \mu\text{M}$, which is high enough to support catalysis. In fact, we demonstrate the successful FOP-mediated whole-cell conversion of ketoisophorone using *E. coli* cells. In *S. cerevisiae*, *in vivo* FOP production by SpRfK using supplied FO was improved through media optimization and enzyme engineering. Through structure-guided enzyme engineering, a SpRfK variant with 7-fold increased catalytic efficiency compared to the wild type was discovered. By using this variant in optimized media conditions, FOP production yield in *S. cerevisiae* was 20-fold increased compared to the very low initial yield of $0.24 \pm 0.04 \text{ nmol per g dry biomass}$. The results show that bacterial and eukaryotic hosts can be engineered to produce the functional deazaflavin cofactor mimic FOP.

4.1 Introduction

Asymmetric hydrogenations are important for the synthesis of high value compounds, such as pharmaceuticals. Some of these can be synthesized under mild conditions by enzymatic reductions of imines, ketones and activated C=C-bonds, with high enantiomeric access.⁴ Cofactor F_{420} -dependent oxidoreductases show a high potential as biocatalysts for these kinds of reactions.^{19,56} The low redox potential of -360 mV ,²¹ when compared to other coenzymes like FAD (-219 mV),²⁷⁵ FMN (-205 mV)²⁷⁶ and NAD(P)⁺ (-320 mV), makes F_{420} an excellent reducing agent. Furthermore, this 7,8-didemethyl-8-hydroxy-5-deazaflavin (**Figure 4.1**) is an obligate

two-electron carrier, like NAD(P)H, which prevents potential radical side reactions and ensures a high tolerance to molecular oxygen.^{22,277} Whereas the flavin (FAD/FMN) and nicotinamide (NAD⁺/NADP⁺) cofactors are ubiquitous in all existing life forms, the deazaflavin cofactor F_{420} is mainly found in Actinobacteria and methanogenic archaeal species.^{27,270}

Despite the potential use of the high reduction power and various reaction scopes of F_{420} for interesting industrial applications,⁵⁶ its low availability hampers further exploration and exploitation of the cofactor and its respective deazaflavin-dependent enzymes. Although F_{420} can be purified from methanogens and Actinobacteria such as *M. smegmatis*, extraction from these organisms only yields several micromoles per liter of culture.^{269,270} Furthermore, using these organisms in industrial settings is not favorable due to the slow growth and potential hazards related to the cultivating condition and pathogenicity.²⁷⁰ Therefore, F_{420} production in more commonly used microorganisms by genetic and metabolic engineering is of great interest. Recent studies show that heterologous expression of the F_{420} -biosynthetic pathway in *E. coli* can produce the cofactor as well, albeit with lower yields than that are produced naturally in *M. smegmatis* ($\sim 27 \text{ nmol L}^{-1}$ of culture in *E. coli*, compared to $1.43 \mu\text{mol L}^{-1}$ in *M. smegmatis*).^{239,240,270} The heterologous production yield of the cofactor can be improved through optimizing growth conditions as it was demonstrated in a follow-up study.²⁷⁸

As an elegant alternative to F_{420} , we previously showed that the chemoenzymatically synthesized artificial biomimetic deazaflavin FOP (FO-5'-phosphate, **Figure 4.1**) is also accepted by a range of F_{420} -dependent enzymes and can be produced in comparatively higher amounts.³² The low water solubility of the chemically synthesized precursor FO, as well as the stability of the employed kinase, make upscaling for industrial applications still challenging. Furthermore, the relatively costly ATP, that is used for *in vitro* phosphorylation, is also an upscaling obstacle. *In vivo* FOP production, however, could overcome the aforementioned complications, as a cost efficient, green and scalable alternative. The two-step biosynthesis of FOP, using a FO synthase and an engineered riboflavin kinase, could also be a more viable alternative to the multi-step biosynthesis of F_{420} . Producing FOP in commonly used microorganisms such as *E. coli* or yeast can help advance F_{420} -related research. These organisms are easy to handle and well-established genetic tools are available for enzyme and strain engineering. And using strains such as *S. cerevisiae*, which is recognized as a GRAS organism ("generally recognized as safe"), is an advantage for industrial production of pharma- or food-related compounds.

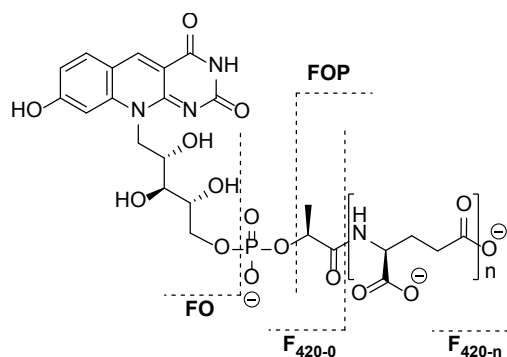
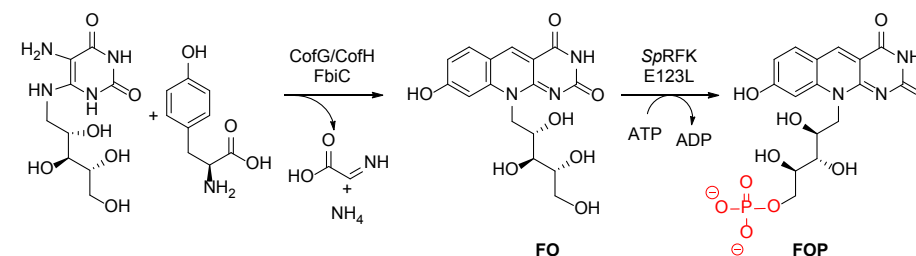


Figure 4.1: Structure of F₄₂₀ and its precursors FO and F_{420-n}, as well as the artificial cofactor analogue FO-5'-phosphate, FOP.

In this study, we explore FOP production in both *E. coli* and *S. cerevisiae* in view of future applications in large scale production of the artificial F₄₂₀ biomimetic for *in vitro* purposes, as well as whole-cell FOP-mediated conversions. These whole-cell approaches could have several advantages, such as: 1) no need for enzyme purification, 2) no need for *in vitro* FOP synthesis, 3) easy catalyst-product separation, 4) low cost, and 5) no need for additional cofactors and sacrificial electron donors, as these are already present in the cell.

In F₄₂₀-producing organisms the catalytic core, FO, is synthesized by radical SAM-dependent reactions that are catalyzed by either a single bifunctional enzyme (FbiC) or two enzymes (CofG and CofH).^{27,237,279} The starting materials for FO biosynthesis, tyrosine and 5-amino-6-ribitylamino-2,4[1H,3H]-pyrimidinedione, are ubiquitous metabolites.²⁸⁰ FO synthesis could therefore also be performed in *E. coli* and *S. cerevisiae* by heterologous expression of a FO synthase (FbiC or a combination of CofG and CofH). Phosphorylating the 5'-position of the D-ribitol moiety of FO would then yield the unnatural cofactor FOP. Herein we show the successful de novo biosynthesis of FOP in *E. coli* by co-expressing FO-synthase and a riboflavin kinase from *Schizosaccharomyces pombe* (*SpRfK*) with a two-plasmid system (**Scheme 4.1**). *SpRfK* showed higher activity than the previously used engineered kinase from *Corynebacterium ammoniagenes* (*CaRfK*).³² Furthermore, unlike *CaRfK* which is a bifunctional riboflavin kinase/FMN adenylyltransferase, *SpRfK* is a monofunctional riboflavin kinase so that the truncation, which may decrease enzyme stability, is not required. The FOP production in *E. coli* was further optimized by structure-guided RFK engineering, as well as varying the FO synthases, *E. coli* expression strains, expression temperatures, expression vectors and growth media. Gratifyingly, this resulted in FOP yields similar to F₄₂₀ yields in *M. smegmatis*.



Scheme 4.1: De novo biosynthesis of FOP in *E. coli*. The FO synthase synthesizes FO using tyrosine and 5-amino-6-ribitylamino-2,4[1H,3H]-pyrimidinedione. Subsequent 5'-phosphorylation by an engineered riboflavin kinase from *S. pombe* yields FOP (FO-5'-phosphate).

A hybrid synthesis approach was used to produce FOP in *S. cerevisiae* by using heterologously expressed *SpRfK* and FO supplemented to the media. We focused on the optimization of *in vivo* phosphorylation of FO in *S. cerevisiae* due to the low FOP yield. We first analyzed the effect of medium composition on FOP production and discovered that supplementary riboflavin and amino acids, as well as FO concentration in media affect the final FOP yield significantly. Engineering of *SpRfK* was also employed to increase the FOP yield. By screening 90 *in silico* designed variants based on the *in vivo* FOP yield, we identified a variant showing more than a 2-fold higher yield than the wild type kinase. By using the optimized FO kinase and growth media optimization, we achieved a significantly improved FOP production in *S. cerevisiae*.

By demonstrating the *in vivo* FOP production in *E. coli* and *S. cerevisiae* and several approaches to improve the yield, this study facilitates further development of both bacterial- and yeast-based whole-cell deazaflavin-mediated reductions and/or production of deazaflavin cofactors.

4.2 Materials and methods

4.2.1 Strains and cloning

The bacterial expression and cloning strains *Escherichia coli* NEB 10-beta, BL21 (DE3) and C41 (DE3) were obtained from New England Biolabs (NEB, Ipswich, MA, U.S.A.). *S. cerevisiae* strain CEN. PK2-1C was purchased from Euroscarf. All genes used for FOP production and whole-cell FOP-mediated conversion in *E. coli* were codon-optimized and synthesized by GenScript Biotech, with flanking 5'-NcoI/3'-HindIII or 5'-NdeI/3'-PacI restriction sites for cloning into multiple cloning site 1 (MCS1) or 2 (MCS2) of the used Duet vectors, respectively. Genes were cloned into the Duet-vectors by restriction/ligation, using standard protocols. For *in vivo* FO phosphorylation experiments in *E. coli*, the codon-optimized *SpRfK* was cloned into

a pBAD vector. The mutant E123L was constructed on this vector using a standard site-directed mutagenesis method. For *in vitro* characterization of SpRfK, a codon-optimized gene was cloned into a pBAD vector with N-terminal 6xHis-tag using the Goldengate assembly method.²⁸¹ These vector constructs were transformed into *E. coli* NEB 10-beta for vector amplification and storage.

All plasmids used for *S. cerevisiae* work were assembled using a modular vector cloning kit (MoClo-YTK, Addgene) following the protocol of Lee et al.²⁸² For FOP production in *S. cerevisiae*, a codon-optimized SpRfK gene with 5'- and 3'- flanking regions containing *BasI* and *BsmbI* restriction sites was purchased from Twist Bioscience and assembled into a 2 μ -based *E. coli* – yeast shuttle vector (pTEF-SpRfK). The transcription of the SpRfK gene in *S. cerevisiae* was regulated by the pTEF1 promoter and a tTDH1 terminator. The URA3 gene was used as an auxotrophic marker. The sequences of the optimized genes can be found in **Table S1**. **Table S2** shows all the constructs from this study. Both tables can be found in the online supplementary information to the article.

4.2.2 Purification of SpRfK

For *in vitro* characterization, SpRfK was expressed in *E. coli* NEB 10-beta. The expression was induced by adding 0.2% (v/v) L-arabinose to the pBAD-N-6xHis-SpRfK harboring *E. coli* culture in Terrific Broth (TB) containing 50 mg/L ampicillin. After the growth at 37 °C for 16 h, the culture was harvested. The N-terminal 6xHis-tagged SpRfK was purified using metal affinity chromatography (Ni-NTA) by the means of gravity flow. The buffers used for the purification are as follow: A – 50 mM KPi, pH 7.4; B - buffer A + DNase (20 μ g/mL) + 1mM MgCl₂ + 1 mM PMSF; C – buffer A + 15 mM imidazole; D – buffer A + 500 mM imidazole. The harvested cells were washed with buffer A and resuspended in buffer B subsequently. The cells were disrupted by sonication (Sonics Vibra-Cell VCX 130 sonicator, cycle of 2 s on and 4 s off for 4 min at 70 % amplitude) and the cell debris was removed by centrifugation for 40 min at 31,000g, 4 °C. The supernatant was applied to the Ni-NTA resin that was pre-equilibrated with buffer A. The column was washed with 10 column volume of buffer A and 20 column volume of buffer C, subsequently. SpRfK was eluted with three column volumes of buffer D. The eluent was desalted using EconoPac 10-DG desalting column (Bio-Rad) pre-equilibrated with buffer A.

4.2.3 FO synthesis

7,8-didemethyl-8-hydroxy-5-deazariboflavin (FO) was chemically synthesized as described previously by Drenth et al.³²

4.2.4 *In vitro* activity of purified SpRfK

1 mL reaction mixtures containing 50 μ M FO, 0.5 mM ATP, 2 mM Mg²⁺ and 1 μ M SpRfK were incubated at 30 °C, pH 7.0 (50 mM HEPES) for 1 h. The reaction was stopped by heating up the sample at 95 °C for 10 min and the precipitants were removed by centrifugation at 17,000g for 10 min. The reaction was analyzed by HPLC and LC-MS.

4.2.5 Steady-state kinetic measurements

To determine the kinetic parameters, wild-type SpRfK and variants were expressed in *E. coli* and purified as described above. The reactions were performed at 30 °C, pH 7.0 (50 mM KPi) in a total volume of 1 mL. The reaction mixtures contained different concentrations of FO, ranging from 5 to 400 μ M, 0.5 mM ATP, 2 mM Mg²⁺ and 0.1 μ M SpRfK. 150 μ L of the mixtures were collected at 5, 10, 15, 20 and 25 min and the reactions were stopped by heating the samples at 95 °C for 5 min. After centrifugation to remove aggregates, the samples were analyzed by HPLC. The concentration of the produced FOP at each time point was calculated using the purified FOP calibration curve and then used to calculate k_{obs} (s⁻¹) at each FO concentration. The calculated k_{obs} values were plotted against the FO concentration and were fitted to the Michaelis-Menten model, using GraphPad Prism 6 to determine the kinetic parameters.

4.2.6 FMN inhibition

1 mL reaction mixtures containing 50 μ M or 200 μ M FO, 0 – 10 μ M FMN, 0.5 mM ATP, 2 mM Mg²⁺ and 1 μ M SpRfK were incubated at 30 °C, pH 7.0 (50 mM HEPES). After 20 min, the reactions were stopped by heating at 95 °C for 10 min. The samples were cleaned up by centrifugation at 17,000 \times g for 10 min and the FOP conversion was analyzed by HPLC

4.2.7 Enzyme expression and FO/FOP production in *E. coli* strains

pETDuet_CofG/H, pETDuet_ScFbiC and pETDuet_MsFbiC were transformed into *E. coli* BL21 (DE3) or C41 (DE3) for FO synthase expression and FO production screening. Either pCDFDuet_SpRfK E123L or pRSFDuet_SpRfK E123L was co-transformed into *E. coli* BL21 (DE3) or C41 (DE3) with either pETDuet_CofG/H, pETDuet_ScFbiC or pETDuet_MsFbiC for *in vivo* FOP production. Single transformation colonies were picked and grown overnight at 37 °C, 135 rpm, in 5 mL terrific broth (TB) with the appropriate antibiotic(s). The overnight cultures were diluted 1:100 in 50 mL fresh TB, LB or M9 medium, supplemented with either 1% glucose (w/v) or 1% glycerol (w/v), in 250 mL Erlenmeyer flasks, with the same antibiotic(s). The cultures were incubated at 37 °C, 135 rpm for 3 h, after which the cultures were induced with 1 mM Isopropyl β -D-1-thiogalactopyranoside (IPTG). The cultures were further incubated at 24 or 37 °C, 135 rpm, for 12 to 20 h.

4.2.8 FO and FOP isolation from *E. coli* and analysis

The cultures described above were harvested by centrifugation (4000g, 20 min, 4 °C, Beckman-Coulter centrifuge) and the pellets were resuspended in 5 mL 50 mM Tris-HCl, pH 8 containing, 1 µg mL⁻¹ DNase, 1 µg mL⁻¹ lysozyme and 0.1 mM phenylmethylsulfonyl fluoride (PMSF). The cells were lysed by sonication, using a Sonics Vibra-Cell VCX 130 sonicator with a 3 mm stepped microtip (5s on, 5s off, 70% amplitude, 10 min) and the extracts were cleared by centrifugation (8000 × g, 45 min, 4 °C). The amount of *in vivo* produced FO and FOP was quantified by HPLC analysis. FO that may leak out of the cells to the media²⁷⁰ was not included in the measurement. Samples were prepared in the following way: 300 µL formic acid and 1 mL of Cell free extracts (CFE) were mixed and incubated on ice for 5 min. Then, 200 µL 1.6 mM NaOH was added and spun down at 8000g, 4 °C, for 15 min. 10 µL supernatant was used for analysis. For further calculations the following assumptions were made: 1 OD₆₀₀ $\hat{=}$ 0.396 gDCW L⁻¹, 1 OD₆₀₀ $\hat{=}$ 7.8·10⁸ cells mL⁻¹ and the *E. coli* cell volume is 4.4·10⁻¹⁵ L.^{283,284}

4.2.9 Whole-cell conversion using FOP-producing *E. coli*

The plasmid vectors pETDuet_MsFbiC, pCDFDuet_SpRfK E123L and pCOLADuet_FSD/FDR were co-transformed into *E. coli* C41 (DE3). Cultures were grown and expressed in TB as described for FOP production. After harvesting, cell pellets were resuspended in M9 medium, containing 1% glycerol (w/v) and 1 mM IPTG. Reactions were initiated by adding cells to a final OD₆₀₀ of 6.25 in M9 medium with 1% glycerol, 1 mM IPTG, 7.5 mM ketoisophorone and 2% DMSO (v/v), in a total volume of 5 mL. Reaction mixtures were incubated at 37 °C, 250 rpm in 24-deep well plates. Reactions were quenched by adding three parts acetonitrile to 1 part of medium, after spinning down the cells. This mixture was incubated on ice for 5 min and then spun down at 8000g in a table top centrifuge at 4 °C, for 15 minutes. Afterwards, 10 µL supernatant was used for HPLC analysis. The depletion of substrate was analyzed at 240 nm, using an isocratic mobile phase of 60:40 acetonitrile:water on an Alltech Alltime HP C18 5µ, 250 mm column. The formation of the correct product was analyzed by GC-MS and chiral GC, as described previously by Mathew and Trajkovic et al.²⁵⁹

4.2.10 Media used for *S. cerevisiae*

Two types of media were used for the growth of *S. cerevisiae* carrying pTEF-SpRfK plasmids and for *in vivo* FOP production. SC medium used here is a synthetic defined medium lacking uracil and, containing 2 % glucose. It is composed of 6.9 g/L yeast nitrogen base without amino acids (YNB) and 0.77 g/L complete supplement mixtures without uracil, both of which were purchased from Formedium. Another medium used is YND medium which contains YNB (6.9 g/L) and 2 % glucose. YND is supplemented with 76 mg/L each L-tryptophan and L-histidine as well as 340 mg/L

L-leucine. Yeast nitrogen base without amino acids and riboflavin (Formedium) was used for testing the effect of riboflavin on FOP production. For *in vivo* FOP production, 200 µM (unless otherwise stated) FO was added to the medium before autoclave sterilization.

4.2.11 *In vivo* FOP production in *S. cerevisiae* and FOP isolation

For *in vivo* FOP production in *S. cerevisiae* an overnight-grown (at 30 °C) pre-inoculum of the yeast cells expressing SpRfK was diluted to OD₆₀₀ 0.4 in 25 mL of either SC or YND medium, with or without riboflavin (YND-RF and YND-RF, respectively), containing 200 µM FO. The pre-inoculum was grown in the respective medium without FO. After growing for 24 h at 30 °C in FO containing medium, cells were harvested by centrifugation (3000g for 10 min) and washed with 50 mL Milli-Q water. For isolation of intracellular FOP, cells were resuspended in 2 mL 70% boiling ethanol, incubated for 5 min at 95 °C and spun down for 10 min at 17,000g. The cell extract solutions were collected and the procedure was repeated once more. The collected extract solutions were lyophilized and resuspended in 250 µL of Milli-Q. After cleaning up by centrifugation the samples were analyzed by HPLC. To estimate the FOP yield per g dry cell weight (DCW), the correlation between the measured OD₆₀₀ and measured cell dry weight was determined. *S. cerevisiae* grown until the late exponential phase was diluted to OD₆₀₀ values of 3 - 8 in 1 mL, in triplicates. The samples were dried by lyophilization and the measured dry cell weights were plotted against the OD₆₀₀/mL.

4.2.12 HPLC analysis of FO and FOP

Samples were separated on a Phenomenex Gemini C18 (4.6 x 250 mm, 5 µm) column. A linear gradient of 50 mM ammonium acetate pH 6.0 with 5% acetonitrile (buffer A) and 100% acetonitrile (buffer B) was applied at a flow rate of 1mL/min: t = 0 min/100:0 (A: B), t = 16 min/80:20 (A: B), t = 19 min/5:95 (A: B), t = 22 min/5:95 (A: B), t = 26 min/95:05 (A: B), t = 28 min/100:0 (A: B). The separation was monitored in time with UV absorbance at 262 nm and fluorescence (ex: 400 nm and em: 470 nm). FOP concentration was calculated based on the peak area calibration curve which was made with the purified FOP. Retention times for FOP and FO are 11 and 12.7 min, respectively.

4.2.13 FOP purification

Enzymatically synthesized FOP using SpRfK was purified on a C18 column (FlashPure 24 mL, Buchi). The quenched and filtered reaction solution was loaded onto the column which was pre-equilibrated sequentially with methanol and Milli-Q. After washing with 50 mL Milli-Q water, FOP was eluted with 5% methanol and lyophilized for further use.

4.2.14 LC-MS analysis of FOP from *in vitro* conversion

To verify the FOP produced by the *Sp*RFK reaction, the mass of the reaction product was analyzed using a UPLC-MS system (Acquity-TQD, Waters). The reaction sample was separated on a ACQUITY UPLC® HSS T3 column (1.8 μm, 2.1 x 150 mm, Waters) using a gradient between solvent A (0.1% formic acid in water) and solvent B (0.1% formic acid in acetonitrile) at a flow rate of 0.31 mL/min: t = 0 min/100:0 (A:B), t = 5 min/75:25 (A:B), t = 6.12 min/5:95 (A:B), t = 7.14 min/5:95 (A:B), t = 8.16 min/75:25 (A:B), t = 9.18 min/100:0 (A:B). Electrospray ionization (ESI) in negative ion mode was used for mass detection.

4.2.15 LC-MS verification for the presence of FOP in *E. coli* cell free extract

The presence of FOP in cell free extracts was determined by UPLC/ESI-QTOF-MS. *E. coli* cell free extract (CFE) samples were processed in the same way as for HPLC (mentioned above), a 3 μL sample was injected onto a Acquity UPLC® BEH C18 (50 × 2.1 mm, 1.7 μm, Waters) column. The mobile phase consisted of solvent A (0.1% formic acid in water) and solvent B (0.1% formic acid in acetonitrile). Compounds were separated by the following program at a flow rate of 0.3 mL/min: linear gradient from 99 to 5% A (v/v) in 10 min, kept at 5% A for 0.5 min, returning to 99% A in 1 min, re-equilibration to 99% A in 3 min. The separation was measured by absorbance at 400 nm. The mass spectrometer detected negative ions over the mass/charge range (m/z) 100 – 600.

4.2.16 *Sp*RFK Library design and construction

The previously solved X-ray structure of *Sp*RFK (PDB: 1N07)²⁸⁵ was used as the initial structure for Rosetta calculations²⁸⁶ of FOP binding. The structure was processed in Schrodinger and a ligand FMN molecule in the structure was turned into FOP manually. The resulting protein-FOP complex was used for flexible backbone design using the CoupledMoves algorithm available in Rosetta 3.5.²⁸⁷ 10 Amino acids (Ile43, Thr45, Val64, Val79, Ser81, Arg121, Glu123, Leu132, Ile136 and Asp139) surrounding the FOP molecule were allowed to be mutated to all possible amino acids in 20 parallel runs (nstruct=20 flag) of 10,000 Monte Carlo sampling steps (ntrials=10000 flag), to ensure full coverage of possible mutations compatible with FOP in the active site. The FOP molecule was allowed to participate in the design via rigid body moves without constraints to further improve acceptance rate of FOP-compatible mutations. Other flags for the CoupledMoves command were kept at their default values, except for the ligand_weight, which was set to 2.0, thus ensuring increased weight of ligand-protein interactions in the Rosetta energy calculations. After removing redundant designs from the 20 parallel runs, 90 amino acid variants were selected based on the most commonly occurring mutations in the 400 designs

with the lowest Rosetta energy and manual inspection of the top design structures produced by the algorithm. The *Sp*RFK mutant library was constructed based on the Goldengate assembly method.²⁸¹ The gene fragments containing the mutations were designed in two parts based on the mutated residues: the N-terminal part of the gene covering the mutations on residues Thr45 and Val79 or Val64 and Ser81 and the C-terminal part of the gene covering the mutations on Glu123 and Leu132. The required 25 gene fragments with flanking regions containing *Bsa*I and *Bsm*BI restriction sites were purchased from Integrated DNA Technologies, Inc. Prior to the library assembly, each fragment was cloned into an entry vector containing the *ColE1* origin of replication and chloramphenicol resistance marker via a *Bsm*BI Goldengate reaction. The resulting plasmids were transformed in *E. coli*, amplified and purified. These plasmids were used for sequencing of the fragments and further library assembly. After verification of the fragment sequences, each entry vector containing the N-terminal part fragment and the C-terminal part fragment were combined to generate all desired 90 variants and assembled into a 2 μ-based expression vector (pTEF-*Sp*RFK) using *Bsa*I Goldengate assembly. The selection of correct mutant constructs was done through *E. coli* transformation, colony picking, amplification and sequencing. The correct variants were transformed in *S. cerevisiae* using an optimized lithium acetate-based method²⁸⁸ and the transformants were plated on a solid SC medium.

4.2.17 Library screening by measuring the *S. cerevisiae* *in vivo* FOP formation

S. cerevisiae cells containing *Sp*RFK variants were grown overnight at 30 °C in 5 mL SC medium in 24-well plates. The pre-inoculum was then diluted in 2 × 5 mL SC medium containing 200 μM FO in 24 well plates and cultivated at 30 °C. After 24h, the cultures were harvested and washed with Milli-Q water by centrifugation at 3200g for 15 min. To isolate FOP, cells were resuspended in 500 μL 70% boiling ethanol, incubated for 5 min at 95 °C and spun down for 10 min at 13,000g. The cell extract solutions were collected and the procedure was repeated once more. The collected extract solutions were lyophilized and resuspended in 100 μL of Milli-Q water. After cleaning up by centrifugation, the samples were analyzed by the aforementioned HPLC method.

4.3 Results

4.3.1 *In vitro* conversion of FO

Owing to the similar structure of riboflavin and FO, riboflavin kinase is a good target enzyme for enzymatic FOP production. Previously, it was shown that an engineered riboflavin kinase from *C. ammoniagenes* (*Ca*RFK) could accept FO as a substrate and produce FOP.³² Three hydrophobic residues near the 7-methyl and 8-methyl groups of riboflavin were mutated to two more polar residues and one longer apolar residue

(F21H/Y_F85H_A66I/V) so that the 7-demethyl and 8-hydroxyl groups of FO could be accommodated. Comparing the X-ray crystal structures of *Ca*RFK and *Sp*RFK, we realized that the mutations at two of the residues already exist in *Sp*RFK; His98 and Val79 correspond to Phe85 and Ala66 in *Ca*RFK, respectively (Figure 4.2). This led us to explore the possibility of using *Sp*RFK for more efficient FOP production.

For testing the substrate acceptance of the wild-type *Sp*RFK, the enzyme was expressed in *E. coli* NEB 10-beta and purified. The expression of the *E. coli*-codon optimized *Sp*RFK gene in this strain yielded a good amount of soluble protein (50 mg/L culture) and the estimated size of the protein (~19 kDa) was confirmed by SDS-PAGE analysis. Surprisingly, after 1 h of incubation at 30 °C, the reaction containing 50 μ M FO showed nearly full conversion, when analyzed by HPLC (Figure 4.3a). The formed product was analyzed by UPLC-MS and showed the corresponding mass of FOP (expected m/z 442.07, $[M - H]^-$) (Figure 4.3c). These data show that wild-type *Sp*RFK can catalyze the phosphorylation of the non-natural substrate FO with higher activity than the previously engineered *Ca*RFK variant.³²

In vivo enzyme applications require the consideration of the possible interaction of the enzyme with any intracellular molecule. Because *Sp*RFK will likely perform its natural reaction of converting riboflavin in *S. cerevisiae*, we sought to test for any inhibition by either riboflavin or FMN in FO conversion. When the reaction was performed with an equimolar amount of riboflavin and FO, even after long incubation of 8 h, there was no conversion of FO, whereas riboflavin was fully converted to FMN. This suggests that the presence of FMN might inhibit the phosphorylation of FO, which should be addressed when engineering the enzyme for *in vivo* conversion.

Structure-guided mutagenesis using the FMN-bound crystal structure of *Sp*RFK,²⁸⁵ was employed to further enhance the activity toward FOP. Mutant E123L was designed to better accommodate the C5 of FO in a more hydrophobic environment. The *in vivo* activity was measured by comparing the amount of FOP in cell free extracts of *E. coli* NEB 10-beta, expressing the enzymes on a pBAD vector. HPLC analysis with UV and fluorescence detection was used to identify and quantify FOP in cell free extracts. The measured FOP yield in cells expressing the mutant enzyme *Sp*RFK E123L was significantly higher than cells expression wild-type enzyme, resulting in roughly double the amount of FOP (Figure 4.4a). Yet no significant differences in apparent expression levels (SDS-PAGE) and final cell densities (OD_{600}) were observed (Figure S 4.1). Therefore, we concluded that the engineered kinase *Sp*RFK E123L is the best performing enzyme for *in vivo* FOP production in *E. coli*.

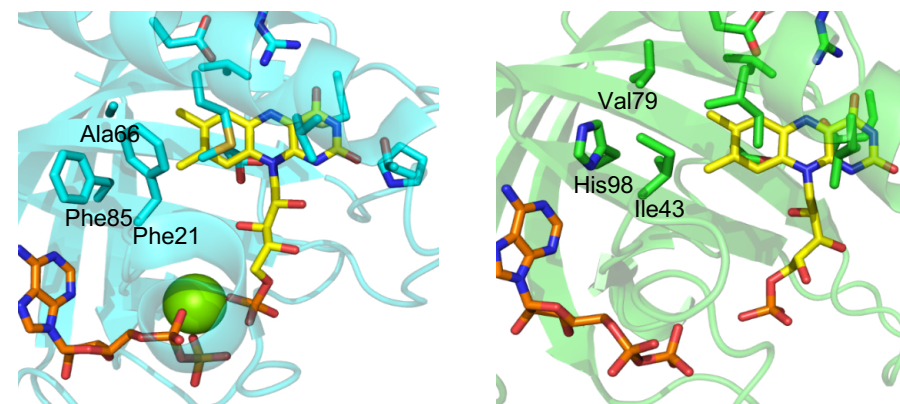


Figure 4.2: Riboflavin binding site structure of *Ca*RFK (left, PDB: 5A89)²⁸⁹ and *Sp*RFK (right, PDB: 1N07)²⁸⁵. Amino acid residues that are within 6 Å radius of the isoalloxazine ring of FMN are shown in sticks. FMN and ADP molecules are depicted as yellow and orange sticks, respectively. Mg²⁺ ion is shown as a green sphere.

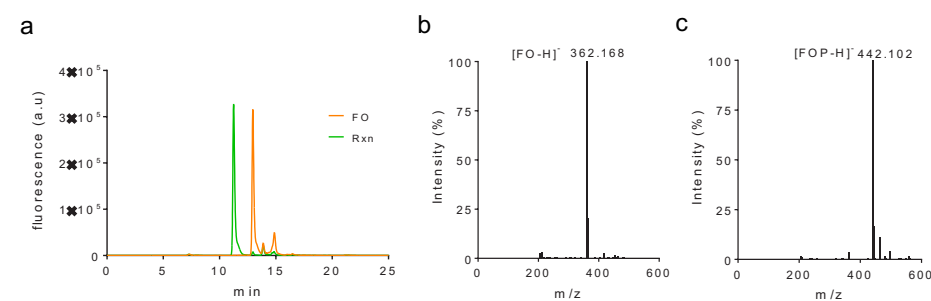


Figure 4.3: FO conversion by *Sp*RFK. a. HPLC chromatogram of FO (orange line) and the formed product (green line). The retention times for FO and the reaction product were 12.9 and 11.2 min, respectively. b. Mass verification of the substrate FO. c. Mass verification of the reaction product FOP.

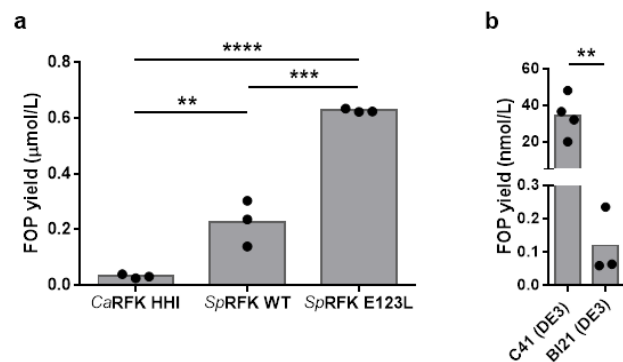


Figure 4.4: a. FOP productivity in μmol FOP per liter of culture in *E. coli* NEB 10-beta cells expressing different riboflavin kinases from pBAD vectors. Bars represent mean values, which were calculated from 3 independent measurements, shown as dots. Data was analyzed by a one-way ANOVA, with Brown-Forsythe test, showing no significant difference in standard deviations.

*: $p \leq 0.05$; **: $p \leq 0.01$; ***: $p \leq 0.001$; ****: $p \leq 0.0001$. b. FOP yield from BL21(DE3) and C41 (DE3) cultures harboring pETDuet_ScFbiC and pCDFDuet_SpRFK E123L. FOP concentrations were measured in cell free extracts of biological replicates by HPLC fluorescence detection. Bars represent average values, calculated from individual data points, shown as dots. An unpaired two-tailed t-test with Welch's correction was applied to confirm a significant difference in FOP yields, with a P-value of 0.0099 (**).

4.3.2 *In vivo* FOP production – *E. coli* expression strain selection

Three FO synthases were screened for their expression and *in vivo* activity in *E. coli* BL21 (DE23) and C41 (DE3). The FbiCs of *Streptomyces coelicolor* (ScFbiC) and *M. smegmatis* (MsFbiC), as well as the combination of CofG from *Methanocaldococcus jannaschii* (MjCofG) and CofH from *Nostoc punctiforme* (NpCofH), were expressed on pETDuet-1 (~40 copies per cell). SDS-PAGE analysis showed the apparent expression of these FO synthases and the expression level was higher in C41 (DE3) than BL21 (DE3) (**Figure S 4.2**). FOP could be produced in both *E. coli* BL21 (DE3) and C41 (DE3) when pETDuet_ScFbiC was co-expressed with pCDFDuet-1 (20 – 40 copies), harboring the SpRFK E123L gene in MSC1. The FOP yield in *E. coli* C41 (DE3) cell free extracts was significantly higher by more than two orders of magnitude, see **Figure 4.4b**, whereas no significant differences in final cell densities were observed. Therefore, C41 (DE3) was selected for further FOP production experiments.

HPLC was used for the detection of FOP (and FO) in cell free extracts. In order to confirm that the peak with a retention time of 11 minutes was really due to the presence of FOP, LC-MS was performed on the samples. LC-MS indeed detected a compound with a corresponding m/z to FOP in *E. coli* C41 (DE3) expressing the two-plasmid system, which was absent in the CFE of wild type *E. coli* C41 (DE3), therefore confirming the presence of FOP with the two-plasmid system. See supplementary **Figure S 4.4**.

4.3.3 *In vivo* FOP production in C41 (DE3) – growth temperature and vector construct selection

The pETDuet vectors with the different FO synthase constructs were co-expressed in *E. coli* C41 (DE3) with pCDFDuet-1 (20 – 40 copies), harboring the SpRFK E123L gene in MSC1. 50 mL Cultures were grown in 250 mL Erlenmeyer flasks, induced with IPTG and grown at either 24 °C for 36 h or 37 °C for 16 h, after which the FOP concentration was measured. The FOP production was significantly larger at 37 °C for cultures expressing MsFbiC and the CofG/CofH combination on pETDuet-1, with at least 10 times more FOP produced (**Figure 4.5a**). In order to see if we could increase the FOP production even more, SpRFK E123L was also cloned into MSC1 of pRSFDuet-1 (>100 copies). The cellular FOP concentration did not significantly increase or decrease as compared to using pCDFDuet-1 (**Figure 4.5b**). Also, the apparent protein concentration, as judged by SDS-PAGE of cell free extracts, was comparable (**Figure S 4.3**). Using pACYCDuet-1 (10 – 12 copies) for SpRFK E123L expression, however, drastically decreased the FOP yield to negligible amounts.

The combination of pETDuet_MsFbiC and either pCDFDuet-1 or pRSFDuet harboring SpRFK E123L were the best performing FOP production systems, and resulted in yields of up to 1.24 μmol FOP per liter of culture (0.3 μmol gDCW⁻¹), within 16 h. This number is comparable to the natural F₄₂₀ yield in *M. smegmatis*, which can reach 1.43 μmol L⁻¹.^{239,270} The FOP production per unit of time, however, is greatly enhanced, as it takes 2 – 4 days of growth for *M. smegmatis* and other natural F₄₂₀-producing organisms before harvesting, whereas our system only takes 16 h, due to the fast growth of *E. coli*. This translates to a FOP productivity of 0.078 μmol L⁻¹ h⁻¹.

4.3.4 FOP production in C41 (DE3) – growth media selection

Terrific broth (TB) was used as the default medium in this study in order to determine the best combination of riboflavin kinase variant, plasmid constructs, temperature and expression strain. Other commonly used media were then screened for their FOP production capacity. We selected the rich medium lysogeny broth (LB) and the defined M9 medium, with either 1% glucose (w/v) or 1% glycerol (w/v) as a carbon source. Using TB medium was the most beneficial, both in FOP production per culture volume per unit of time and in FOP production per gram dry cell weight (gDCW) (**Figure 4.6**). Supplementing TB with a saturating amount of 5 mM tyrosine (a precursor of FO) or 100 μM ammoniumiron(II)sulfate, as previously was shown to benefit FO synthase expression by Graham et al.,²⁷⁹ did not further increase the FOP yield.

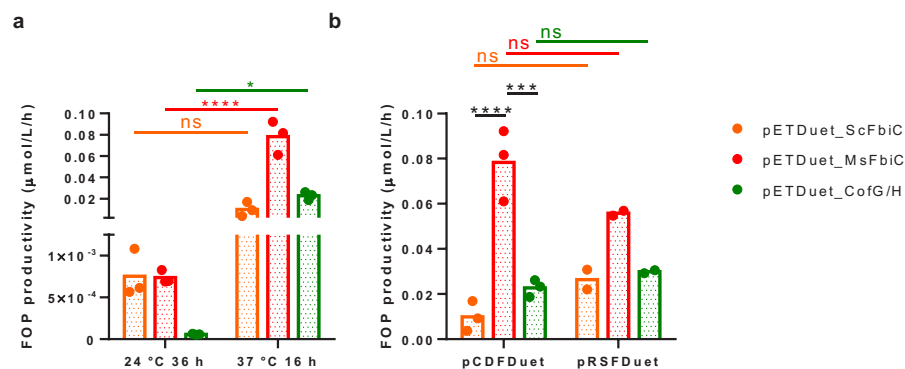


Figure 4.5: FOP productivity in μmol per liter of culture per hour of growth. The amount of FOP in cell free extracts as measured by HPLC, using fluorescence detection. **a:** FOP productivity by C41 (DE3) cells that express an FO synthase on pETDuet-1 and SpRfK E123L on pCDFDuet-1 at 24 °C and 37 °C, after 36 h and 16 h of growth, respectively. **b:** FOP productivity by C41 (DE3) cells that express an FO synthase on pETDuet-1 and SpRfK E123L on either pCDFDuet-1 or pRSFDuet-1. Bars represent mean values of individual data points that are depicted as dots. Data was analyzed by a two-way ANOVA. ns: not significant ($p > 0.05$); *: $p \leq 0.05$; **: $p \leq 0.01$; ***: $p \leq 0.001$; ****: $p \leq 0.0001$.

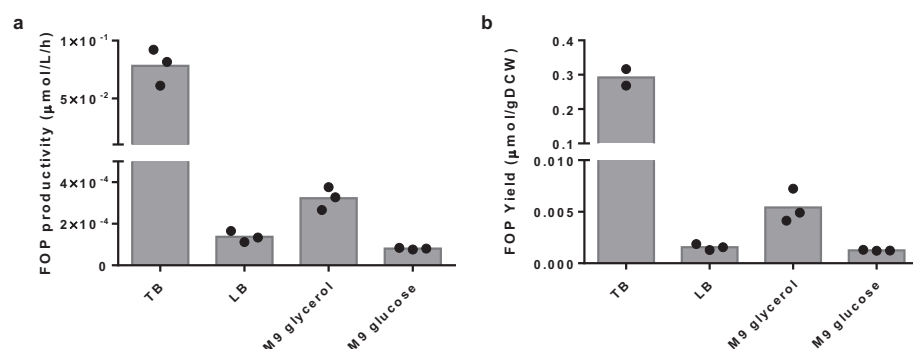


Figure 4.6: The effect of different commonly used growth media on FOP production by *E. coli* C41 (DE3) expressing MsFbiC on pETDuet-1 and SpRfK E123L on pCDFDuet-1. Bars represent mean values of individual data points that are depicted as dots.

4.3.5 Whole-cell conversion of ketoisophorone

We estimated that intracellular FOP concentrations in *E. coli* C41 (DE3) can reach up to about 40 μM when these cells are coexpressing pETDuet_MsFbiC and pCDFDuet_SpRfK E123L and grown at 37 °C in TB medium. For this estimation we used the following experimentally verified parameters: $1 \text{ OD}_{600} \hat{=} 7.8 \cdot 10^8 \text{ cells} \cdot \text{mL}^{-1}$ and the *E. coli* cell volume is $4.4 \cdot 10^{-15} \text{ L}$.^{284,290} This intercellular FOP concentration is high enough to fuel several F_{420} -dependent enzymes.³² Therefore, we attempted to do a whole-cell FOP-mediated conversion of ketoisophorone (2,6,6-trimethyl-2-cyclohexene-1,4-dione), using the

deazaflavoenzymes sugar-6-phosphate dehydrogenase from *Cryptosporangium aryum* (FSD-Cryar) and the ene-reductase from *Mycobacterium hassiacum* (FDR-Mha) (**Figure 4.7a**).^{259,265} Both genes were cloned into pCOLADuet-1 (**Table S 4.1**) and coexpressed with pETDuet_MsFbiC and pCDFDuet_SpRfK E123L in C41 (DE3). After growing cells in TB medium, they were transferred to M9 medium with 1% glycerol and 7.5 mM ketoisophorone. After incubating the cells overnight, samples were taken for analysis. Reverse-phase HPLC showed that ketoisophorone was converted by both cultures of C41 (DE3) with and without the three plasmids. Yet, C41 (DE3) cells that contained the plasmid system converted significantly more ketoisophorone (83% compared to 47%) (**Figure 4.7b**). GC-MS was performed to verify the presence of the reductase product, 2,2,6-trimethylcyclohexane-1,4-dione, which was indeed present (**Figure S 4.5**). Previous *in vitro* data on ketoisophorone reduction by FDR-Mha showed that the product had an e.e. of 72% (S).²⁵⁹ Chiral GC of whole-cell conversions, however, showed an e.e. of 42% (R) for both C41 (DE3) with and without the plasmid system (**Figure S 4.6**). This is probably due to a racemization effect caused by endogenous *E. coli* reductases/dehydrogenases, as was also described previously by Dezavarei and Lee et al. for the whole-cell P450-mediated isophorene hydroxylation in *E. coli*.²⁹¹ Product racemization was also seen in crude extract of *Rhodococcus rhodochrous* ATCC 17895.²⁹²

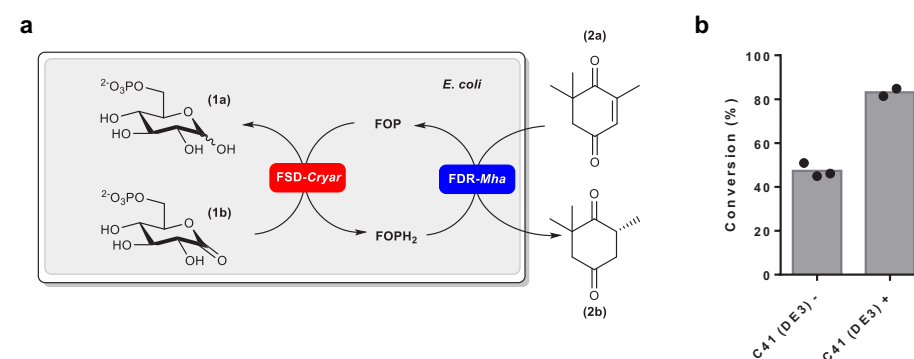


Figure 4.7: **a:** Scheme of whole-cell FOP-mediated conversion of 2,2,6-trimethyl-2-cyclohexen-1,4-dione (2a). The *in vivo* synthesized FOP is reduced by FSD-Cryar, using glucose-6-phosphate (1a) as sacrificial electron source. FDR-Mha catalyzes the reduction of 2a by FOPH₂. **b:** Whole-cell conversion of ketoisophorone by *E. coli* C41 (DE3). C41 (DE3) -: wild-type strain. C41 (DE3) +: cells harboring pETDuet_MsFbiC, pCDFDuet_SpRfK E123L and pCOLA_FSD/FDR.

4.3.6 In vivo FOP production by SpRfK in *S. cerevisiae*

After confirming that SpRfK converts FO to FOP, we tested the expression of the enzyme in *S. cerevisiae* for possible *in vivo* FOP formation in yeast. SDS-PAGE analysis revealed the soluble expression of SpRfK in *S. cerevisiae* (**Figure S 4.7**). The use of different promoters (pTEF1 and pPGK1) did not show any significant differences

in the expression level and we continued further work with the pTEF1 promoter. Next, we tested whether the enzyme can produce a detectable amount of FOP *in vivo*. After growth of the yeast cells expressing SpRfK in the medium supplemented with FO, the cell extracts were analyzed by HPLC. After 24 h of cultivation in the medium supplemented with FO, the cells containing wild-type SpRfK showed FOP production with a yield of 0.24 ± 0.04 nmol per g dry biomass whereas wild-type cells lacking SpRfK did not show any detectable amount of FOP (Figure 4.8). This result indicates that SpRfK performs *in vivo* FO phosphorylation and that the native *S. cerevisiae* riboflavin kinase does not contribute to the FOP production. However, the yield was poor and would not be sufficient for FOP-dependent bioconversion. Therefore, further engineering and optimization is required for increasing the FOP yield and *in vivo* concentration.

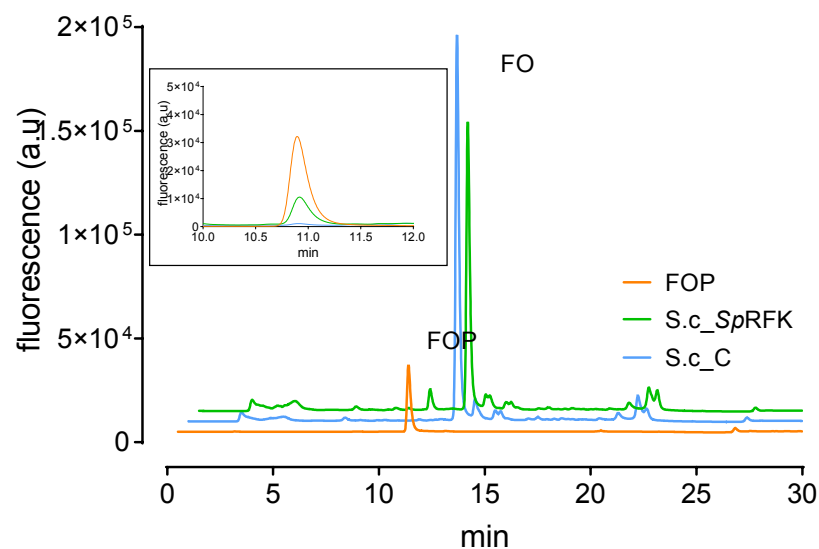


Figure 4.8: *In vivo* FOP production of *S. cerevisiae* expressing wild-type SpRfK. The cell free extract of *S. cerevisiae* expressing SpRfK (green line) shows a peak corresponding to FOP which aligns with the purified FOP standard (orange line). The control strain without SpRfK shows no measurable *in vivo* FOP formation (blue line). The inset shows a zoomed-in chromatogram area of FOP peaks.

For *de novo* biosynthesis of FOP, we attempted expression of several codon-optimized FO synthases in *S. cerevisiae*. However, functional expression of several FO synthases (FbiC from *M. smegmatis*, *Mycobacterium tuberculosis* and *Chlamydomonas reinhardtii* and CofG/H from *M. jannaschii*) in *S. cerevisiae* failed (data not shown). Therefore, we focused on improving the *in vivo* FOP production using the chemically synthesized FO.

Effect of media and FO concentration on FOP production

In addition to the catalytic performance of SpRfK, indirect factors such as the growth condition of *S. cerevisiae* can also influence the *in vivo* FOP conversion. In order to optimize the condition for FOP production, we tested several variables and analyzed the FOP yield. The concentration of FO in the medium may influence the *in vivo* FO concentration and cellular metabolism, which likely affects the final FOP yield. Three different FO concentrations (50, 100 and 200 μM) in the media were tested and showed a significant influence on the final FOP yield. While no apparent influence of FO on the growth of *S. cerevisiae* was observed, increasing FO concentration positively correlated with the final FOP yield (Figure 4.9a). The improvement of FOP yield is possibly due to an increase in intracellular FO concentration. Although it is possible that the uptake efficiency did not reach its maximum within the tested FO concentration range, we continued further experiments using 200 μM FO due to its poor solubility.

Next, we tested the influence of the media composition on the FOP yield. In general, for yeast cultivation, we used a synthetic defined medium (SC) which contains yeast nitrogen base (YNB), amino acids and vitamin supplements as well as 2% glucose. Except for the auxotrophic amino acids (Trp, His, Leu) for the yeast strain used (CEN. PK2-1C), all other supplemented amino acids are not essential for cell growth. To evaluate the effect of the supplements on FOP yield, we compared the FOP yield of wild-type SpRfK containing cells grown on SC medium and YND (YNB + 2% glucose) medium supplemented only with the auxotrophic amino acids. The use of YND medium resulted in a more than 8-fold higher FOP yield compared to the use of SC medium (Figure 4.9b). During cultivation, no apparent effect on growth was observed and similar OD₆₀₀ was measured (~5.6) upon harvesting after 24 h. This result indicates that the additional amino acids supplemented in SC medium negatively influence the *in vivo* FOP conversion. SDS-PAGE analysis (Figure S 4.7) showed that the two different media did not significantly affect the SpRfK expression level.

In *S. cerevisiae*, riboflavin is known to be transported through simple diffusion and/or the riboflavin transporter MCH5 whose expression is up-regulated by low intracellular riboflavin concentration.²⁹³ Due to the structural similarity, FO and riboflavin are likely transported by the same means and may affect the transportation efficiency of each other. We tested whether the absence of riboflavin would improve the FO uptake, thus increasing the FOP conversion, by measuring the FOP yield in both SC and YND medium lacking riboflavin. While using SC medium with and without riboflavin yielded similar amounts of FOP, cells grown in YND medium without riboflavin showed a 1.5 higher FOP yield compared to cells grown in YND medium (Figure 4.9b). Therefore, the effect of the riboflavin in media for FOP

conversion seems to be dependent on the type of media. Whether the increased FOP yield is indeed due to improved transport is yet to be verified, as the current method used for FOP isolation and measurement does not distinguish between the intracellular FO and the FO which remain bound on the cell surfaces after washing steps. Therefore, we do not exclude the possibility of riboflavin affecting FOP conversion through other mechanisms, for example ones related to metabolism. In conclusion, among the conditions we tested, the use of YND medium with 200 μM FO lacking riboflavin seems to provide the best FOP yield.

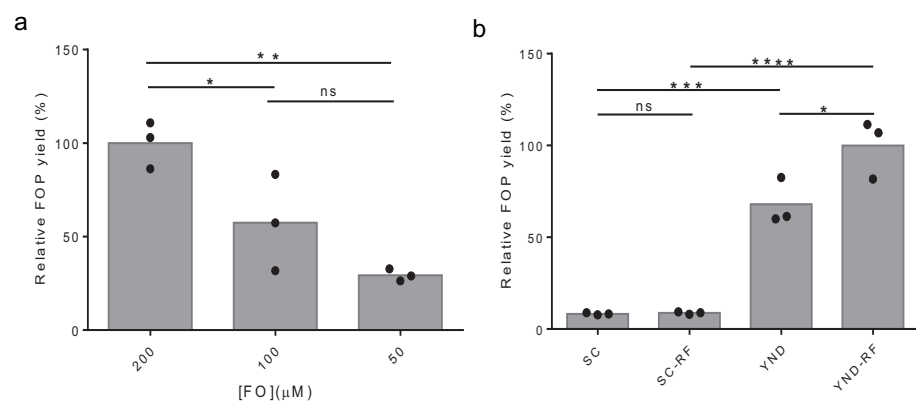


Figure 4.9: Media optimization for improving *in vivo* FOP conversion in *S. cerevisiae*. a. Effect of FO concentration in media on FOP yield. b. Effect of different media and riboflavin supplements. The dots show the individual data points of three independent samples and their averages are presented in bars. The average value of samples with highest FOP yield is set as 100 percent in both a and b. In all experiments the FOP yield was normalized by the cell density (OD600) of the samples. The statistical significance of the data was analyzed by one-way ANOVA. ns $p > 0.05$; * $p \leq 0.05$; ** $p \leq 0.01$; *** $p \leq 0.001$; **** $p \leq 0.0001$.

4.3.7 *In vivo* FOP production using *SpRfK E123L* in *S. cerevisiae*

As *SpRfK* variant E123L showed improved FOP production in *E. coli*, we expressed this mutant *SpRfK* in *S. cerevisiae* and measured the FOP production level after the growth in FO containing medium. Unlike the significant increase of FOP production by the variant in *E. coli*, the yeast cells carrying the *SpRfK* E123L did not show any improvement in FOP production. The mutant *SpRfK* carrying cells produced similar or slightly lower amount of FOP compared to the cells expressing the wild-type *SpRfK*. In fact, SDS-PAGE analysis shows (Figure S 4.7) that the expression level of *SpRfK* E123L is poor compared to the wild-type enzyme. The lower expression level of the mutant may cancel out the effect of its improved catalytic properties, hence resulting in unaffected *in vivo* FOP production levels. In order to discover an improved variant relevant for *in vivo* applications in yeast, we generated an *in silico* designed *SpRfK* mutant library and performed screening based on the *in vivo* FOP production level.

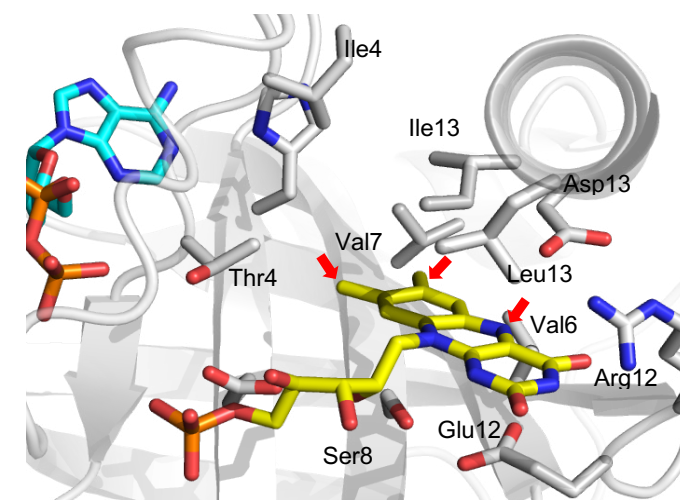


Figure 4.10: The substrate binding site structure of *SpRfK* (1No7).²⁸⁵ The residues surrounding the bound FMN (yellow) are shown in grey sticks and the residues that were subjected to be mutated during the *in silico* calculation are indicated with the residue numbers. The red arrows indicate the structural difference of FMN compared with FOP. A bound ADP molecule is shown in blue.

4.3.7.1 *SpRfK* library construction and screening

To improve the *in vivo* FOP production of *S. cerevisiae* by improving the catalytic properties of *SpRfK*, we designed a structure-guided rational mutant library. We envisioned that modifying the residues that interact with the moieties that distinguish FO from riboflavin could improve binding of FO (Figure 4.10) as well as reduce the binding of riboflavin which could be an inhibitor for *in vivo* FOP production. Based on Rosetta CoupledMoves calculations²⁸⁷ for FOP binding and visual inspection of the structure, we selected 6 residues (Thr45, Val64, Val79, Ser81, Glu123 and Leu132) for the combinatorial mutagenesis library. Each residue was subjected to the substitutions to one, two or three different amino acid residues (Table 4.1). In order to limit the library size, in view of the screening capacity, the library was divided into two sub-libraries based on the locations of the residues in relation to the substrate. By combining gene fragments containing mutations at the respective residues, using the Goldengate assembly method, we obtained all the desired variants including two wild-type constructs.

Table 4.1: *SpRfK* mutant library scheme.

	Library 1				Library 2		
Residues	Val64	Ser81	Glu123	Leu132	Thr45	Val79	Leu132
Substitutions	I	A, V, C	L, M	I, M	D, E	M, L	I, M, E

The screening results revealed five variants (D1, D3, D4, D7 and E1, **Figure 4.11**) which improved *in vivo* FOP production in *S. cerevisiae*. Interestingly, a common mutation in these five variants is E123M and the best variant amongst them is the single mutant E123M showing an over 3-fold increase in FOP production compared to the wild type. This indicates that the mutation E123M is beneficial for the *in vivo* FOP production in *S. cerevisiae* and that additional mutations decrease the positive effect of E123M. Therefore, we carried out further experiments using the E123M mutant kinase.

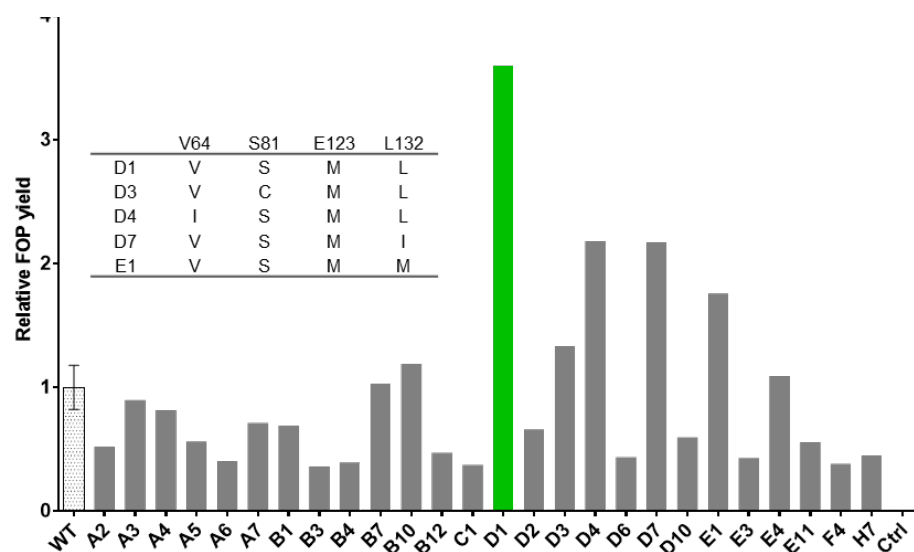


Figure 4.11: SpRfK library screening result. The bars show the relative *in vivo* FOP yield of *S. cerevisiae* expressing the SpRfK variants. Only the variants with measurable FOP production are shown. The mutations of all variants can be found in **Table S 4.2**. The values of the single measurements of each sample were compared to the average value of three independent wild-type samples. The control sample (Ctrl) is *S. cerevisiae* cells without SpRfK expression. The FOP yield is normalized by the cell density (OD_{600}). The inset shows the best five variants.

In order to verify the improvement of the selected variant on *in vivo* FOP production, we measured the FOP yield of cells expressing SpRfK-E123M in bigger culture volumes and compared that to the wild type. Eight biological replicates of each wild type and the mutant containing cells were grown in YND medium lacking riboflavin, supplemented with 200 μ M FOP for 24 h. The cell densities of all cultures at harvest were similar ranging from OD_{600} 5.2 to 6. On average, SpRfK-E123M carrying cells produced 2.5-fold more FOP with the measured yield of 5.2 ± 0.9 nmol/gDCW compared to the wild type kinase carrying cells which produced 2.1 ± 0.2 nmol/gDCW. This translates to the accumulated intracellular FOP concentration of ~ 2 and ~ 0.8 μ M, respectively, estimated based on the reported cell volume to biomass conversion.²⁹⁴

4.3.7.2 Steady-state kinetics of SpRfK variants

Through the *in vivo* FOP production measurement we showed that the SpRfK variants E123L and E123M increase FOP yield when expressed in *E. coli* and *S. cerevisiae*, respectively. Interpreted from the SDS-PAGE analyses, the improvements did not seem to be related with expression levels. Therefore, we measured the kinetic parameters of the purified enzymes in order to understand the factors that contributed to the improvements (**Table 4.2**). The variant E123L showed a slightly higher k_{cat} and half the K_M compared to the wild type, resulting in a 2.5-fold higher catalytic efficiency. The mutation E123M improved the catalytic properties on FO even further with a 2.5-fold higher k_{cat} and almost 3-fold lower K_M (7-fold higher catalytic efficiency compared to the wild type). The improved catalytic properties of both mutants explain the improved *in vivo* FOP yields. The lower K_M values for FO may especially be beneficial for low *in vivo* FO concentrations. Furthermore, the data suggest that the modestly improved catalytic property of the variant SpRfK-E123L was sufficient to improve the FOP yield significantly in *E. coli* while it could not compensate its lowered expression in *S. cerevisiae*. Mutant E123L also seems to be slightly less inhibited by FMN than wild type and mutant E123M *in vitro*, shown by less significant decrease in FO conversion in the presence of FMN, which could also contribute to the increase seen in the *in vivo* FOP yield in *E. coli* (see **Table S 4.3**).

Table 4.2: Kinetic parameters of SpRfK variants.

	k_{cat} (s^{-1})	K_M (μ M)	k_{cat}/K_M ($s^{-1}\cdot M^{-1}$)
SpRfK	0.06 ± 0.006	100 ± 13	600
SpRfK-E123L	0.08 ± 0.003	51 ± 3	1570
SpRfK-E123M	0.15 ± 0.007	35 ± 3	4290

All measurements were done at 30 $^{\circ}$ C, pH 7.0 (50 mM KPi). The k_{cat} values and the K_M values for FO are the average of duplicate measurements and the margins represent the standard deviations.

4.4 Discussion

F_{420} is a naturally occurring deazaflavin redox cofactor found in archaea and Actinobacteria. Its very low redox potential and strict hydride transfer chemistry make it an interesting target for biocatalytic applications. Unfortunately, the low availability of this cofactor prevents it from being used for upscaled biotechnological applications thus far. In previous work we showed that a truncated version of F_{420} , the chemoenzymatically synthesized FO-5'-phosphate (FOP), could be used as an alternative cofactor for F_{420} -dependent enzymes.³² FOP showed similar activities as F_{420} for enzymes from different structural classes, namely the F_{420} :NADPH oxidoreductase from *Thermobifida fusca* (Rossmann fold),²⁵³ the sugar-6-phosphate dehydrogenase from *C. arzum* (TIM barrel)²⁶⁵ and the ene-reductase from *M.*

hassiacum (β -roll/split β -barrel).²⁵⁹ The low solubility of chemically synthesized FO, the relatively high cost and bulk availability of ATP and the instability of the kinase from *C. ammoniagenes*²⁷¹ prompted a search for alternative green synthesis routes for FOP. Whole-cell synthesis of FOP, either by supplying chemically synthesized FO in the media or by *de novo* biosynthesis, could be a scalable, environmentally friendly and cheap way to synthesize this valuable cofactor for large-scale applications.

We pursued *in vivo* FOP synthesis by using either a FO synthase or chemically synthesized FO and a monofunctional riboflavin kinase from *S. pombe*, both in *E. coli* and *S. cerevisiae*. The amino acid sequences of the truncated *Ca*RFK and the *Sp*RFK share only 24% identity. The riboflavin binding site residues of these enzymes show quite some diversification as well. Whereas the *Ca*RFK required engineering for FOP conversion, wild-type *Sp*RFK already accepted FO as a substrate, showing an even higher FOP conversion yield compared to the mutant *Ca*RFK. Interestingly, amino acids at two residues near the 7- and 8- methyl group of riboflavin in *Sp*RFK, Val79 and His98, correspond to the mutations that were previously made in *Ca*RFK for FO conversion. Although few riboflavin kinases were reported to convert various riboflavin analogs including 5-deazariboflavin, *Sp*RFK is the first riboflavin kinase to be reported to accept FO as a substrate without engineering.^{271,295}

Using a FO synthase from *M. smegmatis* and *Sp*RFK variant E123L, we showed that FOP can be produced *in vivo* by *E. coli* C41 (DE3). The yield was 1.24 $\mu\text{mol L}^{-1}$, which is 45 times higher than the F_{420} yield of *E. coli* expressing the heterologous F_{420} biosynthesis pathway.²³⁹ The simple two-step biosynthesis pathway of FOP, compared to the multi-step synthesis of the more complex cofactor F_{420} , could be a possible reason for this observed difference. Recently, Shah et al. showed that the F_{420} yield in *E. coli* can be increased up to 2.33 $\mu\text{mol L}^{-1}$ by varying carbon sources, which demonstrates the potential for improving non-natural cofactor production by using simple methods.²⁷⁸ The FOP yield presented here closely resembles the F_{420} yield from *M. smegmatis*, which is 1.43 $\mu\text{mol L}^{-1}$. The estimated FOP productivity per unit of time (0.078 $\mu\text{mol L}^{-1} \text{h}^{-1}$), however, is much higher than that of F_{420} by *M. smegmatis*. *E. coli* – with doubling times as low as 20 minutes – grows much faster than *M. smegmatis*, with doubling times of 3 to 4 hours. Therefore, expression strains of *E. coli* can be harvested already after 12 to 16 hours, whereas *M. smegmatis* and other F_{420} production strains take 2 – 4 days (Table 4.3).

Table 4.3: F_{420} /FOP yields for several F_{420} producing organisms and the *E. coli* FOP producing system, as presented in this work.

Organism/strain	Yield		Growth time	Cell yield (g/L)	Potential hazards
	$\mu\text{mol/g}$	$\mu\text{mol/L}$			
<i>M. smegmatis</i> ²⁷⁰	0.3	1.43	2 - 4 days	4.8	wound infection
<i>Methanobacterium thermoautotrophicum</i> ²⁷⁰	1.7	0.85	3 - 5 days	0.5	flammable/explosive gas
<i>Streptomyces flocculus</i> ²⁷⁰	0.62	4.43	3 - 4 days	7.2	toxic metabolites
<i>E. coli</i> BL21 (DE3)-F420 ²³⁹	-	0.027			-
<i>E. coli</i> C41 (DE3)-FOP	0.3	1.24	16 h	3.1	-

Another advantage of *E. coli* is the wealth of readily available genetic tools, which could be used to engineer genetically stable FOP production strains, and even whole-cell factories for FOP-mediated conversions. In this work we could indeed show – as a proof of concept – that whole-cell conversions could be performed by expressing the FOP biosynthesis machinery on two separate plasmids, as well as two additional enzymes for FOP reduction and compound conversion on a third plasmid. Although *E. coli* C41 (DE3) has a background reduction activity toward the employed substrate, we could show a significant increase in ketoisophorone conversions when the three plasmids were introduced, albeit with loss of the previously established (S)-selectivity *in vitro*.²⁵⁹ Endogenous ketoisophorone reductions by native enzymes, producing racemic mixtures were also observed in previous studies.^{291,292} In fact, the *E. coli* genome contains several homologues of YqjM, the NAD(P)-dependent ene reductase from *Bacillus subtilis*, capable of reducing ketoisophorone with (R)-enantioselectivity.^{296–298} Identification and subsequent gene knock outs of the responsible enzymes could overcome this observed ‘racemisation’ problem, provided that these enzymes are non-essential.²⁹⁹ Further engineering could result in cell factories for efficient FOP-fueled enantioselective reductions that only require substrate, *E. coli* cells and cheap growth media. The intracellular FOP concentration of up to 40 μM is high enough to support catalysis.³² Also of great importance is the safety of *E. coli*, as compared to natural F_{420} sources, which might be opportunistic pathogens, may produce toxic waste products or need flammable, explosive gases for their growth (Table 4.3).

In addition to developing the FOP-producing *E. coli* strain, we also explored FOP production in *S. cerevisiae*, a representative eukaryotic microorganism. Besides the well-developed genetic and strain engineering tools, the advantage of using the yeast strain also lies on the easy implementation in industrial settings due to its

robustness and harmless nature.³⁰⁰ To the extent of our knowledge, *in vivo* production of F₄₂₀ or other deazaflavins in yeast have not been reported so far. In a recent study, use of chemically synthesized FO for tetracycline biosynthesis in *S. cerevisiae* was demonstrated.³⁰¹ Although FO can be used for some F₄₂₀-dependent conversion, *in vivo* FOP production can expand the reaction scope owing to the phosphate group offering better binding to more F₄₂₀-dependent enzymes and less leakage from the cell. In this study, we show that it is possible to produce FOP in *S. cerevisiae* using the heterologously expressed SpRfK and FO supplemented in the media.

In view of finding a variant for improved *in vivo* FOP conversion in *S. cerevisiae*, some 90 mutants were designed and screened for improved *in vivo* FOP yield. The screening results revealed 5 improved variants of which E123M showed the highest FOP yield. As also shown with the mutant E123L which improved *in vivo* FOP production in *E. coli*, residue Glu123 seems to play an important role for the activity toward FO. This residue in SpRfK interacts with N5 of riboflavin, possibly stabilizing the substrate in the correct orientation.²⁸⁵ We initially anticipated that replacing this residue with a hydrophobic amino acid would improve the *in vivo* FOP production of the enzyme by reduced inhibition by FMN as well as improving the activity toward FO. However, *in vitro* conversion assays measured in the presence of different FMN concentrations showed that both wild type and the variants are significantly inhibited by FMN (Table S 4.3). Albeit that E123L shows slightly less inhibition than wild type and E123M, which might have contributed to the improved FOP yield in *E. coli*.

Even though SpRfK E123L showed a significant improvement in FOP production in *E. coli*, it did not increase the FOP yield in *S. cerevisiae* due to the lower expression level compared to wild-type SpRfK. This result showed that the protein expression level can change due to a single mutation and that change is dependent on the host organism. It also indicates that improved *in vitro* steady state kinetic properties do not always result in better *in vivo* performance, especially when the improvement is modest as in the case of E123L.

Besides the enzyme engineering approach, we also optimized other aspects related to growth condition for improving the final FOP yield in *S. cerevisiae*. Through testing different media, we first discovered that using the minimal medium (YND) yields much higher (~8-fold) amounts of FOP than using medium with amino acid supplements (SC). Essentially, SC medium is a YND medium with supplementary amino acids. There was no apparent effect of the media on growth behavior and the mechanism of the improved FOP conversion is unclear. The availability of extra amino acids in the media may affect the intracellular environment or metabolic flux in such

a way that it influences the FOP production. For example, supplementing glycine, a precursor in purine synthesis, could increase the riboflavin synthesis, which could potentially prevent the FOP formation as more SpRfK would be occupied with riboflavin rather than FO.^{302,303} This result shows that sometimes less supplemented media are more beneficial for whole cell-based production. A previous study on FO production in *E. coli* also showed that using minimal media supplemented only with tyrosine, a FO precursor, gives higher FO yield than using a more completed media.²⁷⁹

Although *S. cerevisiae* is a riboflavin-prototroph and does not require additional riboflavin for growth,^{68,304,305} it is included in generally used media. Omitting riboflavin from the media improved the FOP production in *S. cerevisiae*, which is anticipated to be the effect of less competition in uptake of FO. However, further studies on how riboflavin affects FO uptake or *in vivo* FOP formation is required. The higher FOP yield caused by increased FO concentration (up to 200 μ M) in the media also indirectly indicates a sub-optimal FO transport to the cell, although the result may as well be related with high K_M -value of wild-type SpRfK for FO. Overall, the best condition found in this study for FOP production in *S. cerevisiae* is to use YND medium, lacking riboflavin, supplemented with 200 μ M FO. Using this condition and the best SpRfK variant discovered from the library, E123M, we increased the FOP yield by over 20-fold compared to the unoptimized condition using SC medium and the wild-type SpRfK. However, the final improved yield (5.2 ± 0.9 nmol/gCDW) is still very modest, further improvement by strain and enzyme engineering as well as optimization of growth conditions, FOP-producing *S. cerevisiae* can potentially be used for interesting bioconversion applications.

4.5 Conclusion

In this study, we showed that it is possible to produce the artificial deazaflavin cofactor FOP in both *E. coli* and *S. cerevisiae*. In *E. coli*, *de novo* FOP biosynthesis was achieved by heterologous expression of a FO synthase from *M. smegmatis* and a riboflavin kinase from *S. pombe*. The improved FOP yield obtained through optimization was sufficient to demonstrate a whole-cell conversion with a F₄₂₀-dependent reductase. The FOP yield in *E. coli* is very similar to the F₄₂₀ yield in *M. smegmatis*, which is regarded as the best strain for F₄₂₀-production. The initially very low *in vivo* FOP yield in *S. cerevisiae* was also significantly improved through enzyme engineering and media optimization. In conclusion, our findings presented here may further the development of deazaflavin-dependent whole-cell conversions in both bacteria and yeast strains. Using these strains for the safe, easy to use, scalable and cost effective FOP synthesis might also boost deazaflavin mediated *in vitro* (bio)catalysis.

Author Contributions

M.L., J.D. and M.W.F. designed the project. J.D. designed and performed the experiments and analyzed the results for *in vivo* FOP production in *E. coli*. M.L. designed and performed the experiments and analyzed the results for *in vivo* FOP production in *S. cerevisiae*. R.d.J. designed the *in silico* RFK mutants and M.T. synthesized FO and assisted in chemical analyses. M.L. performed mutagenesis on the RFK gene, and steady-state kinetic analysis on engineered RFK variants. M.L., J.D. and M.W.F. wrote the manuscript.

Funding Sources

The research is financially supported by Dutch research council NWO (NWO-VICI-Fraaije and NWO-LIFT-YeastPlus grants), Royal DSM and Syngenta.

Notes

The authors declare no competing financial interest.

Acknowledgements

We also thank Marcus Hans, Cees Sagt and Alrik Los from Royal DSM, as well as Jason Vincent and Matthew Bennett from Syngenta for valuable scientific discussions.

4.6 Supporting information Chapter 4

Sequences of gene constructs and the mutagenic primers can be found online, in the supporting information to the published article.

Table S 4.1: Gene constructs.

Construct name	Vector backbone	Replicon	marker	MCS1 (NcoI/NdeIII)	MCS2 (NdeI/PacI)
pETDuet_ScFbiC	pETDuet-1	ColE1	amp	-	ScFbiC
pETDuet_MsFbiC	pETDuet-1	ColE1	amp	-	MsFbiC
pETDuet_CofG/H	pETDuet-1	ColE1	amp	NpCofH	MjCofG
pETDuet_ScFbiC_SpRFK E123L	pETDuet-1	ColE1	amp	SpRFK E123L	ScFbiC
pACYCDuet_SpRFK E123L	pACYCDuet-1	P15A	Cam	CaRFK HHI	
pCDFDuet_SpRFK E123L	pCDFDuet-1	CloDF13	strep	SpRFK E123L	-
pRSFDuet_SpRFK E123L	pRSFDuet-1	RSF1030	kan	SpRFK E123L	-
pCOLADuet_FSD/FDR	pCOLADuet-1	COLA	kan	SUMO-FSD- <i>Cryar</i>	SUMO-FDR- <i>Mha</i>

Genes were cloned into either MCS1 or MCS2 using NcoI/HindIII or NdeI/PacI, respectively. Amp = ampicillin, strep = streptomycin and kan = kanamycin, Cam is chloramphenicol. Gene sequences are shown in Table S1 of the online supplementary information to the article.

Table S 4.2: SpRFK library

Residues - Library 1					Residues - Library 2			
Mutants	Val64	Ser81	Glu123	Leu132	Mutants	Thr45	Val79	Leu132
A1 (WT)	V	S	E	L	E7 (WT)	T	V	L
A2	V	A	E	L	E8	T	M	L
A3	V	C	E	L	E9	T	L	L
A4	I	S	E	L	E10	D	V	L
A5	I	A	E	L	E11	D	M	L
A6	I	C	E	L	E12	D	L	L
A7	V	S	E	I	F1	E	V	L
A8	V	A	E	I	F2	E	M	L
A9	V	C	E	I	F3	E	L	L
A10	I	S	E	I	F4	T	V	I
A11	I	A	E	I	F5	T	M	I
A12	I	C	E	I	F6	T	L	I
B1	V	S	E	M	F7	D	V	I
B2	V	A	E	M	F8	D	M	I
B3	V	C	E	M	F9	D	L	I
B4	I	S	E	M	F10	E	V	I
B5	I	A	E	M	F11	E	M	I
B6	I	C	E	M	F12	E	L	I
B7	V	S	L	L	G1	T	V	M
B8	V	A	L	L	G2	T	M	M
B9	V	C	L	L	G3	T	L	M
B10	I	S	L	L	G4	D	V	M
B11	I	A	L	L	G5	D	M	M
B12	I	C	L	L	G6	D	L	M
C1	V	S	L	I	G7	E	V	M
C2	V	A	L	I	G8	E	M	M
C3	V	C	L	I	G9	E	L	M
C4	I	S	L	I	H1	T	V	E
C5	I	A	L	I	H2	T	M	E
C6	I	C	L	I	H3	T	L	E
C7	V	S	L	M	H4	D	V	E
C8	V	A	L	M	H5	D	M	E
C9	V	C	L	M	H6	D	L	E

Table S 4.2: Continued

Residues - Library 1					Residues - Library 2			
Mutants	Val64	Ser81	Glu123	Leu132	Mutants	Thr45	Val79	Leu132
C10	I	S	L	M	H7	E	V	E
C11	I	A	L	M	H8	E	M	E
C12	I	C	L	M	H9	E	L	E
D1	V	S	M	L				
D2	V	A	M	L				
D3	V	C	M	L				
D4	I	S	M	L				
D5	I	A	M	L				
D6	I	C	M	L				
D7	V	S	M	I				
D8	V	A	M	I				
D9	V	C	M	I				
D10	I	S	M	I				
D11	I	A	M	I				
D12	I	C	M	I				
E1	V	S	M	M				
E2	V	A	M	M				
E3	V	C	M	M				
E4	I	S	M	M				
E5	I	A	M	M				
E6	I	C	M	M				

Table S 4.3: Relative FO conversion in the presence of FMN

[FMN](μ M)	50 μ M FO			200 μ M FO		
	WT	E123M	E123L	WT	E123M	E123L
1	32 \pm 0.4	12.3 \pm 0.4	35.3 \pm 2.5	26.7 \pm 7.4	14.7 \pm 0.5	42.3 \pm 0.4
5	4.9 \pm 3.1	4.3 \pm 1.4	9.0 \pm 3.3	6.2 \pm 2.5	5.2 \pm 0.2	10.3 \pm 0.6
10	0.5 \pm 0.2	1.3 \pm 0.3	1.4 \pm 0.3	1.1 \pm 0.2	2.1 \pm 1.4	4.3 \pm 0.8

FOP conversion of *Sp*RFK variants with 50 and 200 μ M FO in the presence of 0, 1, 5 and 10 μ M of FMN was tested. The average FO conversion yield in the presence of 0 μ M FMN in each cases were set to 100% and the values represent the relative FO conversion in percentage. All measurements were done in duplicates and errors show the standard deviation.

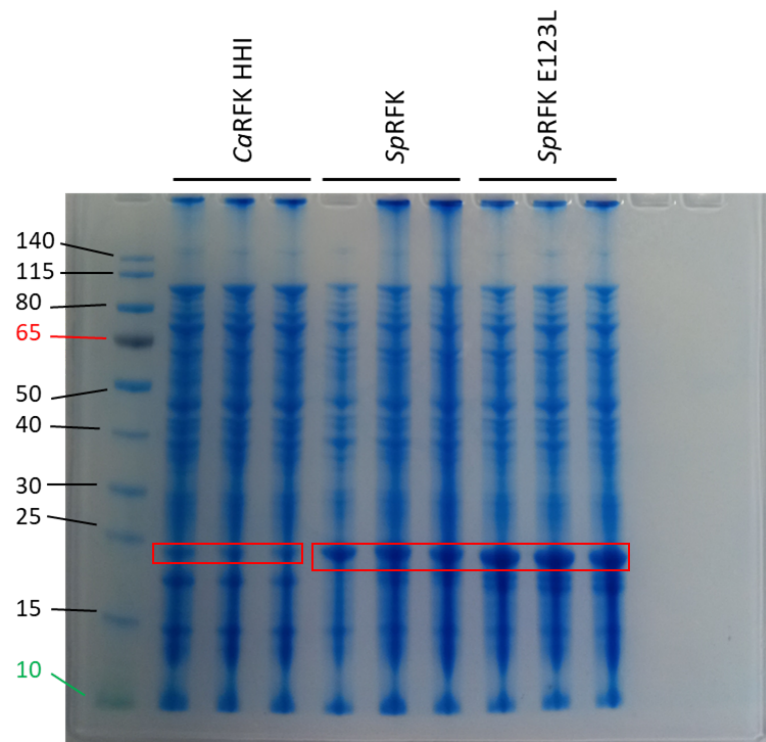


Figure S 4.1: SDS-PAGE analysis of *E. coli* NEB 10-beta cell free extracts expressing different C-terminally His-tagged riboflavin kinase mutants on pBAD Myc/His. CaRFK 6 \times His has a molecular weight of 18 kDA, SpRFK 6 \times His has a molecular weight of 19.7 kDA.

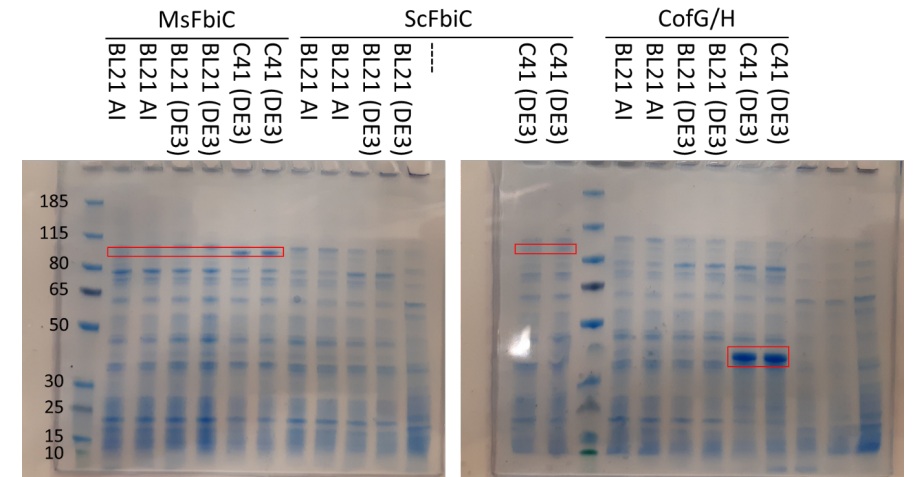


Figure S 4.2: 4 – 12% polyacrylamide gel with cell extracts from 5 mL cultures that were grown for 36 h at 24 °C, in the presence of 1 mM isopropyl β - D-1-thiogalactopyranoside (IPTG). Red bars highlight FO synthase bands.

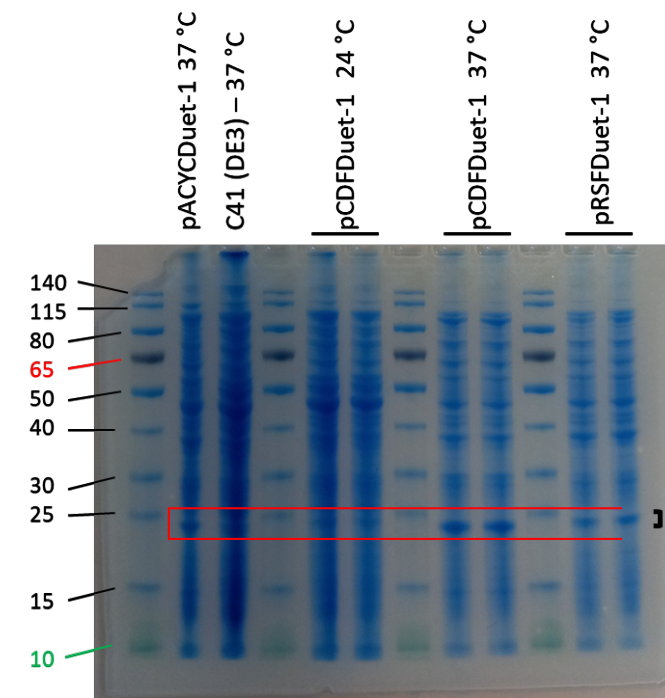


Figure S 4.3: SDS-PAGE analysis on cell free extract samples of C41 (DE3) expressing pETDuet_MsFbiC (Mw = 95.2 kDA) and SpRFK E123L (Mw = 18.9 kDA; red rectangles) on different vectors at different temperatures.

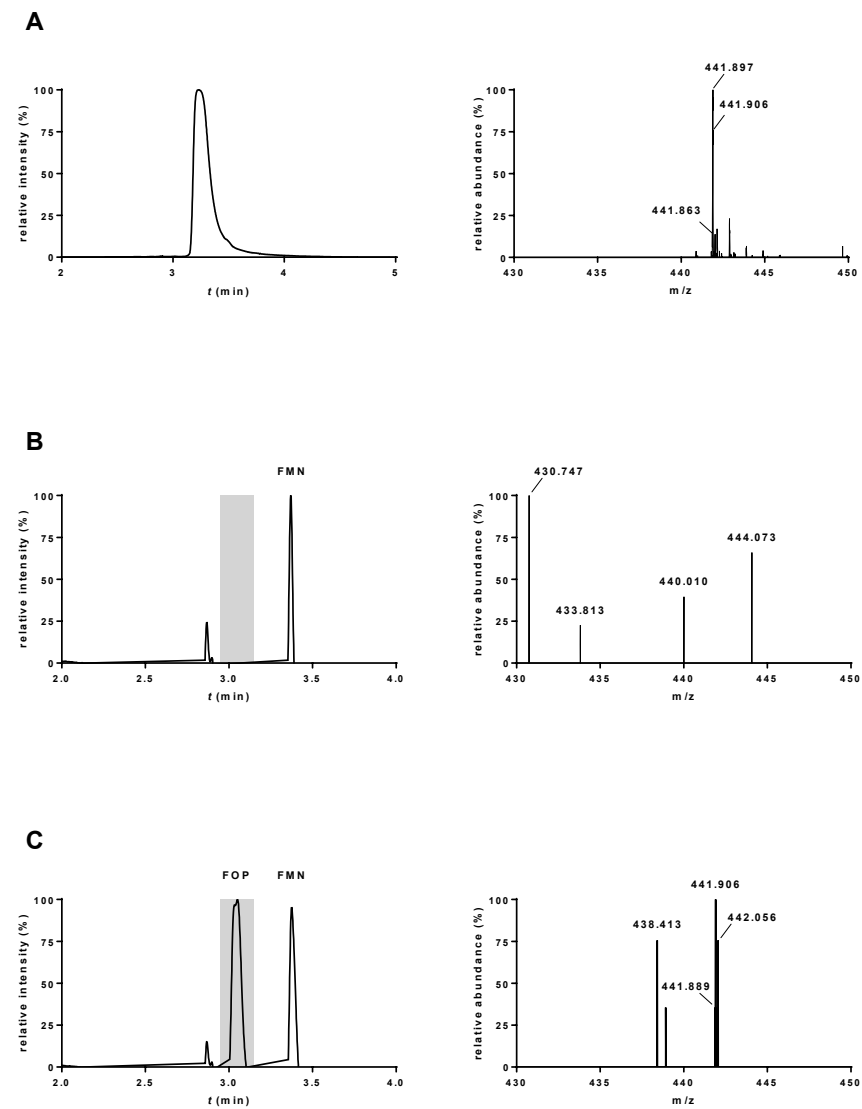


Figure S 4.4: UPLC/ESI-QTOF Mass spectrometry for FOP detection in cell free extracts. Graphs on the left show chromatograms, graphs on the right are corresponding mass spectra of highlighted areas (shown in light grey) **A:** In vitro synthesized FOP, dissolved in water. **B:** CFE of wild-type C41 (DE3). **C:** CFE of C41 (DE3) expressing MsFbiC on pETDuet-1 and SpRfK E123L on pCDFDuet-1.

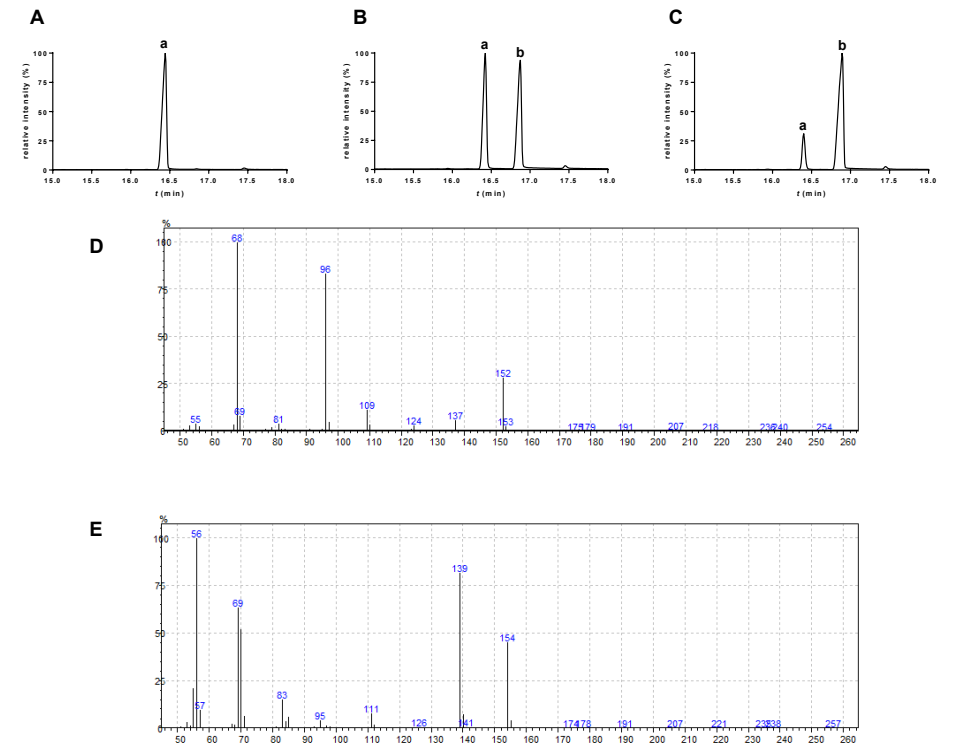


Figure S 4.5: GC-MS analysis of whole cell conversion samples. **A:** Ketoisophorone blank sample. **B:** wild-type C41 (DE3) conversion sample. **C:** C41 (DE3) expressing MsFbiC on pETDuet-1 and SpRfK E123L on pCDFDuet-1. **D:** Mass spectrum of peak a, showing exact mass and fragmentation pattern corresponding to ketoisophorone (substrate). **E:** Mass spectrum of peak b, showing exact mass and fragmentation pattern for 2,2,6-trimethylcyclohexane-1,4-dione, which is the desired product. The x-axis in figures D and E represent m/z values and the y-axis represent relative abundance.

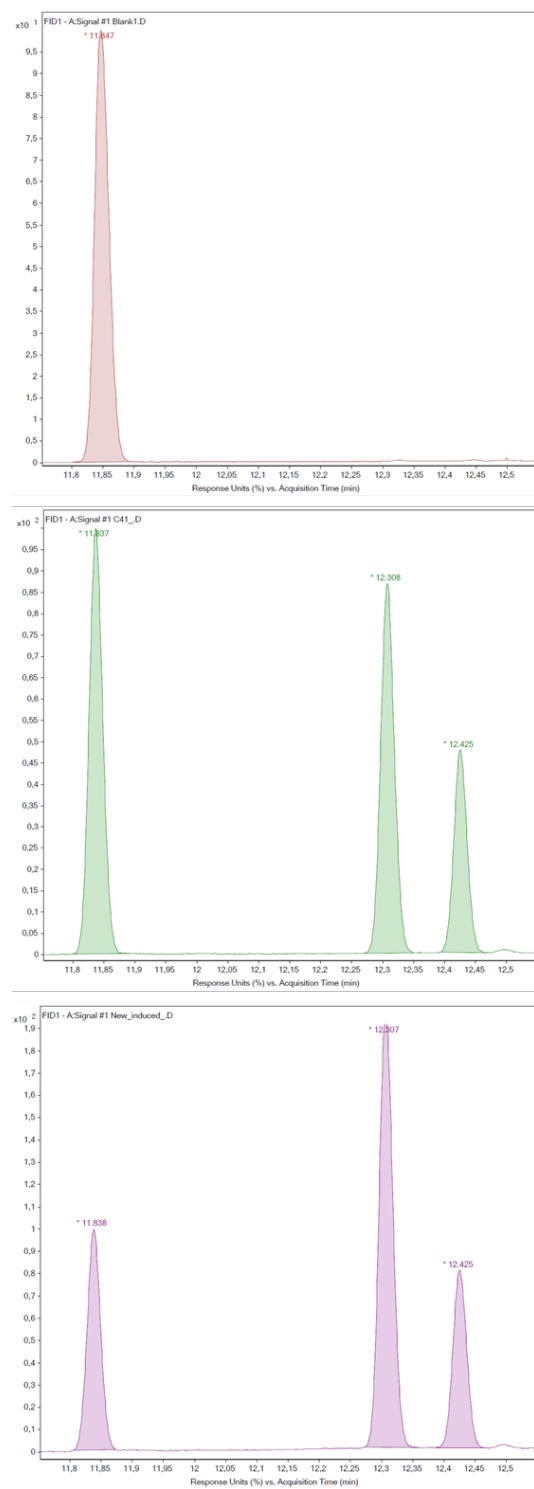


Figure S 4.6: Chiral GC analysis of whole cell conversion samples. Top: Ketoisophorone blank. Middle: wild-type C41 (DE3) conversion sample. Bottom: C41 (DE3) expressing MsFbiC on pETDuet-1 and SpRfK E123L on pCDFDuet-1. Left ($t_R = 12.3$) and right ($t_R = 12.425$) product peak correspond to the (R)-enantiomer and the (S)-enantiomer of 2,2,6-trimethylcyclohexane-1,4-dione, respectively, as was described before.

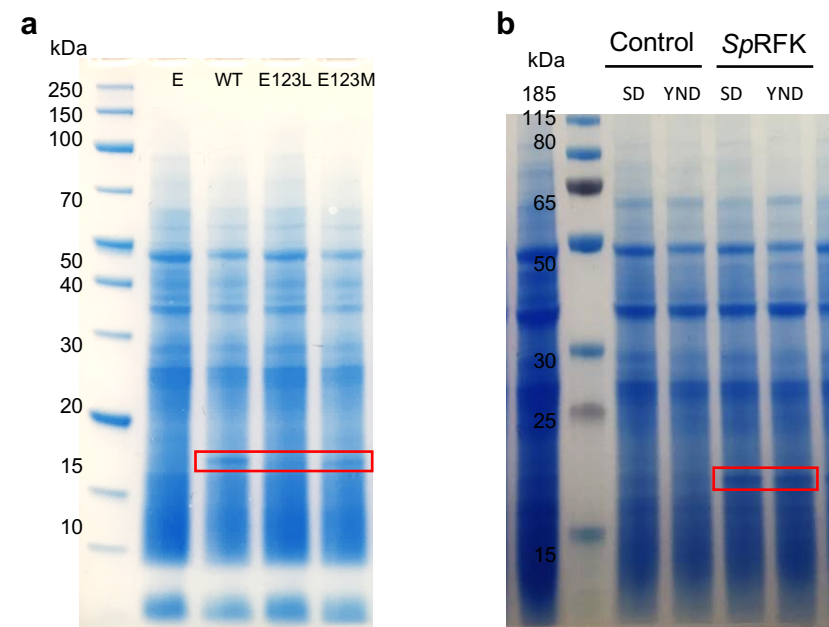


Figure S 4.7: SpRfK expression in *S. cerevisiae*. **a.** SDS-PAGE of cell free extract of *S. cerevisiae* expressing wild-type, E123L and E123M SpRfK. E: control cells carrying empty plasmids. **b.** SDS-PAGE of cell free extracts of *S. cerevisiae*, expressing wild-type SpRfK, grown on SD or YND media. Controls are cells carrying empty plasmids. Protein bands corresponding SpRfK (~19 kDa) are marked in red rectangles.

CHAPTER 5

A tailor-made deazaflavin-mediated recycling system for artificial nicotinamide cofactor biomimetics

Jeroen Drenth^{†*}, Guang Yang^{†*}, Caroline E. Paul[§] and Marco W. Fraaije[†]

This chapter is based on a published article: ACS Catal. 2021, 11, 18, 11561–11569

[†]*Molecular Enzymology Group, University of Groningen, Nijenborgh 4, 9747AG Groningen, The Netherlands*

[§]*Department of Biotechnology, Delft University of Technology, Van der Maasweg 9, 2629HZ Delft, The Netherlands*

^{*}*These authors contributed equally to this work*

Abstract

Nicotinamide adenine dinucleotide (NAD) and its 2'-phosphorylated form NADP are crucial cofactors for a large array of biocatalytically important redox enzymes. Their high cost and relatively poor stability, however, make them less attractive electron mediators for industrial processes. Nicotinamide cofactor biomimetics (NCBs) are easily synthesized, inexpensive, and also generally more stable than their natural counterparts. A bottleneck for the application of these artificial hydride carriers is the lack of efficient cofactor recycling methods. Therefore, we engineered the thermostable F_{420} :NADPH oxidoreductase from *Thermobifida fusca* (*Tfu*-FNO), by structure-inspired site-directed mutagenesis, to accommodate the unnatural N1-substituents of eight NCBs. The extraordinarily low redox potential of the natural cofactor $F_{420}H_2$ was then exploited to reduce these NCBs. Wild-type enzyme had detectable activity toward all selected NCBs, with K_m -values in the millimolar range and k_{cat} -values ranging from 0.09 to 1.4 min⁻¹. Saturation mutagenesis at positions Gly-29 and Pro-89 resulted in mutants with up to 139 times higher catalytic efficiencies. Mutant G29W showed a k_{cat} of 4.2 s⁻¹ toward 1-benzyl-3-acetylpyridine (BAP⁺), which is similar to the k_{cat} for the natural substrate NADP⁺. The best *Tfu*-FNO variants for a specific NCB were then used for the recycling of catalytic amounts of these nicotinamides in conversion experiments with the thermostable ene-reductase from *Thermus scotoductus* (*Ts*OYE). We were able to fully convert 10 mM ketoisophorone with BAP⁺ within 16 hours, using F_{420} or its artificial biomimetic FOP (FO-2'-phosphate) as efficient electron mediators and glucose-6-phosphate as electron donor. The generated toolbox of thermostable and NCB-dependent *Tfu*-FNO variants offers powerful cofactor regeneration biocatalysts for the reduction of several artificial nicotinamide biomimetics at both ambient and high temperatures. In fact, to our knowledge, this enzymatic method seems to be the best performing NCB-recycling system for BNAH and BAPH, thus far.

5.1 Introduction

An increased use of oxidoreductases for biocatalytic applications was seen in surveys of patent literature filed in the last two decades.^{306–308} In fact, in between 2000 and 2015, 68% of those patents was based on these enzymes.³⁰⁸ Oxidoreductases make up nearly one third of all enzymes³⁰⁹ and about half of them use a nicotinamide cofactor.³¹⁰ Nicotinamides and their *in vitro* performance are therefore of great importance to modern biocatalytic applications.

β -Nicotinamide adenine dinucleotide (NAD⁺/NADH) and β -nicotinamide adenine dinucleotide 2'-phosphate (NADP⁺/NADPH) are the two naturally occurring

nicotinamide cofactor variants, see **Figure 5.1A**. The nicotinamide moiety (pyridine-3-carboxylic acid amide) is the redox active part of the molecule, capable of accepting or donating a hydride. The adenosine diphosphate portion (ADP) serves as a recognition and anchoring point for enzymes. The presence or absence of the 2'-phosphate enables the cofactors to be discriminated by enzymes, while there are also enzymes that accept both nicotinamide cofactors.

The use of NAD(P)-dependent enzymes *in vitro* requires either a stoichiometric amount of the cofactor or a catalytic amount in combination with an *in situ* regeneration system. Although efficient enzymatic and non-enzymatic recycling systems already exist,^{310,311} the stability and cost of NAD and especially NADP remain an issue for large scale applications.^{312,313} The ADP and ADP-2'-phosphate moieties of the natural nicotinamides are partially responsible for these issues, but are not necessary for *in vitro* biocatalysis. Therefore, an array of synthetic analogues known as nicotinamide cofactor biomimetics (NCBs), have been synthesized to overcome these problems. These relatively simple molecules are 1- and 3-substituted pyridines (see **Figure 5.1B**), which are easily synthesized from inexpensive, commercially available building blocks,^{314,315} and are generally more stable than NAD(P) under standard *in vitro* conditions.^{312,314}

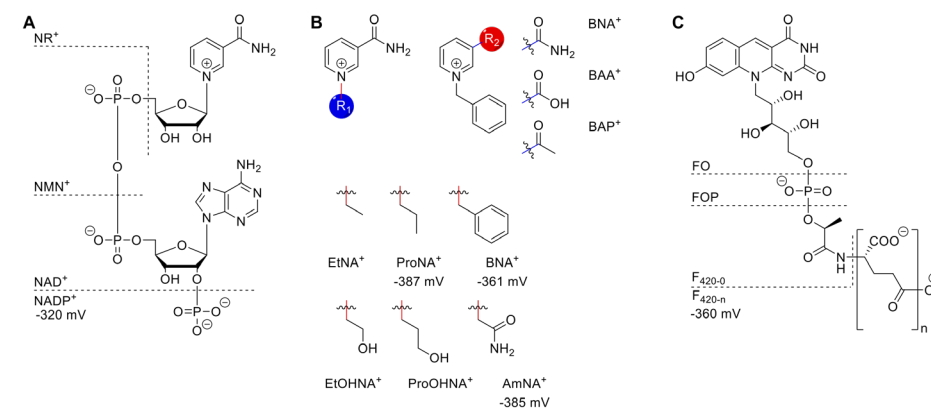


Figure 5.1: Nicotinamide and F_{420} cofactors. **A:** The natural nicotinamides β -nicotinamide adenine dinucleotide (NAD) and β -nicotinamide adenine dinucleotide 2'-phosphate (NADP) and their redox active natural precursors nicotinamide mononucleotide (NMN) and nicotinamide ribose (NR). **B:** The artificial nicotinamide biomimetics that were investigated in this study. Their abbreviated names and redox potentials (when known) are shown below the structural formulas.³¹⁶ Their full names can be found in the list of abbreviations. **C:** The naturally occurring 5-deazaflavin cofactor F_{420} and its redox active natural precursor FO and the artificial biomimetic FOP.^{30,21,32}

NCBs have been employed in several studies as reducing agents for oxidoreductases. Reduced 1-methylnicotinamide (MNAH) was the first of these synthetic cofactors that was successfully applied to reduce two redox enzymes, namely a DT diaphorase from Walker 256 rat carcinoma cells and a nitroreductase from *Escherichia coli*, with the same efficiency as NAD(P)H.^{317,318} Thereafter, reduced 1-benzyl nicotinamide (BNAH) and its *para*-methoxy analogue were used to reduce a mutant cytochrome P450 BM3 from *Bacillus megaterium* and P450cam from *Pseudomonas putida*, showing slightly lower specific activities of hydroxylation as compared to NAD(P)H.³¹⁹ BNAH also works with 2-hydroxybiphenyl 3-monooxygenase (HbpA) from *Pseudomonas azelaica* HBP1,³²⁰ with 3-hydroxybenzoate 6-hydroxylase (3HB6H) from *Rhodococcus jostii* RHA1, *para*-hydroxybenzoate hydroxylase (PHBH) from *Pseudomonas fluorescens*, salicylate hydroxylase (SalH) from *P. putida*,³²¹ and even improved the dye degrading activity of the oxygen-insensitive azoreductase (AzoRo) from *Rhodococcus opacus* 1CP.³²² Several reduced NCBs were used on ene-reductases from the old yellow enzyme family (OYE), with varying activities between different OYE-NCB combinations.^{323–327} In several cases the nicotinamide biomimetics outperformed the native cofactors NADH and NADPH.^{323–325} Alcohol dehydrogenases however, generally show no or very low activity toward NCBs, apart from horse liver ADH, which showed activity with BNAH as hydride donor.^{328–330} Their greater stability, lower cost and sometimes enhanced performance with oxidoreductases make them lucrative alternatives for (NAD(P)).

Although these NCBs are significantly cheaper than their natural counterparts, stoichiometric addition of reduced NCB would still not be economically feasible. Therefore, several *in situ* recycling methods have been developed over the last few years. Two enzymatic recycling methods have been reported for the oxidation of reduced NCBs, namely a hydrogen peroxide driven myoglobin system for BNAH and the water forming NADH oxidase from *Lactobacillus pentosus* for MNAH and BNAH.^{331,332} Recycling reduced NCBs is considerably more challenging, due to their low redox potentials. The most popular recycling method for reduced NCBs, thus far, is the formate-driven organometallic rhodium catalyst pentamethylcyclopentadienyl rhodium bipyridine, $[\text{Cp}^*\text{Rh}(\text{bpy})(\text{H}_2\text{O})]^{2+}$,³³³ which has been used in several studies.^{319,320,324,328,329} Two studies, however, have reported low initial activity and mutual inactivation of organometallic catalyst and enzyme, which form major bottlenecks for biocatalysis.^{320,334} Several attempts to overcome these problems were published, such as the use of different counter ions for the rhodium catalyst,^{319,328} catalyst separation,³³⁵ carbon-nanodot-sensitized regeneration systems,³³⁶ and artificial metalloenzymes that were based on streptavidin variants with biotinylated iridium catalysts.³³⁷ To our knowledge, two studies have investigated enzymatic recycling systems of reduced NCBs. The two enzymes are an engineered

6-phosphogluconate dehydrogenase from *Thermotoga maritima* and an engineered glucose dehydrogenase from *Sulfolobus solfataricus* (SsGDH).^{338,339} Unfortunately, these recycling systems still have low catalytic efficiencies. The low catalytic activity might be caused by two separate, yet equally important factors: 1) the poor structural complementarity between the 1-substituents of the NCBs and the enzyme scaffold, and 2) the incompatibility of the low redox potentials of NCBs with most natural redox systems. The naturally occurring redox cofactor F_{420} (see **Figure 5.1C**), found in many archaea and actinobacteria, has an extremely low redox potential of -360 mV, which is close to the potentials of most NCBs.^{20,21,25,211,316} Some organisms use F_{420} : NADPH oxidoreductases to catalyze the reversible hydride transfer between F_{420} and the natural nicotinamide NADPH. Therefore, these enzymes may form effective recycling systems for reduced NCBs, harnessing the strong reducing power of F_{420} .

Herein we describe the engineering of the thermostable F_{420} : NADPH oxidoreductase from *Thermobifida fusca* (*Tfu*-FNO)²⁵³ to efficiently reduce a selection of NCBs (see **Figure 5.1B**). Structure-guided site-directed mutagenesis was used to make variants that better accommodate NCBs. These variants were then screened for improved activity toward selected NCBs and the best mutants were further characterized with steady-state kinetics. The best *Tfu*-FNO variants for a given biomimetic were then used as recycling systems in conversion experiments with the ene-reductase from *Thermus scotoductus* (*Ts*OYE), using glucose-6-phosphate as sacrificial electron donor. Also the artificial deazaflavin biomimetic FOP,³² see **Figure 5.1C**, was employed as an equally efficient electron mediator, demonstrating that engineered FNO enables regeneration of catalytic amounts of reduced NCBs through the use of a catalytic amount of either F_{420} or an artificial deazaflavin biomimetic. In fact, this study presents the first mutagenesis study on an F_{420} -dependent enzyme for biocatalytic purposes, resulting in an efficient recycling system for a broad selection of NCBs at ambient and elevated temperatures.

5.2 Materials and Methods

5.2.1 Materials

All chemicals and mutagenic primers were purchased from Sigma Aldrich (Merck; St. Louis, MO, U.S.A.), unless stated otherwise. The natural nicotinamides NMN^+ , NR^+ , NADP^+ and NADPH were ordered at Sigma Aldrich, all artificial nicotinamide biomimetics were synthesized as described before by Norris et al. and Knox et al.^{314,315} Ligase, and restriction endonucleases, as well as the bacterial expression and cloning strains *E. coli* NEB 10-beta, BL21 (DE3) and C41 (DE3) were obtained from New England Biolabs (NEB, Ipswich, MA, U.S.A.). PfuUltra Hotstart PCR Mastermix (Agilent Technologies) was used for mutagenic PCR (QuikChange). Plasmid DNA was

isolated using the QIAprep Miniprep Kit, and PCR products were purified with the QIAquick PCR Purification Kit (Qiagen, Valencia, CA, U.S.A.). F_{420} was isolated from *Mycobacterium smegmatis* mc² 4517, as described by Bashiri et al. and Isabelle et al.^{269,270} FOP was synthesized as previously described by Drenth et al.³²

5.2.2 Expression and purification of F_{420} -dependent enzymes

The F_{420} :NADPH oxidoreductase from *T. fusca* (*Tfu*-FNO) was expressed and purified as previously described by Kumar et al.²⁵³ The F_{420} -dependent glucose-6-phosphate dehydrogenase from *R. jostii* RHA1 (FGD-RHA1) and the F_{420} -dependent sugar-6-phosphate dehydrogenase from *Cryptosporangium arvum* (FSD-*Cryar*) were expressed and purified as N-terminally SUMO-fused proteins, as previously described by Nguyen et al.²³⁰ and Mascotti et al.,²⁶⁵ respectively. The same plasmid constructs and expression strains were used as in the aforementioned literature.

5.2.3 TsOYE expression and purification

The thermostable ene-reductase from *T. scotoeductus* (TsOYE) was expressed and purified as previously described by Knaus et al. and Opperman et al.^{324,340} with the following exceptions: TsOYE was heat-purified at 70 °C for 90 min, saturated with FMN, desalted (PD10) and concentrated (Amicon 10 kDa cutoff), and stored in 20 mM MOPS-NaOH pH 7.0.

5.2.4 *Tfu*-FNO mutagenesis

Site-directed mutagenesis was performed on the *Tfu*-FNO gene with the use of mutagenic primers, using the QuikChange mutagenesis kit (Stratagene), following the procedure of the manufacturer. Primers were designed with the Agilent QuikChange primer design tool (<http://www.genomics.agilent.com/primerDesignProgram.jsp>). The used primers are listed in Table S1 of the online supplementary information to the article. Sequencing was performed at GATC/Eurofins Genomics (Konstanz, Germany). The plasmids were transformed into calcium chloride chemically competent *E. coli* NEB 10-beta for plasmid amplification and protein expression, using standard protocols.

5.2.5 Steady-state activity assays and mutant activity screens

Steady-state parameters for the activity of wild-type and mutant *Tfu*-FNO variants toward NCBs were obtained by a spectrophotometric assay. The measurements were performed at 25 °C by adding 0.1 – 5 μ M enzyme to 50 mM Tris-HCl, 100 mM NaCl, 3% (v/v) DMSO, pH 8.0 with a constant F_{420} :H₂ concentration of 40 μ M and varying concentrations of NCBs between 0.1 and 250 mM. The absorbance at 400 nm was followed in time, and observed slopes (k_{obs}) were calculated with $\epsilon_{400}(F_{420}) = 25.7 \text{ mM}^{-1} \text{ cm}^{-1}$

cm^{-1} . All experiments were performed in triplicates. The k_{obs} values were plotted against de NCB concentration, and the data were fitted to the Michaelis–Menten equation (eq 1) or Michaelis–Menten equation with substrate inhibition (eq 2) by nonlinear regression, using GraphPad Prism v. 6.0 (GraphPad Software Inc., La Jolla, CA, U.S.A.).

$$k_{obs} = \frac{k_{cat} \cdot [S]}{K_m + [S]} \quad (1)$$

$$k_{obs} = \frac{k_{cat} \cdot [S]}{K_m + [S] \cdot \left(1 + \frac{[S]}{K_i}\right)} \quad (2)$$

F_{420} :H₂ was prepared by incubating 400 μ M F_{420} with 10 μ M FGD-RHA1 and 5 mM glucose-6-phosphate in 50 mM Tris-HCl, pH 8.0, until the yellow color disappeared. Then, the mixture was passed through an Amicon Ultra 0.5 mL centrifugal filter, 10 kDa molecular weight cutoff. The filtrate, containing 400 μ M F_{420} :H₂, was then immediately used for a spectrophotometric assay.

The mutant activities toward certain NCBs were screened at 25 °C by adding 1 μ M enzyme to 50 mM Tris-HCl, 100 mM NaCl, 3% (v/v) DMSO pH 8.0, with 40 μ M F_{420} :H₂ and either 1 or 40 mM NCB. The absorbance at 400 nm was followed in time, and observed initial slopes (k_{obs}) were calculated with $\epsilon_{400}(F_{420}) = 25.7 \text{ mM}^{-1} \text{ cm}^{-1}$. All experiments were performed in duplicates. For the best performing mutants this activity assay was also performed at 50 °C in triplicates.

5.2.6 Conversion experiments

The reaction mixture, with a total volume of 500 μ L, contained of 50 mM Tris-HCl, 100 mM NaCl, 3% (v/v) DMSO, pH 8.0 supplemented with 10 mM 2,6,6-trimethyl-2-cyclohexene-1,4-dione (ketoisophorone), 400 μ M FOP or 100 μ M F_{420} , 1.0 mM NCB (in the oxidized form), 5 μ M TsOYE, 5 μ M *Tfu*-FNO, 10 μ M FSD-*Cryar*, and 50 mM glucose-6-phosphate. The reactions were performed in closed 2 mL glass vials in the dark at 30 °C and 135 rpm for 3 to 24 h. The reaction was quenched by adding 100 μ L of the mixture to 400 μ L acetonitrile and was then incubated on ice for 5 min. This mixture was spun down at 8000g in a table top centrifuge at 4 °C, and 10 μ L supernatant was used for analysis on HPLC. The depletion of substrate was analyzed at 240 nm, using an isocratic mobile phase of 60:40 water:acetonitrile on an Alltech Alltime HP C18 5 μ , 250 mm column.

5.3 Results

5.3.1 *Tfu*-FNO wild-type activity toward selected NCBs

The thermostable F_{420} :NADPH oxidoreductase from *T. fusca* (*Tfu*-FNO) was expressed and purified as described before.²⁵³ Then, the activity of *Tfu*-FNO for a selection of nicotinamide biomimetics (NCBs), see **Figure 5.1B**, was assessed spectrophotometrically. First, the optimal pH for NCB reduction was investigated by reducing 40 mM BNA⁺ and AmNA⁺ at pH 6 to 8. The optimal pH was determined to be 8 (**Figure S 5.9**), which is the same as the previously published optimal pH for NADP⁺ reduction.²⁵³ Steady-state kinetic parameters were measured by varying the concentration of the NCBs, while maintaining a constant, saturating F_{420} :H₂ concentration. The initial slopes of absorbance increase at 400 nm were measured, and the observed rates (k_{obs}) were calculated using $\epsilon_{400} = 25.7 \text{ mM}^{-1} \text{ cm}^{-1}$. The observed rates were plotted against the cofactor concentration and fitted to the Michaelis–Menten model, with or without substrate inhibition (eqs 1 and 2, respectively). The resulting steady-state parameters are shown in **Table 5.1**. The Michaelis–Menten curves are shown in **Figure S 5.1** and **Figure S 5.2**. All tested biomimetics had detectable activity that could be fitted to the Michaelis–Menten models, with and without substrate inhibition. All compounds showed substrate inhibition at high concentrations (>40 mM). All K_m values were in the millimolar range, with the lowest value for BNA⁺ (6.4 mM) and the highest for ProOHNA⁺ and EtNA⁺ (25 mM). The k_{cat} values span from 0.09 min⁻¹ for ProNA⁺, to 1.4 min⁻¹ for AmNA⁺ and EtOHNA⁺. This shows that wild-type *Tfu*-FNO has a very high specificity for NADP⁺, as this native co-substrate has a k_{cat} of 4.9 s⁻¹ and a K_m of 1.1 μM .²⁵³

5.3.2 *Tfu*-FNO mutagenesis

Structure-guided site-directed mutagenesis was performed on *Tfu*-FNO, in order to improve the catalytic efficiency toward the nicotinamide biomimetics. The crystal structure of *Tfu*-FNO (PDB ID: 5N2I), with co-crystallized NADP⁺, was used to identify sites for mutagenesis. See **Figure S 5.10**. Glycine-29, proline-89, alanine-87 and valine-113 were chosen as sites for mutagenesis, as these residues are in close proximity to the ribose moiety of NADP⁺, which is substituted by small, similarly sized substituents in NCBs. Mutants A87S, V113S, G29X and P89X, were created with QuikChange-PCR, where X stands for F, H, I, L, M, N, Q, S, V, W, and Y. Single point mutations were introduced and screened for their activity toward the NCBs. All mutant FNOs had similar expression levels as wild-type. Also, their apparent melting temperature, as measured by the ThermoFluor assay, did not change (data not shown), which is ideal for high temperature conversion.

5.3.3 Mutant activity screens and subsequent steady-state activity measurements

The engineered *Tfu*-FNO variants G29X and P89X, harboring a single point mutation, were screened for their activity toward the different NCBs. The G29X and P89X mutants with a polar amino acid side-chain (H, N, Q, S and Y) were tested for their activity toward EtOHNA⁺, ProOHNA⁺ and AmNA⁺, as these have a compatible polar N1-substituent. Similarly, the G29X and P89X with apolar amino acid side-chains (F, H, I, L, M, V, W and Y) were tested for their activity with EtNA⁺, ProNA⁺ and BNA⁺, which have apolar N1-substituents. The mutants were screened in 96-well format with a constant, saturating F_{420} :H₂ concentration and an NCB concentration of either 1 or 40 mM. All mutants were also screened for their activity toward nicotinamide ribose (NR) and nicotinamide mononucleotide (NMN), which are the redox active natural precursors of NAD(P). **Figure S 5.3–S5.5** of the supporting information summarize the results. No mutant was found with a significantly higher activity toward EtNA⁺, NR⁺ or NMN⁺ when compared with the wild-type enzyme. All other NCBs had at least one *Tfu*-FNO variant with significantly increased reduction rates. The kinetic parameters of these hits were then characterized spectrophotometrically, as was done before with wild-type *Tfu*-FNO. For 1-aminoethylnicotinamide (AmNA⁺), variants G29S, G29Y and P89H were identified as hits, and indeed showed higher k_{cat} values than wild-type *Tfu*-FNO. The same trend was seen with G29Y, P89H and P89Y for 1-hydroxyethylnicotinamide (EtOHNA⁺), P89Y for 1-hydroxypropylnicotinamide (ProOHNA⁺), and G29L, P89L and P89Y for 1-propylnicotinamide (ProNA⁺), where the mutants show a significant increase in maximum velocity of up to 7 times that of wild type *Tfu*-FNO. Mutants G29Y and G29W had an even more dramatic increase in activity toward 1-benzylnicotinamide (BNA⁺), with 32 and 93 times higher reduction rates than wild type, respectively. The K_m , however, was hardly changed. So, most mutations do not seem to affect the overall binding affinity of these NCBs, but – probably – do induce subtle changes in the binding conformation that lead to more efficient hydride transfer.

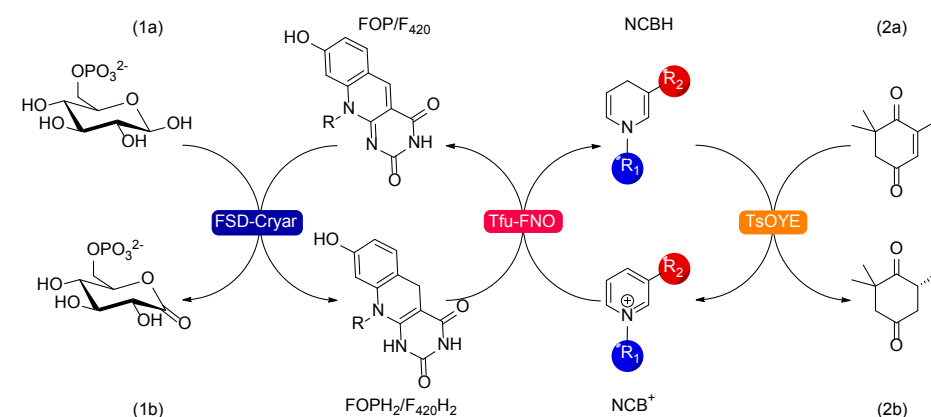
Variant G29W, the variant with 139 times higher catalytic efficiency toward BNA⁺ than wild type, was also tested for its activity toward 1-benzylnicotinic acid (BAA⁺) and 1-benzyl-3-acetylpyridine (BAP⁺), as all of which have the same N1-substituent. Although no apparent activity could be measured for BAA⁺, profound activity was observed for BAP⁺, with a k_{cat} of 4.2 s⁻¹ (252 min⁻¹). This maximum velocity is very similar to that of wild type toward its natural substrate NADP⁺, which is 4.9 s⁻¹. The aforementioned results show that G29S, G29Y and P89H, and especially G29W could serve as effective recycling agents for AmNAH, BNAH and BAPH.

Table 5.1: Steady-state kinetic parameters for wild-type *Tfu*-FNO and selected *Tfu*-FNO G29X and P89X variants toward selected NCBs. The measurements were performed at 25 °C by adding 0.1 – 5 μM enzyme to 50 mM Tris-HCl, 100 mM NaCl, 3% (v/v) DMSO, pH 8.0 with a constant $F_{420}H_2$ concentration of 40 μM and varying concentrations of NCBs between 0.1 and 250 mM. Absorbance traces over time were measured and fitted to the Michaelis–Menten model. Values are means from 3 independent measurements ± standard deviations. N.A.: not active. The corresponding Michaelis–Menten plots are shown in Figure S 5.6 and Figure S 5.7 of the supporting information.

NCB	variant	k_{cat} (min ⁻¹)	K_m (mM)	k_{cat}/K_m (s ⁻¹ M ⁻¹)	$(k_{cat}/K_m)_{mutant}/(k_{cat}/K_m)_{wt}$
AmNA ⁺	wt	1.4 ± 0.07	12 ± 1.7	1.9 ± 0.29	
	G29S	9.6 ± 0.56	18 ± 2.5	8.8 ± 1.3	4.6 ± 0.98
	G29Y	3.2 ± 0.23	23 ± 3.5	2.3 ± 0.39	1.2 ± 0.28
	P89H	2.5 ± 0.21	14 ± 3.0	3.0 ± 0.69	1.6 ± 0.44
EtOHNA ⁺	wt	1.4 ± 0.06	20 ± 2.5	1.2 ± 0.15	
	G29Y	6.2 ± 0.58	23 ± 4.7	4.5 ± 1.0	3.8 ± 0.96
	P89H	2.9 ± 0.22	20 ± 3.3	2.4 ± 0.44	2.0 ± 0.44
	P89Y	5.0 ± 0.63	33 ± 9.2	2.5 ± 0.77	2.1 ± 0.69
ProOHNA ⁺	wt	0.25 ± 0.013	25 ± 3.0	0.17 ± 0.022	
	P89Y	0.71 ± 0.096	35 ± 10	0.34 ± 0.11	2.0 ± 0.7
EtNA ⁺	wt	0.44 ± 0.01	25 ± 1.4	0.29 ± 0.018	
ProNA ⁺	wt	0.09 ± 0.007	10 ± 2.8	0.15 ± 0.044	
	G29L	0.36 ± 0.057	18 ± 7.9	0.33 ± 0.16	2.2 ± 1.3
	P89H	0.27 ± 0.026	5.7 ± 1.9	0.79 ± 0.27	5.3 ± 2.4
	P89L	0.44 ± 0.048	27 ± 6.9	0.27 ± 0.075	1.8 ± 0.73
	P89Y	0.59 ± 0.11	35 ± 14	0.28 ± 0.12	1.9 ± 0.97
BNA ⁺	wt	0.27 ± 0.01	6.4 ± 0.60	0.70 ± 0.071	
	G29W	25 ± 1.1	4.3 ± 0.68	97 ± 15	139 ± 26
	G29Y	8.7 ± 0.64	9.5 ± 2.0	15 ± 3.4	21 ± 5.3
BAP ⁺	G29W	252 ± 14	7.4 ± 1.2	568 ± 97	
BAA ⁺	G29W	N.A.	N.A.	N.A.	

Double mutants G29S/P89H, G29Y/P89H and G29Y/P89Y were made for AmNA⁺, EtOHNA⁺, and ProOHNA⁺, where hits in activity increase for both position 29 and 89 were seen. These double mutants were screened in a 96-well format for their activity toward 1 mM AmNA⁺, EtOHNA⁺, ProOHNA⁺, NR⁺ and NMN⁺. Unfortunately, none of these mutants showed better activity than the single mutants or wild-type. Double mutants with two large, aromatic side chains might form steric clashes with the NCB or with their surroundings, therefore abolishing the NCB reduction activity.

The activity of the single mutants was also tested for the native substrate NADP⁺ (see Table S 5.1). Most mutations significantly decrease the activity toward NADP⁺, but do not completely inhibit the enzyme for this co-substrate. Adding mutations in the 2'-phosphate binding site, as was previously done by Kumar et al., might completely abolish NADP⁺-reduction activity.²⁵³ These *Tfu*-FNO variants might then be used for biorthogonal pathways that use NCBs and are not affected by the presence of NAD(P).



Scheme 5.1: The TsOYE-catalyzed reduction of ketoisophorone (2,6,6-trimethyl-2-cyclohexene-1,4-dione; **2a**) by NCBs. Glucose-6-phosphate (**1a**) is used as a sacrificial electron donor for the reduction of F_{420} or FOP, as catalyzed by FSD-Cryar. Reduced F_{420} /FOP can then efficiently reduce several NCBs for the formation of chiral product.

Tfu-FNO variants as NCB-recycling systems for TsOYE-mediated conversions

TsOYE is known to efficiently hydrogenate ketoisophorone (2,6,6-trimethyl-2-cyclohexene-1,4-dione) to form the chiral product (*R*)-2,2,6-trimethylcyclohexane-1,4-dione with high *ee*-values of 94 – 97%, when using several NCBs as more efficient electron donors than NADPH.^{323,324} The *Tfu*-FNO variants G29Y, G29W and P89H, which showed high activity toward AmNA⁺, BNA⁺ and BAP⁺, were selected for the use in conversion experiments as recycling catalysts for these NCBs. The catalytic amount of 1 mM oxidized NCB was used for the TsOYE-catalyzed reduction of 10 mM ketoisophorone at 30 °C. F_{420} (100 μM) or FOP (400 μM) was used as electron mediator and glucose-6-phosphate was used as sacrificial electron donor to fuel the reduction of NCBs through the action of the deazaflavin-dependent glucose-6-phosphate dehydrogenase FSD-Cryar, see Scheme 5.1. Reaction mixtures that contained *Tfu*-FNO G29W and P89H, in combination with BNA⁺ or AmNA⁺ as their respective nicotinamides, converted 5 mM of the substrate within 16 h of incubation. Mixtures containing the combination of G29W with the artificial nicotinamide BAP⁺ showed even full conversion of 10 mM ketoisophorone within 16 h (see Figure 5.2A).

Therefore, we could demonstrate the use of *Tfu*-FNO as a recycling method for catalytic amounts of several artificial nicotinamide biomimetics in ene-reductase catalyzed conversions.

To demonstrate the potential use of these thermostable *Tfu*-FNO variants as NCB recycling systems at high temperatures, we measured the activity of a selection of variants toward 5 mM of AmNA⁺, BNA⁺ and BAP⁺ at both 25 and 50 °C. Gratifyingly, the performance increased at elevated temperature. This makes *Tfu*-FNO variants especially suitable as NCB recycling method for conversions at relatively high temperatures (see **Figure 5.2B**).

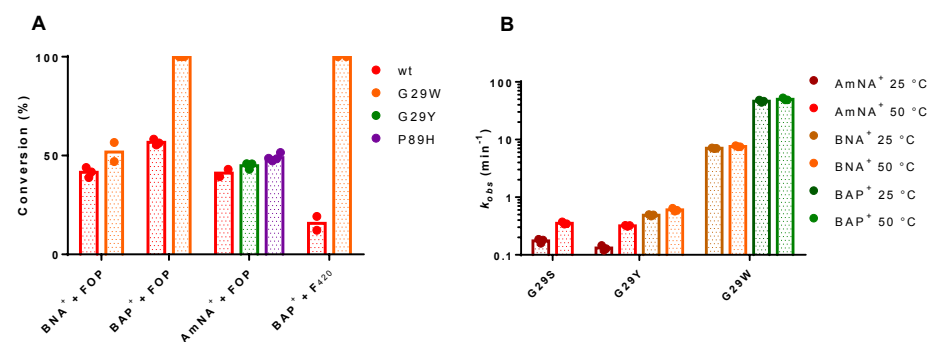


Figure 5.2: **A:** The TsOYE-catalyzed conversion of 10 mM ketoisophorone, using 1 mM NCB, 100 μM F420 or 400 μM FOP and glucose-6-phosphate as sacrificial electron donor after 16 h at 30 °C. **B:** The activity of selected *Tfu*-FNO variants toward 5 mM of nicotinamide biomimetic at either 25 or 50 °C. Bars represent average values of individual data points, which are represented by dots.

Table 5.2: Turnover numbers for the reduction of BNA⁺ and BAP⁺ for several recycling systems.

Recycling catalyst	Turnover number (min ⁻¹)	
	BNA ⁺	BAP ⁺
<i>Tfu</i> -FNO G29W	25	252
SsGDH I192T/V306I ³³⁸	0.54	-
[Cp ³ Rh(bpy)H] ³³³	0.15	0.15
ATHase IrC-Sav S112K ³³⁷	4.0	-
ATHase IrC-Sav No Sav ³³⁷	7.2	-

5.4 Discussion

Nicotinamide-dependent oxidoreductases make up one third of all redox enzymes and are of paramount importance in biocatalysis. The stability and cost of NAD(P), however, make these compounds less attractive for green chemistry.^{312,313} Therefore, a range of artificial biomimetics were introduced as alternative nicotinamide cofactors. These small 1 and 3 substituted pyridines were first introduced for mechanistic studies and thereafter also proved their value as stable and low cost cofactors.^{312–314} Many NCBs have a lower redox potential than their natural counterparts as an additional benefit. The challenge with these NCBs however, is proper cofactor recycling of the reduced form. Several metal-based catalysts have been proposed as recycling agents,^{333,337} which are hard to reconcile with white biotechnology.

The low redox potential of these artificial cofactors, as well as their non-natural structure make it hard to find efficient enzyme-mediated recycling systems. The naturally occurring cofactor F₄₂₀, which is found in a plethora of archaea and actinobacteria,²⁶ has a compatibly low redox potential (–360 mV) to many of these NCBs.²¹ This makes the cofactor suitable for the use in NCB recycling systems. In fact, we could indeed show for the thermostable F₄₂₀:NADPH oxidoreductase from *T. fusca*, which naturally catalyzes the hydride transfer between the redox pairs F₄₂₀/F₄₂₀H₂ and NADP⁺/NADPH, that it is also able to reduce a range of nicotinamide biomimetics (see **Figure 5.1** and **Table 5.1**). In fact, this is, to the best of our knowledge, the first study to consider such a large and diverse array of artificial nicotinamides. Although the wild type FNO activity toward these NCBs is relatively low, we could show that several structure-inspired variants with single amino acid substitutions at position 29 and 89 have drastically increased reduction rates for several NCBs. Especially the G29W variant, which has a 139 times increase in catalytic efficiency toward 1-benzylnicotinamide (BNA⁺) as compared to wild type *Tfu*-FNO, and has a *k_{cat}* for 1-benzyl-3-acetyl-pyridine (DAP⁺) which is similar to the wild type activity toward the native substrate NADP⁺.²⁵³ To the best of our knowledge, this *Tfu*-FNO variant is in fact the best recycling catalyst for BNA⁺ and BAP⁺ reported thus far, see **Table 5.2**. The reduced form of these NCBs are especially interesting for the reduction of α,β-unsaturated carbonyl compounds, as they were shown to outperform NADPH as reducing agent for several ene-reductases.³²⁴

We could show that variants P89H, G29Y and G29W are indeed efficient NCB recycling systems in bioconversions, in combination with an ene-reductase. Only a catalytic amount of 1 mM of NCB was necessary to convert 5 to 10 mM ketoisophorone within 16 hours. Not only F₄₂₀, but also its artificial biomimetic FOP³² could be used for these conversions. The use of FOP might overcome the upscaling problems that F₄₂₀ could face, as it needs to be isolated from slow growing organisms, thus far.²⁷⁰

The catalytic activity toward the native substrate, NADP⁺, was drastically decreased for most of the variants that are described in this study. Therefore, these *Tfu*-FNO variants could also be employed as a biorthogonal system in parallel with NAD(P)-dependent systems, when one or several additional mutations are introduced that completely inhibit NADP⁺-binding. Kumar et al. have already shown that they could drastically decrease the catalytic efficiency for the natural substrate by introducing single or several point mutations at positions that would not interfere with NCB-binding.²⁵³

In this study the F₄₂₀-dependent glucose-6-phosphate dehydrogenase from *R. jostii* RHA1 (FGD-RHA1) and the F₄₂₀-dependent sugar-6-phosphate dehydrogenase from *C. arvum* (FSD-*Cryar*) were used as recycling enzymes in the conversion experiments as a proof of concept, which use the somewhat expensive sacrificial electron donor glucose-6-phosphate. For industrial applications other cheaper and more accessible electron donors might be used, such as isopropanol, formate or hydrogen gas in combination with F₄₂₀-dependent alcohol dehydrogenases, formate dehydrogenases or hydrogenases, respectively.^{214,216,218,341–343} The use of these electron donors could make this an inexpensive and scalable recycling system.

Moreover, the thermostability of the *Tfu*-FNO variants make them lucrative for high temperature conversions. Not only are they stable at elevated temperatures they were also shown to have greater NCB reduction rates when used at 50 °C, as compared to room temperature. Thermostability often also ensures organic co-solvent tolerance, which would make this NCB recycling method also ideal for processes that involve highly hydrophobic compounds.

The toolbox of F₄₂₀:NADPH oxidoreductases that were tailor-made to accept NCBs, as presented in this study, could make the application of NAD(P)-dependent oxidoreductases in large-scale biocatalysis more feasible. These thermostable enzymes can be implemented as efficient enzymatic recycling systems for catalytic amounts of NCBs at ambient and elevated temperatures, harnessing the reductive power of F₄₂₀ and FOP.

List of abbreviations

AmNA ⁺	1-aminoethylnicotinamide
BAA ⁺	1-benzylnicotinic acid
BAP ⁺	1-benzyl-3-acetylpyridine
BNA ⁺	1-benzylnicotinamide
EtNA ⁺	1-ethylnicotinamide
EtOHNA ⁺	1-hydroxyethylnicotinamide
FGD-RHA1	<i>Rhodococcus jostii</i> RHA1 F ₄₂₀ -dependent glucose-6-phosphate dehydrogenase
FSD- <i>Cryar</i>	<i>Cryptosporangium arvum</i> F ₄₂₀ -dependent sugar-6-phosphate dehydrogenase
MNA ⁺	1-methylnicotinamide
ProNA ⁺	1-propylnicotinamide
ProOHNA ⁺	1-hydroxypropylnicotinamide
<i>Tfu</i> -FNO	<i>Thermobifida fusca</i> F ₄₂₀ :NADPH oxidoreductase
TsOYE	<i>Thermus scotoeductus</i> ene-reductase

Author Contributions

M.W.F., C.E.P. and J.D. designed the project. J.D., G.Y. and C.E.P. designed and performed the experiments and analyzed the results. J.D. and M.W.F. wrote the manuscript.

Funding Sources

Funding came from the Dutch research council; NWO (VICI grant).

Notes

The authors declare no competing financial interest.

Acknowledgements

We thank Martijn Deinum for help in experimental work.

5.5 Supporting information Chapter 5

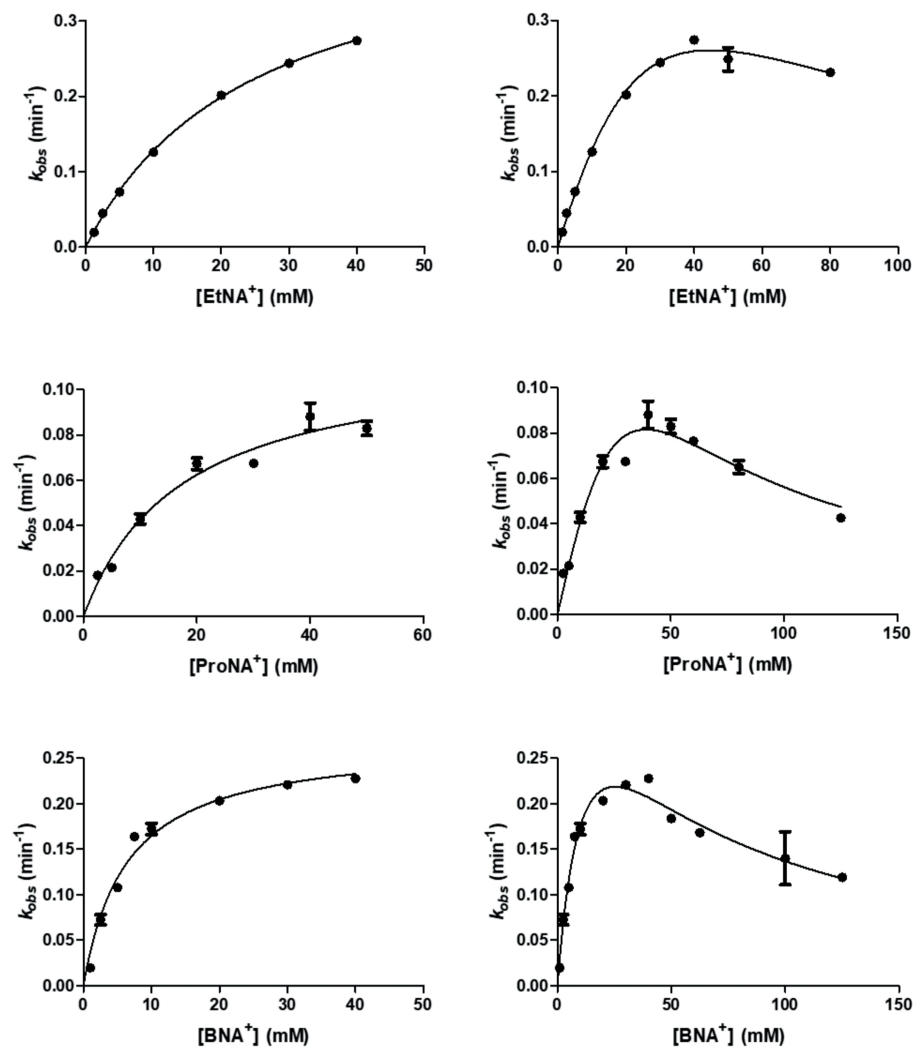


Figure S 5.1: The observed initial rates, k_{obs} , of wild-type Tfu-FNO plotted against the concentrations of artificial nicotinamide cofactor biomimetics (NCBs) with apolar groups at position 1 of the nicotinamide. Data in the left column is fitted to the Michaelis–Menten formula and data in the right column is fitted to the Michaelis–Menten formula with substrate inhibition. Data was fitted by non-linear regression, GraphPad Prism v. 6.0 (GraphPad Software Inc., La Jolla, CA, U.S.A.). Data points and error bars represent means and standard deviations of triplicates, respectively. EtNA+: 1-ethylnicotinamide, ProNA+: 1-propylnicotinamide, BNA+: 1-benzylnicotinamide.

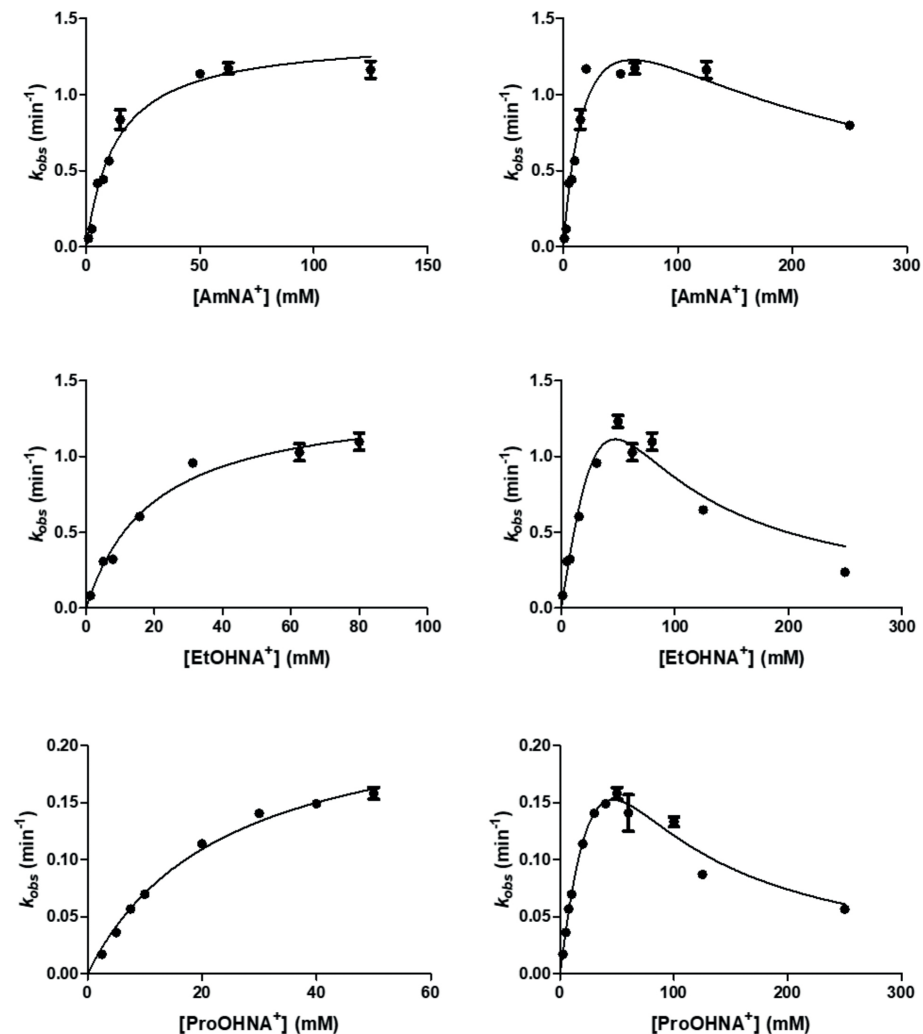


Figure S 5.2: The observed initial rates, k_{obs} , of wild-type Tfu-FNO plotted against the concentrations of artificial nicotinamide cofactor biomimetics (NCBs) with polar groups at position 1 of the nicotinamide. Data in the left column is fitted to the Michaelis–Menten formula and data in the right column is fitted to the Michaelis–Menten formula with substrate inhibition. Data was fitted by non-linear regression, GraphPad Prism v. 6.0 (GraphPad Software Inc., La Jolla, CA, U.S.A.). Data points and error bars represent means and standard deviations of triplicates, respectively. EtOHNA+: 1-hydroxyethylnicotinamide, ProNA+: 1-hydroxypropylnicotinamide, AmNA+: 1-carbamylethylnicotinamide.

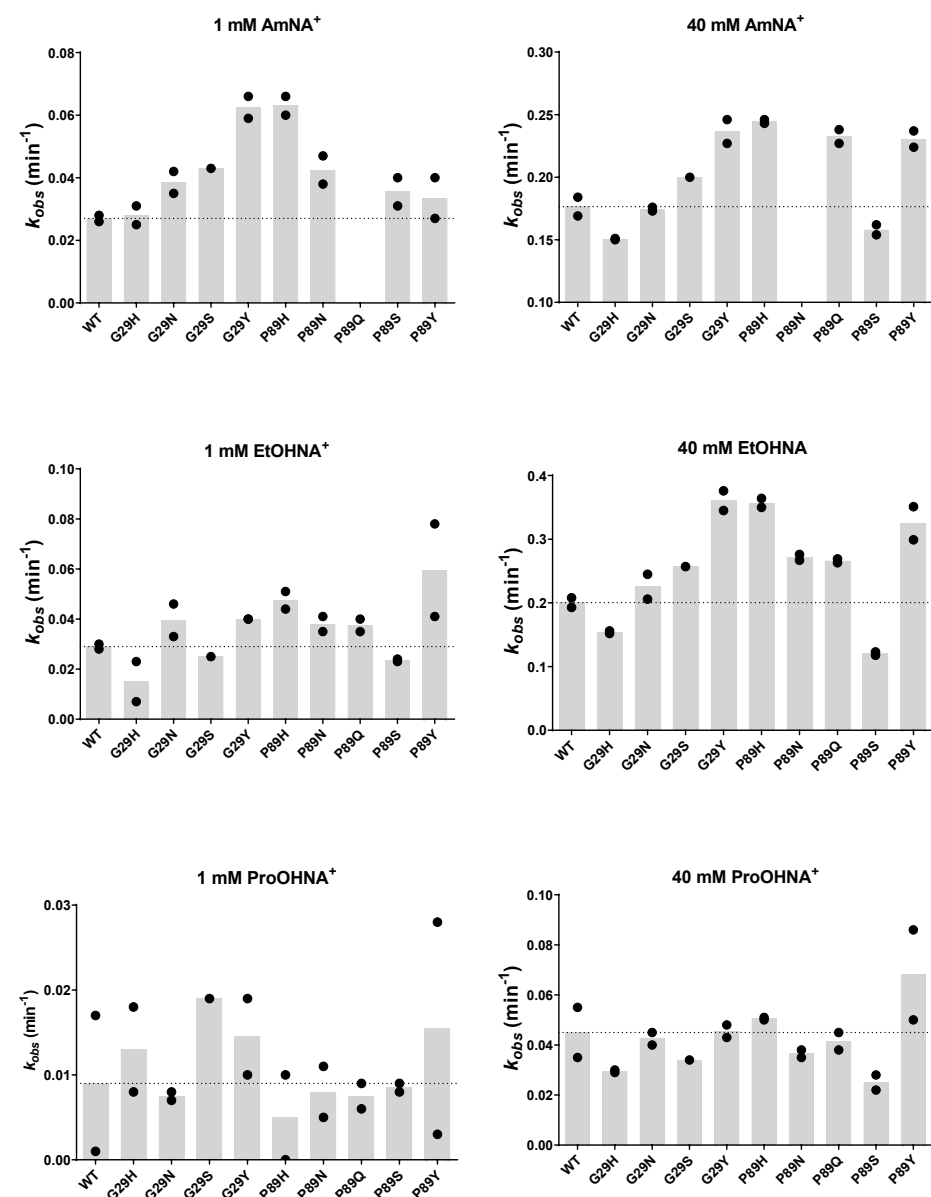


Figure S 5.3: Activity screen of selected Tfu-FNO G29X and P89X variants with polar amino acid side chains toward artificial nicotinamide cofactor biomimetics (NCBs) with polar groups at position 1 of the nicotinamide. Data in the left column and right column are the activity measured with 1 mM NCB and 40 mM NCB, respectively. Data points represents individual k_{obs} measurements and bars represent the mean value of these two data points. The horizontal dotted line is the mean value of wild-type activity.

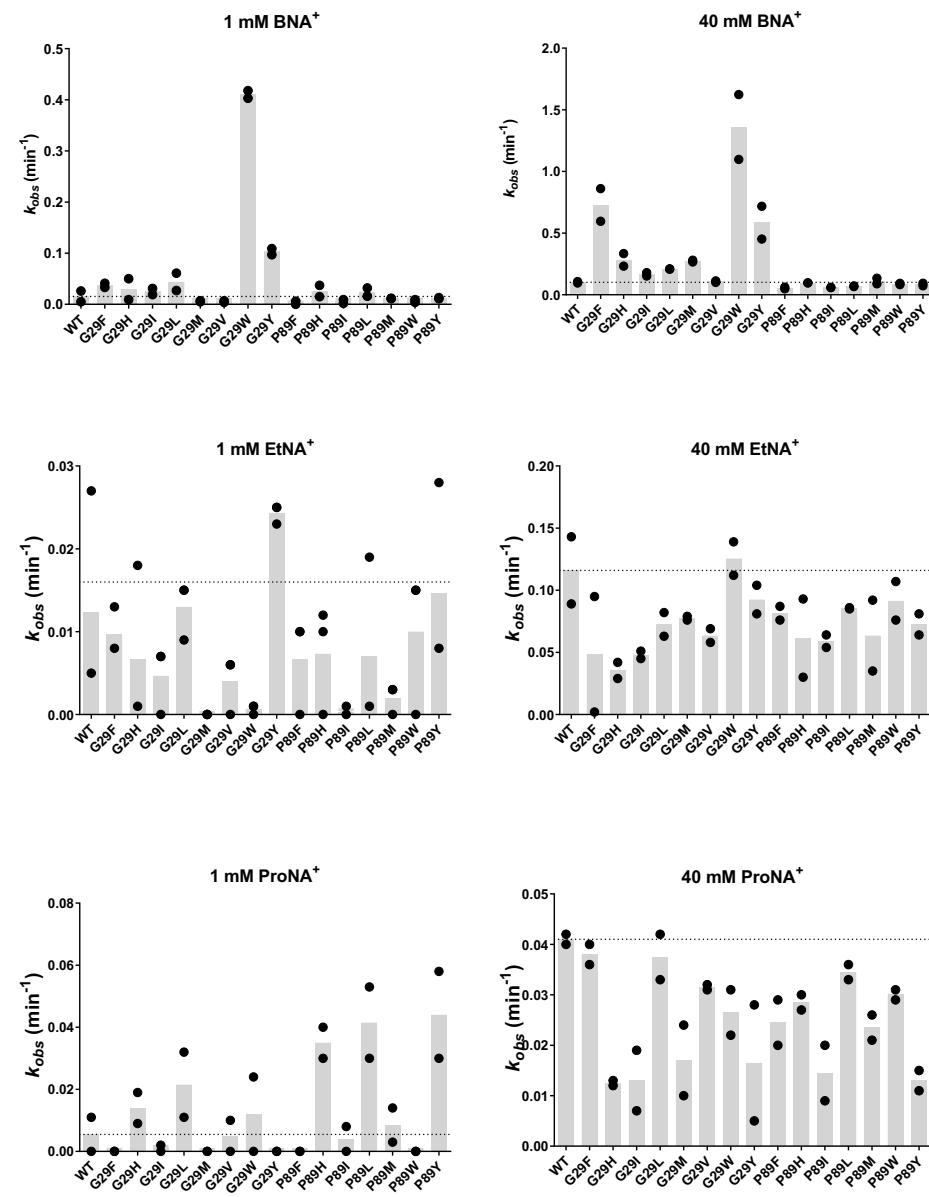


Figure S 5.4: Activity screen of selected Tfu-FNO G29X and P89X variants with apolar amino acid side chains toward artificial nicotinamide cofactor biomimetics (NCBs) with apolar groups at position 1 of the nicotinamide. Data in the left column and right column are the activity measured with 1 mM NCB and 40 mM NCB, respectively. Data points represents individual k_{obs} measurements and bars represent the mean value of these two data points. The horizontal dotted line is the mean value of wild-type activity.

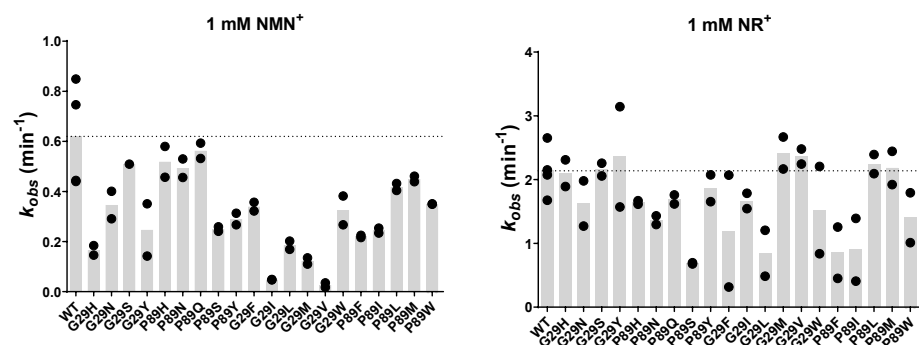


Figure S 5.5: Activity screen of selected Tfu-FNO G29X and P89X variants toward the natural NAD(P) precursors nicotinamide ribose (NR) and nicotinamide mononucleotide (NMN). Data points represent individual k_{obs} measurements and bars represent the mean value of these two data points. The horizontal dotted line is the mean value of wild-type activity.

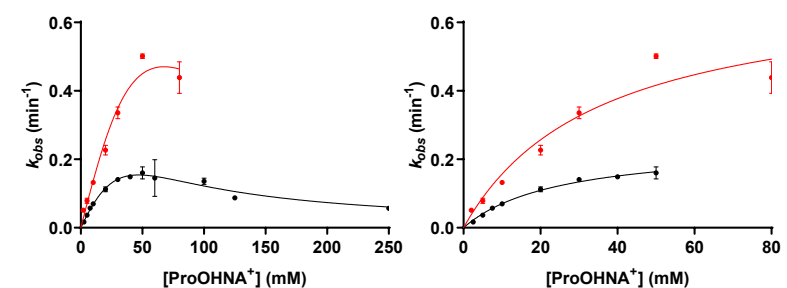
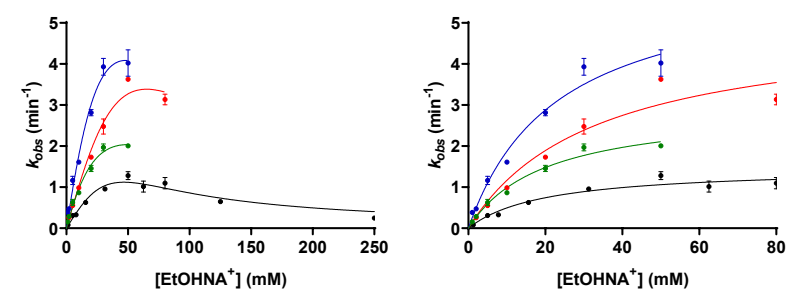
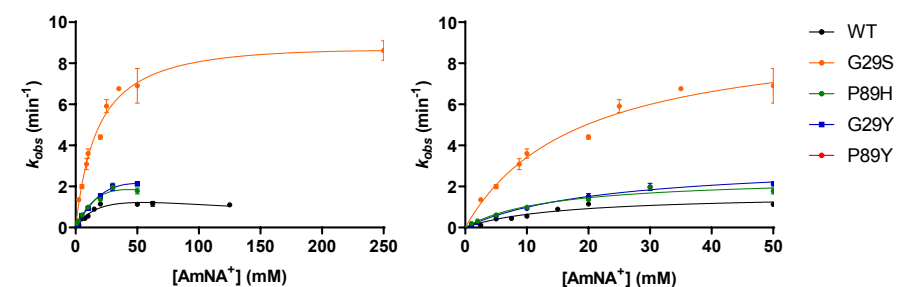


Figure S 5.6: The observed initial rates, k_{obs} , of selected Tfu-FNO G29X and P89X variants with polar side chains plotted against the concentrations of artificial nicotinamide cofactor biomimetics (NCBs) with polar groups at position 1 of the nicotinamide. Data in the left column is fitted to the Michaelis–Menten formula with substrate inhibition and data in the right column is fitted to the Michaelis–Menten formula. Data was fitted by non-linear regression, GraphPad Prism v. 6.0 (GraphPad Software Inc., La Jolla, CA, U.S.A.). Data points and error bars represent means and standard deviations of triplicates, respectively. EtOHNA+: 1-hydroxyethylnicotinamide, ProNA+: 1-hydroxypropylnicotinamide, AmNA+: 1-carbamoylethylnicotinamide.

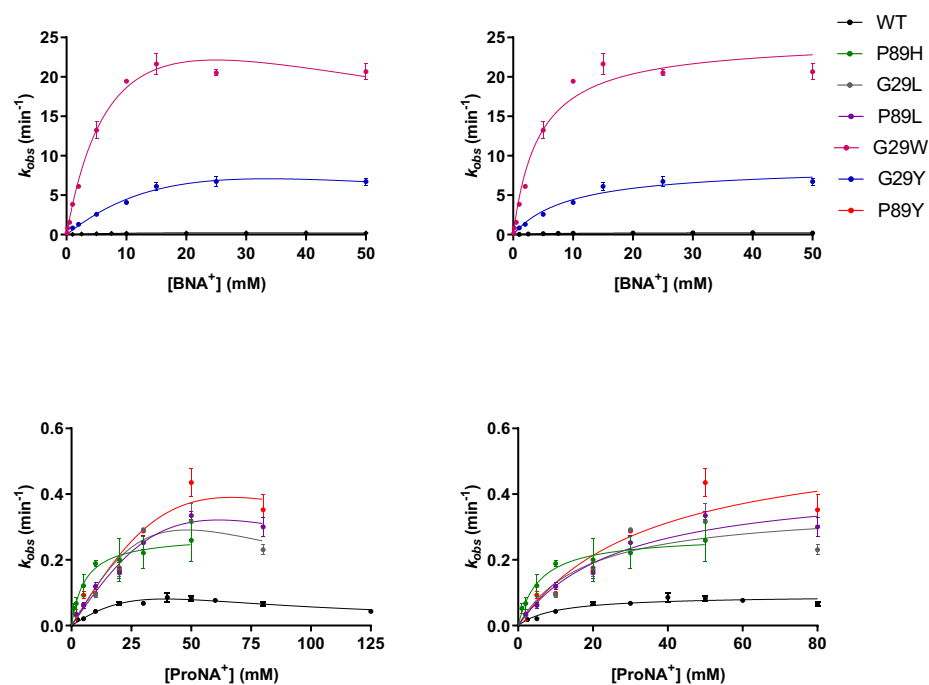


Figure S 5.7: The observed initial rates, k_{obs} , of selected Tfu-FNO G29X and P89X variants plotted against the concentrations of artificial nicotinamide cofactor biomimetics (NCBs) with apolar groups at position 1 of the nicotinamide. Data in the left column is fitted to the Michaelis–Menten formula with substrate inhibition and data in the right column is fitted to the Michaelis–Menten. Data was fitted by non-linear regression, GraphPad Prism v. 6.0 (GraphPad Software Inc., La Jolla, CA, U.S.A.). Data points and error bars represent means and standard deviations of triplicates, respectively. EtNA+: 1-ethylnicotinamide, ProNA+: 1-propylnicotinamide, BNA+: 1-benzyl nicotinamide.

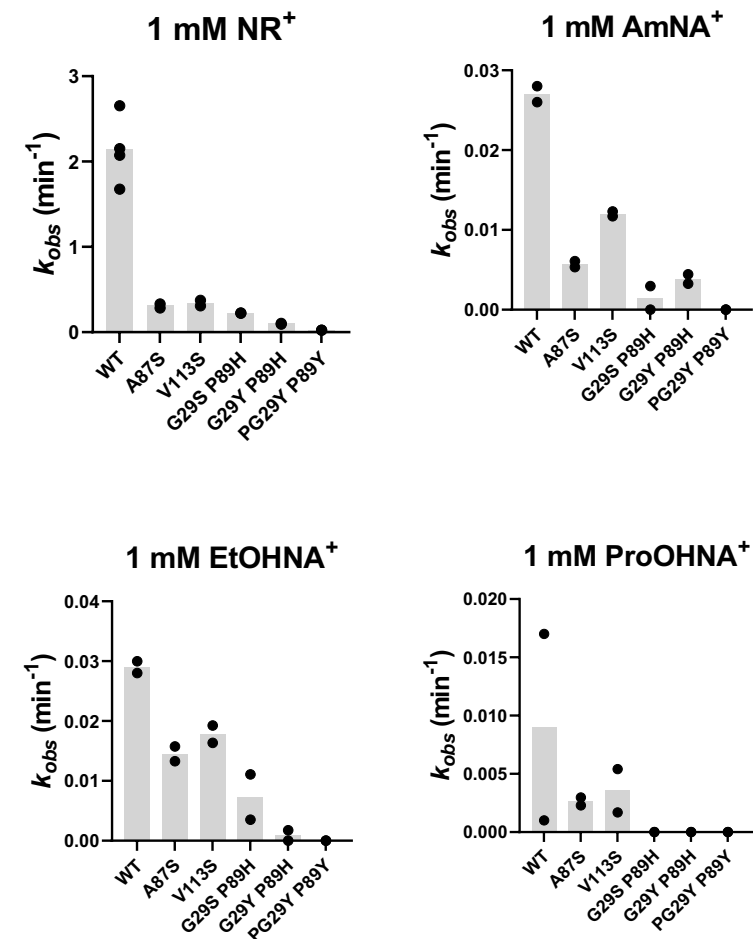
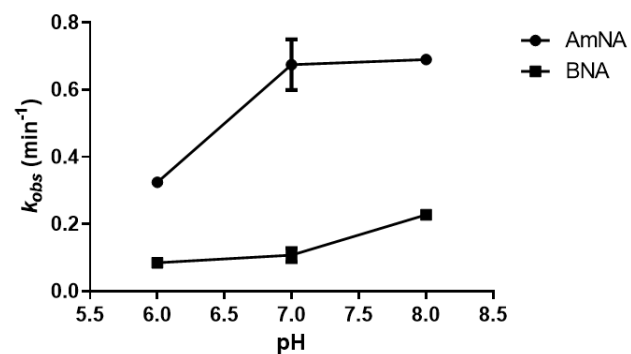
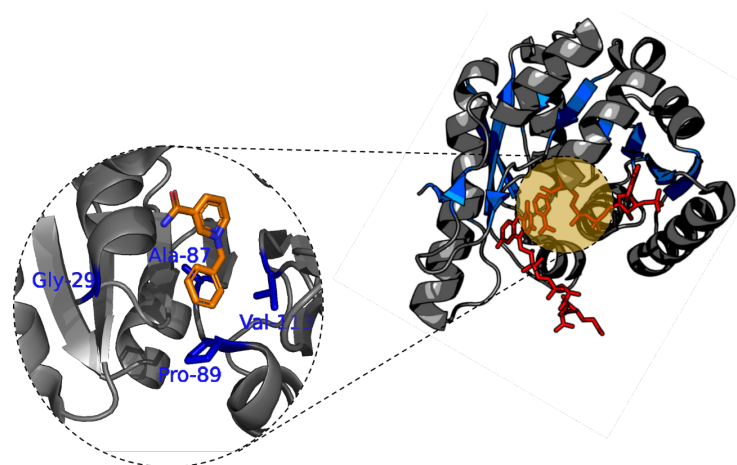


Figure S 5.8: Activity screen of selected Tfu-FNO G29X/P89X double mutant variants, as well as A87S and V113S, toward the natural NAD(P) precursor nicotinamide ribose (NR) and the polar artificial nicotinamides AmNA+, EtOHNA+ and ProOHNA+. Data points represent individual k_{obs} measurements and bars represent the mean value of these two data points.

Table S 5.1: Steady-state kinetic parameters for wild-type Tfu-FNO and selected Tfu-FNO G29X and P89X variants toward selected NADP+. Values are means from 3 independent measurements \pm standard deviations.

variant	k_{cat} (s ⁻¹)	K_m (μ M)	k_{cat}/K_m (s ⁻¹ M ⁻¹)	$(k_{cat}/K_m)_{mutant}/(k_{cat}/K_m)_{wt}$
wt	4.9 \pm 0.21	1.1 \pm 0.21	4.5 \cdot 10 ⁶ \pm 8.7 \cdot 10 ⁵	
G29L	0.63 \pm 0.03	1.2 \cdot 10 ³ \pm 140	522 \pm 65	1.2 \cdot 10 ⁻⁴ \pm 2.7 \cdot 10 ⁻⁵
G29W	2.6 \pm 0.13	697 \pm 109	3.7 \cdot 10 ³ \pm 612	8.4 \cdot 10 ⁻⁴ \pm 2.1 \cdot 10 ⁻⁴
G29Y	0.17 \pm 0.005	8.2 \pm 0.72	2.1 \cdot 10 ⁴ \pm 1.9 \cdot 10 ³	4.7 \cdot 10 ⁻³ \pm 1.0 \cdot 10 ⁻³
P89H	20 \pm 0.61	14 \pm 1.5	1.4 \cdot 10 ⁶ \pm 1.5 \cdot 10 ⁵	0.3 \pm 0.07
P89L	0.55 \pm 0.02	65 \pm 8.0	8.4 \cdot 10 ³ \pm 1.1 \cdot 10 ³	1.9 \cdot 10 ⁻³ \pm 4.4 \cdot 10 ⁻⁴
P89Y	3.9 \pm 0.16	86 \pm 15	4.5 \cdot 10 ⁴ \pm 8.1 \cdot 10 ³	1.0 \cdot 10 ⁻² \pm 2.7 \cdot 10 ⁻³

**Figure S 5.9:** pH dependence of NCB-reduction by Tfu-FNO.**Figure S 5.10:** The active site of Tfu-FNO. BNA+ was built in the active site, using co-crystallized NADP+ as a template, and is shown in orange. Residues that were selected for mutagenesis are shown as blue sticks. PDB ID: 5N2I.

CHAPTER 6

Boosting the reductive power of OYE1 by cofactor engineering

Jeroen Drenth & Marco W. Fraaije

Molecular Enzymology Group, University of Groningen, Nijenborgh 4, 9747AG Groningen,
The Netherlands

Abstract

The asymmetric reduction of alkenes is of great importance for the production of pharmaceuticals and other fine chemicals. Ene reductases (ERs) of the Old Yellow Enzyme (OYE) family are especially suitable as biocatalysts for these conversions. OYE-catalyzed reduction of olefins can only happen when they are properly activated by a suitable electron withdrawing group (EWG), which limits their substrate scope. Lowering the redox potential by cofactor substitution, however, could enable OYEs to accept lesser activated olefins as substrates. In this work we successfully exchanged the FMN prosthetic group of OYE1 from *Saccharomyces pastorianus* for the artificial deazaflavin FO-5'-phosphate, FOP, with a lower redox potential. We could demonstrate with activity and conversion measurements that OYE1-FOP was functional as it could fully convert cinnamaldehyde, a well-accepted substrate of OYE1, albeit with much lower activity than the native enzyme ($3.8 \pm 0.3 \text{ min}^{-1}$ vs. 125 min^{-1}). Activity measurements showed that OYE1-FOP was active on cinnamic acid, and conversion experiments showed full conversion of cinnamic acid within 20 h. This compound is normally not activated enough for the reduction by OYEs, demonstrating an enhanced reductive power by cofactor engineering.

6.1 Introduction

The asymmetric reduction of olefins is an important tool for the production of enantiopure pharmaceuticals and other fine chemicals.^{344,345} Many enzymes show high enantioselectivity and regiospecificity, enabling production of an optically pure product. Moreover enzymes are green catalyst that are produced by environmentally friendly procedures and normally perform best under ambient conditions.^{3,346} Ene reductases (ERs) from the Old Yellow Enzyme family (OYE) are well characterized flavoproteins that contain FMN as a noncovalently bound prosthetic group. The best characterized member of this family is OYE1 from bottom brewer's yeast (*Saccharomyces pastorianus*).^{347–353} The biocatalytic reduction of double bonds, as performed by ERs from the OYE family, happens through the addition of a hydride from reduced FMN.³⁵¹ This mechanism is very similar to a Michael type addition, in which the hydride acts as a nucleophile and attacks the most electron-deficient carbon of the olefinic bond (see **Figure 6.2**). This implies that the double bond needs to be sufficiently activated by a C α -electron withdrawing group (EWG). Good EWGs for OYE-catalyzed reactions are aldehydes, ketones, lactams and nitro groups. Carboxylic acids, esters and nitriles are relatively poor EWGs and need an additional EWG for double bond activation.^{354–360} The reduction of lesser activated alkenes – thus lower redox potentials – however, would be attractive for organic synthesis. Therefore, enzymes with a lower redox potential are needed. The enzyme scaffold

modulates the redox potential of the cofactor,⁹⁴ as is also seen in OYE1 with its redox potential of -230 mV , which is lower than the -210 mV of free FMN in solution.³⁶¹ Enzyme engineering could be employed to alter the redox potential of an enzyme.³⁶² Another strategy is engineering the cofactor by substituting the prosthetic group for an analogous cofactor with different redox properties. This was already done in the past for OYE1 by substituting FMN with several artificial FMN-analogues.³⁶¹

Previously we synthesized the artificial deazaflavin cofactor FOP, FO-5'-phosphate, as an alternative to the naturally occurring deazaflavin cofactor F_{420} (see **Chapters 3 and 4**).^{32,363} F_{420} is a cofactor with an extremely low redox potential of -360 mV .²¹ This cofactor would therefore be ideal as a reducing agent in biocatalysis, which is unfortunately prevented by its low availability. We designed FOP as an easily producible substitute in order to exploit F_{420} -dependent enzymes for biocatalysis. The biosynthesis of FMN was a source of inspiration for the (bio)synthesis of FOP. Consequently, as an additional outcome, FOP is a 7-demethyl-8-hydroxyl-5-deazaflavin analogue of FMN (see **Figure 6.1**). Therefore, we set out to replace the FMN cofactor of OYE1 with FOP, aiming to generate a biocatalyst with potentially stronger reductive power.

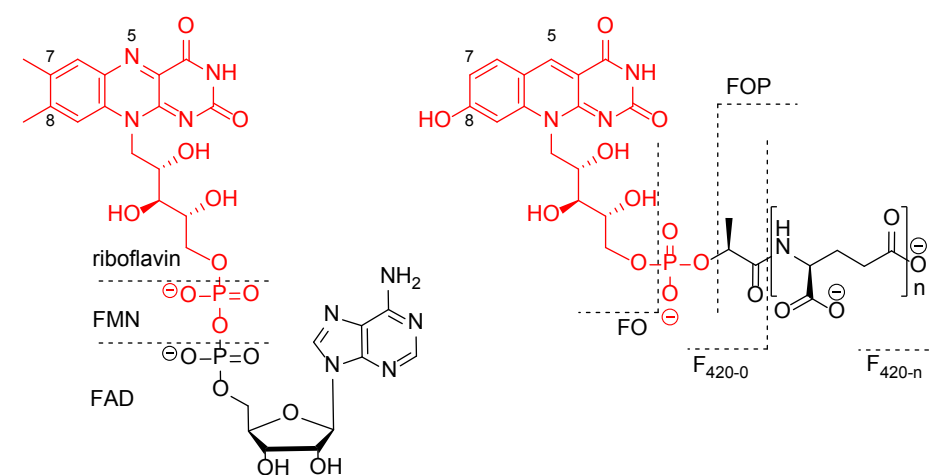


Figure 6.1: The structures of flavin and deazaflavin cofactors. Flavin mononucleotide (FMN) and its artificial deazaflavin analogue FO-5'-phosphate (FOP) are colored red.

In this work we reconstituted OYE1 with FOP and tested its ability to reduce olefins with a range of EWGs, harboring different activation strengths. The cofactor substitution can be achieved by preparing apo OYE1 and subsequent reconstitution with FOP. Previous studies have shown that OYE1 indeed binds modified forms of

FMN.³⁶¹ A set of cinnamyl compounds with a variety of α,β -unsaturated carbonyl and nitril groups were chosen as substrates for this proof of concept studies, both for their structural similarity and their ability to be accepted by OYE1 as substrate.^{351,358} See **Figure 6.2**. The artificial nicotinamide biomimetic 1-benzyl-1,4-dihyronicotinamide (BNAH) was used electron donor in this work, as its low redox potential of -361 mV is close to that of the deazaflavins.³¹³ By performing steady-state kinetic measurements and conversion experiments we show that FOP-reconstituted OYE1 is able to convert cinnamic acid. This compound is normally not converted by OYE1, demonstrating the success of this novel cofactor engineering approach.

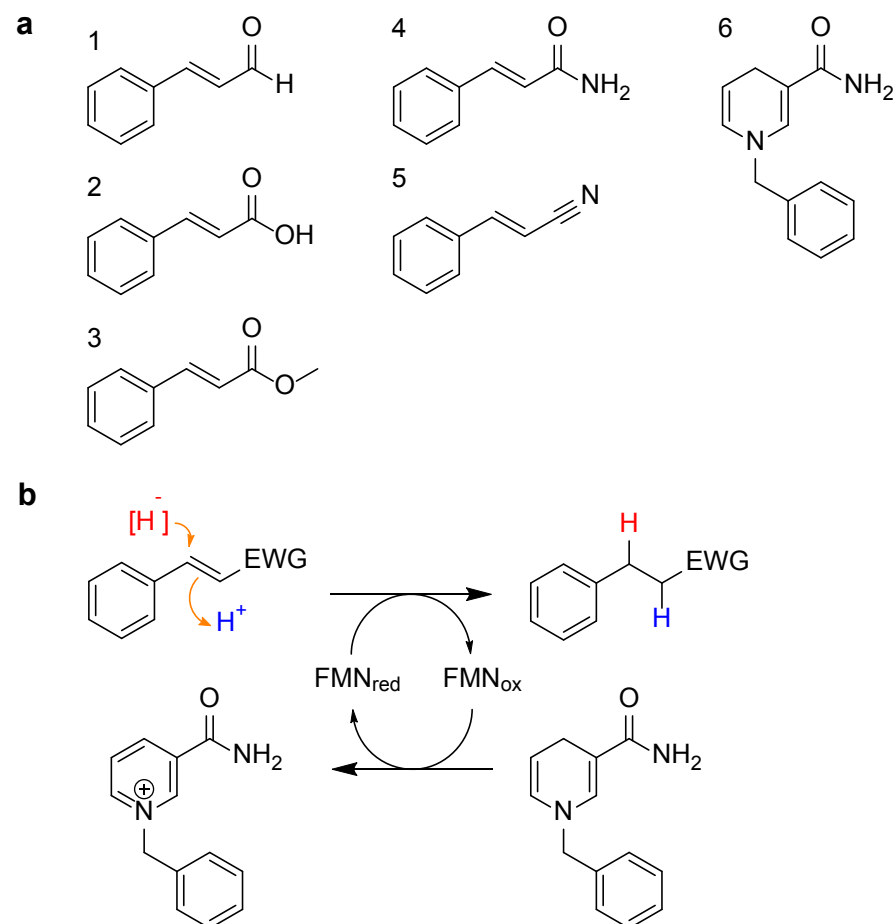


Figure 6.2: Cinnamyl compounds used in this study, the nonnatural nicotinamide cofactor benzyl nicotinamide (BNAH), and the studied OYE1-catalyzed reaction. **a:** cinnamyl compounds; (1) cinnamaldehyde, (2) cinnamic acid, (3) methyl cinnamate, (4) cinnamamide, (5) cinnamitrile and (6) the nicotinamide biomimetic BNAH. **b:** Reaction mechanism of OYE1 catalyzed ene-reductions of cinnamyl compounds. EWG = electron withdrawing group.

6.2 Materials and methods

6.2.1 Materials

All compounds were purchased from Sigma Aldrich (Merck), unless stated otherwise. *E. coli* NEB 10-beta was ordered from New England Biolabs. Reduced benzyl nicotinamide (BNAH) was a kind gift from dr. Caroline E. Paul from the Delft University of Technology.

6.2.2 Expression and purification

The native OYE1 sequence from *Saccharomyces pastorianus* was cloned into a pBAD vector, which was subsequently transformed into CaCl_2 -competent *E. coli* NEB 10-beta cells, using standard protocols.²⁷² Cells were grown overnight in terrific broth (TB) at 37°C , 200 rpm and were then diluted $100\times$ in 300 mL fresh TB in a 1-L Erlenmeyer flask. The culture was incubated at 37°C , 200 rpm until the OD_{600} reached 0.5. The expression of OYE1 was then induced by the addition of 1% L-arabinose (final concentration), and the culture was grown for an additional 12 h.

The cells were harvested by centrifugation, and subsequently resuspended in 20 mM Tris/HCl, pH 8, with $1\ \mu\text{g}/\text{mL}$ lysozyme and $1\ \mu\text{g}/\text{mL}$ DNaseI. The suspension was incubated on ice for 20 min, after which it was homogenized by sonication (5 s on, 5 s off, 70% amplitude, for 15 min). The homogenate was cleared by centrifugation at 8000g for 45 min. The supernatant was passed through a DEAE Sepharose Fast Flow column, pre-equilibrated with 20 mM Tris/HCl, pH 8. The column was washed with several column volumes of 20 mM Tris/HCl, pH 8. Yellow protein was then eluted in small fractions by applying a 200 mM Tris/HCl (pH 8) buffer to the column. The purity of the protein was estimated by SDS-PAGE and the protein concentration was measured with the Bradford assay. Pure OYE1-containing fractions were pooled and stored at -20°C .

6.2.3 Cofactor reconstitution

Apo protein was prepared by dialysis against 200 mM KPi pH 5.3 containing 2 M KBr and 6.7 mM EDTA, for 24 h, as previously described by Abramovitz and Massey.³⁵² The enzyme was then dialyzed against 50 mM Tris/HCl pH 8.0 with 100 mM NaCl, and subsequently reconstituted with FOP by adding 500 μM FOP (final concentration) in 50 mM Tris/HCl pH 8.0 with 100 mM NaCl for 30 min on ice. Free cofactor was removed by buffer exchange with the use of an Amicon Ultra-0.5 Centrifugal Filter Unit 10,000 MWCO.

6.2.4 Spectrophotometric steady-state activity measurements

The measurements were performed at 25°C by adding 1 – 5 μM enzyme to 50 mM Tris-HCl, 100 mM NaCl, 10% (v/v) DMSO, pH 8.0 with 1 mM cinnamyl compound and

250 μM BNAH. The absorbance trace at 385 nm was followed in time and an ϵ_{385} of $1350 \text{ M}^{-1} \text{ cm}^{-1}$ was used for calculating the observed rates (k_{obs}) for BNAH oxidation.³²¹

6.2.5 Conversion experiments

Reaction mixtures contained 10 μM enzyme, 7.5 mM BNAH and 1 mM substrate in 50 mM Tris-HCl pH 8.0 with 10% DMSO. Reactions were incubated for 20 h at 30 °C in closed cap glass vials, after which a sample was taken. For HPLC analysis, the reaction mixture was mixed 1:1 with acetonitrile and incubated on ice for 5 min, after which the mixture was spun down and 10 μL of the mixture was injected. The compounds were separated by an isocratic mobile phase of 60% acetonitrile (v/v) in water on a Phenomenex Gemini C18 (4.6 x 250 mm, 5 μm) column with a flow rate of 0.5 mL/min. Compounds were detected using UV/VIS absorbance at 240 nm. For GCMS the reaction mixtures were extracted with an equal volume of ethyl acetate, supplemented with 2 mM mesitylene as an internal standard. The organic layer was passed over anhydrous magnesium sulfate and then injected into the GCMS for analysis. The GCMS method was described previously by Mathew and Trajkovic et al.²⁵⁹

6.3 Results

6.3.1 Apoprotein formation and reconstitution with FOP

The flavin mononucleotide prosthetic group, FMN, in Old Yellow Enzyme from bottom brewer's yeast, OYE1, was removed by dialysis with chaotropic salts. A UV/VIS spectrum was taken before and after dialysis to confirm loss of the cofactor, as shown in **Figure 6.3**. The figure shows that apo OYE1 lost the characteristic flavin absorbance peaks around 375 and 450 nm, which indicates complete loss of cofactor. This could also be seen by loss of yellow color in the enzyme solution. Apo OYE1 was then reconstituted with the artificial deazaflavin FOP to yield OYE1-FOP, by incubation with 500 μM FOP on ice. After buffer exchange to remove free FOP in solution, the absorbance spectrum of the newly formed holoprotein was recorded (see **Figure 6.3**). A single absorbance band with a maximum at 420 nm confirmed the incorporation of FOP into OYE1, which is characteristic for the deazaflavins FOP and F₄₂₀.²⁰⁹

6.3.2 Spectrophotometric activity measurements of BNAH reduction by OYE1-FOP

Spectrophotometric steady-state kinetic measurements of BNAH oxidation activity by OYE1-FOP showed some background activity of $1.7 \pm 0.2 \text{ min}^{-1}$ in the absence of substrate. In the presence of several cinnamyl compounds the activity was significantly larger than the background activity, see **Figure 6.4**. The substrates cinnamaldehyde, cinnamic acid and methyl cinnamate showed similar observed

activities of 3.8 ± 0.3 , 4.4 ± 0.5 and $4.0 \pm 0.4 \text{ min}^{-1}$, respectively. The observed activity for cinnamaldehyde with OYE1-FOP is about 33 times lower than that of native OYE1 (125 min^{-1}).³⁵⁸ The native enzyme, however, has no activity toward cinnamic acid and methyl cinnamate.³⁵⁸ The amide and nitril groups in cinnamamide and cinnamonnitrile seem to show slightly higher activities than background oxidation of BNAH.

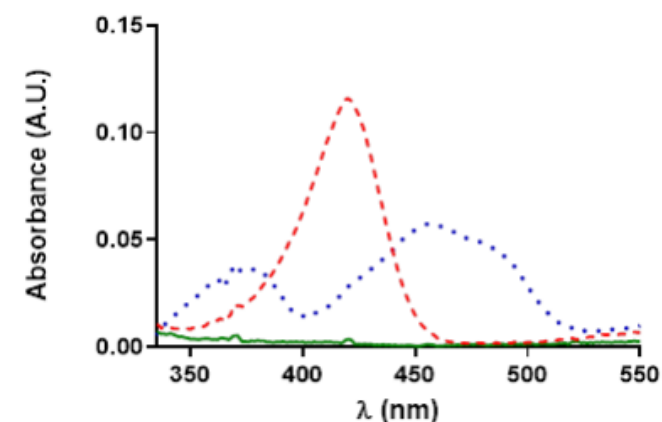


Figure 6.3: Absorbance spectra of OYE1 (blue dotted line), apo OYE1 (green solid line), and OYE1 reconstituted with FOP (red dashed line). All enzymes were dissolved in 50 mM Tris/HCl pH 8.0 with 100 mM NaCl to a final concentration of 5 μM .

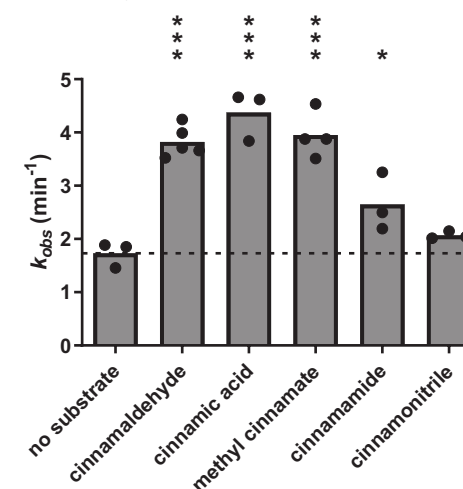


Figure 6.4: Observed rates (k_{obs}) for BNAH oxidation by FOP reconstituted OYE1 in the presence of different substrates. Bars represent mean values of replicate data points that are depicted as dots. Dashed line represents the mean value of the measured activity without substrate. Data was analyzed by a one-way ANOVA. Activities with certain substrates that are significantly higher than that without substrate are marked *: $p = 0.0305$; **: $p \leq 0.0001$.

Conversion of cinnamyl compounds with OYE1-FOP

After the promising results from the spectrophotometric activity measurements, we conducted conversion experiments. For these conversions, 10 μM enzyme was incubated with 1 mM substrate and 7.5 mM BNAH for 20 h at 30 °C in 50 mM Tris-HCl pH 8.0. GCMS results clearly show full conversion of cinnamaldehyde to the expected product. See **Figure 6.5**. Strikingly, methyl cinnamate does not show any apparent conversion under these conditions, which contradicts the spectrophotometric steady-state activity measurement.

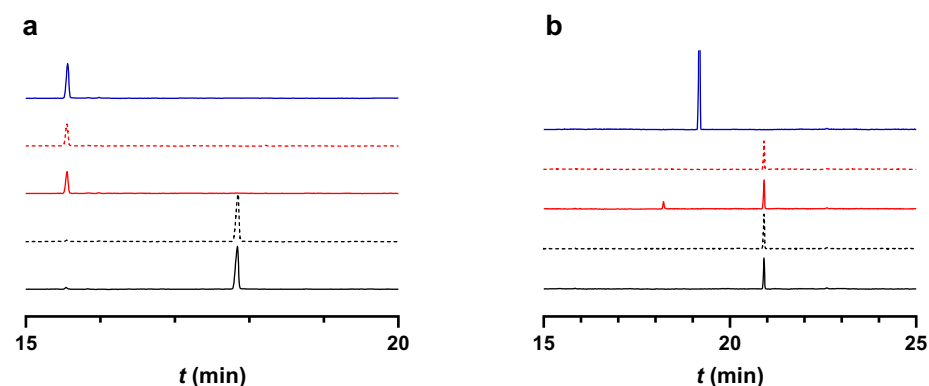


Figure 6.5: GCMS chromatograms for the conversion of (a) cinnamaldehyde and (b) methyl cinnamate. 1 mM Substrate was incubated in the presence of 10 μM OYE1-FOP and 7.5 mM BNAH for 20 h at 30 °C. Black lines are reaction mixtures without enzyme, red lines are reaction mixtures with OYE1-FOP, blue line is product standard, solid and dotted lines represent biological duplicates.

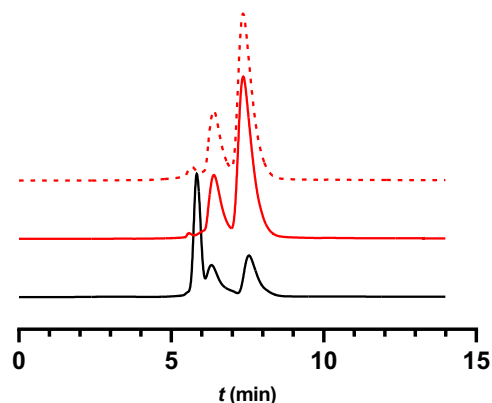


Figure 6.6: HPLC chromatogram of the conversion of 1 mM cinnamic acid in the presence of 10 μM OYE1-FOP and 7.5 mM BNAH in 50 mM Tris-HCl pH 8.0 with 10% DMSO, after 20 h at 30 °C. Black line is the blank sample without enzyme, red lines are biological duplicates with enzyme. $R_f = 5.83$: cinnamic acid, $R_f = 6.39$: BNA+, $R_f = 7.36$: BNAH. Product could not be visualized with the HPLC conditions used in this experiment.

The conversion of cinnamic acid was analyzed by HPLC and revealed that the reaction went toward full depletion of substrate within 20 h, see **Figure 6.6**. The product could not be visualized with the used settings.

6.4 Discussion

The formation of enantiopure chiral compounds is crucial for the production of pharmaceuticals and other fine chemicals, like fragrances.^{298,344,345,357} And asymmetric reduction of olefins is of key importance in the synthesis of many of these compounds. Ene reductases (ERs) of the Old Yellow Enzyme (OYE) family are biocatalysts that can perform this trick under mild, ambient conditions with high regio- enantioselectivity, for a wide variety of compounds.^{298,357} A bottleneck in using these enzymes, however, is the need for strong electron withdrawing groups (EWGs) for the activation of double bonds, like ketones, aldehydes and nitro groups. Both enzyme and cofactor engineering could be employed to reduce the redox potential of the enzyme and, therefore, create an enzyme that can reduce less strongly activated double bonds.

In this work we chose the latter by replacing the native prosthetic group (FMN) by an artificial deazaflavin cofactor (FOP) (see **Figure 6.1**). FOP is a cofactor biomimetic of the naturally occurring coenzyme F_{420} . In the design of FOP we took inspiration from FMN biosynthesis and phosphorylated the biological precursor of F_{420} , FO, on the 5'-position to form FOP. This truncated version of F_{420} is more easily synthesized than its elaborate, parent structure.³² As FO is 7-demethyl-8-hydroxy-5-deazariboflavin, and FMN is the 5'-phosphorylated version of riboflavin, FOP is also a cofactor analogue of FMN. Massey and coworkers have shown in several instances that FMN could be substituted by analogues with modified isoalloxazine ring structures in OYE1.^{184,361} As the isoalloxazine ring system is mainly bound by π - π stacking in between aromatic amino acid side chains, FOP would theoretically also be able to bind.³⁵³ We could indeed show that FOP was successfully introduced as a novel prosthetic group in OYE1 as is seen in **Figure 6.3**. The characteristic absorbance bands of FMN-containing OYE1 were replaced by the typical absorbance band around 420 nm for FOP. Further research still has to be conducted on establishing the precise binding affinity (K_d) of OYE1 for this novel prosthetic group.

The lower redox potential of deazaflavins, as compared to flavins, could significantly reduce the overall redox potential of OYE1, when reconstituted with a deazaflavin. Therefore, we hypothesized that OYE1-FOP would be able to reduce lesser activated olefins (i.e. alkenes with a relatively low redox potential), although the exact redox potential for OYE1-FOP has yet to be determined. To prove our hypothesis, we

tested the reductive activity of OYE1-FOP toward a set of cinnamyl compounds with different EWGs, see **Figure 6.2**. Steady-state activity measurements showed significant BNAH oxidation rates in the presence of cinnamaldehyde, which is also a good substrate for the native enzyme. The reaction rates for OYE1-FOP, however, were significantly lower than that for OYE1. This could be due to the smaller difference in redox potentials between the redox pairs OYE1-FOP and BNAH, as compared to OYE1 and NAD(P)H, leading to lower rates in the reductive half-reaction. Stopped-flow experiments could give more insight into the exact cause of the reduction in activity. Nevertheless, we could show that OYE1 reconstituted with FOP is still active. The activity loss seen in this work is also no exception, as it has been reported that cofactor substitutions in flavoenzymes could result in significant activity loss.¹⁸⁴ More importantly, we could also show a significant activity toward cinnamic acid, which is not converted by native OYE1 at all. Conversion experiments indeed showed full depletion of 1 mM of cinnamic acid after 20 h, in the presence of 10 mM OYE1-FOP and 7.5 mM BNAH as an electron donor. Although the expected product, 3-phenylpropanoic acid, could not be detected by the methods used in this chapter, we cannot think of any other possible cause for substrate depletion, as the vials were sealed tight and the alternative product, cinnamaldehyde, was not detected. More volatile cinnamyl compounds were indeed retained inside the glass vials.

Carboxylic acids are generally weak activators of unsaturated bonds but do occur relatively frequently in fine chemicals of significant importance. The ability to reduce mono-activated α,β -unsaturated carboxylic acids under mild, biological conditions with OYEs could be an important tool for synthetic chemistry.

The selected cinnamyl compounds with weaker EWGs, as judged by the acidity of the α -proton, showed no apparent conversion in the presence of enzyme and electron donor after 20 h of incubation. The reducing power of FOP seems to be sufficient for aldehydes and acids, but not enough to convert the other compounds. Strikingly, in spectrophotometric steady-state experiments BNAH oxidation was significantly higher in the presence of methyl cinnamate and – to a lesser extent – cinnamamide, as compared to the absence of substrate. It is still unclear why these elevated BNAH oxidation rates were observed. Research by Park et al. has shown that BNAH is slowly oxidized in the presence of molecular oxygen.³⁶⁴ Massey and coworkers also showed that OYE1 has substantial uncoupling activity in the presence of oxygen ($3.8 \cdot 10^3 \text{ M}^{-1} \text{ s}^{-1}$).³⁵¹ The presence of certain compounds, like methyl cinnamate, might induce an enzyme conformation that facilitates BNAH oxidation by molecular oxygen, and therefore promotes greater uncoupling rates.

Although further characterization of OYE1-FOP is necessary, this study has demonstrated that the created holoenzyme, carrying an unnatural redox cofactor, is active and capable of reducing compounds that are normally recalcitrant to reduction by members of the OYE family. Enzyme engineering could potentially further optimize the activity of this enzyme to lesser activated olefins. Other traits of FOP, like its relatively low reactivity toward molecular oxygen and possible photocatalytic properties, as seen for 5-deazaflavins, could also be investigated and potentially be exploited for biocatalytic purposes.

APPENDICES

Summary and Conclusions

References

Nederlandse samenvatting

Acknowledgements

Curriculum vitae

List of publications

Summary and Conclusions

In this work we developed a novel artificial cofactor that resembles the structures of both F_{420} and flavin mononucleotide (FMN) and mimics F_{420} chemistry. This was done as a means to overcome the problem of F_{420} scarcity for biocatalytic applications.

F_{420} is found in a great number of microorganisms, ranging from archaea to Actinobacteria and even some proteobacteria, in which it performs different physiological roles.^{25–27,210} For instance, it forms a crucial link in the central C1-metabolism of methanogens and methanotrophs and is exploited by Actinobacteria for the synthesis of secondary metabolites and detoxification of xenobiotics.^{25,26,219,221,223,224,241,246,301,365} These organisms are relatively hard to cultivate, which makes F_{420} extraction complicated, and results in low yields. Moreover, complete synthesis of the cofactor is also tedious and cannot provide enough material for large-scale applications.²⁹ Other cofactors, like flavins, nicotinamides and ATP, however, are produced on industrial scale by fermentation and can be easily purchased from many suppliers.

Because of its low availability to biocatalysis and the believe that it could only be found in rare microorganisms, research on deazaflavoenzymes has been scarce, until very recently. Genome studies and revaluation of published data shows a wealth of F_{420} -producing organisms with intriguing metabolic functions for this coenzyme, which could potentially be exploited for biocatalytic purposes. Moreover, its greatest selling point, the extremely low physiological redox potential of -340 to -380 mV, makes it an interesting reducing agent for compounds that are otherwise relatively inert to biocatalytic reductions performed by flavins and nicotinamides.^{21,22} In fact, this coenzyme was already used in at least two biocatalytic applications, namely the enantiospecific reduction of ketones and olefins, and is speculated to be of use in many more synthetic applications.^{27,56,259,343}

In order to aid the use of F_{420} -dependent enzymes for large scale applications, we set out to design an artificial cofactor that could be produced on larger scales than its native counterpart and could function equally well as a redox coenzyme (**Chapter 3**). As a starting point for the design we used FO, see **Figure 1.1**. This is the natural biosynthetic precursor of F_{420} and contains the catalytic 7,8-didemethyl-8-hydroxy-5-deazaalloxazine core structure. FO was previously shown to be relatively easily synthesized, and chemically active, but unfortunately shows low affinity for several F_{420} -dependent enzymes.^{31,32} Other research by Ney et al. had previously shown that the elaborate polar 5'-phospho-L-lactyl- γ -L-glutamyl tail that is added to FO to form F_{420}

is indeed important for protein binding.²¹³ This 'tail' is 2 glutamate residues long in Archaea and is of variable length in Proteobacteria and Actinobacteria, which can reach up to 9 glutamate residues in length, but is normally around 3 to 8 residues in length. Ney et al. also showed that the length of the glutamyl-tail had impact on enzyme activity. In fact, the researchers showed that the observed rates were slightly higher with shorter glutamyl-tails, but had consequently higher K_m -values.²¹³ This insinuates that a charged or polar extension on the 5'-position of FO is necessary for efficient binding to enzymes, and prompted us to design a cofactor based on the FO core structure with an additional hydrophilic group on the 5'-position, but smaller than F_{420} . Inspired by the biosynthesis and structure of flavin mononucleotide (FMN; see **Figure 1.1**), we came up with FO-5'-phosphate, in short FOP. Recent studies also showed that some F_{420} -dependent enzymes have FMN-dependent ancestors, which would possibly make an FMN analogue also effectively bind to these enzymes.^{265,366}

As FO and riboflavin are strikingly similar in structure, we anticipated that riboflavin kinase, the enzyme that forms FMN out of its precursor riboflavin by 5'-phosphorylation, would also be able to convert chemically synthesized FO to FOP.²⁷³ The well characterized kinase from *Corynebacterium ammoniagenes* (CaRFK) was selected for FO phosphorylation, but this enzyme had unfortunately no apparent activity toward this compound.²⁷¹ Several rounds of structure-inspired side-directed mutagenesis were then performed to adapt the kinase toward accepting FO as a substrate. Targeting apolar active site residues that surround the C8-position of the isoalloxazine and exchanging them for polar residues, enabled the binding of FO with its 8-hydroxyl group. A threefold mutant of CaRFK (F21H/F85H/A66I) was able to convert up to 80% of FO to FOP within 12 h and could produce 1 mg (2.5 μ mol) FOP in a 50 mL of reaction volume, which translates to a production of 50 μ mol/L. Which is higher than the F_{420} yield from *Mycobacterium smegmatis*, being only 1.4 μ mol/L of culture.^{269,270}

After we synthesized the artificial deazaflavin cofactor FOP by this chemoenzymatic method, we tested the activity of several F_{420} -dependent enzymes of different structural classes with this novel coenzyme. The sugar-6-phosphate dehydrogenase from *Cryptosporangium arzum* (FSD-Cryar), the F_{420} :NADPH oxidoreductase from *Thermobifida fusca* (TfuFNO), and the F_{420} -dependent reductases from *Mycobacterium hassiacum* (FDR-Mha) all showed activity with FOP. Although the activity toward FOP was lower than that toward F_{420} , the catalytic efficiencies were only 2.0, 12.6, and 22.4 times lower for TfuFNO, FSD-Cryar, and FDR-Mha, respectively. Thereby we could showcase that FOP is a serious alternative for F_{420} , as discussed in more detail in **Chapter 3**.

The chemoenzymatic synthesis of FOP still requires a relatively expensive supply of ATP and high yields are hindered by the low solubility of FO in water. To work around these problems, we designed a biosynthetic pathway to produce FOP in *Escherichia coli*, which is the topic of **Chapter 4**. By heterologously expressing the best performing enzymes, selected from a set of FO synthases and riboflavin kinases, we were able to successfully produce FOP *in vivo*. The combined efforts of protein engineering and expression system optimization lead to an estimated production rate of 0.078 $\mu\text{mol L}^{-1} \text{h}^{-1}$. The overall yield is comparable to that of F_{420} in *Mycobacterium smegmatis*, but the production rate of FOP in *E. coli* is much faster. Moreover, the intracellular FOP concentration of about 40 μM should be sufficient to power F_{420} -dependent enzymes *in vivo*. As a proof of concept, we could indeed demonstrate an increase in whole-cell reduction of ketoisophorone by co-expressing an F_{420} -dependent reductase and an F_{420} -dependent glucose dehydrogenase together with the FOP biosynthesis constructs.

As deazaflavin-dependent whole-cell conversions could have high potential for the biocatalytic production of valuable compounds, we also produced FOP in the yeast *Saccharomyces cerevisiae*, which is widely used in industrial biosynthesis. Unlike the *de novo* biosynthetic approach in *E. coli* we used a semi-synthetic approach for yeast. Heterologous expression of the riboflavin kinase from *Schizosaccharomyces pombe* (*Sp*RFK) enabled *in vivo* phosphorylation of chemically synthesized FO, which was supplied in the growth medium. Production in *S. cerevisiae* was further improved through medium optimization and enzyme engineering. Through structure-guided and computational enzyme engineering, a *Sp*RFK variant with 7-fold increased catalytic efficiency compared to the wild type was discovered. By using this variant in optimized medium conditions, the FOP production yield in *S. cerevisiae* was 20-fold increased compared to the very low initial yield of 0.24 ± 0.04 nmol per g dry biomass. The results from **Chapter 4** show that prokaryotic and eukaryotic lab strains can be engineered to produce the functional deazaflavin cofactor mimic FOP. FOP production strains could be exploited for the biosynthesis of valuable compounds in the future.

We exploited the findings of **Chapter 3**, that show the activity of several F_{420} -dependent enzymes from different structural classes toward FOP, for the reduction of several artificial nicotinamide cofactor biomimetics (NCBs), as discussed in **Chapter 5**. These compounds have been proven to be cheaper, more easily synthesized, and more stable than their natural counterparts nicotinamide adenine dinucleotide (NAD) and its 2'-phosphorylated form NADP. And were even shown to outcompete NAD(P)H in reduction rates for ene-reductases of the Old Yellow Enzyme family.^{313,316,317,324,367,368} But

these artificial hydride carriers lack efficient cofactor recycling methods. Therefore, we engineered the thermostable F_{420} :NADPH oxidoreductase from *Thermobifida fusca* (*Tfu*-FNO), by structure-inspired site-directed mutagenesis, to accommodate the unnatural N1-substituents of eight NCBs. The extraordinarily low redox potential of the natural cofactor $F_{420}\text{H}_2$ and its synthetic counterpart FOP were then exploited to reduce these NCBs. Wild-type enzyme had already detectable activity toward all selected NCBs, but showed high K_m -values in the millimolar range and low k_{cat} -values ranging up to 1.4 min^{-1} . Saturation mutagenesis at positions Gly-29 and Pro-89 resulted in mutants with up to 139 times higher catalytic efficiencies. Moreover, mutant G29W showed a k_{cat} of 4.2 s^{-1} toward 1-benzyl-3-acetylpyridine (BAP⁺), which is similar to the k_{cat} for the natural substrate NADP⁺. The best *Tfu*-FNO variants for a specific NCB were then used for the recycling of catalytic amounts of these nicotinamides in conversion experiments with the thermostable ene-reductase from *Thermus scotoductus* (*Ts*OYE). It enabled full conversion of 10 mM ketoisophorone with BAP⁺ within 16 hours. The generated set of thermostable and NCB-dependent *Tfu*-FNO variants are powerful cofactor regeneration biocatalysts for the reduction of several artificial nicotinamide biomimetics at both ambient and high temperatures. And, to our knowledge, this enzymatic method seems to be the best performing NCB-recycling system for BNAH and BAPH yet.

As FOP also resembles the structure of FMN, see **Figure 1.1**, we envisioned that this biomimetic could potentially not only be used for F_{420} -dependent enzymes, but also those depending on FMN. The lower redox potential of deazaflavins compared to that of flavins could serve as a means to reduce compounds with redox potentials that are too low for FMN. We tested this hypothesis in **Chapter 6** by exchanging the FMN prosthetic group of OYE1, an ene-reductase from *Saccharomyces pastorianus*, with FOP. Just as previously shown for other artificial FMN analogues, FOP was successfully built in as prosthetic group.³⁶¹ Then, we measured the activity of OYE1-FOP toward a range of cinnamyl compounds with different electron withdrawing groups. This revealed that cofactor replacement with FOP introduces a novel reductase activity toward cinnamic acid, a compound that is normally not well accepted as substrate by members of the OYE family. Although more research needs to be done on this system, it forms a good foundation for future studies on deazaflavin reconstituted ene-reductases.

Overall we could show that FOP is a feasible alternative to F_{420} , with its straightforward and scalable (bio)synthesis and its activity being similar to that of the original natural cofactor. Furthermore, we also show that FOP can be used as an alternative to FMN, where its lower redox potential and inertness to molecular oxygen can lead to novel

activities. The biosynthesis of FOP, as well as the astonishing recent advances of F₄₂₀ production in *E. coli*^{239,240,369} could boost the application of F₄₂₀-dependent enzymes in biocatalysis and whole cell biosynthesis. With growing (meta)genomic data, better sequencing methods and more powerful bioinformatics tools, more F₄₂₀-dependent enzymes will emerge, as well as the possible discovery of new synthesis routes for novel metabolites. Characterization of new and predicted F₄₂₀-enzymes from the large amount of organisms could complement the enzymes that have already shown to be interesting biocatalysts, and could lead to novel biocatalytic applications and new biosynthesis pathways for compounds in various applications.^{19,25,27,56,370} FOP specifically, can be used as an alternative for FMN, exploiting the low redox potential and inertness to molecular oxygen of this deazaflavin to known enzyme scaffolds. As shown before, cofactor engineering can lead to remarkable new activities^{183,185–187,361} or enhance certain traits to better perform a certain task.^{176,177,324}

References

- (1) de Carvalho, C. C. R. Whole Cell Biocatalysts: Essential Workers from Nature to the Industry. *Microb. Biotechnol.* **2017**, *10*, 250–263.
- (2) Lin, B.; Tao, Y. Whole-Cell Biocatalysts by Design. *Microb. Cell Fact.* **2017**, *16*, 106.
- (3) Sheldon, R. A.; Woodley, J. M. Role of Biocatalysis in Sustainable Chemistry. *Chem. Rev.* **2018**, *118*, 801–838.
- (4) Sheldon, R. A.; Brady, D.; Bode, M. L. The Hitchhiker's Guide to Biocatalysis: Recent Advances in the Use of Enzymes in Organic Synthesis. *Chem. Sci.* **2020**, *11*, 2587–2605.
- (5) Cano-Flores, A.; Gómez, J.; S. Escalona-Torres, I.; Velasco-Bejarano, B. Microorganisms as Biocatalysts and Enzyme Sources. In *Microorganisms*; Blumenberg, M., Shaaban, M., Eds.; IntechOpen: London, UK, 2020.
- (6) Behrens, G. A.; Hummel, A.; Padhi, S. K.; Schätzle, S.; Bornscheuer, U. T. Discovery and Protein Engineering of Biocatalysts for Organic Synthesis. *Adv. Synth. Catal.* **2011**, *353*, 2191–2215.
- (7) Marshall, J. R.; Mangas-Sanchez, J.; Turner, N. J. Expanding the Synthetic Scope of Biocatalysis by Enzyme Discovery and Protein Engineering. *Tetrahedron* **2021**, *82*, 131926.
- (8) Miller, D. C.; Athavale, S. V.; Arnold, F. H. Combining Chemistry and Protein Engineering for New-to-Nature Biocatalysis. *Nat. Synth.* **2022**, *1*, 18–23.
- (9) Broderick, J. B. Coenzymes and Cofactors. *eLS* **2001**.
- (10) Guengerich, F. P. Reactions and Significance of Cytochrome P-450 Enzymes". *J. Biol. Chem.* **1991**, *266*, 10019–10022.
- (11) O'Reilly, E.; Köhler, V.; Flitsch, S. L.; Turner, N. J. Cytochromes P450 as Useful Biocatalysts: Addressing the Limitations. *Chem. Commun.* **2011**, *47*, 2490–2501.
- (12) Urlacher, V. B.; Eiben, S. Cytochrome P450 Monooxygenases: Perspectives for Synthetic Application. *Trends Biotechnol.* **2006**, *24*, 324–330.
- (13) Cosgrove, S. C.; Brzezniak, A.; France, S. P.; Ramsden, J. I.; Mangas-Sanchez, J.; Montgomery, S. L.; Heath, R. S.; Turner, N. J. Imine Reductases, Reductive Aminases, and Amine Oxidases for the Synthesis of Chiral Amines: Discovery, Characterization, and Synthetic Applications. *Methods Enzymol.* **2018**, *608*, 131–149.
- (14) Grogan, G.; Turner, N. J. InspiRED by Nature: NADPH-Dependent Imine Reductases (IREDS) as Catalysts for the Preparation of Chiral Amines. *Chem. – A Eur. J.* **2016**, *22*, 1900–1907.
- (15) de Miranda, A. S.; Milagre, C. D. F.; Hollmann, F. Alcohol Dehydrogenases as Catalysts in Organic Synthesis. *Front. Catal.* **2022**, *2*.
- (16) Baker Dockrey, S. A.; Narayan, A. R. H. Flavin-Dependent Biocatalysts in Synthesis. *Tetrahedron* **2019**, *75*, 1115–1121.
- (17) *Flavin-Based Catalysis*; Cibulka, R., Fraaije, M. W., Eds.; Wiley, 2021.
- (18) Shah, M.; Antoney, J.; Kang, S. W.; Warden, A.; Hartley, C.; Nazem-Bokaee, H.; Jackson, C.; Scott, C. Cofactor F420-Dependent Enzymes: An Under-Explored Resource for Asymmetric Redox Biocatalysis. *Catalysts* **2019**, *9*, 868.

- (19) Taylor, M.; Scott, C.; Grogan, G. F₄₂₀-Dependent Enzymes - Potential for Applications in Biotechnology. *Trends Biotechnol.* **2013**, *31*, 63–64.
- (20) Wolfe, R. S.; Vogels, G. D.; Eirich, L. D. Proposed Structure for Coenzyme F₄₂₀ from *Methanobacterium*. *Biochemistry* **1978**, *17*, 4583–4593.
- (21) Walsh, C. Naturally Occurring 5-Deazaflavin Coenzymes: Biological Redox Roles. *Acc. Chem. Res.* **1986**, *19*, 216–221.
- (22) Jacobson, F.; Walsh, C. Properties of 7,8-Didemethyl-8-Hydroxy-5-Deazaflavins Relevant to Redox Coenzyme Function in Methanogen Metabolism. *Biochemistry* **1984**, *23*, 979–988.
- (23) de Poorter, L. M. I.; Geerts, W. J.; Keltjens, J. T. Hydrogen Concentrations in Methane-Forming Cells Probed by the Ratios of Reduced and Oxidized Coenzyme F₄₂₀. *Microbiology* **2005**, *151*, 1697–1705.
- (24) Jacobson, F.; Walsh, C. Properties of 7,8-Didemethyl-8-Hydroxy-5-Deazaflavins Relevant to Redox Coenzyme Function in Methanogen Metabolism. *Biochemistry* **1984**, *23*, 979–988.
- (25) Greening, C.; Ahmed, F. H.; Mohamed, A. E.; Lee, B. M.; Pandey, G.; Warden, A. C.; Scott, C.; Oakeshott, J. G.; Taylor, M. C.; Jackson, C. J. Physiology, Biochemistry, and Applications of F₄₂₀- and Fo-Dependent Redox Reactions. *Microbiol. Mol. Biol. Rev.* **2016**, *80*, 451–493.
- (26) Ney, B.; Ahmed, F. H.; Carere, C. R.; Biswas, A.; Warden, A. C.; Morales, S. E.; Pandey, G.; Watt, S. J.; Oakeshott, J. G.; Taylor, M. C.; Stott, M. B.; Jackson, C. J.; Greening, C. The Methanogenic Redox Cofactor F₄₂₀ Is Widely Synthesized by Aerobic Soil Bacteria. *ISME J.* **2017**, *11*, 125–137.
- (27) Grinter, R.; Greening, C. Cofactor F₄₂₀: An Expanded View of Its Distribution, Biosynthesis and Roles in Bacteria and Archaea. *FEMS Microbiol. Rev.* **2021**, *45*, 1–46.
- (28) Tanaka, K.; Kimachi, T.; Kawase, M.; Yoneda, F. First Total Synthesis of Redox Coenzyme Factor 420. *J. Chem. Soc. Chem. Commun.* **1988**, *8*, 524–526.
- (29) Kimachi, T.; Kawase, M.; Matsuki, S.; Tanaka, K.; Yoneda, F. First Total Synthesis of Coenzyme Factor 420. *J. Chem. Soc. Perkin Trans. 1* **1990**, No. 2, 253–256.
- (30) Ashton, W. T.; Brown, R. D. Synthesis of 8-demethyl-8-hydroxy-5-deazariboflavins. *J. Heterocycl. Chem.* **1980**, *17*, 1709–1712.
- (31) Hossain, M. S.; Le, C. Q.; Joseph, E.; Nguyen, T. Q.; Johnson-Winters, K.; Foss, F. W. Convenient Synthesis of Deazaflavin Cofactor FO and Its Activity in F₄₂₀-Dependent NADP Reductase. *Org. Biomol. Chem.* **2015**, *13*, 5082–5085.
- (32) Drenth, J.; Trajkovic, M.; Fraaije, M. W. Chemoenzymatic Synthesis of an Unnatural Deazaflavin Cofactor That Can Fuel F₄₂₀-Dependent Enzymes. *ACS Catal.* **2019**, *9*, 6435–6443.
- (33) Warburg, O.; Christian, W. Ein Zweites Sauerstoffübertragendes Ferment Und Sein Absorptionsspektrum. *Naturwissenschaften* **1932**, *20*, 688.
- (34) Scholtissek, A.; Tischler, D.; Westphal, A. H.; van Berkel, W. J. H.; Paul, C. E. Old Yellow Enzyme-Catalysed Asymmetric Hydrogenation: Linking Family Roots with Improved Catalysis. *Catalysts* **2017**, *7*, 130.
- (35) Romero, E.; Gadda, G. Alcohol Oxidation by Flavoenzymes. *Biomol. Concepts* **2014**, *5*, 299–318.
- (36) Pickl, M.; Fuchs, M.; Glueck, S. M.; Faber, K. The Substrate Tolerance of Alcohol Oxidases. *Appl. Microbiol. Biotechnol.* **2015**, *99*, 6617–6642.
- (37) Koshiba, T.; Saito, E.; Ono, N.; Yamamoto, N.; Satô, M. Purification and Properties of Flavin- and Molybdenum-Containing Aldehyde Oxidase from Coleoptiles of Maize. *Plant Physiol.* **1996**, *110*, 781–789.
- (38) Dijkman, W. P.; Fraaije, M. W. Discovery and Characterization of a 5-Hydroxymethylfurfural Oxidase from *Methylovorus* Sp. Strain MP688. *Appl. Environ. Microbiol.* **2014**, *80*, 1082–1090.
- (39) Wilson, R.; Turner, A. P. F. Glucose Oxidase: An Ideal Enzyme. *Biosens. Bioelectron.* **1992**, *7*, 165–185.
- (40) Martin, C.; Trajkovic, M.; Fraaije, M. W. Production of Hydroxy Acids: Selective Double Oxidation of Diols by Flavoprotein Alcohol Oxidase. *Angew. Chemie Int. Ed.* **2020**, *59*, 4869–4872.
- (41) Li, L.; Liu, X.; Yang, W.; Xu, F.; Wang, W.; Feng, L.; Bartlam, M.; Wang, L.; Rao, Z. Crystal Structure of Long-Chain Alkane Monooxygenase (LadA) in Complex with Coenzyme FMN: Unveiling the Long-Chain Alkane Hydroxylase. *J. Mol. Biol.* **2007**, *376*, 453–465.
- (42) Entsch, B.; Van Berkel, W. J. H. Structure and Mechanism of Para-hydroxybenzoate Hydroxylase. *FASEB J.* **1995**, *9*, 476–483.
- (43) Chakraborty, S.; Ortiz-Maldonado, M.; Entsch, B.; Ballou, D. P. Studies on the Mechanism of *p*-Hydroxyphenylacetate 3-Hydroxylase from *Pseudomonas Aeruginosa*: A System Composed of a Small Flavin Reductase and a Large Flavin-Dependent Oxygenase. *Biochemistry* **2010**, *49*, 372–385.
- (44) Donoghue, N. A.; Norris, D. B.; Trudgill, P. W. The Purification and Properties of Cyclohexanone Oxygenase from *Nocardia Globerulea* CL1 and *Acinetobacter* NCIB 9871. *Eur. J. Biochem.* **1976**, *63*, 175–192.
- (45) Fürst, M. J. L. J.; Gran-Scheuch, A.; Aalbers, F. S.; Fraaije, M. W. Baeyer-Villiger Monooxygenases: Tunable Oxidative Biocatalysts. *ACS Catal.* **2019**, *9*, 11207–11241.
- (46) Walsh, C. T.; Chen, Y.-C. J. Enzymic Baeyer-Villiger Oxidations by Flavin-Dependent Monooxygenases. *Angew. Chemie Int. Ed. English* **1988**, *27*, 333–343.
- (47) Van Pée, K. H.; Unversucht, S. Biological Dehalogenation and Halogenation Reactions. *Chemosphere* **2003**, *52*, 299–312.
- (48) Sutton, W. B. Mechanism of Action and Crystallization of Alctic Oxidative Decarboxylase From *Mycobacterium Phlei*. *J. Biol. Chem.* **1957**, *226*, 395–405.
- (49) Zhao, Y. Auxin Biosynthesis: A Simple Two-Step Pathway Converts Tryptophan to Indole-3-Acetic Acid in Plants. *Mol. Plant* **2012**, *5*, 334–338.
- (50) Brodl, E.; Winkler, A.; Macheroux, P. Molecular Mechanisms of Bacterial Bioluminescence. *Comput. Struct. Biotechnol. J.* **2018**, *16*, 551–564.
- (51) Massey, V. The Chemical and Biological Versatility of Riboflavin. *Biochem. Soc. Trans.* **2000**, *28*, 283–296.
- (52) Huijbers, M. M. E.; Montersino, S.; Westphal, A. H.; Tischler, D.; Van Berkel, W. J. H. Flavin Dependent Monooxygenases. *Arch. Biochem. Biophys.* **2014**, *544*, 2–17.
- (53) Romero, E.; Rubén, J.; Gómez, R.; Castellanos, G.; Gadda, G.; Fraaije, M. W.; Mattevi, A. Same Substrate, Many Reactions: Oxygen Activation in Flavoenzymes. *Chem. Rev.* **2018**, *118*, 1742–1769.
- (54) Teufel, R.; Stull, F.; Meehan, M. J.; Michaudel, Q.; Dorrestein, P. C.; Palfey, B.; Moore, B. S. Biochemical Establishment and Characterization of EncM's Flavin-N5-Oxide Cofactor. *J. Am. Chem. Soc.* **2015**, *137*, 8078–8085.

- (55) Wang, P. H.; Khusnutdinova, A. N.; Luo, F.; Xiao, J.; Nemr, K.; Flick, R.; Brown, G.; Mahadevan, R.; Edwards, E. A.; Yakunin, A. F. Biosynthesis and Activity of Prenylated FMN Cofactors. *Cell Chem. Biol.* **2018**, *25*, 560–570.e6.
- (56) Shah, M. V.; Antoney, J.; Kang, S. W.; Warden, A. C.; Hartley, C. J.; Nazem-Bokae, H.; Jackson, C. J.; Scott, C. Cofactor F₄₂₀-Dependent Enzymes: An Under-Explored Resource for Asymmetric Redox Biocatalysis. *Catalysts* **2019**, *9*, 868.
- (57) Foor, F.; Brown, G. M. GTP Cyclohydrolase II from Escherichia Coli. *Methods Enzymol.* **1980**, *66*, 303–307.
- (58) Mailänder, B.; Bacher, A. Biosynthesis of Riboflavin; Structure of the Purine Precursor and Origin of the Ribityl Side Chain. *J. Biol. Chem.* **1976**, *251*, 3623–3628.
- (59) Richter, G.; Fischer, M.; Krieger, C.; Eberhardt, S.; Lüttgen, H.; Gerstenschlager, I.; Bacher, A. Biosynthesis of Riboflavin: Characterization of the Bifunctional Deaminase-Reductase of *Escherichia Coli* and *Bacillus Subtilis*. *J. Bacteriol.* **1997**, *179*, 2022–2028.
- (60) Hollander, I.; Brown, G. M. Biosynthesis of Riboflavin: Reductase and Deaminase of *Ashbya Gossypii*. *Biochem. Biophys. Res. Commun.* **1979**, *89*, 759–763.
- (61) Haase, I.; Sarge, S.; Illarionov, B.; Laudert, D.; Hohmann, H.-P.; Bacher, A.; Fischer, M. Enzymes from the Haloacid Dehalogenase (HAD) Superfamily Catalyse the Elusive Dephosphorylation Step of Riboflavin Biosynthesis. *ChemBioChem* **2013**, *14*, 2272–2275.
- (62) Kis, K.; Volk, R.; Bacher, A. Biosynthesis of Riboflavin. Studies on the Reaction Mechanism of 6,7-Dimethyl-8-Ribityllumazine Synthase. *Biochemistry* **1995**, *34*, 2883–2892.
- (63) Neuberger, G.; Bacher, A. Biosynthesis of Riboflavin. Enzymatic Formation of 6,7-Dimethyl-8-Ribityllumazine by Heavy Riboflavin Synthase from *Bacillus Subtilis*. *Biochem. Biophys. Res. Commun.* **1986**, *139*, 1111–1116.
- (64) Volk, R.; Bacher, A. Biosynthesis of Riboflavin. The Structure of the Four-Carbon Precursor. *J. Am. Chem. Soc.* **1988**, *110*, 3651–3653.
- (65) Neuberger, G.; Bacher, A. Biosynthesis of Riboflavin. An Aliphatic Intermediate in the Formation of 6,7-Dimethyl-8-Ribityllumazine from Pentose Phosphate. *Biochem. Biophys. Res. Commun.* **1985**, *127*, 175–181.
- (66) Volk, R.; Bather, A. Studies on the 4-Carbon Precursor in the Biosynthesis of Riboflavin; Purification and Properties of L-3,4-Dihydroxy-2-Butanone-4-Phosphate Synthase. *J. Biol. Chem.* **1990**, *265*, 19479–19485.
- (67) Winestock, C. H.; Aogaichi, T.; Plaut, G. W. E. The Substrate Specificity of Riboflavin Synthetase. *J. Biol. Chem.* **1963**, *233*, 2866–2874.
- (68) Abbas, C. A.; Sibirny, A. A. Genetic Control of Biosynthesis and Transport of Riboflavin and Flavin Nucleotides and Construction of Robust Biotechnological Producers. *Microbiol. Mol. Biol. Rev.* **2011**, *75*, 321–360.
- (69) Walsh, C. T.; Wencewicz, T. A. Flavoenzymes: Versatile Catalysts in Biosynthetic Pathways. *Nat. Prod. Rep.* **2013**, *30*, 175–200.
- (70) Lowe, H. J.; Mansfield Clark, W. On Oxidation-Reduction. *J. Biol. Chem.* **1956**, *221*, 983–992.
- (71) Christgen, S. L.; Becker, S. M.; Becker, D. F. Methods for Determining the Reduction Potentials of Flavin Enzymes. In *Methods in Enzymology, Volume 620*; 2019; pp 1–25.
- (72) Frisell, W. R.; Chung, C. W.; Mackenzie, C. G. Catalysis of Oxidation of Nitrogen Compounds by Flavin Coenzymes in the Presence of Light*. *J. Biol. Chem.* **1959**, *234*, 1297–1302.
- (73) Massey, V.; Palmer, G. On the Existence of Spectrally Distinct Classes of Flavoprotein A New Method for the Quantitative Production of Flavoprotein Semiquinones. *J. Ant. Chem. Soc.* **1966**, *5*, 2089.
- (74) Müller, F. NMR Spectroscopy on Flavins and Flavoproteins. *Methods Mol. Biol.* **2014**, *1146*, 229–306.
- (75) Massey, V.; Ghisla, S.; Moore, E. G. 8-Mercaptoflavins as Active Site Probes of Flavoenzymes. *J. Biol. Chem.* **1979**, *254*, 9640–9650.
- (76) Walsh, C. T. Flavin Coenzymes: At the Crossroads of Biological Redox Chemistry. *Acc. Chem. Res.* **1980**, *13*, 148–155.
- (77) Walsh, C. Chemical Approaches to the Study of Enzymes Catalyzing Redox Transformations. *Annu. Rev. Biochem.* **1978**, *47*, 881–931.
- (78) Geissler, J.; Ghisla, S.; Kroneck, P. M. H. Flavin-dependent Alcohol Oxidase from Yeast: Studies on the Catalytic Mechanism and Inactivation during Turnover. *Eur. J. Biochem.* **1986**, *160*, 93–100.
- (79) Kong, X.; Ouyang, S.; Liang, Z.; Lu, J.; Chen, L.; Shen, B.; Li, D.; Zheng, M.; Li, K. K.; Luo, C.; Jiang, H. Catalytic Mechanism Investigation of Lysine-Specific Demethylase 1 (LSD1): A Computational Study. *PLoS One* **2011**, *6*.
- (80) Pollegioni, L.; Blodig, W.; Ghisla, S. On the Mechanism of D-Amino Acid Oxidase: Structure/Linear Free Energy Correlations and Deuterium Kinetic Isotope Effects Using Substituted Phenylglycines. *J. Biol. Chem.* **1997**, *272*, 4924–4934.
- (81) Weibel, M. K.; Brights, H. J. The Glucose Oxidase Mechanism; Interpretation of the PH Dependence. *J. Biol. Chem.* **1971**, *246*, 2734–2744.
- (82) Schulz, G. E.; Schirmer, R. H.; Sachsenheimer, W.; Pai, E. F. The Structure of the Flavoenzyme Glutathione Reductase. *Nature* **1978**, *273*, 120–124.
- (83) Porter, D. J. T.; Voet, J. G.; Brights, H. J. Direct Evidence for Carbanions and Covalent N5-Flavin-Carbanion Adducts as Catalytic Intermediates in the Oxidation of Nitroethane by D-Amino Acid Oxidase. *J. Biol. Chem.* **1973**, *248*, 4400–4416.
- (84) Massey, V. Activation of Molecular Oxygen by Flavins and Flavoproteins. *J. Biol. Chem.* **1994**, *269*, 22459–22462.
- (85) Bruice, T. C. Oxygen-Flavin Chemistry. *Isr. J. Chem.* **1984**, *24*, 54–61.
- (86) Eberlein, G.; Bruice, T. C. The Chemistry of a 1,5-Diblocked Flavin. 2. Proton and Electron Transfer Steps in the Reaction of Dihydroflavins with Oxygen. *J. Am. Chem. Soc.* **1983**, *105*, 6685–6697.
- (87) Sucharitakul, J.; Prongjit, M.; Haltrich, D.; Chaiyen, P. Detection of a C4a-Hydroperoxyflavin Intermediate in the Reaction of a Flavoprotein Oxidase. *Biochemistry* **2008**, *47*, 8485–8490.
- (88) Visitsatthawong, S.; Chenprakhon, P.; Chaiyen, P.; Surawatanawong, P. Mechanism of Oxygen Activation in a Flavin-Dependent Monooxygenase: A Nearly Barrierless Formation of C4a-Hydroperoxyflavin via Proton-Coupled Electron Transfer. *J. Am. Chem. Soc.* **2015**, *137*, 9363–9374.
- (89) Oppenheimer, N. J. NAD⁺ and NADP⁺ as Prosthetic Groups for Enzymes. In *Encyclopedia of Life Sciences*; John Wiley & Sons, Ltd: Chichester, UK, 2010.

- (90) Reche, P.; Perham, R. N. Structure and Selectivity in Post-Translational Modification: Attaching the Biotinyl-Lysine and Lipoyl-Lysine Swinging Arms in Multifunctional Enzymes. *EMBO J.* **1999**, *18*, 2673–2682.
- (91) Xie, L.; Van Der Donk, W. A. Homemade Cofactors: Self-Processing in Galactose Oxidase. *PNAS* **2001**, *98*, 12863–12865.
- (92) Dooley, D. M. Structure and Biogenesis of Topaquinone and Related Cofactors. *J. Biol. Inorg. Chem.* **1999**, *4*, 1–11.
- (93) Mure, M. Tyrosine-Derived Quinone Cofactors. *Acc. Chem. Res.* **2004**, *37*, 131–139.
- (94) Heuts, D. P. H. M.; Scrutton, N. S.; McIntire, W. S.; Fraaije, M. W. What's in a Covalent Bond? *FEBS J.* **2009**, *276*, 3405–3427.
- (95) Kearney, E. B.; Singer, T. P. On the Prosthetic Group of Succinic Dehydrogenase. *BBA - Biochim. Biophys. Acta* **1955**, *17*, 596–597.
- (96) Walker, W. H.; Singer, T. P.; Ghisla, S.; Hemmerich, P. Studies on Succinate Dehydrogenase. 8alpha-Histidyl-FAD as the Active Center of Succinate Dehydrogenase. *Eur. J. Biochem.* **1972**, *26*, 279–289.
- (97) Mewies, M.; McIntire, W. S.; Scrutton, N. S. Covalent Attachment of Flavin Adenine Dinucleotide (FAD) and Flavin Mononucleotide (FMN) to Enzymes: The Current State of Affairs. *Protein Sci.* **1998**, *7*, 7–21.
- (98) Starbird, C. A.; Maklashina, E.; Cecchini, G.; Iverson, T. Flavoenzymes: Covalent versus Noncovalent. In *eLS*; John Wiley & Sons, Ltd: Chichester, UK, 2015.
- (99) Huang, C. H.; Lai, W. L.; Lee, M. H.; Chen, C. J.; Vasella, A.; Tsai, Y. C.; Liaw, S. H. Crystal Structure of Glucooligosaccharide Oxidase from *Acremonium Strictum*: A Novel Flavinylation of 6-S-Cysteinyll, 8α-N1-Histidyl FAD. *J. Biol. Chem.* **2005**, *280*, 38831–38838.
- (100) Alexeev, I.; Sultana, A.; Mäntsälä, P.; Niemi, J.; Schneider, G. Aclacinomycin Oxidoreductase (AknOx) from the Biosynthetic Pathway of the Antibiotic Aclacinomycin Is an Unusual Flavoenzyme with a Dual Active Site. *Proc. Natl. Acad. Sci. U. S. A.* **2007**, *104*, 6170–6175.
- (101) Winkler, A.; Hartner, F.; Kutchan, T. M.; Glieder, A.; Macheroux, P. Biochemical Evidence That Berberine Bridge Enzyme Belongs to a Novel Family of Flavoproteins Containing a Bi-Covalently Attached FAD Cofactor. *J. Biol. Chem.* **2006**, *281*, 21276–21285.
- (102) Rand, T.; Qvist, K. B.; Walter, C. P.; Poulsen, C. H. Characterization of the Flavin Association in Hexose Oxidase from *Chondrus Crispus*. *FEBS J.* **2006**, *273*, 2693–2703.
- (103) Heuts, D. P. H. M.; Janssen, D. B.; Fraaije, M. W. Changing the Substrate Specificity of a Chito oligosaccharide Oxidase from *Fusarium Graminearum* by Model-Inspired Site-Directed Mutagenesis. *FEBS Lett.* **2007**, *581*, 4905–4909.
- (104) Taura, F.; Sirikantaramas, S.; Shoyama, Y.; Morimoto, S. Phytocannabinoids in *Cannabis Sativa*: Recent Studies on Biosynthetic Enzymes. *Chem. Biodivers.* **2007**, *4*, 1649–1663.
- (105) Leferink, N. G. H.; Heuts, D. P. H. M.; Fraaije, M. W.; van Berkel, W. J. H. The Growing VAO Flavoprotein Family. *Arch. Biochem. Biophys.* **2008**, *474*, 292–301.
- (106) Fraaije, M. W.; Van Berkel, W. J. H.; Benen, J. A. E.; Visser, J.; Mattevi, A. A Novel Oxidoreductase Family Sharing a Conserved FAD-Binding Domain. *Trends Biochem. Sci.* **1998**, *23*, 206–207.
- (107) Edmondson, D. E.; Binda, C.; Mattevi, A. The FAD Binding Sites of Human Monoamine Oxidases A and B. *Neurotoxicology* **2004**, *25*, 63–72.
- (108) Hassan-Abdallah, A.; Bruckner, R. C.; Zhao, G.; Jorns, M. S. Biosynthesis of Covalently Bound Flavin: Isolation and in Vitro Flavinylation of the Monomeric Sarcosine Oxidase Apoprotein. *Biochemistry* **2005**, *44*, 6452–6462.
- (109) Scruttons, N. S.; Packman, L. C.; Mathews, F. S.; Rohlf, R. J.; Hille, R. Assembly of Redox Centers in the Trimethylamine Dehydrogenase of Bacterium Wfi, Properties of Wild-Type Enzyme and a C30A Mutant Expressed From a Cloned Gene in *Escherichia Coli*. *J. Biol. Chem.* **1994**, *269*, 13942–13950.
- (110) Packman, L. C.; Mewies, M.; Scrutton, N. S. The Flavinylation Reaction of Trimethylamine Dehydrogenase: Analysis by Directed Mutagenesis and Electrospray Mass Spectrometry. *J. Biol. Chem.* **1995**, *270*, 13186–13191.
- (111) Mathews, F. S.; Chen, Z. W.; Bellamy, H. D.; McIntire, W. S. Three-Dimensional Structure of p-Cresol Methylhydroxylase (Flavocytochrome c) from *Pseudomonas Putida* at 3.0-Å Resolution. *Biochemistry* **1991**, *30*, 238–247.
- (112) McIntire, W.; Edmondson, D. E.; Hopper, D. J.; Singer, T. P. 8α-(O-Tyrosyl)Flavin Adenine Dinucleotide, the Prosthetic Group of Bacterial p-Cresol Methylhydroxylase. *Biochemistry* **1981**, *20*, 3068–3075.
- (113) Podzelinska, K.; Latimer, R.; Bhattacharya, A.; Vining, L. C.; Zechel, D. L.; Jia, Z. Chloramphenicol Biosynthesis: The Structure of CmlS, a Flavin-Dependent Halogenase Showing a Covalent Flavin–Aspartate Bond. *J. Mol. Biol.* **2010**, *397*, 316–331.
- (114) Hayashi, M.; Nakayama, Y.; Yasui, M.; Maeda, M.; Furuishi, K.; Unemoto, T. FMN Is Covalently Attached to a Threonine Residue in the NqrB and NqrC Subunits of Na⁺-Translocating NADH-Quinone Reductase from *Vibrio Alginolyticus*. *FEBS Lett.* **2001**, *488*, 5–8.
- (115) Steuber, J.; Vohl, G.; Casutt, M. S.; Vorburger, T.; Diederichs, K.; Fritz, G. Structure of the V. Cholerae Na⁺-Pumping NADH:Quinone Oxidoreductase. *Nature* **2014**, *516*, 62–67.
- (116) Bullock, F. J.; Jardetzky, O. An Experimental Demonstration of the Nuclear Magnetic Resonance Assignments in the 6,7-Dimethylisalloxazine Nucleus. *J. Org. Chem.* **1965**, *30*, 2056–2057.
- (117) Bramson, N. H.; Thomas, N.; DeGrado, W. F.; Kaiser, E. T. Biomimetic 8α Functionalization of Riboflavin. *J. Am. Chem. Soc.* **1980**, *102*, 7157–7159.
- (118) Jin, J.; Mazon, H.; van den Heuvel, R. H. H.; Heck, A. J.; Janssen, D. B.; Fraaije, M. W. Covalent Flavinylation of Vanillyl-Alcohol Oxidase Is an Autocatalytic Process. *FEBS J.* **2008**, *275*, 5191–5200.
- (119) Van Hellemond, E. W.; Mazon, H.; Heck, A. J.; Van Den Heuvel, R. H. H.; Heuts, D. P. H. M.; Janssen, D. B.; Fraaije, M. W. ADP Competes with FAD Binding in Putrescine Oxidase. *J. Biol. Chem.* **2008**, *283*, 28259–28264.
- (120) Brandschs, R.; Bichler, V. Autoflavinylation of Apo6-Hydroxy-Nicotine Oxidase. *J. Biol. Chem.* **1991**, *266*, 19056–19062.
- (121) Efimov, I.; McIntire, W. S. A Study of the Spectral and Redox Properties and Covalent Flavinylation of the Flavoprotein Component of P-Cresol Methylhydroxylase Reconstituted with FAD Analogues. *Biochemistry* **2004**, *43*, 10532–10546.

- (122) Cunane, L. M.; Chen, Z.-W.; McIntire, W. S.; Mathews, F. S. P-Cresol Methylhydroxylase: Alteration of the Structure of the Flavoprotein Subunit upon Its Binding to the Cytochrome Subunit. *Biochemistry* **2005**, *44*, 2963–2973.
- (123) Kim, J.; Fuller, J. H.; Kuusk, V.; Cunane, L.; Chen, Z.; Scott Mathews, F.; McIntire, W. S. The Cytochrome Subunit Is Necessary for Covalent FAD Attachment to the Flavoprotein Subunit of P-Cresol Methylhydroxylase. *J. Biol. Chem.* **1995**, *270*, 31202–31209.
- (124) Koetter, J. W. A.; Schulz, G. E. Crystal Structure of 6-Hydroxy-D-Nicotine Oxidase from *Arthrobacter Nicotinovorans*. *J. Mol. Biol.* **2005**, *352*, 418–428.
- (125) Hao, H.-X.; Khalimonchuk, O.; Schraders, M.; Dephoure, N.; Bayley, J.-P.; Kunst, H.; Devile, P.; Cremers, C. W. R. J.; Schiffman, J. D.; Bentz, B. G.; Gygi, S. P.; Winge, D. R.; Kremer, H.; Rutter, J. SDH5, a Gene Required for Flavination of Succinate Dehydrogenase, Is Mutated in Paraganglioma. *Science*. **2009**, *325*, 1139–1142.
- (126) McNeil, M. B.; Clulow, J. S.; Wilf, N. M.; Salmond, G. P. C.; Fineran, P. C. SdhE Is a Conserved Protein Required for Flavinylation of Succinate Dehydrogenase in Bacteria. *J. Biol. Chem.* **2012**, *287*, 18418–18428.
- (127) Lim, K.; Doseeva, V.; Demirkan, E. S.; Pullalarevu, S.; Krajewski, W.; Galkin, A.; Howard, A.; Herzberg, O. Crystal Structure of the YgfY from *Escherichia Coli*, a Protein That May Be Involved in Transcriptional Regulation. *Proteins Struct. Funct. Bioinforma.* **2004**, *58*, 759–763.
- (128) Eletsky, A.; Jeong, M. Y.; Kim, H.; Lee, H. W.; Xiao, R.; Pagliarini, D. J.; Prestegard, J. H.; Winge, D. R.; Montelione, G. T.; Szyperski, T. Solution NMR Structure of Yeast Succinate Dehydrogenase Flavinylation Factor Sdh5 Reveals a Putative Sdh1 Binding Site. *Biochemistry* **2012**, *51*, 8475–8477.
- (129) McNeil, M. B.; Fineran, P. C. The Conserved RGxxE Motif of the Bacterial FAD Assembly Factor SdhE Is Required for Succinate Dehydrogenase Flavinylation and Activity. *Biochemistry* **2013**, *52*, 7628–7640.
- (130) Starbird, C. A.; Maklashina, E.; Sharma, P.; Qualls-Histed, S.; Cecchini, G.; Iverson, T. M. Structural and Biochemical Analyses Reveal Insights into Covalent Flavinylation of the *Escherichia Coli* Complex II Homolog Quinol:Fumarate Reductase. *J. Biol. Chem.* **2017**, *292*, 12921–12933.
- (131) Maklashina, E.; Rajagukguk, S.; Starbird, C. A.; McDonald, W. H.; Koganitsky, A.; Eisenbach, M.; Iverson, T. M.; Cecchini, G. Binding of the Covalent Flavin Assembly Factor to the Flavoprotein Subunit of Complex II. *J. Biol. Chem.* **2015**, *291*, 2904–2916.
- (132) Kounosu, A. Analysis of Covalent Flavinylation Using Thermostable Succinate Dehydrogenase from *Thermus Thermophilus* and *Sulfolobus Tokodaii* Lacking SdhE Homologs. *FEBS Lett.* **2014**, *588*, 1058–1063.
- (133) Barquera, B.; Häse, C. C.; Gennis, R. B. Expression and Mutagenesis of the NqrC Subunit of the NQR Respiratory Na⁺ Pump from *Vibrio Cholerae* with Covalently Attached FMN. *FEBS Lett.* **2001**, *492*, 45–49.
- (134) Bertsova, Y. V.; Fadeeva, M. S.; Kostyrko, V. A.; Serebryakova, M. V.; Baykov, A. A.; Bogachev, A. V. Alternative Pyrimidine Biosynthesis Protein ApbE Is a Flavin Transferase Catalyzing Covalent Attachment of FMN to a Threonine Residue in Bacterial Flavoproteins. *J. Biol. Chem.* **2013**, *288*, 14276–14286.
- (135) Deka, R. K.; Brautigam, C. A.; Liu, W. Z.; Tomchick, D. R.; Norgard, M. V.; Greenberg, E. E. P. Evidence for Posttranslational Protein Flavinylation in the Syphilis Spirochete *Treponema Pallidum*: Structural and Biochemical Insights from the Catalytic Core of a Periplasmic Flavin-Trafficking Protein. *MBio* **2015**, *6*, 1–9.
- (136) Boyd, J. M.; Endrizzi, J. A.; Hamilton, T. L.; Christopherson, M. R.; Mulder, D. W.; Downs, D. M.; Peters, J. W. FAD Binding by ApbE Protein from *Salmonella Enterica*: A New Class of FAD-Binding Proteins. *J. Bacteriol.* **2011**, *193*, 887–895.
- (137) Bogachev, A. V.; Baykov, A. A.; Bertsova, Y. V. Flavin Transferase: The Maturation Factor of Flavincontaining Oxidoreductases. *Biochem. Soc. Trans.* **2018**, *46*, 1161–1169.
- (138) Fang, X.; Osipiuk, J.; Chakravarthy, S.; Yuan, M.; Menzer, W. M.; Nissen, D.; Liang, P.; Raba, D. A.; Tuz, K.; Howard, A. J.; Joachimiak, A.; Minh, D. D. L.; Juarez, O. Conserved Residue His-257 of *Vibrio Cholerae* Flavin Transferase ApbE Plays a Critical Role in Substrate Binding and Catalysis. *J. Biol. Chem.* **2019**, *294*, 13800–13810.
- (139) Zhou, Z.; Swenson, R. P. The Cumulative Electrostatic Effect of Aromatic Stacking Interactions and the Negative Electrostatic Environment of the Flavin Mononucleotide Binding Site Is a Major Determinant of the Reduction Potential for the Flavodoxin from *Desulfovibrio Vulgaris*. *Biochemistry* **1996**, *35*, 15980–15988.
- (140) Zhou, Z.; Swenson, R. P. Electrostatic Effects of Surface Acidic Amino Acid Residues on the Oxidation-Reduction Potentials of the Flavodoxin from *Desulfovibrio Vulgaris* (Hildenborough). *Biochemistry* **1995**, *34*, 3183–3192.
- (141) Edmondson, D. E.; Ghisla, S. Electronic Effects of 7 and 8 Ring Substituents as Predictors of Flavin Oxidation-Reduction Potentials. In *Flavins and flavoproteins*; 1999; pp 71–76.
- (142) Fraaije, M. W.; Van Den Heuvel, R. H. H.; Van Berkel, W. J. H.; Mattevi, A. Covalent Flavinylation Is Essential for Efficient Redox Catalysis in Vanillyl-Alcohol Oxidase. *J Biol Chem.* **1999**, *274*, 35514–35520.
- (143) Fraaije, M. W.; Van Den Heuvel, R. H. H.; Van Berkel, W. J. H.; Mattevi, A. Structural Analysis of Flavinylation in Vanillyl-Alcohol Oxidase. *J. Biol. Chem.* **2000**, *275*, 38654–38658.
- (144) Efimov, I.; Cronin, C. N.; McIntire, W. S. Effects of Noncovalent and Covalent FAD Binding on the Redox and Catalytic Properties of P-Cresol Methylhydroxylase. *Biochemistry* **2001**, *40*, 2155–2166.
- (145) Lim, L.; Molla, G.; Guinn, N.; Ghisla, S.; Pollegioni, L.; Vrielink, A. Structural and Kinetic Analyses of the H121A Mutant of Cholesterol Oxidase. *Biochem. J.* **2006**, *400*, 13–22.
- (146) Motteran, L.; Pilone, M. S.; Molla, G.; Ghisla, S.; Pollegioni, L.; Coulombe, R.; Yue, K. Q.; Ghisla, S.; Vrielink, A. Cholesterol Oxidase from *Brevibacterium Sterolicum*; The Relationship Between Covalent Flavinylation and Redox Properties. *J. Biol. Chem.* **2001**, *276*, 18024–18030.
- (147) Winkler, A.; Kutchan, T. M.; Macheroux, P. 6-S-Cysteinylation of Bi-Covalently Attached FAD in Berberine Bridge Enzyme Tunes the Redox Potential for Optimal Activity. *J. Biol. Chem.* **2007**, *282*, 24437–24443.
- (148) Heuts, D. P. H. M.; Winter, R. T.; Damsma, G. E.; Janssen, D. B.; Fraaije, M. W. The Role of Double Covalent Flavin Binding in Chito-Oligosaccharide Oxidase from *Fusarium Graminearum*. *Biochem. J.* **2008**, *413*, 175–183.

- (149) Hassan-Abdallah, A.; Zhao, G.; Jorns, M. S. Role of the Covalent Flavin Linkage in Monomeric Sarcosine Oxidase. *Biochemistry* **2006**, *45*, 9454–9462.
- (150) Caldinelli, L.; Iametti, S.; Barbiroli, A.; Bonomi, F.; Fessas, D.; Molla, G.; Pilone, M. S.; Pollegioni, L. Dissecting the Structural Determinants of the Stability of Cholesterol Oxidase Containing Covalently Bound Flavin. *J. Biol. Chem.* **2005**, *280*, 22572–22581.
- (151) Lu, X.; Nikolic, D.; Mitchell, D. J.; Van Breemen, R. B.; Mersfelder, J. A.; Hille, R.; Silverman, R. B. A Mechanism for Substrate-Induced Formation of 6-Hydroxyflavin Mononucleotide Catalyzed by C30A Trimethylamine Dehydrogenase. *Bioorganic Med. Chem. Lett.* **2003**, *13*, 4129–4132.
- (152) Mayhew, S. G.; Whitfield, C. D.; Ghisla, S.; Schuman-jorns, M. Identification and Properties of New Flavins in Electron-Transferring Flavoprotein from *Peptostreptococcus Elsdonii* and Pig-Liver Glycolate Oxidase. *Eur. J. Biochem.* **1974**, *44*, 579–591.
- (153) Ghisla, S.; Mayhew, S. G. Identification and Properties of 8-Hydroxyflavin : Adenine Dinucleotide in Electron-Transferring Flavoprotein from *Peptostreptococcus Elsdonii*. *Eur. J. Biochem.* **1976**, *63*, 373–390.
- (154) Bergner, T.; Tabib, C. R.; Winkler, A.; Stipsits, S.; Kayer, H.; Lee, J.; Malthouse, J. P.; Mayhew, S.; Müller, F.; Gruber, K.; Macheroux, P. Structural and Biochemical Properties of LuxF from *Photobacterium Leioognathi*. *Biochim. Biophys. Acta - Proteins Proteomics* **2015**, *1854*, 1466–1475.
- (155) Tabib, C. R.; Brodl, E.; Macheroux, P. Evidence for the Generation of Myristylated FMN by Bacterial Luciferase. *Mol. Microbiol.* **2017**, *104*, 1027–1036.
- (156) Eckstein, J. W.; Hastings, J. W.; Ghisla, S. Mechanism of Bacterial Bioluminescence: 4a,5-Dihydroflavin Analogs as Models for Luciferase Hydroperoxide Intermediates and the Effect of Substituents at the 8-Position of Flavin on Luciferase Kinetics. *Biochemistry* **1993**, *32*, 404–411.
- (157) Moore, S. A.; James, M. N. G. Structural Refinement of the Non-Fluorescent Flavoprotein from *Photobacterium Leioognathi* at 1.60 Å Resolution. *J. Mol. Biol.* **1995**, *249*, 195–214.
- (158) Wei, C. J.; Lei, B.; Tu, S. C. Characterization of the Binding of *Photobacterium Phosphoreum* P-Flavin by *Vibrio Harveyi* Luciferase. *Arch. Biochem. Biophys.* **2001**, *396*, 199–206.
- (159) Tachibana, S.; Murakami, T. The Isolation and Some Properties Of New Flavins (“Schizoflavin”) Formed By Schizophyllum Commune. *J. Nutr. Sci. Vitaminol. (Tokyo)*. **1975**, *21*, 61–63.
- (160) Tachibana, S.; Murakami, T.; Ninomiya, T. Identification of the Chemical Structures of Schizoflavins as 7,8-Dimethyl-10-(2,3,4-Trihydroxy-4-Formylbutyl)Isoalloxazine and 7,8-Dimethyl-10-(2,3,4-Trihydroxy-4-Carboxybutyl)Isoalloxazine. *J. Nutr. Sci. Vitaminol. (Tokyo)*. **1975**, *21*, 4.
- (161) Tachibana, S.; Oka, M. NADPH-Dependence of Vitamin B₂-Aldehyde-Forming Enzyme. *J. Nutr. Sci. Vitaminol.* **1982**, *28*, 335–342.
- (162) Matsui, K.; Kasai, S. Identification of Nekoflavin as 7a-Hydroxyriboflavin. *J. Biochem.* **1996**, *119*, 441–447.
- (163) Owen, E. C.; West, D. W. Metabolites of Riboflavine in Milk, Urine and Tissues of Animals in Relation to Alimentary Symbiotic Bacteria. *Br. J. Nutr.* **1970**, *24*, 45.
- (164) Susin, S.; Abián, J.; Sanchez-Baeza, F.; Peleato, M. L.; Abadia, A.; Gelpi, E.; Abadia, J. Riboflavin 3'-and 5'-Sulfate, Two Novel Flavins Accumulating in the Roots of Iron-Deficient Sugar Beet (*Beta Vulgaris*). *J. Biol. Chem.* **1993**, *268*, 2095–20965.
- (165) Otani, S.; Takatsu, M.; Nakano, M.; Kasai, S.; Miura, R.; Matsui, K. Roseoflavin, A New Antimicrobial Pigment From *Streptomyces*. *J. Antibiot. (Tokyo)*. **1974**, *27*, 86–87.
- (166) Mansjö, M.; Johansson, J. The Riboflavin Analog Roseoflavin Targets an FMN-Riboswitch and Blocks *Listeria Monocytogenes* Growth, but Also Stimulates Virulence Gene-Expression and Infection. *RNA Biol.* **2011**, *8*, 674–680.
- (167) Langer, S.; Nakanishi, S.; Mathes, T.; Knaus, T.; Binter, A.; Macheroux, P.; Mase, T.; Miyakawa, T.; Tanokura, M.; Mack, M. The Flavoenzyme Azobenzene Reductase AzoR from *Escherichia Coli* Binds Roseoflavin Mononucleotide (RoFMN) with High Affinity and Is Less Active in Its RoFMN Form. *Biochemistry* **2013**, *52*, 4288–4295.
- (168) Grill, S.; Busenbender, S.; Pfeiffer, M.; Köhler, U.; Mack, M. The Bifunctional Flavokinase/Flavin Adenine Dinucleotide Synthetase from *Streptomyces Davawensis* Produces Inactive Flavin Cofactors and Is Not Involved in Resistance to the Antibiotic Roseoflavin. *J. Bacteriol.* **2008**, *190*, 1546–1553.
- (169) Pedrolli, D. B.; Nakanishi, S.; Barile, M.; Mansurova, M.; Carmona, E. C.; Lux, A.; Gärtner, W.; Mack, M. The Antibiotics Roseoflavin and 8-Demethyl-8-Amino-Riboflavin from *Streptomyces Davawensis* Are Metabolized by Human Flavokinase and Human FAD Synthetase. *Biochem. Pharmacol.* **2011**, *82*, 1853–1859.
- (170) Shinkai, S.; Kameoka, K.; Honda, N.; Ueda, K.; Manabe, O.; Lindsey, J. Coenzyme Models. 40. Spectral and Reactivity Studies of Roseoflavin Analogs: Correlation between Reactivity and Spectral Parameters. *Bioorg. Chem.* **1986**, *14*, 119–133.
- (171) Lee, E. R.; Blount, K. F.; Breaker, R. R. Roseoflavin Is a Natural Antibacterial Compound That Binds to FMN Riboswitches and Regulates Gene Expression. *RNA Biol.* **2009**, *6*, 187–194.
- (172) Schwarz, J.; Konjik, V.; Jankowitsch, F.; Sandhoff, R.; Mack, M. Identification of the Key Enzyme of Roseoflavin Biosynthesis. *Angew. Chemie Int. Ed.* **2016**, *55*, 6103–6106.
- (173) Konjik, V.; Brünle, S.; Demmer, U.; Vanselow, A.; Sandhoff, R.; Ermler, U.; Mack, M. The Crystal Structure of RosB: Insights into the Reaction Mechanism of the First Member of a Family of Flavodoxin-like Enzymes. *Angew. Chemie Int. Ed.* **2017**, *56*, 1146–1151.
- (174) Mora-Lugo, R.; Stegmüller, J.; Mack, M. Metabolic Engineering of Roseoflavin-Overproducing Microorganisms. *Microb. Cell Fact.* **2019**, *18*, 1–13.
- (175) Jankowitsch, F.; Kühm, C.; Kellner, R.; Kalinowski, J.; Pelzer, S.; Macheroux, P.; Mack, M. A Novel N,N-8-Amino-8-Demethyl-D-Riboflavin Dimethyltransferase (RosA) Catalyzing the Two Terminal Steps of Roseoflavin Biosynthesis in *Streptomyces Davawensis*. *J. Biol. Chem.* **2011**, *286*, 38275–38285.
- (176) Yorita, K.; Matsuoka, T.; Misaki, H.; Massey, V. Interaction of Two Arginine Residues in Lactate Oxidase with the Enzyme Flavin: Conversion of FMN to 8-Formyl-FMN. *Proc. Natl. Acad. Sci. U. S. A.* **2000**, *97*, 13039–13044.
- (177) Robbins, J. M.; Souffrant, M. G.; Hamelberg, D.; Gadda, G.; Bommarius, A. S. Enzyme-Mediated Conversion of Flavin Adenine Dinucleotide (FAD) to 8-Formyl FAD in Formate Oxidase Results in a Modified Cofactor with Enhanced Catalytic Properties. *Biochemistry* **2017**, *56*, 3800–3807.

- (178) Augustin, P.; Toplak, M.; Fuchs, K.; Gerstmann, E. C.; Prassl, R.; Winkler, A.; Macheroux, P. Oxidation of the FAD Cofactor to the 8-Formyl Derivative in Human Electron Transferring Flavoprotein. *J. Biol. Chem.* **2018**, *293*, 2829–2840.
- (179) Marshall, S. A.; Fisher, K.; Cheallaigh, A. N.; White, M. D.; Payne, K. A. P.; Parker, D. A.; Rigby, S. E. J.; Leys, D. Oxidative Maturation and Structural Characterization of Prenylated FMN Binding by UbiD, a Decarboxylase Involved in Bacterial Ubiquinone Biosynthesis. *J. Biol. Chem.* **2017**, *292*, 4623–4637.
- (180) Payne, K. A. P.; White, M. D.; Fisher, K.; Khara, B.; Bailey, S. S.; Parker, D.; Rattray, N. J. W.; Trivedi, D. K.; Goodacre, R.; Beveridge, R.; Barran, P.; Rigby, S. E. J.; Scrutton, N. S.; Hay, S.; Leys, D. New Cofactor Supports a,b-Unsaturated Acid Decarboxylation via 1,3-Dipolar Cycloaddition. *Nature* **2015**, *522*, 497–501.
- (181) White, M. D.; Payne, K. A. P.; Fisher, K.; Marshall, S. A.; Parker, D.; Rattray, N. J. W.; Trivedi, D. K.; Goodacre, R.; Rigby, S. E. J.; Scrutton, N. S.; Hay, S.; Leys, D. UbiX Is a Flavin Prenyltransferase Required for Bacterial Ubiquinone Biosynthesis. *Nature* **2015**, *522*, 502–506.
- (182) Marshall, S. A.; Payne, K. A. P.; Fisher, K.; White, M. D.; Ni Cheallaigh, A.; Balaikaite, A.; Rigby, S. E. J.; Leys, D. The UbiX Flavin Prenyltransferase Reaction Mechanism Resembles Class I Terpene Cyclase Chemistry. *Nat. Commun.* **2019**, *10*, 1–10.
- (183) Biemann, M.; Claiborne, A.; Ghisla, S.; Massey, V. 4-Thioflavins as Active Site Probes of Flavoproteins. Reactions with Sulfite. *J. Biol. Chem.* **1984**, *259*, 13355–13362.
- (184) Ghisla, S.; Massey, V. New Flavins for Old: Artificial Flavins as Active Site Probes of Flavoproteins. *Biochem. J.* **1986**, *239*, 1–12.
- (185) Massey, V.; Ghisla, S.; Yagi, K. 6-Thiocyanatoflavins and 6-Mercaptoflavins as Active-Site Probes of Flavoproteins. *Biochemistry* **1986**, *25*, 8103–8112.
- (186) Su, Q.; Boucher, P. A.; Rokita, S. E. Conversion of a Dehalogenase into a Nitroreductase by Swapping Its Flavin Cofactor with a 5-Deazaflavin Analogue. *Angew. Chemie Int. Ed.* **2017**, *56*, 10862–10866.
- (187) De Gonzalo, G.; Smit, C.; Jin, J.; Minnaard, A. J.; Fraaije, M. W. Turning a Riboflavin-Binding Protein into a Self-Sufficient Monooxygenase by Cofactor Redesign. *Chem. Commun.* **2011**, *47*, 11050–11052.
- (188) Lalpalikar, G. V.; Taylor, M. C.; Warden, A. C.; Onagi, H.; Hennessy, J. E.; Mulder, R. J.; Scott, C.; Brown, S. E.; Russell, R. J.; Easton, C. J.; Oakshott, J. G. Cofactor Promiscuity among F₄₂₀-Dependent Reductases Enables Them to Catalyse Both Oxidation and Reduction of the Same Substrate. *Catal. Sci. Technol.* **2012**, *2*, 1560–1567.
- (189) Karunan Partha, S.; van Straaten, K. E.; Sanders, D. A. R. Structural Basis of Substrate Binding to UDP-Galactopyranose Mutase: Crystal Structures in the Reduced and Oxidized State Complexed with UDP-Galactopyranose and UDP. *J. Mol. Biol.* **2009**, *394*, 864–877.
- (190) Zhang, Q.; Liu, H.-W. Mechanistic Investigation of UDP-Galactopyranose Mutase from Escherichia Coli Using 2- and 3-Fluorinated UDP-Galactofuranose as Probes. *J. Am. Chem. Soc.* **2001**, *123*, 6756–6766.
- (191) Mehra-Chaudhary, R.; Dai, Y.; Sobrado, P.; Tanner, J. J. In Crystallo Capture of a Covalent Intermediate in the UDP-Galactopyranose Mutase Reaction. *Biochemistry* **2016**, *55*, 833–836.
- (192) Tanner, J. J.; Boechi, L.; Andrew McCammon, J.; Sobrado, P. Structure, Mechanism, and Dynamics of UDP-Galactopyranose Mutase. *Archives of Biochemistry and Biophysics*. Academic Press February 15, 2014, pp 128–141.
- (193) Razeto, A.; Mattioli, F.; Carpanelli, E.; Aliverti, A.; Pandini, V.; Coda, A.; Mattevi, A. The Crucial Step in Ether Phospholipid Biosynthesis: Structural Basis of a Noncanonical Reaction Associated with a Peroxisomal Disorder. *Structure* **2007**, *15*, 683–692.
- (194) Urbonavič, J.; Phane Skouloubris, S.; Myllykallio, H.; Grosjean, H. Identification of a Novel Gene Encoding a Flavin-Dependent TRNA:M 5 U Methyltransferase in Bacteria-Evolutionary Implications. *Nucleic Acids Res.* **2005**, *33*, 3955–3964.
- (195) Myllykallio, H.; Lipowski, G.; Leduc, D.; Filee, J.; Forterre, P.; Liebl, U. An Alternative Flavin-Dependent Mechanism for Thymidylate Synthesis. *Science*. **2002**, *297*, 105–107.
- (196) Hamdane, D.; Argentini, M.; Cornu, D.; Myllykallio, H.; Skouloubris, S.; Hui-Bon-Hoa, G.; Golinelli-Pimpaneau, B. Insights into Folate/FAD-Dependent TRNA Methyltransferase Mechanism: Role of Two Highly Conserved Cysteines in Catalysis. *J. Biol. Chem.* **2011**, *286*, 36268–36280.
- (197) Myllykallio, H.; Skouloubris, S.; Grosjean, H.; Liebl, U. Folate-Dependent Thymidylate-Forming Enzymes: Parallels between DNA and RNA Metabolic Enzymes and Evolutionary Implications. In *DNA and RNA Modification Enzymes: Comparative Structure, Mechanism, Functions, Cellular Interactions and Evolution*; Henri Grosjean, Ed.; Landes Bioscience, 2009.
- (198) Mishanina, T. V.; Yu, L.; Karunaratne, K.; Mondal, D.; Corcoran, J. M.; Choi, M. A.; Kohen, A. An Unprecedented Mechanism of Nucleotide Methylation in Organisms Containing ThyX. *Science*. **2016**, *351*, 507–510.
- (199) Sobrado, P. Noncanonical Reactions of Flavoenzymes. *Int. J. Mol. Sci.* **2012**, *13*, 14219–14242.
- (200) Xiang, L.; Kalaitzis, J. A.; Moore, B. S. EncM, a Versatile Enterocin Biosynthetic Enzyme Involved in Favorskii Oxidative Rearrangement, Aldol Condensation, and Heterocycle-Forming Reactions. *Proc. Natl. Acad. Sci. U. S. A.* **2004**, *101*, 15609–15614.
- (201) Teufel, R.; Miyanaga, A.; Michaudel, Q.; Stull, F.; Louie, G.; Noel, J. P.; Baran, P. S.; Palfey, B.; Moore, B. S. Flavin-Mediated Dual Oxidation Controls an Enzymatic Favorskii-Type Rearrangement. *Nature* **2013**, *503*, 552–556.
- (202) Teufel, R.; Stull, F.; Meehan, M. J.; Michaudel, Q.; Dorrestein, P. C.; Palfey, B.; Moore, B. S. Biochemical Establishment and Characterization of EncM's Flavin-N5-Oxide Cofactor. *J. Am. Chem. Soc.* **2015**, *137*, 8078–8085.
- (203) Saleem-Batcha, R.; Stull, F.; Sanders, J. N.; Moore, B. S.; Palfey, B. A.; Houk, K. N.; Teufel, R. Enzymatic Control of Dioxygen Binding and Functionalization of the Flavin Cofactor. *Proc. Natl. Acad. Sci. U. S. A.* **2018**, *115*, 4909–4919.
- (204) Matthews, A.; Saleem-Batcha, R.; Sanders, J. N.; Stull, F.; Houk, K. N.; Teufel, R. Aminoperoxide Adducts Expand the Catalytic Repertoire of Flavin Monooxygenases. *Nat. Chem. Biol.* **2020**, *16*, 556–563.
- (205) Mukherjee, T.; Zhang, Y.; Abdelwahed, S.; Ealick, S. E.; Begley, T. P. Catalysis of a Flavoenzyme-Mediated Amide Hydrolysis. *J. Am. Chem. Soc.* **2010**, *132*, 5550–5551.
- (206) Adak, S.; Begley, T. P. Ruta-Catalyzed Oxidative Cleavage of the Uracil Amide Involves Formation of a Flavin-N5-Oxide. *Biochemistry* **2017**, *56*, 3708–3709.
- (207) Adak, S.; Begley, T. P. Dibenzothiophene Catabolism Proceeds via a Flavin-N5-Oxide Intermediate. *J. Am. Chem. Soc.* **2016**, *138*, 6424–6426.

- (208) Adak, S.; Begley, T. P. Hexachlorobenzene Catabolism Involves a Nucleophilic Aromatic Substitution and Flavin-N5-Oxide Formation. *Biochemistry* **2019**, *58*, 1181–1183.
- (209) Eirich, L. D.; Vogels, G. D.; Wolfe, R. S. Distribution of Coenzyme F₄₂₀ and Properties of Its Hydrolytic Fragments. *J. Bacteriol.* **1979**, *140*, 20–27.
- (210) Selengut, J. D.; Haft, D. H. Unexpected Abundance of Coenzyme F₄₂₀-Dependent Enzymes in *Mycobacterium Tuberculosis* and Other Actinobacteria. *J. Bacteriol.* **2010**, *192*, 5788–5798.
- (211) Cheeseman, P.; Toms-Wood, A.; Wolfe, R. S. Isolation and Properties of a Fluorescent Compound, Factor420, from *Methanobacterium* Strain M.o.H. *J. Bacteriol.* **1972**, *112*, 527–531.
- (212) Edmondson, D. E.; Barman, B.; Toliin, G. On the Importance of the N-5 Position in Flavin Coenzymes. Properties of Free and Protein-Bound 5-Deaza Analogs. *Biochemistry* **1972**, *11*, 1133–1138.
- (213) Ney, B.; Carere, C. R.; Sparling, R.; Jirapanjawan, T.; Stott, M. B.; Jackson, C. J.; Oakeshott, J. G.; Warden, A. C.; Greening, C. Cofactor Tail Length Modulates Catalysis of Bacterial F₄₂₀-Dependent Oxidoreductases. *Front. Microbiol.* **2017**, *8*, 1902.
- (214) Schauer, N. L.; Ferry, J. G. Composition of the Coenzyme F₄₂₀-Dependent Formate Dehydrogenase from *Methanobacterium Formicicum*. *J. Bacteriol.* **1986**, *165*, 405–411.
- (215) Tzeng, S. F.; Wolfe, R. S.; Bryant, M. P. Factor 420-Dependent Tyridine Nucleotide-Linked Hydrogenase System of *Methanobacterium Ruminantium*. *J. Bacteriol.* **1975**, *121*, 184–191.
- (216) Aufhammer, S. W.; Warkentin, E.; Berk, H.; Shima, S.; Thauer, R. K.; Ermler, U. Coenzyme Binding in F₄₂₀-Dependent Secondary Alcohol Dehydrogenase, a Member of the Bacterial Luciferase Family. *Structure* **2004**, *12*, 361–370.
- (217) Widdel, F.; Rouvière, P. E.; Wolfe, R. S. Classification of Secondary Alcohol-Utilizing Methanogens Including a New Thermophilic Isolate. *Arch. Microbiol.* **1988**, *150*, 477–481.
- (218) Vitt, S.; Ma, K.; Warkentin, E.; Moll, J.; Pierik, A. J.; Shima, S.; Ermler, U. The F₄₂₀-Reducing [NiFe]-Hydrogenase Complex from *Methanothermobacter Marburgensis*, the First X-Ray Structure of a Group 3 Family Member. *J. Mol. Biol.* **2014**, *426*, 2813–2826.
- (219) Hagemeyer, C. H.; Shima, S.; Thauer, R. K.; Bourenkov, G.; Bartunik, H. D.; Ermler, U. Coenzyme F₄₂₀-Dependent Methylenetetrahydromethanopterin Dehydrogenase (Mtd) from *Methanopyrus Kandleri*: A Methanogenic Enzyme with an Unusual Quarternary Structure. *J. Mol. Biol.* **2003**, *332*, 1047–1057.
- (220) Shima, S.; Warkentin, E.; Grabarse, W.; Sordel, M.; Wicke, M.; Thauer, R. K.; Ermler, U. Structure of Coenzyme F₄₂₀ Dependent Methylenetetrahydromethanopterin Reductase from Two Methanogenic Archaea. *J. Mol. Biol.* **2000**, *300*, 935–950.
- (221) Johnson, E. F.; Mukhopadhyay, B. A New Type of Sulfite Reductase, a Novel Coenzyme F₄₂₀-Dependent Enzyme, from the Methanarchaeon *Methanocaldococcus Jannaschii*. *J. Biol. Chem.* **2005**, *280*, 38776–38786.
- (222) Bäumer, S.; Ide, T.; Jacobi, C.; Johann, A.; Gottschalk, G.; Deppenmeier, U. The F₄₂₀H₂ Dehydrogenase from *Methanosarcina Mazei* Is a Redox-Driven Proton Pump Closely Related to NADH Dehydrogenases. *J. Biol. Chem.* **2000**, *275*, 17968–17973.
- (223) Welte, C.; Deppenmeier, U. Re-Evaluation of the Function of the F₄₂₀ Dehydrogenase in Electron Transport of *Methanosarcina Mazei*. *FEBS J.* **2011**, *278*, 1277–1287.
- (224) Berk, H.; Thauer, R. K. Function of Coenzyme F₄₂₀-Dependent NADP Reductase in Methanogenic Archaea Containing an NADP-Dependent Alcohol Dehydrogenase. *Arch. Microbiol.* **1997**, *168*, 396–402.
- (225) Seedorf, H.; Dreisbach, A.; Hedderich, R.; Shima, S.; Thauer, R. K. F420H₂ Oxidase (FprA) from *Methanobrevibacter Arboriphilus*, a Coenzyme F₄₂₀-Dependent Enzyme Involved in O₂ Detoxification. *Arch. Microbiol.* **2004**, *182*, 126–137.
- (226) Möller-Zinkhan, D.; Börner, G.; Thauer, R. K. Function of Methanofuran, Tetrahydromethanopterin, and Coenzyme F₄₂₀ in *Archaeoglobus Fulgidus*. *Arch. Microbiol.* **1989**, *152*, 362–368.
- (227) Gurumurthy, M.; Rao, M.; Mukherjee, T.; Rao, S. P. S.; Boshoff, H. I.; Dick, T.; Barry, C. E.; Manjunatha, U. H. A Novel F₄₂₀-Dependent Anti-Oxidant Mechanism Protects *Mycobacterium Tuberculosis* against Oxidative Stress and Bactericidal Agents. *Mol. Microbiol.* **2013**, *87*, 744–755.
- (228) Purwantini, E.; Mukhopadhyay, B. Conversion of NO₂ to NO by Reduced Coenzyme F₄₂₀ Protects *Mycobacteria* from Nitrosative Damage. *Proc. Natl. Acad. Sci. U. S. A.* **2009**, *106*, 6333–6338.
- (229) Bashiri, G.; Squire, C. J.; Moreland, N. J.; Baker, E. N. Crystal Structures of F₄₂₀-Dependent Glucose-6-Phosphate Dehydrogenase FGD1 Involved in the Activation of the Anti-Tuberculosis Drug Candidate PA-824 Reveal the Basis of Coenzyme and Substrate Binding. *J. Biol. Chem.* **2008**, *283*, 17531–17541.
- (230) Nguyen, Q.-T.; Trinco, G.; Binda, C.; Mattevi, A.; Fraaije, M. W.; Nguyen, Q.-T.; Trinco, G.; Binda, C.; Mattevi, A. Discovery and Characterization of an F₄₂₀-Dependent Glucose-6-Phosphate Dehydrogenase (Rh-FGD1) from *Rhodococcus Jostii* RHA1. *Appl. Microbiol. Biotechnol.* **101**, 2831–2842.
- (231) Manjunatha, U.; Boshoff, H. I. M.; Barry, C. E. The Mechanism of Action of PA-824. *Commun. Integr. Biol.* **2009**, *2*, 215–218.
- (232) Purwantini, E.; Mukhopadhyay, B. Rv0132c of *Mycobacterium Tuberculosis* Encodes a Coenzyme F₄₂₀-Dependent Hydroxymycolic Acid Dehydrogenase. *PLoS One* **2013**, *8*, e81985.
- (233) Ahmed, F. H.; Carr, P. D.; Lee, B. M.; Afriat-Jurnou, L.; Mohamed, A. E.; Hong, N.-S.; Flanagan, J.; Taylor, M. C.; Greening, C.; Jackson, C. J. Sequence–Structure–Function Classification of a Catalytically Diverse Oxidoreductase Superfamily in *Mycobacteria*. *J. Mol. Biol.* **2015**, *427*, 3554–3571.
- (234) Kuo, M.-S. T.; Yurek, D. A.; Coats, J. H.; Li, G. P. Isolation and Identification of 7,8-Didemethyl-8-Hydroxy-5-Deazariboflavin, an Unusual Cosynthetic Factor in Streptomycetes, from *Streptomyces Lincolnensis*. *J. Antibiot. (Tokyo)*. **1989**, *42*, 475–478.
- (235) Li, W.; Chou, S.; Khullar, A.; Gerratana, B. Cloning and Characterization of the Biosynthetic Gene Cluster for Tomaymycin, an Sjc-136 Monomeric Analog. *Appl. Environ. Microbiol.* **2009**, *75*, 2958–2963.
- (236) Coats, J. H.; Li, G. P.; Kuo, M.-S. T.; Yurek, D. A. Discovery, Production and Biological Assay of an Unusual Flavenoid Cofactor Involved in Lincomycin Biosynthesis. *J. Antibiot. (Tokyo)*. **1989**, *42*, 472–474.
- (237) Choi, K. P.; Kendrick, N.; Daniels, L. Demonstration That FbiC Is Required by *Mycobacterium Bovis* BCG for Coenzyme F₄₂₀ and FO Biosynthesis. *J. Bacteriol.* **2002**, *184*, 2420–2428.
- (238) Philmus, B.; Decamps, L.; Berteau, O.; Begley, T. P. Biosynthetic Versatility and Coordinated Action of 5'-Deoxyadenosyl Radicals in Deazaflavin Biosynthesis. *J. Am. Chem. Soc.* **2015**, *137*, 5406–5413.
- (239) Bashiri, G.; Antoney, J.; Jirgis, E. N. M.; Shah, M. V.; Ney, B.; Copp, J.; Stuteley, S. M.; Sreebhavan, S.; Palmer, B.; Middleditch, M.; Tokuriki, N.; Greening, C.; Scott, C.; Baker, E. N.; Jackson, C. J. A Revised Biosynthetic Pathway for the Cofactor F₄₂₀ in Prokaryotes. *Nat. Commun.* **2019**, *10*, 1558.

- (240) Braga, D.; Last, D.; Hasan, M.; Guo, H.; Lechnitz, D.; Uzum, Z.; Richter, I.; Schalk, F.; Beemelmans, C.; Hertweck, C.; Lackner, G. Metabolic Pathway Rerouting in *Paraburkholderia rhizoxinica* Evolved Long-Overlooked Derivatives of Coenzyme F₄₂₀. *ACS Chem. Biol.* **2019**, *14*, 2088–2094.
- (241) Daniels, L.; Bakhiet, N.; Harmon, K. Widespread Distribution of a 5-Deazaflavin Cofactor in Actinomyces and Related Bacteria. *Syst. Appl. Microbiol.* **1985**, *6*, 12–17.
- (242) Taylor, M. C.; Jackson, C. J.; Tattersall, D. B.; French, N.; Peat, T. S.; Newman, J.; Briggs, L. J.; Lapalikal, G. V.; Campbell, P. M.; Scott, C.; Russell, R. J.; Oakeshott, J. G. Identification and Characterization of Two Families of F₄₂₀H₂-Dependent Reductases from Mycobacteria That Catalyse Aflatoxin Degradation. *Mol. Microbiol.* **2010**, *78*, 561–575.
- (243) Wang, P.; Bashiri, G.; Gao, X.; Sawaya, M. R.; Tang, Y. Uncovering the Enzymes That Catalyze the Final Steps in Oxytetracycline Biosynthesis. *J. Am. Chem. Soc.* **2013**, *135*, 7138–7141.
- (244) Ebert, S.; Rieger, P.; Knackmuss, H.-J. Function of Coenzyme F₄₂₀ in Aerobic Catabolism of 2,4,6-Trinitrophenol and 2,4-Dinitrophenol by *Nocardioides simplex* FJ2-1A. *J. Bacteriol.* **1999**, *181*, 2669–2674.
- (245) Heiss, G.; Hofmann, K. W.; Trachtmann, N.; Walters, D. M.; Rouvière, P.; Knackmuss, H.-J. Npd Gene Functions of *Rhodococcus (Opacus) erythropolis* HL PM-1 in the Initial Steps of 2,4,6-Trinitrophenol Degradation. *Microbiology* **2002**, *148*, 799–806.
- (246) Jirapanjawan, T.; Ney, B.; Taylor, M. C.; Warden, A. C.; Afroze, S.; Russell, R. J.; Lee, B. M.; Jackson, C. J.; Oakeshott, J. G.; Pandey, G.; Greening, C. The Redox Cofactor F₄₂₀ Protects Mycobacteria from Diverse Antimicrobial Compounds and Mediates a Reductive Detoxification System. *Appl. Environ. Microbiol.* **2016**, *82*, 6818.
- (247) Hasan, M. R.; Rahman, M.; Jaques, S.; Purwantini, E.; Daniels, L. Glucose 6-Phosphate Accumulation in Mycobacteria: Implications for a Novel F₄₂₀-Dependent Anti-Oxidant Defense System. *J. Biol. Chem.* **2010**, *285*, 19135–19144.
- (248) Denny, W. TBA-354 : A New Drug for the Treatment of Persistent Tuberculosis. *Chem. New Zeal.* **2015**, *1*, 18–22.
- (249) Matsumoto, M.; Hashizume, H.; Tomishige, T.; Kawasaki, M.; Tsubouchi, H.; Sasaki, H.; Shimokawa, Y.; Komatsu, M. OPC-67683, a Nitro-Dihydro-Imidazooxazole Derivative with Promising Action against Tuberculosis in Vitro and in Mice. *PLoS Med.* **2006**, *3*, 2131–2144.
- (250) Stover, C.; Warren, P.; VanDevanter, D.; Sherman, D.; Arain, T.; Langhorne, M.; Anderson, S.; Towell, J.; Yuan, Y.; McMurray, D.; Kreiswirth, B.; Barry, C.; Baker, W. A Small-Molecule Nitroimidazopyran Drug Candidate for the Treatment of Tuberculosis. *Nature* **2000**, *405*, 962–966.
- (251) Bashiri, G.; Rehan, A. M.; Sreebhavan, S.; Baker, H.; Baker, E. N.; Squire, C. J. Elongation of the Poly-γ-Glutamate Tail of F₄₂₀ Requires Both Domains of the F₄₂₀-γ-Glutamyl Ligase (FbiB) of *Mycobacterium tuberculosis*. *J. Biol. Chem.* **2016**, *291*, 6882–6894.
- (252) Aufhammer, S. W.; Warkentin, E.; Berk, H.; Shima, S.; Thauer, R. K.; Ermler, U. Coenzyme Binding in F₄₂₀-Dependent Secondary Alcohol Dehydrogenase, a Member of the Bacterial Luciferase Family. *Structure* **2004**, *12*, 361–370.
- (253) Kumar, H.; Nguyen, Q. T.; Binda, C.; Mattevi, A.; Fraaije, M. W. Isolation and Characterization of a Thermostable F₄₂₀:NADPH Oxidoreductase from *Thermobifida fusca*. *J. Biol. Chem.* **2017**, *292*, 10123–10130.
- (254) Nguyen, Q. T.; Trinco, G.; Binda, C.; Mattevi, A.; Fraaije, M. W. Discovery and Characterization of an F₄₂₀-Dependent Glucose-6-Phosphate Dehydrogenase (Rh-FGD1) from *Rhodococcus jostii* RHA1. *Appl. Microbiol. Biotechnol.* **2017**, *101*, 2831–2842.
- (255) Aufhammer, S. W.; Warkentin, E.; Ermler, U.; Hagemeyer, C. H.; Thauer, R. K.; Shima, S. Crystal Structure of Methylene-tetrahydromethanopterin Reductase (Mer) in Complex with Coenzyme F₄₂₀: Architecture of the F₄₂₀/FMN Binding Site of Enzymes within the Nonprolyl Cis-Peptide Containing Bacterial Luciferase Family. *Protein Sci.* **2005**, *14*, 1840–1849.
- (256) Warkentin, E.; Mamat, B.; Sordel-Klippert, M.; Wicke, M.; Thauer, R. K.; Iwata, M.; Iwata, S.; Ermler, U.; Shima, S. Structures of F₄₂₀H₂:NADP⁺ Oxidoreductase with and without Its Substrates Bound. *EMBO J.* **2001**, *20*, 6569.
- (257) Ichikawa, H.; Bashiri, G.; Kelly, W. L. Biosynthesis of the Thiopeptides and Identification of an F₄₂₀H₂-Dependent Dehydropiperidine Reductase. *J. Am. Chem. Soc.* **2018**, *140*, 10749–10756.
- (258) Lapalikal, G. V.; Taylor, M. C.; Warden, A. C.; Scott, C.; Russell, R. J.; Oakeshott, J. G. F₄₂₀H₂-Dependent Degradation of Aflatoxin and Other Furanocoumarins Is Widespread throughout the Actinomycetales. *PLoS One* **2012**, *7*, e30114.
- (259) Mathew, S.; Trajkovic, M.; Kumar, H.; Nguyen, Q. T.; Fraaije, M. W. Enantio- and Regioselective Ene-Reductions Using F₄₂₀H₂-Dependent Enzymes. *Chem. Commun.* **2018**, *54*, 11208–11211.
- (260) de Wit, L. E. A.; Eker, A. P. M. 8-Hydroxy-5-Deazaflavin-Dependent Electron Transfer in the Extreme Halophile *Halobacterium cutirubrum*. *FEMS Microbiol. Lett.* **1987**, *48*, 121–125.
- (261) Dudley Eirich, L.; Dugger, R. S. Purification and Properties of an F₄₂₀-Dependent NADP Reductase from *Methanobacterium thermoautotrophicum*. *Biochim. Biophys. Acta - Gen. Subj.* **1984**, *802*, 454–458.
- (262) Elias, D. A.; Juck, D. F.; Berry, K. A.; Sparling, R. Purification of the NADP⁺: F₄₂₀ Oxidoreductase of *Methanosphaera stadtmanae*. *Can. J. Microbiol.* **2000**, *46*, 998–1003.
- (263) Kunow, J.; Schwörer, B.; Stetter, K. O.; Thauer, R. K. A F₄₂₀-Dependent NADP Reductase in the Extremely Thermophilic Sulfate-Reducing *Archaeoglobus fulgidus*. *Arch. Microbiol.* **1993**, *160*, 199–205.
- (264) Bashiri, G.; Squire, C. J.; Baker, E. N.; Moreland, N. J. Expression, Purification and Crystallization of Native and Selenomethionine Labeled *Mycobacterium tuberculosis* FGD1 (Rv0407) Using a *Mycobacterium smegmatis* Expression System. *Protein Expr. Purif.* **2007**, *54*, 38–44.
- (265) Mascotti, M. L.; Kumar, H.; Nguyen, Q. T.; Ayub, M. J.; Fraaije, M. W. Reconstructing the Evolutionary History of F₄₂₀-Dependent Dehydrogenases. *Sci. Rep.* **2018**, *8*, 17571.
- (266) Purwantini, E.; Daniels, L. Purification of a Novel Coenzyme F₄₂₀-Dependent Glucose-6-Phosphate Dehydrogenase from *Mycobacterium smegmatis*. *J. Bacteriol.* **1996**, *178*, 2861–2866.
- (267) Purwantini, E.; Gillis, T. P.; Daniels, L. Presence of F₄₂₀-Dependent Glucose-6-Phosphate Dehydrogenase in *Mycobacterium* and *Nocardia* Species, but Absence from *Streptomyces* and *Corynebacterium* Species and Methanogenic Archaea. *FEMS Microbiol. Lett.* **1997**, *146*, 129–134.

- (268) Purwantini, E.; Daniels, L. Molecular Analysis of the Gene Encoding F₄₂₀-Dependent Glucose-6-Phosphate Dehydrogenase from *Mycobacterium Smegmatis*. *J. Bacteriol.* **1998**, *180*, 2219.
- (269) Bashiri, G.; Rehan, A. M.; Greenwood, D. R.; Dickson, J. M. J.; Baker, E. N. Metabolic Engineering of Cofactor F₄₂₀ Production in *Mycobacterium Smegmatis*. *PLoS One* **2010**, *5*, e15803.
- (270) Isabelle, D.; Simpson, D. R.; Daniels, L. Large-Scale Production of Coenzyme F₄₂₀-5,6 by Using *Mycobacterium Smegmatis*. *Appl. Environ. Microbiol.* **2002**, *68*, 5750–5755.
- (271) Iamurri, S. M.; Daugherty, A. B.; Edmondson, D. E.; Lutz, S. Truncated FAD Synthetase for Direct Biocatalytic Conversion of Riboflavin and Analogs to Their Corresponding Flavin Mononucleotides. *Protein Eng. Des. Sel.* **2013**, *26*, 791–795.
- (272) Sambrook, J.; Green, M. *Molecular Cloning: A Laboratory Manual*, 4th ed.; Cold Spring Harbor Laboratory Press: Cold Spring Harbor, 2012.
- (273) Herguedas, B.; Lans, I.; Sebastián, M.; Hermoso, J. A.; Martínez-Júlvez, M.; Medina, M. Structural Insights into the Synthesis of FMN in Prokaryotic Organisms. *Acta Crystallogr. D. Biol. Crystallogr.* **2015**, *71*, 2526–2542.
- (274) Le, C. Q.; Oyugi, M.; Joseph, E.; Nguyen, T.; Ullah, M. H.; Aubert, J.; Phan, T.; Tran, J.; Johnson-Winters, K. Effects of Isoleucine 135 Side Chain Length on the Cofactor Donor-Acceptor Distance within F₄₂₀H₂:NADP⁺ Oxidoreductase: A Kinetic Analysis. *Biochem. Biophys. Reports* **2017**, *9*, 120.
- (275) Clark, W. M.; Lowe, H. J. Studies on Oxidation-Reduction. XXIV. Oxidation-Reduction Potentials of Flavin Adenine Dinucleotide. *J. Biol. Chem.* **1956**, *221*, 983–992.
- (276) Draper, R. D.; Ingraham, L. L. A Potentiometric Study of the Flavin Semiquinone Equilibrium. *Arch. Biochem. Biophys.* **1968**, *125*, 802–808.
- (277) Hemmerich, P.; Massey, V. Flavin and 5-Deazaflavin: A Chemical Evaluation of ‘Modified’ Flavoproteins with Respect to the Mechanisms of Redox Biocatalysis. *FEBS Lett.* **1977**, *84*, 5–21.
- (278) Shah, M. V.; Nazem-Bokae, H.; Antoney, J.; Kang, S. W.; Jackson, C. J.; Scott, C. Improved Production of the Non-Native Cofactor F₄₂₀ in *Escherichia Coli*. *Sci. Rep.* **2021**, *11*, 21774.
- (279) Graham, D. E.; Xu, H.; White, R. H. Identification of the 7,8-Didemethyl-8-Hydroxy-5-Deazariboflavin Synthase Required for Coenzyme F₄₂₀ Biosynthesis. *Arch. Microbiol.* **2003**, *180*, 455–464.
- (280) Decamps, L.; Philmus, B.; Benjdia, A.; White, R.; Begley, T. P.; Berteau, O. Biosynthesis of F₄₂₀, Precursor of the F₄₂₀ Cofactor, Requires a Unique Two Radical-SAM Domain Enzyme and Tyrosine as Substrate. *J. Am. Chem. Soc.* **2012**, *134*, 18173–18176.
- (281) Engler, C.; Kandzia, R.; Marillonnet, S. A One Pot, One Step, Precision Cloning Method with High Throughput Capability. *PLoS One* **2008**, *3*.
- (282) Lee, M. E.; DeLoache, W. C.; Cervantes, B.; Dueber, J. E. A Highly Characterized Yeast Toolkit for Modular, Multipart Assembly. *ACS Synth. Biol.* **2015**, *4*, 975–986.
- (283) Volkmer, B.; Heinemann, M. Condition-Dependent Cell Volume and Concentration of *Escherichia Coli* to Facilitate Data Conversion for Systems Biology Modeling. *PLoS One* **2011**, *6*, e23126.
- (284) Myers, J. A.; Curtis, B. S.; Curtis, W. R. Improving Accuracy of Cell and Chromophore Concentration Measurements Using Optical Density. *BMC Biophys.* **2013**, *6*, 4.
- (285) Bauer, S.; Kemter, K.; Bacher, A.; Huber, R.; Fischer, M.; Steinbacher, S. Crystal Structure of *Schizosaccharomyces Pombe* Riboflavin Kinase Reveals a Novel ATP and Riboflavin-Binding Fold. *J. Mol. Biol.* **2003**, *326*, 1463–1473.
- (286) Leman, J. K.; Weitzner, B. D.; Lewis, S. M.; Adolf-Bryfogle, J.; Alam, N.; Alford, R. F.; Aprahamian, M.; Baker, D.; Barlow, K. A.; Barth, P.; Basanta, B.; Bender, B. J.; Blacklock, K.; Bonet, J.; Boyken, S. E.; Bradley, P.; Bystroff, C.; Conway, P.; Cooper, S.; Correia, B. E.; Coventry, B.; Das, R.; De Jong, R. M.; DiMaio, F.; Dsilva, L.; Dunbrack, R.; Ford, A. S.; Frenz, B.; Fu, D. Y.; Geniesse, C.; Goldschmidt, L.; Gowthaman, R.; Gray, J. J.; Gront, D.; Guffy, S.; Horowitz, S.; Huang, P. S.; Huber, T.; Jacobs, T. M.; Jeliakov, J. R.; Johnson, D. K.; Kappel, K.; Karanicolas, J.; Khakzad, H.; Khar, K. R.; Khare, S. D.; Khatib, F.; Khramushin, A.; King, I. C.; Kleffner, R.; Koepnick, B.; Kortemme, T.; Kuenze, G.; Kuhlman, B.; Kuroda, D.; Labonte, J. W.; Lai, J. K.; Lapidath, G.; Leaver-Fay, A.; Lindert, S.; Linsky, T.; London, N.; Lubin, J. H.; Lyskov, S.; Maguire, J.; Malmström, L.; Marcos, E.; Marcu, O.; Marze, N. A.; Meiler, J.; Moretti, R.; Mulligan, V. K.; Nerli, S.; Norn, C.; ÓConchúir, S.; Ollikainen, N.; Ovchinnikov, S.; Pacella, M. S.; Pan, X.; Park, H.; Pavlovicz, R. E.; Pethe, M.; Pierce, B. G.; Pilla, K. B.; Raveh, B.; Renfrew, P. D.; Burman, S. S. R.; Rubenstein, A.; Sauer, M. F.; Scheck, A.; Schief, W.; Schueler-Furman, O.; Sedan, Y.; Sevy, A. M.; Sgourakis, N. G.; Shi, L.; Siegel, J. B.; Silva, D. A.; Smith, S.; Song, Y.; Stein, A.; Szegedy, M.; Teets, F. D.; Thyme, S. B.; Wang, R. Y. R.; Watkins, A.; Zimmerman, L.; Bonneau, R. Macromolecular Modeling and Design in Rosetta: Recent Methods and Frameworks. *Nat. Methods* **2020**, *17*, 665–680.
- (287) Ollikainen, N.; de Jong, R. M.; Kortemme, T. Coupling Protein Side-Chain and Backbone Flexibility Improves the Re-Design of Protein-Ligand Specificity. *PLoS Comput. Biol.* **2015**, *11*, e1004335.
- (288) Gietz, R. D.; Schiestl, R. H. High-Efficiency Yeast Transformation Using the LiAc/SS Carrier DNA/PEG Method. *Nat. Protoc.* **2007**, *2*, 31–34.
- (289) Herguedas, B.; Lans, I.; Sebastián, M.; Hermoso, J. A.; Martínez-Júlvez, M.; Medina, M. Structural Insights into the Synthesis of FMN in Prokaryotic Organisms. *Acta Crystallogr. Sect. D Biol. Crystallogr.* **2015**, *71*, 2526–2542.
- (290) Volkmer, B.; Heinemann, M. Condition-Dependent Cell Volume and Concentration of *Escherichia Coli* to Facilitate Data Conversion for Systems Biology Modeling. *PLoS One* **2011**, *6*, e23126.
- (291) Dezvarei, S.; Lee, J. H. Z.; Bell, S. G. Stereoselective Hydroxylation of Isophorone by Variants of the Cytochromes P450 CYP102A1 and CYP101A1. *Enzyme Microb. Technol.* **2018**, *111*, 29–37.
- (292) Chen, B. S.; Médici, R.; van der Helm, M. P.; van Zwet, Y.; Gjonaj, L.; van der Geest, R.; Otten, L. G.; Hanefeld, U. *Rhodococcus* Strains as Source for Ene-Reductase Activity. *Appl. Microbiol. Biotechnol.* **2018**, *102*, 5545–5556.
- (293) Reihl, P.; Stolz, J. The Monocarboxylate Transporter Homolog Mch5p Catalyzes Riboflavin (Vitamin B₂) Uptake in *Saccharomyces Cerevisiae*. *J. Biol. Chem.* **2005**, *280*, 39809–39817.
- (294) Klis, F. M.; de Koster, C. G.; Brul, S. Cell Wall-Related Bionumbers and Bioestimates of *Saccharomyces Cerevisiae* and *Candida Albicans*. *Eukaryot. Cell* **2014**, *13*, 2–9.
- (295) Kearney, E. B. The Interaction of Yeast Flavokinase with Riboflavin Analogues. *J. Biol. Chem.* **1952**, *194*, 747–754.

- (296) Brewster, R. C.; Sutor, J. T.; Bennett, A. W.; Wallace, S. Transition Metal-Free Reduction of Activated Alkenes Using a Living Microorganism. *Angew. Chemie - Int. Ed.* **2019**, *58*, 12409–12414.
- (297) Miura, K.; Tomioka, Y.; Suzuki, H.; Yonezawa, M.; Hishinuma, T.; Mizugaki, M. Molecular Cloning of the *NemA* Gene Encoding *N*-Ethylmaleimide Reductase from *Escherichia Coli*. *Biol. Pharm. Bull.* **1997**, *20*, 110–112.
- (298) Winkler, C. K.; Tasnádi, G.; Clay, D.; Hall, M.; Faber, K. Asymmetric Bioreduction of Activated Alkenes to Industrially Relevant Optically Active Compounds. *J. Biotechnol.* **2012**, *162*, 381–389.
- (299) Fitzpatrick, T. B.; Amrhein, N.; Macheroux, P. Characterization of YqjM, an Old Yellow Enzyme Homolog from *Bacillus Subtilis* Involved in the Oxidative Stress Response. *J. Biol. Chem.* **2003**, *278*, 19891–19897.
- (300) Parapouli, M.; Vasileiadis, A.; Afendra, A. S.; Hatziloukas, E. *Saccharomyces Cerevisiae* and Its Industrial Applications. *AIMS Microbiol.* **2020**, *6*, 1–31.
- (301) Herbst, E.; Lee, A.; Tang, Y.; Snyder, S. A.; Cornish, V. W. Heterologous Catalysis of the Final Steps of Tetracycline Biosynthesis by *Saccharomyces Cerevisiae*. *ACS Chem. Biol.* **2021**.
- (302) Liu, S.; Hu, W.; Wang, Z.; Chen, T. Production of Riboflavin and Related Cofactors by Biotechnological Processes. *Microb. Cell Fact.* **2020**, *19*, 1–16.
- (303) Schlüpen, C.; Santos, M. A.; Weber, U.; De Graaf, A.; Revuelta, J. L.; Stahmann, K. P. Disruption of the SHM2 Gene, Encoding One of Two Serine Hydroxymethyltransferase Isoenzymes, Reduces the Flux from Glycine to Serine in *Ashbya Gossypii*. *Biochem. J.* **2003**, *369*, 263–273.
- (304) Santos, M. A.; Garcia-Ramirez, J. J.; Revuelta, J. L. Riboflavin Biosynthesis in *Saccharomyces Cerevisiae*. Cloning, Characterization, and Expression of the RIB5 Gene Encoding Riboflavin Synthase. *J. Biol. Chem.* **1995**, *270*, 437–444.
- (305) Gudipati, V.; Koch, K.; Lienhart, W. D.; Macheroux, P. The Flavoproteome of the Yeast *Saccharomyces Cerevisiae*. *Biochim. Biophys. Acta - Proteins Proteomics* **2014**, *1844*, 535–544.
- (306) Hughes, D. L. Biocatalysis in Drug Development - Highlights of the Recent Patent Literature. *Org. Process Res. Dev.* **2018**, *22*, 1063–1080.
- (307) Hecht, K.; Meyer, H.-P.; Wohlgemuth, R.; Buller, R. Biocatalysis in the Swiss Manufacturing Environment. *Catalysts* **2020**, *10*, 1420.
- (308) Buller, R.; Hecht, K.; Mirata, M. A.; Meyer, H. P. CHAPTER 1: An Appreciation of Biocatalysis in the Swiss Manufacturing Environment. In *RSC Catalysis Series*; Royal Society of Chemistry, 2018; Vol. 2018-January, pp 3–43.
- (309) Schomburg, I.; Jeske, L.; Ulbrich, M.; Placzek, S.; Chang, A.; Schomburg, D. The BRENDA Enzyme Information System—From a Database to an Expert System. *J. Biotechnol.* **2017**, *261*, 194–206.
- (310) Sellés Vidal, L.; Kelly, C. L.; Mordaka, P. M.; Heap, J. T. Review of NAD(P)H-Dependent Oxidoreductases: Properties, Engineering and Application. *Biochim. Biophys. Acta - Proteins Proteomics* **2018**, *1866*, 327–347.
- (311) Wu, H.; Tian, C.; Song, X.; Liu, C.; Yang, D.; Jiang, Z. Methods for the Regeneration of Nicotinamide Coenzymes. *Green Chem.* **2013**, *15*, 1773–1789.
- (312) Wu, J. T.; Wu, L. H.; Knight, J. A. Stability of NADPH: Effect of Various Factors on the Kinetics of Degradation. *Clin. Chem.* **1986**, *32*, 314–319.
- (313) Paul, C. E.; Arends, I. W. C. E.; Hollmann, F. Is Simpler Better? Synthetic Nicotinamide Cofactor Analogues for Redox Chemistry. *ACS Catal.* **2014**, *4*, 788–797.
- (314) Norris, D. J.; Stewart, R. Synthesis of a Series of Substituted Pyridinium Ions and Their 1,4-Dihydro Reduction Products and a Determination of Their Stabilities in Aqueous Buffers. *Can. J. Chem.* **1977**, *55*, 1687–1695.
- (315) Knox, R. J.; Jenkins, T. C.; Hobbs, S. M.; Chen, S.; Melton, R. G.; Burke, P. J. Bioactivation of 5-(Aziridin-1-yl)-2,4-Dinitrobenzamide (CB 1954) by Human NAD(P)H Quinone Oxidoreductase 2: A Novel Co-Substrate-Mediated Antitumor Prodrug Therapy. *Cancer Res.* **2000**, *60*, 4179–4186.
- (316) Paul, C. E.; Hollmann, F. A Survey of Synthetic Nicotinamide Cofactors in Enzymatic Processes. *Appl. Microbiol. Biotechnol.* **2016**, *100*, 4773–4778.
- (317) Friedlos, F.; Jarman, M.; Davies, L. C.; Boland, M. P.; Knox, R. J. Identification of Novel Reduced Pyridinium Derivatives as Synthetic Co-Factors for the Enzyme DT Diaphorase (NAD(P)H Dehydrogenase (Quinone), EC 1.6.99.2). *Biochem. Pharmacol.* **1992**, *44*, 25–31.
- (318) Knox, R. J.; Friedlos, F.; Jarman, M.; Davies, L. C.; Goddard, P.; Anlezark, G. M.; Melton, R. G.; Sherwood, R. F. Virtual Cofactors for an *Escherichia Coli* Nitroreductase Enzyme: Relevance to Reductively Activated Prodrugs in Antibody Directed Enzyme Prodrug Therapy (ADEPT). *Biochem. Pharmacol.* **1995**, *49*, 1641–1647.
- (319) Ryan, J. D.; Fish, R. H.; Clark, D. S. Engineering Cytochrome P450 Enzymes for Improved Activity towards Biomimetic 1,4-NADH Cofactors. *ChemBioChem* **2008**, *9*, 2579–2582.
- (320) Lutz, J.; Hollmann, F.; Ho, T. V.; Schnyder, A.; Fish, R. H.; Schmid, A. Bioorganometallic Chemistry: Biocatalytic Oxidation Reactions with Biomimetic NAD⁺/NADH Co-Factors and [Cp^{*}Rh(Bpy)H]⁺ for Selective Organic Synthesis. *J. Organomet. Chem.* **2004**, *689*, 4783–4790.
- (321) Guarneri, A.; Westphal, A. H.; Leertouwer, J.; Lunsonga, J.; Franssen, M. C. R.; Opperman, D. J.; Hollmann, F.; van Berkel, W. J. H.; Paul, C. E. Flavoenzyme-Mediated Regioselective Aromatic Hydroxylation with Coenzyme Biomimetics. *ChemCatChem* **2020**, *12*, 1368–1375.
- (322) Qi, J.; Paul, C. E.; Hollmann, F.; Tischler, D. Changing the Electron Donor Improves Azoreductase Dye Degrading Activity at Neutral PH. *Enzyme Microb. Technol.* **2017**, *100*, 17–19.
- (323) Paul, C. E.; Gargiulo, S.; Opperman, D. J.; Lavandera, I.; Gotor-Fernández, V.; Gotor, V.; Taglieber, A.; Arends, I. W. C. E.; Hollmann, F. Mimicking Nature: Synthetic Nicotinamide Cofactors for C=C Bioreduction Using Enoate Reductases. *Org. Lett.* **2013**, *15*, 180–183.
- (324) Knaus, T.; Paul, C. E.; Levy, C. W.; De Vries, S.; Mutti, F. G.; Hollmann, F.; Scrutton, N. S. Better than Nature: Nicotinamide Biomimetics That Outperform Natural Coenzymes. *J. Am. Chem. Soc.* **2016**, *138*, 1033–1039.
- (325) Löw, S. A.; Löw, I. M.; Weissenborn, M. J.; Hauer, B. Enhanced Ene-Reductase Activity through Alteration of Artificial Nicotinamide Cofactor Substituents. *ChemCatChem* **2016**, *8*, 911–915.

- (326) Riedel, A.; Mehnert, M.; Paul, C. E.; Westphal, A. H.; van Berkel, W. J. H.; Tischler, D. Functional Characterization and Stability Improvement of a 'Thermophilic-like' Ene-Reductase from *Rhodococcus Opacus* 1CP. *Front. Microbiol.* **2015**, *6*, 1073.
- (327) Geddes, A.; Paul, C. E.; Hay, S.; Hollmann, F.; Scrutton, N. S. Donor-Acceptor Distance Sampling Enhances the Performance of "Better than Nature" Nicotinamide Coenzyme Biomimetics. *J. Am. Chem. Soc.* **2016**, *138*, 11089–11092.
- (328) Lo, H. C.; Fish, R. H. Biomimetic NAD⁺ Models for Tandem Cofactor Regeneration, Horse Liver Alcohol Dehydrogenase Recognition of 1,4-NADH Derivatives, and Chiral Synthesis. *Angew. Chemie Int. Ed.* **2002**, *41*, 478–481.
- (329) Fish, R. H. 1,4-NADH Biomimetic Co-Factors with Horse Liver Alcohol Dehydrogenase (HLADH), Utilizing [Cp^{*}Rh(Bpy)H](OTf) for Co-Factor Regeneration, Do in Fact, Produce Chiral Alcohols from Reactions with Achiral Ketones. *Catalysts* **2019**, *9*, 562.
- (330) Josa-Culleré, L.; Lahdenperä, A.; Ribaucourt, A.; Höfler, G.; Gargiulo, S.; Liu, Y.-Y.; Xu, J.-H.; Cassidy, J.; Paradisi, F.; Opperman, D.; Hollmann, F.; Paul, C. Synthetic Biomimetic Coenzymes and Alcohol Dehydrogenases for Asymmetric Catalysis. *Catalysts* **2019**, *9*, 207.
- (331) Nowak, C.; Beer, B.; Pick, A.; Roth, T.; Lommès, P.; Sieber, V. A Water-Forming NADH Oxidase from *Lactobacillus Pentosus* Suitable for the Regeneration of Synthetic Biomimetic Cofactors. *Front. Microbiol.* **2015**, *6*, 957.
- (332) Jia, H. Y.; Zong, M. H.; Zheng, G. W.; Li, N. Myoglobin-Catalyzed Efficient in Situ Regeneration of NAD(P)⁺ and Their Synthetic Biomimetic for Dehydrogenase-Mediated Oxidations. *ACS Catal.* **2019**, *9*, 2196–2202.
- (333) Lo, H. C.; Leiva, C.; Buriez, O.; Kerr, J. B.; Olmstead, M. M.; Fish, R. H. Bioorganometallic Chemistry. 13. Regioselective Reduction of NAD⁺ Models, 1-Benzylnicotinamide Triflate and b-Nicotinamide Ribose-5'-Methyl Phosphate, with in Situ Generated [Cp^{*}Rh(Bpy)H]⁺: Structure-Activity Relationships, Kinetics, and Mechanistic Aspects in the Formation of the 1,4-NADH Derivatives. *Inorg. Chem.* **2001**, *40*, 6705–6716.
- (334) Knaus, T.; Paul, C. E.; Levy, C. W.; De Vries, S.; Mutti, F. G.; Hollmann, F.; Scrutton, N. S. Better than Nature: Nicotinamide Biomimetics That Outperform Natural Coenzymes. *JACS* **2016**, *138*, 1033–1039.
- (335) Hildebrand, F.; Lütz, S. Stable Electroenzymatic Processes by Catalyst Separation. *Chem. - A Eur. J.* **2009**, *15*, 4998–5001.
- (336) Kim, J.; Lee, S. H.; Tieves, F.; Choi, D. S.; Hollmann, F.; Paul, C. E.; Park, C. B. Biocatalytic C=C Bond Reduction through Carbon Nanodot-Sensitized Regeneration of NADH Analogues. *Angew. Chemie - Int. Ed.* **2018**, *57*, 13825–13828.
- (337) Okamoto, Y.; Köhler, V.; Paul, C. E.; Hollmann, F.; Ward, T. R. Efficient in Situ Regeneration of NADH Mimics by an Artificial Metalloenzyme. *ACS Catal.* **2016**, *6*, 3553–3557.
- (338) Nowak, C.; pick, A.; Lommès, P.; Sieber, V. Enzymatic Reduction of Nicotinamide Biomimetic Cofactors Using an Engineered Glucose Dehydrogenase: Providing a Regeneration System for Artificial Cofactors. *ACS Catal.* **2017**, *17*, 5202–5208.
- (339) Huang, R.; Chen, H.; Upp, D. M.; Lewis, J. C.; Zhang, Y.-H. P. J. A High-Throughput Method for Directed Evolution of NAD(P)⁺-Dependent Dehydrogenases for the Reduction of Biomimetic Nicotinamide Analogues. *ACS Catal.* **2019**, *9*, 11709–11719.
- (340) Opperman, D. J.; Sewell, B. T.; Litthauer, D.; Isupov, M. N.; Littlechild, J. A.; van Heerden, E. Crystal Structure of a Thermostable Old Yellow Enzyme from *Thermus Scotoductus* SA-01. *Biochem. Biophys. Res. Commun.* **2010**, *393*, 426–431.
- (341) Schauer, N. L.; Ferry, J. G.; Honek, J. F.; Orme-Johnson, W. H.; Walsh, C. Mechanistic Studies of the Coenzyme F₄₂₀ Reducing Formate Dehydrogenase from *Methanobacterium Formicicum*. *Biochemistry* **1986**, *25*, 7163–7168.
- (342) Thauer, R. K.; Kaster, A. K.; Goenrich, M.; Schick, M.; Hiromoto, T.; Shima, S. Hydrogenases from Methanogenic Archaea, Nickel, a Novel Cofactor, and H₂ Storage. *Annu. Rev. Biochem.* **2010**, *79*, 507–536.
- (343) Martin, C.; Tjallinks, G.; Trajkovic, M.; Fraaije, M. Facile Stereoselective Reduction of Prochiral Ketones by Using an F₄₂₀-Dependent Alcohol Dehydrogenase. *ChemBioChem* **2021**, *22*, 156–159.
- (344) Hecht, K.; Buller, R. Ene-Reductases in Pharmaceutical Chemistry. In *Pharmaceutical Biocatalysis*; Grunwald, P., Ed.; Jenny Stanford Publishing: New York, 2019; pp 311–347.
- (345) Saudan, L. A. Hydrogenation Processes in the Synthesis of Perfumery Ingredients. *Acc. Chem. Res.* **2007**, *40*, 1309–1319.
- (346) Kumar Roy, T.; Sreedharan, R.; Ghosh, P.; Gandhi, T.; Maiti, D. Ene-Reductase: A Multifaceted Biocatalyst in Organic Synthesis. *Chem. - A Eur. J.* **2022**, *28*, e202103949.
- (347) Massey, V.; Schopfer, L. M. Reactivity of Old Yellow Enzyme with α -NADPH and Other Pyridine Nucleotide Derivatives. *J. Biol. Chem.* **1986**, *261*, 1215–1222.
- (348) Brown, B. J.; Hyun, J. W.; Duvvuri, S.; Andrew Karplus, P.; Massey, V. The Role of Glutamine 114 in Old Yellow Enzyme. *J. Biol. Chem.* **2002**, *277*, 2138–2145.
- (349) Xu, D.; Kohli, R. M.; Massey, V. The Role of Threonine 37 in Flavin Reactivity of the Old Yellow Enzyme. *Proc. Natl. Acad. Sci. U. S. A.* **1999**, *96*, 3556–3561.
- (350) Karplus, P. A.; Fox, K. M.; Massey, V. Structure-Function Relations for Old Yellow Enzyme. *FASEB J.* **1995**, *9*, 1518–1526.
- (351) Kohli, R. M.; Massey, V. The Oxidative Half-Reaction of Old Yellow Enzyme: The Role of Tyrosine 196. *J. Biol. Chem.* **1998**, *273*, 32763–32770.
- (352) Abramovitz, A. S.; Massey, V. Interaction of Phenols with Old Yellow Enzyme. Physical Evidence for Charge-Transfer Complexes. *J. Biol. Chem.* **1976**, *251*, 5327–5336.
- (353) Brown, B. J.; Deng, Z.; Karplus, P. A.; Massey, V. On the Active Site of Old Yellow Enzyme: Role of Histidine 191 and Asparagine 194. *J. Biol. Chem.* **1998**, *273*, 32753–32762.
- (354) Kawai, Y.; Hayashi, M.; Inaba, Y.; Saitou, K.; Ohno, A. Asymmetric Reduction of α,β -Unsaturated Ketones with a Carbon-Carbon Double-Bond Reductase from Baker's Yeast. *Tetrahedron Lett.* **1998**, *39*, 5225–5228.
- (355) Koul, S.; Crout, D. H. G.; Errington, W.; Tax, J. Biotransformation of $\alpha\beta$ -Unsaturated Carbonyl Compounds: Sulfides, Sulfoxides, Sulfones, Nitriles and Esters by Yeast Species: Carbonyl Group and Carbon-Carbon Double Bond Reduction. *J. Chem. Soc. Perkin Trans. 1* **1995**, No. 23, 2969–2988.

- (356) Tasnádi, G.; Winkler, C. K.; Clay, D.; Sultana, N.; Fabian, W. M. F.; Hall, M.; Ditrich, K.; Faber, K. A Substrate-Driven Approach to Determine Reactivities of α,β -Unsaturated Carboxylic Esters Towards Asymmetric Bioreduction. *Chem. – A Eur. J.* **2012**, *18*, 10362–10367.
- (357) Hall, M. Enzymatic Strategies for Asymmetric Synthesis. *RSC Chem. Biol.* **2021**, *2*, 958–989.
- (358) Vaz, A. D. N.; Chakraborty, S.; Massey, V. Old Yellow Enzyme: Aromatization of Cyclic Enones and the Mechanism of A Novel Dismutation Reaction. *Biochemistry* **1995**, *34*, 4246–4256.
- (359) Garzón-Posse, F.; Becerra-Figueroa, L.; Hernández-Arias, J.; Gamba-Sánchez, D. Whole Cells as Biocatalysts in Organic Transformations. *Molecules* **2018**, *23*, 1265.
- (360) Oroz-Guinea, I.; Winkler, C. K.; Glueck, S. M.; Ditrich, K.; Weingarten, M.; Breuer, M.; Schachtschabel, D.; Kroutil, W. Ene-Reductase Catalyzed Regio- and Stereoselective 1,4-Mono-Reduction of Pseudoionone to Geranylacetone. *ChemCatChem* **2022**, *14*, e202101557.
- (361) Stewart, R. C.; Massey, V. Potentiometric Studies of Native and Flavin-Substituted Old Yellow Enzyme*. *J. Biol. Chem.* **1985**, *260*, 13639–13647.
- (362) Prabhulkar, S.; Tian, H.; Wang, X.; Zhu, J. J.; Li, C. Z. Engineered Proteins: Redox Properties and Their Applications. *Antioxid. Redox Signal.* **2012**, *17*, 1822.
- (363) Lee, M.; Drenth, J.; Trajkovic, M.; de Jong, R. M.; Fraaije, M. W. Introducing an Artificial Deazaflavin Cofactor in *Escherichia Coli* and *Saccharomyces Cerevisiae*. *ACS Synth. Biol.* **2022**, *11*, 938–952.
- (364) Woo Park, J.; Hoe Yun, S.; Koh Park, K. Interaction of Metal Ions with NADH Model Compounds. Cupric Ion Oxidation of Dihyronicotinamides. *Bull. Korean Chem. Soc.* **1988**, *9*, 298–303.
- (365) Lin, X. L.; White, R. H. Occurrence of Coenzyme F_{420} and Its γ -Monoglutamyl Derivative in Nonmethanogenic Archaeobacteria. *J. Bacteriol.* **1986**, *168*, 444–448.
- (366) Mascotti, M. L.; Juri Ayub, M.; Fraaije, M. W. On the Diversity of F_{420} -Dependent Oxidoreductases: A Sequence- and Structure-Based Classification. *Proteins Struct. Funct. Bioinforma.* **2021**, *89*, 1497–1507.
- (367) Kim, J.; Lee, S. H.; Tieves, F.; Choi, D. S.; Hollmann, F.; Paul, C. E.; Park, C. B. Biocatalytic C=C Bond Reduction through Carbon Nanodot-Sensitized Regeneration of NADH Analogues. *Angew. Chemie Int. Ed.* **2018**, *57*, 13825–13828.
- (368) Zachos, I.; Nowak, C.; Sieber, V. Biomimetic Cofactors and Methods for Their Recycling. *Curr. Opin. Chem. Biol.* **2019**, *49*, 59–66.
- (369) Last, D.; Hasan, M.; Rothenburger, L.; Braga, D.; Lackner, G. High-Yield Production of Coenzyme F_{420} in *Escherichia Coli* by Fluorescence-Based Screening of Multi-Dimensional Gene Expression Space. *Metab. Eng.* **2022**, *73*, 158–167.
- (370) Bashiri, G. Cofactor F_{420} , an Emerging Redox Power in Biosynthesis of Secondary Metabolites. *Biochem. Soc. Trans.* **2022**, *50*, 253–267.

Nederlandse samenvatting

In dit werk beschrijven we de design en (bio)synthese van een nieuwe, artificiële cofactor die structureel gelijkend is aan de natuurlijke cofactoren F_{420} en flavine mononucleotide (FMN) en de chemie van F_{420} nabootst. Deze nieuwe cofactor heeft als doel om het toepassen van F_{420} -afhankelijke enzymen voor biokatalytische doeleinden te bevorderen en om nieuwe functionaliteiten te creëren voor FMN-afhankelijke enzymen.

F_{420} is een cofactor die voorkomt in veel micro-organismen, van archaea tot actinobacteriën en zelfs sommige proteobacteriën (niet in *Escherichia coli*). Hierin vervult het hele verschillende fysiologische rollen.^{25–27,210} In methanogene en methanotrofe archaea heeft dit co-enzym een essentiële rol in het centrale C_1 -metabolisme. En in actinobacteriën wordt het juist gebruikt voor de synthese van secundaire metabolieten en voor de detoxificatie van xenobiotica.^{25,26,219,221,223,224,241,246,301,365} Al deze organismen zijn vrij moeilijk te kweken, waardoor extractie van F_{420} lastig is en resulteert in lage opbrengsten. Ook is de synthese van deze cofactor moeilijk door haar omvangrijke, heterogene structuur en dit resulteert dus ook in hele lage opbrengsten.²⁹

Door de lage beschikbaarheid van deze cofactor zijn biokatalytische toepassingen op grote schaal niet mogelijk, ook al laten recente publicaties zien dat F_{420} -afhankelijke enzymen juist wel hele interessante reacties katalyseren met biotechnologisch relevantie. Twee recente studies hebben zelfs al laten zien dat deze cofactor kan worden gebruikt voor biocatalyse op labschaal, namelijk voor de enantiospecifieke reductie van ketonen en geactiveerde alkenen.^{27,56,259,343} Vooral de extreem lage redoxpotentiaal van -340 tot wel -380 mV maakt het een interessante reductor voor stoffen die relatief inert zijn voor andere redoxcofactoren, zoals flavines en nicotinamides. Ook is de ongevoeligheid voor moleculair zuurstof een handige eigenschap in bepaalde biokatalytische toepassingen.^{21,22}

Om F_{420} -afhankelijke enzymen juist ook op grote schaal toe te kunnen passen, hebben we een artificiële cofactor ontwikkeld die op grotere schaal geproduceerd kan worden en even goed functioneert als redoxcofactor (**Hoofdstuk 3**). Als startpunt voor de design hebben we FO gebruikt. Dit is de natuurlijke, biosynthetische precursor van F_{420} en bevat de 7,8-didemethyl-8-hydroxy-5-deazaisoalloxazine katalytische kern van de cofactor (zie **Figuur 1.1**). Eerder onderzoek heeft laten zien dat chemisch actief FO relatief makkelijk te synthetiseren is, maar dat deze stof een lage affiniteit heeft voor F_{420} -afhankelijke enzymen.^{31,32} Ander onderzoek van Ney et al. heeft inderdaad

laten zien dat de lange, polaire 5'-phospho-L-lactyl- γ -L-glutamyl 'staart' – die aan FO wordt gezet om F_{420} te genereren – inderdaad belangrijk is voor de binding aan eiwitten.²¹³ Deze staart is veelal twee glutamylresiduen lang in archaea en kan tot 9 residuen lang zijn in actinobacteriën en proteobacteriën, maar is in deze organismen vaak tussen de drie en acht residuen lang. Dezelfde studie heeft ook laten zien dat het aantal glutamylresiduen invloed heeft op enzymactiviteit, waarbij kleinere staarten in een iets hogere k_{cat} resulteren en tegelijkertijd ook een iets hogere K_m hebben.²¹³ Hieruit blijkt dat een polaire/geladen staart op de 5'-positie essentieel is voor de binding aan enzymen, maar dat de lengte van deze staart niet van hele grote invloed is. Daarom hebben wij besloten om FO te decoreren met een kleinere polaire groep dan F_{420} op de 5'-positie, voor eenvoudige en schaalbare synthese.

Geïnspireerd door de biosynthese van flavine mononucleotide (FMN; zie **Figuur 1.1**) hebben wij FO-5'-fosfaat, kortweg FOP bedacht. Riboflavine, de precursor van FMN lijkt namelijk sterk op FO. Tevens blijken een aantal F_{420} -afhankelijke enzymen evolutionair af te stammen van FMN-afhankelijke enzymen, waardoor een FMN gelijkende cofactor mogelijk ook effectief kan binden aan deze enzymen.^{265,366}

Door de structurele overeenkomsten tussen FO en riboflavine verwachtten wij dat riboflavine kinase – het enzym dat FMN synthetiseert uit riboflavine door 5'-fosforylering vanuit ATP – ook zou werken op chemisch gesynthetiseerd FO.²⁷³ De goed gekarakteriseerde riboflavine kinase uit *Corynebacterium ammoniagenes* (CaRFK) werd geselecteerd voor FO fosforylering, maar dit enzym had helaas geen detecteerbare activiteit met FO als substraat.²⁷¹ Meerdere rondes van structuur-geïnspireerde positie-specifieke mutagenese werden uitgevoerd om de kinase actief te laten zijn op het nieuwe substraat FO. De apolaire residuen in de riboflavine bindingsplaats, rond de C8-positie van de isoalloxazine, werden vervangen door polaire residuen, waardoor de 8-hydroxylgroep van FO beter kan worden geacommodeerd. De mutagenese-studie resulteerde in een aantal FOP producerende varianten. De beste variant, de drievoudige mutant F21H/F85H/A66I, is in staat om 80% van de FO om te zetten in FOP binnen 12 uur en kan 1 mg (2.5 μ mol) FOP produceren in 50 mL reactievolume, dat vertaalt naar een FOP productie van 50 μ mol/L. Dit is hoger dan de F_{420} opbrengst door extractie uit *Mycobacterium smegmatis* – de beste F_{420} productiestam – welke maar 1.4 μ mol/L culture is.^{269,270}

Na de succesvolle chemo-enzymatische synthese van FOP hebben we dit artificiële co-enzym getest op verschillende F_{420} -afhankelijke enzymen uit verschillende structurele classes. De suiker-6-fosfaatdehydrogenase uit *Cryptosporangium arvum* (FSD-*Cryar*), de F_{420} :NADPH oxidoreductase uit *Thermobifida fusca* (Tfu-FNO) en de

F_{420} -afhankelijke reductase uit *Mycobacterium hassiacum* (FDR-*Mha*) lieten allemaal detecteerbare activiteit zien met de nieuwe cofactor. Hoewel de specifieke activiteiten met FOP lager waren dan met de natuurlijke cofactor F_{420} , waren deze maar 2.0, 12.6, en 22.4 keer lager voor respectievelijk TfuFNO, FSD-*Cryar*, and FDR-*Mha*. Hiermee konden we dus aantonen dat FOP inderdaad een serieus en schaalbaar alternatief is voor F_{420} , zoals in meer detail besproken wordt in **Hoofdstuk 3**.

De chemo-enzymatische synthese van FOP is nog steeds suboptimaal, omdat het grote hoeveelheden relatief dure ATP nodig heeft en omdat grote opbrengsten worden verhinderd door de lage oplosbaarheid van de precursor FO in water. Ook is CaRFK redelijk instabiel, wat resulteert in een kleine hoeveelheid totale omzettingen. Om deze problemen te verhelpen hebben we een biosynthetische route ontwikkeld in *Escherichia coli*. Dit is het onderwerp van **Hoofdstuk 4**. De combinatie van een FO synthase en riboflavine kinase stelde ons in staat om FOP te synthetiseren *in vivo* uit metaboliëten die voorkomen in *E. coli*. De FOP productie werd geoptimaliseerd door het variëren van groeiomstandigheden, expressievectoren en combinaties van enzymen uit verschillende organismen, al dan niet geëngineerd. Deze combinatie van enzymengineering en optimalisatie van het expressiesysteem resulteerde in een productiesnelheid van 0.078 μ mol L⁻¹ h⁻¹. De totale opbrengst is soortgelijk aan die van F_{420} in *Mycobacterium smegmatis*, maar de productiesnelheid van FOP in *E. coli* is veel hoger. De intracellulaire FOP-concentratie van ongeveer 40 μ M zou bovendien hoog genoeg moeten zijn om F_{420} -afhankelijke enzymen te faciliteren *in vivo*. We konden inderdaad demonstreren dat er een toename in ketoisophorone reductie was in cellen waarin zowel een F_{420} -afhankelijke reductase als een F_{420} -afhankelijke suiker-6-fosfaat dehydrogenase tot expressie werden gebracht, samen met de FOP productie constructen.

Omdat deazaflavine-afhankelijke conversies in levende cellen zouden kunnen leiden tot de milieu vriendelijke en veilige productie van fijnchemicaliën, hebben we ook geprobeerd om de FOP biosynthesemachinerie in bakker's gist, *Saccharomyces cerevisiae*, te zetten. Dit organisme wordt namelijk al veel gebruikt voor de productie van verschillende stoffen op industriële schaal en is tevens veilig voor gebruik in producten voor menselijke consumptie. Anders dan de *de novo* biosynthese van FOP in *E. coli* hebben we in gist juist gebruik gemaakt van een semi-synthetische benadering. Heterologe expressie van de riboflavine kinase uit *Schizosaccharomyces pombe* (SpRFK) stelde ons in staat om *in vivo* chemisch gesynthetiseerd FO te fosforyleren, welke werd toegediend aan het groeimedium. De FOP productie in *S. cerevisiae* werd verder geoptimaliseerd door mediumoptimalisatie en enzymengineering. Zowel structuur-geïnspireerde positie-specifieke mutagenese als computer gefaciliteerde mutagenese werden toegepast op SpRFK, waardoor er een variant ontstond die

een zevenvoudige toename in katalytische efficiëntie liet zien. Door deze variant toe te passen in combinatie met geoptimaliseerde groeiomstandigheden werd de lage initiële FOP productie in gist van 0.24 nmol per gram droge biomassa 20 keer verhoogd. De resultaten van **Hoofdstuk 4** laten zien dat zowel prokaryote als eukaryote laboratoriumstammen gebruikt kunnen worden om deze artificiële deazaflavine cofactor te produceren. Deze FOP producerende stammen zouden in de toekomst gebruikt kunnen worden voor zowel de productie van FOP, evenals de FOP-gemedieerde biosynthese van fijnchemicaliën in levende cellen.

Onze bevindingen uit **Hoofdstuk 3** laten zien dat FOP succesvol gebruikt kan worden als cofactor voor verschillende F_{420} -afhankelijke enzymen. In **Hoofdstuk 5** gebruiken we deze kennis om met FOP en F_{420} verschillende artificiële biomimetische nicotinamide cofactoren (nicotinamide cofactor biomimetics; NCB's) te reduceren. Uit onderzoek blijkt dat NCB's stabiel, goedkoper en gemakkelijker te synthetiseren zijn dan hun natuurlijke tegenhangers nicotinamide adenine dinucleotide (NAD) en de 2'-gefosforyleerde vorm NADP. Sommige studies hebben zelfs bewezen dat enkele NCB's beter werken als cofactor dan NAD(P)H voor reductasen uit de Old Yellow Enzyme familie (OYE),^{313,316,317,324,367,368} Hoewel deze artificiële hydridecarriers ideaal lijken voor biocatalytische reducties, hebben ze één groot nadeel: er bestaan nog geen efficiënte cofactorrecyclingsystemen. Dit komt mede door hun lage redoxpotentiaal. Wij hebben de thermostabiele F_{420} : NADPH oxidoreductase uit *Thermobifida fusca* (*Tfu*-FNO) aangepast met structuur-geïnspireerde positie-specifieke mutagenese om de onnatuurlijke N1-substituenten van acht NCB's te kunnen accommoderen, waardoor de uitzonderlijk lage redoxpotentiaal van F_{420} en Fop gebruikt kon worden voor de recycling van deze stoffen. Wildtype *Tfu*-FNO had al detecteerbare activiteit met de geselecteerde NCB's, maar met hoge K_m -waarden in het millimolair bereik en lage k_{cat} -waarden niet hoger dan 1.4 min⁻¹. Saturatie mutagenese op posities Gly-29 en Pro-89 resulteerde in mutanten met tot 139 keer hogere katalytische efficiënties. Mutant G29W had een opmerkelijk hoge k_{cat} van 4.2 s⁻¹ voor 1-benzyl-3-acetylpyridine (BAP⁺), welke overeenkomt met de k_{cat} -waarde voor het natuurlijke co-enzym NADP⁺. De best presterende *Tfu*-FNO varianten werden gebruikt voor conversie-experimenten waarbij katalytische hoeveelheden van de NCB's en van FOP/ F_{420} werden gebruikt in combinatie met de thermostabiele alkeenreductase uit *Thermus scotoductus* (TsOYE) om ketoisophorone te reduceren. Na 16 uur kon 10 mM ketoisophorone volledig gereduceerd worden met BAP⁺ als cofactor. Deze set van thermostabiele NCB-afhankelijke *Tfu*-FNO varianten zijn krachtige cofactorregeneratiesystemen voor de reductie van verschillende artificiële nicotinamide cofactoren op zowel kamertemperatuur als hoge temperaturen. En, voor zover bij ons bekend, zijn dit de best presterende recyclingsystemen voor BNAH en BAPH tot nu toe.

Omdat FOP sterk lijkt op FMN, zie **Figuur 1.1**, zagen we de mogelijkheid om ook FMN te vervangen door FOP als prothetische groep in FMN-afhankelijke enzymen. De lagere redoxpotentiaal van FOP zou FMN-afhankelijke enzymen in staat kunnen stellen om stoffen te reduceren die inert zijn voor FMN-afhankelijke reductie. Wij hebben deze hypothese getest in **hoofdstuk 6** door FMN te verwisselen met FOP in OYE1, een alkeenreductase uit *Saccharomyces pastorianus*. Net als met andere FMN-analogen, zoals aangetoond in eerdere onderzoeken, kon ook FOP succesvol worden geïntroduceerd als prothetische groep in OYE1.³⁶¹ Daarna hebben we de activiteit van OYE1-FOP getest op een aantal cinnamylverbindingen met verschillende elektronenonttrekkende groepen (EWG's) met verschillende sterktes. Hieruit bleek dat de introductie van FOP resulteerde in activiteit met kaneelzuur, een stof die normaalgesproken niet kan worden gereduceerd met OYE1, door de aanwezigheid van een carboxylgroep als zwakke EWG. Alhoewel er nog veel onderzoek moet worden gedaan naar OYE1-FOP, legt dit wel de basis voor verder onderzoek en toekomstig gebruik van FOP-gereconstitueerde reductasen.

Dit proefschrift laat zien dat FOP een goed alternatief is voor F_{420} , met een relatief simpele, schaalbare (bio)synthese en biochemische eigenschappen die sterk lijken op de originele, natuurlijke cofactor. We hebben ook kunnen laten zien dat FOP gebruikt kan worden om FMN te vervangen als cofactor, waarbij de lage redoxpotentiaal en ongevoeligheid voor moleculair zuurstof leiden tot nieuwe enzymactiviteit. De biosynthese van FOP, evenals dat van F_{420} in *E. coli* – zoals recentelijk bewerkstelligd door andere onderzoeksgroepen,^{239,240,369} kunnen een boost geven aan het gebruik van F_{420} -afhankelijke enzymen in biokatalyse en biosynthese. Bovendien zullen de flinke groei in (meta)gnomische data, betere sequencing technieken en krachtigere bio-informaticatools ervoor zorgen dat er meer F_{420} -afhankelijke enzymen ontdekt gaan worden. Deze nieuwe F_{420} -afhankelijke enzymen kunnen de toolbox van bestaande enzymen complementeren en kunnen daardoor leiden tot nieuwe biokatalytische routes.^{19,25,27,56,370} FOP kan ook specifiek worden toegepast als prothetische groep in FMN-afhankelijke enzymen, waardoor nieuwe functionaliteiten ontstaan met minimale engineering. Zoals in dit proefschrift wordt beschreven, als ook door andere studies, kan cofactorengineering leiden tot verrassende nieuwe activiteiten^{183,185-187,361} en kan dit de katalytische kracht van bepaalde enzymen versterken.^{176,177,324}

Acknowledgements

First of all I would like to thank my promotors. Marco, ik ben enorm dankbaar voor het krijgen van een aanstelling bij jou in de onderzoeksgroep én voor alle vrijheid die je mij hebt gegeven tijdens mij promotietraject. Ik heb tijdens mijn PhD en mijn studie jaren enorm veel van je geleerd en heb vooral ook genoten van onze ‘brainstormsessies’ die spontaan ontstonden op willekeurige momenten als je even over het lab liep. Jouw input, kritische blik en management skills waren ook essentieel voor de afronding van dit project. Je wist me op de juiste momenten te motiveren en te laten focussen, want ik was inderdaad vaak best koppig en verstrooid. Al met al had het eindresultaat slechter kunnen zijn!

Dick, bedankt voor de mogelijkheden om mijn bachelor- én masterproject bij jou te doen. In deze tijd heb ik enorm veel van je kunnen leren. Ook heb je bijgedragen aan mijn PhD onderzoek met jouw waardevolle input en kritische vragen tijdens werkbesprekingen. Enorm bedankt voor de mogelijkheid om leservaring op te doen tijdens jouw vakken! Want ik heb veel geleerd van het lesgeven. Het doet me deugd dat je me genoeg vertrouwdde om mij ook de hoorcollege te laten verzorgen en de toetsen te laten maken. Al moest ik soms dan wel even op het ‘strafbankje’ zitten als je weer een foutje had ontdekt in de toets of de uitwerkingen.

I would also like to thank the reading and defense committees for finding time in your busy schedules to read my thesis and for all of your constructive and helpful feedback.

A PhD defense is nothing without a great pair of Paranympths. Elvira and Gertie, I can't overstate my gratitude. Elvira, you are one of the most genuine and unique people I've met in my life. I've also never met someone who can complain and freak out as much as you! Our daily walks to the coffee machine, during which we'd complain (you more so than me...) about our PhDs and other things in life, were one of the highlights of my lab days. We had loads of fun together during our PhD years, and I hope we can continue our friendship. On top of that, I also enjoyed the scientific discussions we had – you are one smart cookie! Gelato, gelato, gelato! Gertie, mijn *allerliebste*. Je bent een geweldig persoon en ik ben zo blij dat ik jou mijn bestie mag noemen. De connectie die wij hebben is uniek. Ik voel me vereerd dat jij ook een van mijn paranympthen wilt zijn. Hierdoor wordt mijn promotiedag een stuk *løker* en makkelijker. Bedankt voor álles!

Over the past few years, I have been very lucky to be part of such an amazing crew of people who made PhD life very enjoyable. To those who have become dear friends of

mine, Estela, Gautier, Nikolas, Yapei, Antonija, Eduardo and Elvira, you made it fun to come to the lab every day. We joked around, laughed, gossiped, and complained so much and yet somehow still found the time to do some science. Estela, you are a wonderful chica with great humor! We had great fun during office hours and in the clubs (when we were shaking our booties)! Since we started this journey together, we've become mezcal drinking, dancing cholas, gossip girls and PhD soulmates. I hope to see you soon in Eindhoven! Yapei, when you first joined the group, you were shy and timid! I'm so proud to see the strong, independent and inspiring researcher you've become over the last few years. Scientifically, we were a great match and I am honored to be on one of your publications. It is a shame you'll be on the other side of the world, but I'll definitely visit you in China. Gautier, you are one crazy person who somehow never lost his inner child. But you're not just a clown, you're also a great, hardworking scientist. Although you guarded the borders of your part of the bench like the Maginot line you were a great bench mate. Soon I shall visit you in beautiful Switzerland and we'll be yodeling like Takeo Ischi. Nikolarrrr, I hope your fish is just as tasty as your bad jokes! I always had great fun when you were around. I admire your creativity and the way you could somehow combine ALL your hobbies with your PhD work. I hope I can sip a teeny weeny espresso with you in beautiful Sardinia soon. Eduardo, we had great conversations about any topic. You always surprised me with your well-read worldly knowledge and your eye for modern art, next to your extensive knowledge of the field.

Much of the scientific output in this thesis is the result of fruitful collaborations with colleagues. The instrumental contributions of my co-authors elevated the research to a point I could not have imagined six years ago. Dr. Caroline Paul, it was an honor to work with you. Your perceptive insights formed a crucial part of our joint NBC-FOP paper. Guang, thank you for all your hard work on our NCB paper! You were able to create a large set of mutants and manually screen a huge set of mutant-substrate combinations in such a short time. I admire your focus, hard work and dedication. Misun, not only should I thank you for the fun times we had, but also for your hard work on our joint paper! Your expertise on yeast systems really elevated the paper. It felt like ages before we could finally obtain some good results, but your perseverance and positive attitude got us there. Milos, you were instrumental to this thesis! Your amazing skills in organic synthesis and chemical analysis were vital to our joint paper, and the rest of the thesis for that matter!

Without the training I received from my former internship supervisors I would not have been able to start my PhD. They showed me how to perform rigorous scientific research, and were a source of inspiration, with their knowledge, enthusiasm, and

perseverance. Anna, thank you for teaching me scientific rigor and patience. Marcelo, thank you for sharing your passion for enzyme engineering. You are a great coach, both in the lab and in the gym. Although my legs hated you so much after every GRIT lesson, I had a lot of fun with you! Antonija, Mäuschen, not only did I learn a lot from you, you also made my masters project and my PhD a super fun period! It was a joy to work together with you – both as a student and as a PhD colleague – and I am happy that we became friends. Hope to see you soon! Marleen, ik heb veel van jou kunnen leren tijdens mijn masterproject met Antonija. Jouw betrokkenheid, expertise en ervaring hebben mij flink geholpen.

Sytze, Jeroen, Eline en de andere mensen bij *Bioclear Earth*, bedankt voor de leuke en leerzame stage. Ik had nooit gedacht dat ik tijdens mijn masterproject bio-bouwmaterialen zou maken, gas zou produceren uit koeienmest én allerlei xenobioticum-degraderende bacteriën zou isoleren. Ik heb veel geleerd van jullie brede wetenschappelijke kennis en kunde. Er zijn maar weinig stageadressen waar een student zulke goede begeleiding krijgt en tevens heel veel vrijheid heeft om het project zelf invulling te geven.

Meneer Gankema, meneer Meijers, Johan en Gerrit, jullie enthousiasme, kennis en kunnen maakten de β -vakken nóg leuker en hebben mij gemotiveerd om (bio) chemie te gaan studeren. Bedankt voor alle extracurriculaire experimenten die ik heb mogen uitvoeren op het Dollard College. Jullie maakten mijn middelbareschooltijd niet alleen leerzaam, maar juist ook super leuk!

It is impossible to perform research in our field without a team of dedicated technicians, researchers, lab supervisors and management-assistants. Peter, Henriette, Christiaan, Piet, Hein and Xiaoyu, thank you for all your help with the HPLC, FPLC, spectrophotometer and computer problems! Without your help the lab would definitely not run as smoothly as it does. Sandra, jij hebt me enorm veel geholpen met allerlei zaken en zonder jouw hulp was ik nooit tot dit punt gekomen! Hoe vaak heb jij mijn contract wel niet moeten verlengen? Ook was het altijd heel gezellig tijdens de administratie van Bioenergetics and Metabolism. Bedankt voor alle hulp en gezelligheid!

To all the members of Marco's and Dick's research groups, as well as those from the research groups of Clemens and Gerard that dared to venture into our labs: thank you for creating such a great environment for research. You were all instrumental to this thesis in your own way, be it with advice, scientific discussions and constructive criticism during our meetings on Mondays and Thursdays or with fun stuff like

lunch conversations and Friday beers. My office mates were especially important contributors to the environment I so much enjoyed. Brenda, you were the best officemate one can imagine. Fun, funny and direct. Thanks! (BTW: Sorry for my loud typing!) Nyoman, Friso and Fabiola thank you for all the fun moments in the office! You were also great scientific sparring partners. Linda, you are so much fun! Each workspace should have a Linda like you! It still amazes me how you managed to raise a kid, do a PhD and still have energy to smile and joke around. You definitely made me laugh a lot. Nikola, Hugo and Caterina from *Gecco Biotech*, thank you for all your help during my PhD and for the kind contributions to the education at *Saxion*. Good luck with your company!

During my PhD, I also had the pleasure to supervise some wonderful master's and bachelor's projects. The contributions of these students were instrumental to the work in this thesis. Marnix, Juan, Jisk and Martijn you were great students! Thank you for all your help!

I could not have done this without my partner and my family. Nate, love of my life. You were one of the main forces that drove me to finally completing the thesis, as a tough coach, motivator and proofreader. Or should I say drill sergeant? As you always reminded me very persistently of my unfinished thesis. Moreover your endless love and compassion helped me through stressful and frustrating periods. Putting up with me during this very LONG period in which I tried to finish my thesis must have been hard on you, as a lot of our plans were put on hold. Hopefully soon we can finally put our plans into action! We make a perfect team! Pap, mam, hartstikke bedankt veur aal joen laifde, steun en motivatie! Al van jongs af aan hebben jullie mijn fascinatie voor de natuur geprikkeld met schepnetjes, scheikundedozen en microscopen. Zonder al jullie hulp, motivatie en een luisterend oor was ik nooit zo ver gekomen.

Aan alle Saxion collega's van BML en Chemie, bedankt voor alle support!

And, finally, to all my friends outside of the PhD you all mean a lot to me! Jonkjes, Hillbillies, Dushis, Arnhemse meisjes, M&M, Erik, Jorn, Marieke, Eline, Stefan, Amaranta and all the other people, without your friendship this PhD would have been so much harder. Loads of kisses, hugs, rosé and many, many THANKS to you all!

Curriculum Vitae

Jeroen was born and raised in north-east Groningen, The Netherlands. From a young age, he had a passion for science and often borrowed lab equipment from his high school so that he could perform experiments at home. He pursued his interest in the natural sciences by obtaining a Bachelor's degree in chemistry with a specialization in biochemistry from the University of Groningen. Subsequently, he completed a Master's in molecular biology and biotechnology. While studying, Jeroen worked on two thesis projects under the supervision of prof. dr. Dick Janssen in the field of biocatalysis and enzyme engineering: broadening the substrate scope of peptidylase for efficient peptide segment condensation and altering the substrate scope and enantiospecificity of a thermostable diaminopimelate decarboxylase, both of which contributed to peer-reviewed articles. During a 6-months internship at Bioclear Earth, Jeroen worked on the biological pretreatment of second-generation feedstock for improved biogas production with Basidiomycota, as well as on the isolation and characterization of microorganisms for the bioremediation of certain xenobiotics. In 2017, Jeroen started his PhD training in the group of prof. dr. Marco Fraaije, where his research focused on the (bio)synthesis of the novel artificial deazaflavin cofactor FOP and on its applications in biocatalysis. Since 2021 he has been working as a lecturer in biochemistry and molecular biology at Saxion University of Applied Sciences in Deventer, the Netherlands.

List of Publications

- Nuijens, T., Toplak, A., Quaedflieg, P. J. M., Drenth, J., Wu, B., & Janssen, D. B. (2016). Engineering a diverse ligase toolbox for peptide segment condensation. *Advanced Synthesis & Catalysis*, 358(24), 4041-4048.
- Drenth, J., Trajkovic, M., & Fraaije, M. W. (2019). Chemoenzymatic synthesis of an unnatural deazaflavin cofactor that can fuel F420-dependent enzymes. *ACS Catalysis*, 9(7), 6435-6443.
- Drenth, J., Yang, G., Paul, C. E., & Fraaije, M. W. (2021). A Tailor-Made Deazaflavin-Mediated Recycling System for Artificial Nicotinamide Cofactor Biomimetics. *ACS catalysis*, 11(18), 11561-11569.
- Tong, Y., Lee, M., Drenth, J., & Fraaije, M. W. (2021). Flavin-tag: A Facile Method for Site-Specific Labeling of Proteins with a Flavin Fluorophore. *Bioconjugate Chemistry*, 32(8), 1559-1563.
- Marjanovic, A., Ramírez-Palacios, C. J., Masman, M. F., Drenth, J., Otzen, M., Marrink, S. J., & Janssen, D. B. (2021). Thermostable D-amino acid decarboxylases derived from *Thermotoga maritima* diaminopimelate decarboxylase. *Protein Engineering, Design and Selection*, 34.
- Lee, M., Drenth, J., Trajkovic, M., de Jong, R. M., & Fraaije, M. W. (2022). Introducing an Artificial Deazaflavin Cofactor in *Escherichia coli* and *Saccharomyces cerevisiae*. *ACS synthetic biology*, 11(2), 938-952.
- Drenth, J., & Fraaije, M. W. (2021). Natural Flavins: Occurrence, Role, and Noncanonical Chemistry. *Flavin-Based Catalysis: Principles and Applications*, 29-65.